

This file is part of the following work:

Montalvo-Proano, Jose L. (2020) *Beneficial acclimation and stress-hardening of corals to climate change conditions*. PhD Thesis, James Cook University.

Access to this file is available from:

<https://doi.org/10.25903/72sk%2Dbc97>

Copyright © 2020 Jose L. Montalvo-Proano.

The author has certified to JCU that they have made a reasonable effort to gain permission and acknowledge the owners of any third party copyright material included in this document. If you believe that this is not the case, please email

researchonline@jcu.edu.au

Beneficial acclimation and stress-hardening of corals to climate change conditions

Thesis submitted by

Jose L. MONTALVO-PROANO

(B.Sc., M.Sc.)

ARC Centre of Excellence for Coral Reef Studies

Australian Institute of Marine Science

James Cook University, AIMS@JCU

October 2020

For the degree of Doctor of Philosophy in Science

Submitted to the ARC Centre of Excellence for Coral Reef Studies

James Cook University

Townsville, Australia

Acknowledgements

I wish to acknowledge the Bindal people as the Traditional Owners of the land on which I worked at Cape Ferguson, and also the sea country of Davies Reef where I collected coral colonies for my experiments. I pay my respects to past, present and future Bindal elders. I honour their culture, knowledge, beliefs and spiritual relationship and connection to land and sea country which has continued for millennia. I also recognise them as the first scientists to work in this region some tens of thousands of years ago.

I thank the Australian Institute of Marine Science, in particular the National Sea Simulator team for their effort on maintaining high quality standards to run the experiments. I also thank AIMS@JCU for the unconditional support and care of their students. I also thank the Great Barrier Reef Marine Park Authority for the corresponding permits.

I wish to thank my supervisors (Line Bay, Philip Munday, Madeleine van Oppen, and Nicole Webster) for their constant support, patience, and guidance throughout this process. I have learnt so much from each of you and your different areas of expertise and I consider myself lucky that I was able to work with a great team of well-recognised research scientists.

I would like to acknowledge all the additional help that I received during the multiple and challenging experiments and laboratory work. I will be forever thankful with these extraordinary people: Mariana Alvarez-Noriega, Mikayla Hiuzer, Merle Schlawinsky, Sara Bell, Sebastian Comarmond, and Matthew-James Bennett.

I would like to dedicate this work to corals and nature in general, and of course to my family for their unconditional support and endless love. It would have been just impossible without you, and I am grateful for having a very special connection with every one of you. Thanks for teaching me to adventure with purpose, to dream and pursue challenges but always keeping humble feet on the ground.

Statement of the Contribution of Others

Research funding:

- AIMS@JCU – PhD Scholarship
- Australian Institute of Marine Science (AIMS) – all chapters
- King Abdullah University of Science and Technology (KAUST) – Chapter 4

Supervision – all chapters:

- Dr. Line K. Bay
- Prof. Philip L. Munday
- Prof Madeleine J. H. van Oppen
- Dr. Nicole Webster

Experimental set-up or instrumentation:

- Staff of the National Sea Simulator (SeaSim – AIMS)
- Laboratory facilities at AIMS

Editorial assistance:

- Dr. Line K. Bay, Prof. Philip L. Munday, Prof Madeleine J. van Oppen, Dr. Nicole Webster
- Dr Mariana Alvarez-Noriega (statistical modelling support)

Volunteers provided help in the experiments during this PhD and their names are listed in the acknowledgments.

General Abstract

Anthropogenic carbon dioxide emissions are projected to continue to increase, leading to significant increases in sea-surface temperature and a reduction in seawater pH. The physiological limits of corals may be surpassed by the cumulative effects of ocean warming and acidification, and the increased frequency and intensity of extreme heat events (marine heat waves). Although corals have survived environmental stressors through geological time, it is unclear how corals, and their symbiotic associates, will respond to the current rapid pace of climate change. Coral populations might genetically adapt across multiple generations although this is expected to be a lengthy process for some species. Alternatively, corals may acclimate over shorter timeframes via phenotypic plasticity. Furthermore, coral symbionts, such as Symbiodiniaceae and bacteria, have evolved mechanisms to maintain their homeostasis in response to environmental change and may enhance the acclimation response of the coral holobiont. Nevertheless, it is still unclear how different life stages of corals will respond to the combined effects of ocean warming and acidification, and if beneficial phenotypic plasticity can occur in sensitive early life stages. Furthermore, it remains unknown how climate change conditions will shape the community structure of symbionts, and if their acclimatory responses will influence thermal tolerance of the holobiont. The objective of this thesis was to determine the potential for beneficial acclimation and thermal hardening in early-life and adult stages of a common coral (*Acropora loripes*) from the Great Barrier Reef. In particular, I aimed to quantify acclimation responses to projected future climate change conditions in a range of phenotypic traits of the coral holobiont, and to evaluate the potential contribution of the Symbiodiniaceae and bacterial communities to host acclimation. Quantifying the acclimation potential of corals to future climate change conditions has important implications for modelling reef futures and for reef restoration and adaptation approaches.

Experimental treatments encompassed two levels of combined elevated temperature and $p\text{CO}_2$ relative to ambient seawater conditions (27.5°C, 410 $\mu\text{atm } p\text{CO}_2$) that were consistent with moderate (mid: 28.5°C, 670 $\mu\text{atm } p\text{CO}_2$) and high (29.5°C, 900 $\mu\text{atm } p\text{CO}_2$) CO_2 emissions scenarios. In Chapter 2 I tested how the thermal tolerance and development of coral early life stages are affected by these two predicted future ocean conditions. Gametes from 12 *A. loripes* colonies were fertilised and larvae and recruits were reared for 10 weeks under ambient, mid, and high treatment conditions. A subset of aposymbiotic larvae were exposed to an acute heat stress (35.5°C) at 10 days post-fertilization. Larval survival under acute heat stress (35.5°C) differed among rearing conditions, with larvae from the high treatment surviving longer than those reared under mid and ambient conditions. Treatment was found to have a significant effect on growth rate of coral recruits after six and ten

weeks of treatment, but the effect size was small (< 11 % difference in growth rate for mid and high relative to ambient) and post-hoc comparisons did not detect a significant difference between pairs of treatments. Symbiodiniaceae and bacterial communities in 6-week old coral recruits significantly differed among treatments, with treatment explaining 25 and 6% of the variation, respectively.

To experimentally test for beneficial acclimation and stress-hardening in early life stages (chapter 3), coral larvae and recruits (from cross-fertilization of 14 *A. loripes* colonies) were reared in the three treatment conditions for a period of 23 weeks. The experiment included a full reciprocal transplant among all treatment conditions at 8 weeks of age, and a heat stress experimental test after 16 weeks of age. As in chapter 2, evidence for thermal hardening in larvae was observed, with treated larvae displaying enhanced tolerance to acute heat stress (35.5°C) after 10-days preconditioning under elevated conditions. Subtle evidence for beneficial acclimation to climate change conditions in the maximum photochemical efficiency (Fv/Fm) of 16-week old recruits following transplantation across treatment combinations was also observed. Furthermore, the negative effect of 35 days of heat stress at 31°C on Fv/Fm was buffered in recruits that had experienced elevated conditions during the reciprocal transplantation stage, providing evidence for thermal hardening. Overall, there was no clear effect of treatment conditions on the growth of recruits during transplantation or heat stress.

In the final thesis chapter, I examined the role of beneficial acclimation and stress-hardening in adult corals. Twenty-one *A. loripes* colonies were collected, fragmented and exposed to the three treatment conditions for four weeks, followed by a full reciprocal transplant among conditions for another four weeks. Following a 2-week pre-acclimation to ambient conditions, fragments were exposed to a ramp and hold bleaching experiment with a maximum temperature of 31°C for four weeks. Clear evidence of beneficial acclimation in photochemical efficiency was observed after reciprocal transplantation, as Fv/Fm decreased with increasingly severe treatment conditions, but this effect was dampened in fragments that experienced mid or high conditions prior to transplantation. There was also clear evidence for thermal hardening of coral fragments. Fv/Fm was significantly lower at 31°C, but the reduction was buffered in fragments that had experienced changes in treatment conditions following transplantation. In contrast, an effect of treatment on growth could not be detected and thus did not provide evidence of beneficial acclimation in this trait. Finally, no significant effect of treatment history was evident in the community structure of Symbiodiniaceae or bacteria, suggesting that beneficial acclimation and hardening of Fv/Fm was due to photoacclimation of Symbiodiniaceae rather than symbiont shuffling or switching.

In summary, this thesis presents a comprehensive appraisal of the potential for beneficial acclimation and thermal hardening in corals to future climate change conditions, via phenotypic

plasticity. An elaborate experimental design and a wide range of phenotypic traits was used in a holistic approach to evaluate acclimatory responses in different life stages of a common species of scleractinian coral, including the community composition of its symbionts. My findings suggest that preconditioning of aposymbiotic larvae to future ocean conditions can increase their tolerance to acute heat stress, without reducing short-term survival or growth of recruits after settlement. Furthermore, my results suggest that corals with past exposure to climate change conditions may be more tolerant to chronic heat stress. These results provide insights into the effects of future climate scenarios on the performance of coral early life stages, and their ability to withstand thermal stress events, to better inform predictions of future reef states. Furthermore, these results show that acclimation of corals to dynamic environments may be beneficial for inducing more temperature resilient phenotypes and are thus of relevance to proposed reef restoration and adaptation approaches.

Table of Contents

Acknowledgements	i
Statement of the Contribution of Others	ii
General Abstract	iii
Table of Contents.....	vi
List of Tables	x
List of Figures	xviii
Chapter 1: General Introduction.....	25
Chapter 2: Thermal preconditioning of coral larvae increases their tolerance to heat waves and affects phenotypic traits of the recruit.....	33
2.1 Abstract	33
2.2 Introduction.....	34
2.3 Material and Methods.....	37
2.3.1 Study species collection	37
2.3.2 Experimental parameters and coral spawning.....	37
2.3.3 Larval acute heat stress experiment	39
2.3.4 Recruit performance experiment.....	39
2.3.5 DNA extraction, Amplification and Sequencing Protocol.....	40
2.3.5.1 Preparation of ITS2 and 16S libraries for sequencing.....	40
2.3.5.2 Metabarcoding analyses.....	41
2.3.6 Statistical analysis	42
2.3.6.1 Larval heat tolerance, settlement and basal growth.....	42
2.3.6.2 Symbiont associations	43
2.4 Results	44
2.4.1 Phenotypic performance.....	44
2.4.1.1 Larval heat stress survival.....	44
2.4.1.2 Settlement success and survival of recruits over time	45
2.4.1.3 Recruit basal growth over time	46
2.4.2 Symbiotic associations	47
2.4.2.1 Symbiodiniaceae communities of 6-week old recruits.....	47
2.4.2.2 Bacterial communities for 6-week old recruits	49
2.4.2.3 Correlation of relative abundances across symbiont members.....	51
2.5 Discussion	53
2.5.1 Larval and recruit survival	53
2.5.2 Symbiodiniaceae diversity and community structure.....	56

2.5.3 Bacterial diversity and community structure	57
2.5.4 Conclusions	58
Chapter 3: An experimental test of beneficial acclimation and thermal hardening to climate change conditions in coral early life stages	59
3.1 Abstract	59
3.2 Introduction.....	60
3.3 Material and Methods.....	63
3.3.1 Study species and coral collection	63
3.3.2 Experimental parameters and coral spawning.....	63
3.3.3 Acute heat tolerance of coral larvae	65
3.3.4 Settlement and follow up of recruit development	65
3.3.5 Recruit performance under chronic conditions	66
3.3.6 Statistical analysis	68
3.3.6.1 Larval survival under acute heat stress	68
3.3.6.2 Settlement and survival of coral recruits.....	68
3.3.6.3 Basal growth of coral recruits.....	68
3.3.6.4 Maximum quantum yield (Fv/Fm)	70
3.3.6.5 Correlation of traits	70
3.4 Results	70
3.4.1 Larvae survival during acute heat stress	70
3.4.2 Settlement success of recruits	71
3.4.3 Coral recruit survival	72
3.4.4 Coral recruit growth	73
3.4.4.1 Growth before and after transplantation.....	73
3.4.4.2 Growth during heat stress exposure	76
3.4.5 Photochemical efficiency (Fv/Fm) across experimental stages	78
3.4.5.1 Fv/Fm before and after transplantation.....	78
3.4.5.2 Fv/Fm during heat stress exposure	80
3.4.6 Correlation between growth and Fv/Fm.....	81
3.5 Discussion	82
3.5.1 Thermal tolerance of larvae under heat stress	82
3.5.2 Settlement, survival, growth and Fv/Fm of coral recruits.....	84
3.5.3 Conclusions	87
Chapter 4: Beneficial acclimation through preconditioning may enhance coral tolerance to acute heat.....	89
4.1 Abstract	89
4.2 Introduction.....	90
4.3 Material and Methods.....	92

4.3.1 Study species collection	92
4.3.2 Coral propagation and experimental parameters.....	93
4.3.3 Experimental design and trait assessment.....	94
4.3.4 DNA extraction, Amplification and Sequencing Protocol.....	96
4.3.4.1 Preparation of ITS2 and 16S libraries for sequencing.....	97
4.3.4.2 Metabarcoding analyses.....	97
4.3.5 Statistical analysis – phenotypic and physiological measurements	97
4.3.5.1 Growth.....	97
4.3.5.2 Maximum quantum yield (Fv/Fm).....	99
4.3.5.3 Symbiont associations	99
4.4 Results	100
4.4.1 Growth	100
4.4.1.1 Growth before and after transplantation (plasticity)	100
4.4.1.2 Growth during heat stress exposure (31 °C).....	102
4.4.2 Photochemical efficiency (Fv/Fm).....	104
4.4.2.1 Fv/Fm before and after transplantation (plasticity)	104
4.4.2.2 Fv/Fm during heat stress exposure (31 °C).....	106
4.4.3 Correlation between growth and Fv/Fm at different experimental stages	108
4.4.4 Symbiotic associations	109
4.4.4.1 Symbiodiniaceae communities 4 weeks after transplantation (plasticity stage; t=8 weeks)	109
4.4.4.2 Bacterial communities 4 weeks after transplantation (plasticity stage; t=8 weeks)	110
4.4.4.3 Correlation of relative abundances across symbiont members	113
4.5 Discussion	114
4.5.1 Growth	115
4.5.1.1 Plasticity stage	115
4.5.1.2 Heat tolerance stage	115
4.5.2 Maximum photochemical efficiency (Fv/Fm).....	116
4.5.2.1 Plasticity stage	116
4.5.2.2 Heat tolerance stage	118
4.5.3 Host genotypic effects on growth and Fv/Fm	119
4.5.4 Symbiodiniaceae and bacterial community composition structure.....	119
4.5.5 Conclusions	120
Chapter 5 – General Discussion	122
References	128
Appendix A – Chapter 2	147
A.1 Recruits: settlement success	147

A.2 Recruits: growth	148
A.3 Symbiotic associations	149
A.3.1 Symbiodiniaceae communities at t=6 weeks.....	149
A.3.2 Bacterial communities at t=6 weeks	157
Appendix B – Chapter 3	179
B.1 Coral recruits: settlement success.....	179
B.2 Coral recruits: survival	180
B.3 Coral recruits: growth.....	193
B.4 Coral recruits: photochemical efficiency (Fv/Fm)	208
Appendix C – Chapter 4	223
C.1 Adult fragments: growth	223
C.2 Adult fragments: Fv/Fm	234
C.3 Adult fragments: Symbiodiniaceae	248
C.4 Adult fragments: Bacteria.....	249

List of Tables

Table 2. 1 Coefficient estimates for survival of recruits among treatments corresponding to all time intervals over a total period of 8 weeks (2 to 10 weeks).....	46
Table A.S 1 Coefficients of the generalised linear mixed effect model predicting the number of recruits settling among treatments.....	147
Table A.S 2 List of statistical models used to predict basal growth of coral recruits relative to the exposure to treatment, size (diameter) and time. The shaded area indicates the best-fit model.	148
Table A.S 3 Coefficient estimates for the best-fit linear model to estimate recruit basal growth relation to treatment, diameter and time.	148
Table A.S 4 Tukey Posthoc Test estimates of pairwise comparisons among treatments.....	148
Table A.S 5 PERMANOVA test results (partial R2 and p-values) for the effect of treatment on Symbiodiniaceae relative composition using Bray-Curtis similarity distance. Number of permutations=999.	149
Table A.S 6 Proportion of Symbiodiniaceae types present in individuals from a general approach and also for each treatment at t = 6 weeks.	149
Table A.S 7 Proportion of Symbiodiniaceae types present in individuals from AMBIENT treatment at t=6 weeks.	150
Table A.S 8 Proportion of Symbiodiniaceae types present in individuals from MID treatment at t=6 weeks.....	152
Table A.S 9 Proportion of Symbiodiniaceae types present in individuals from HIGH treatment at t=2.....	154
Table A.S 10 Coefficient estimates of the observed ASVs in 6-week old recruit corals among treatments.....	159
Table A.S 11 Coefficient estimates for Shannon diversity index in 6-week old recruit corals among treatments.....	159
Table A.S 12 Coefficient estimates of the observed ASVs in 6-week old recruit corals among treatments.....	159
Table A.S 13 PERMANOVA test results (partial R2 and p-values) for the effect of treatment on the relative composition of bacterial communities using Bray-Curtis similarity distance. Number of permutations=999	160
Table A.S 14 Permutation test for homogeneity of multivariate dispersions. Number of permutations=999	160

Table A.S 15 Indicator taxa for 6-week old coral recruits under different treatments. Indval analysis done at the species level (ASV) and included alpha parameters of 0.05.	161
Table A.S 16 Indicator taxa for 6-week old coral recruits under different treatments. Indval analysis done at the genus level and included alpha parameters of 0.05.	161
Table A.S 17 Indicator taxa for 6-week old coral recruits under different treatments. Indval analysis done at the family level and included alpha parameters of 0.05.....	162
Table A.S 18 Individual models among bacterial families used to estimate difference in relative abundances from the top ten most abundant following a zero-inflated beta-regression. ...	163
Table A.S 19 Results from the posterior distribution of difference as the outcome for each model and bacterial family	166
Table A.S 20 Individual models among bacterial genera used to estimate difference in relative abundances from the top ten most abundant following a zero-inflated beta-regression. ...	169
Table A.S 21 Results from the posterior distribution of difference as the outcome for each model and bacterial family	171
Table A.S 22 Estimates of differentially abundant bacteria (non-rarefied dataset) between mid and ambient treatments. Only significantly different taxa displayed. Log2FoldChange (x) values compare abundances found in mid as reference treatment compared to abundances found in ambient. Its value represents magnitude of difference (2^x), whereas its sign represents direction: negative favours reference treatment mid and positive favours ambient.....	174
Table A.S 23 Estimates of differentially abundant bacteria (non-rarefied dataset) between high and ambient treatments. Only significantly different taxa displayed. Log2FoldChange (x) values compare abundances found in high as reference treatment compared to abundances found in ambient. Its value represents magnitude of difference (2^x), whereas its sign represents direction: negative favours reference treatment high and positive favours ambient.....	175
Table A.S 24 Estimates of differentially abundant bacteria (non-rarefied dataset) between mid and high treatments. Only significantly different taxa displayed. Log2FoldChange (x) values compare abundances found in mid as reference treatment compared to abundances found in high. Its value represents magnitude of difference (2^x), whereas its sign represents direction: negative favours reference treatment mid and positive favours high.....	176
Table B.S 1 List of statistical models used to predict variation in settlement success across treatments at t=0 weeks. The shaded area indicates the best-fit model.	179
Table B.S 2 Coefficients of the generalised linear mixed effect model predicting the number of recruits settling among treatments.....	179

Table B.S 3 Tukey Posthoc Test estimates of pairwise comparisons among treatments for settlement.	179
Table B.S 4 List of statistical models used to predict survival of coral recruits relative to the exposure to treatment at t=8 weeks. The shaded area indicates the best-fit model.....	180
Table B.S 5 Coefficients of the generalised linear mixed effect model predicting the survival rate of number of recruits among treatments at t=8 weeks. Number of observations: total=10689, tank=36.....	180
Table B.S 6 Tukey Posthoc Test estimates of pairwise comparisons among treatments for survival at t=8 weeks; confidence level used: 0.95.....	180
Table B.S 7 List of statistical models used to predict survival of coral recruits relative to the exposure to treatment at t=16 weeks. The shaded area indicates the best-fit model.	181
Table B.S 8 Coefficients of the generalised linear mixed effect model predicting the survival rate of number of recruits among treatments at t=16 weeks. Number of observations: total=10689, tank=36.....	181
Table B.S 9 Tukey Posthoc Test estimates of pairwise comparisons among treatments for survival at t=16 weeks; confidence level used: 0.95.....	182
Table B.S 10 List of statistical models used to predict survival of coral recruits relative to the exposure to treatment at t=18 weeks. The shaded area indicates the best-fit model.	183
Table B.S 11 Coefficients of the generalised linear mixed effect model predicting the survival rate of number of recruits among treatments at t=18 weeks. Number of observations: total=10689, tank=36.....	183
Table B.S 12 Tukey Posthoc Test estimates of pairwise comparisons among treatments for survival at t=18 weeks; confidence level used: 0.95.....	184
Table B.S 13 List of statistical models used to predict survival of coral recruits relative to the exposure to treatment at t=23 weeks. The shaded area indicates the best-fit model.	185
Table B.S 14 Coefficients of the generalised linear mixed effect model predicting the survival rate of number of recruits among treatments at t=23 weeks. Number of observations: total=10689, tank=24.....	185
Table B.S 15 Tukey Posthoc Test estimates of pairwise comparisons among treatments for survival at t=23 weeks; confidence level used: 0.95.....	186
Table B.S 16 List of statistical models used to predict basal growth rate of coral recruits relative to the exposure to treatment at t=8 weeks. The shaded area indicates the best-fit model.	193

Table B.S 17 Coefficients of the generalised linear mixed effect model predicting the basal growth rate of recruits among treatments at t=8 weeks. Number of observations: total=360, tank=36.	193
Table B.S 18 Tukey Posthoc Test estimates of pairwise comparisons among treatments for basal growth rate at t=8 weeks; confidence level used: 0.95.....	194
Table B.S 19 List of statistical models used to predict basal growth rate of coral recruits relative to the exposure to treatment at t=16 weeks. The shaded area indicates the best-fit model.	194
Table B.S 20 Coefficients of the generalised linear mixed effect model predicting the basal growth rate of recruits among treatments at t=16 weeks. Number of observations: total=360, tank=36.....	194
Table B.S 21 Tukey Posthoc Test estimates of pairwise comparisons among treatments for basal growth rate at t=16 weeks; confidence level used: 0.95.....	195
Table B.S 22 List of statistical models used to predict basal growth rate of coral recruits relative to the exposure to treatment at t=18 weeks. The shaded area indicates the best-fit model.	196
Table B.S 23 Coefficients of the generalised linear mixed effect model predicting the basal growth rate of recruits among treatments at t=18 weeks. Number of observations: total=358, tank=24, tray=62.....	197
Table B.S 24 Tukey Posthoc Test estimates of pairwise comparisons among treatments for basal growth rate at t=18 weeks; confidence level used: 0.95.....	197
Table B.S 25 List of statistical models used to predict basal growth rate of coral recruits relative to the exposure to treatment at t=23 weeks. The shaded area indicates the best-fit model.	200
Table B.S 26 Coefficients of the generalised linear mixed effect model predicting the basal growth rate of recruits among treatments at t=23 weeks. Number of observations: total=347, tank=24.....	201
Table B.S 27 Tukey Posthoc Test estimates of pairwise comparisons among treatments for basal growth rate at t=23 weeks; confidence level used: 0.95.....	202
Table B.S 28 List of statistical models used to predict Fv/Fm of coral recruits relative to the exposure to treatment at t=8 weeks. The shaded area indicates the best-fit model.....	208
Table B.S 29 Coefficients of the generalised linear mixed effect model predicting Fv/Fm of recruits among treatments at t=8 weeks. Number of observations: total=288, tank=36.....	208

Table B.S 30 Tukey Posthoc Test estimates of pairwise comparisons among treatments for Fv/Fm at t=8 weeks; confidence level used: 0.95.....	208
Table B.S 31 List of statistical models used to predict Fv/Fm of coral recruits relative to the exposure to treatment at t=16 weeks. The shaded area indicates the best-fit model.	209
Table B.S 32 Coefficients of the generalised linear mixed effect model predicting Fv/Fm of recruits among treatments at t=16 weeks. Number of observations: total=288, tank=36.	209
Table B.S 33 Tukey Posthoc Test estimates of pairwise comparisons among treatments for Fv/Fm at t=16 weeks; confidence level used: 0.95.....	210
Table B.S 34 List of statistical models used to predict Fv/Fm of coral recruits relative to the exposure to treatment at t=18 weeks. The shaded area indicates the best-fit model.	211
Table B.S 35 Coefficients of the generalised linear mixed effect model predicting Fv/Fm of recruits among treatments at t=18 weeks. Number of observations: total=288, tank=24, tray=62..	212
Table B.S 36 Tukey Posthoc Test estimates of pairwise comparisons among treatments for Fv/Fm at t=18 weeks; confidence level used: 0.95.....	213
Table B.S 37 List of statistical models used to predict Fv/Fm of coral recruits relative to the exposure to treatment at t=23 weeks. The shaded area indicates the best-fit model.	215
Table B.S 38 Coefficients of the generalised linear mixed effect model predicting Fv/Fm of recruits among treatments at t=23 weeks. Number of observations: total=288.	216
Table B.S 39 Tukey Posthoc Test estimates of pairwise comparisons among treatments for Fv/Fm at t=23 weeks; confidence level used: 0.95.....	217
Table C.S 1 List of statistical models used to assess growth among treatments during incubation period t=1 (4 weeks). The shaded area indicates the best-fit model.	223
Table C.S 2 Coefficient estimates for the best-fit linear model predicting proportional growth rate at t=4 weeks. Asterisks indicate significant effects.	223
Table C.S 3 Posthoc test estimates for growth at t=4 weeks for individual comparisons among treatments.....	224
Table C.S 4 List of statistical models used to predict the difference in proportional linear extension between time t=8 and t=4 weeks [i.e., ($\log_{10}A_{reat} = 2A_{reat} = 1$)] among treatments during incubation period t=8, after transplanted occurred. The shaded area indicates the best-fit model.....	224
Table C.S 5 Coefficient estimates for the linear model comparing proportional linear extension of fragments under the different treatments at t=8 in relation to the exposure of their previous treatment at t=4. Asterisks indicate significant effects.	224

Table C.S 6 Post Hoc results of coefficient estimates for the linear model comparing predicted growth of fragments under the different treatments at t=8 in relation to the exposure of their previous treatment at t=4 (treatment combinations). Asterisks indicate significant effects. ...	225
Table C.S 7 Summary statistics of the linear mixed effect models testing for acclimation at t=8, considering all treatment combinations.	226
Table C.S 8 List of statistical models predicting linear growth at t=10 weeks (all fragments under ambient treatment for 2 weeks) relative to the exposure to previous treatments at t=4 and t=8. The shaded area indicates the best-fit model.	228
Table C.S 9 Coefficient estimates for the best-fit linear model predicting the linear growth at t=10 weeks as a function of treatment at t=4 weeks and treatment at t=8 weeks and size at t=8 weeks. Asterisks indicate significant effects. Total observations=378, genotypes=21.....	228
Table C.S 10 Tukey Post hoc test estimates of all combinations of treatments confirming no significant differences on growth at t=10 weeks.....	229
Table C.S 11 List of statistical models predicting linear growth at t=14 (fragments under acute or ambient treatment) relative to the exposure to previous treatments at t=4 and t=8. The shaded area indicates the best-fit model.....	231
Table C.S 12 Coefficient estimates for the best-fit linear model predicting the linear growth at t=14 as a function of treatment at t=4 and treatment at t=8 and size at t=10 weeks. Asterisks indicate significant effects.....	232
Table C.S 13 Tukey Post hoc test estimates of growth rate at t=14 considering combinations of treatments.....	233
Table C.S 14 List of statistical models used to assess maximum quantum yield (Fv/Fm) among treatments during incubation period t=4 weeks. The shaded area indicates the best-fit model.	234
Table C.S 15 Coefficient estimates for the best-fit linear model predicting Fv/Fm at t=4 as a function of treatment at t=4 weeks, Fv/fm at t=0 and size at t=4 weeks. Asterisks indicate significant effects.	235
Table C.S 16 Tukey Post hoc test estimates of Fv/Fm at t=4 weeks considering comparisons between treatments.....	235
Table C.S 17 List of statistical models used to predict maximum quantum yield [Fv/Fm] at time t=8 weeks relative to treatment t=4 weeks, i.e., after transplantation occurred. The shaded area indicates the best-fit model.....	236
Table C.S 18 Coefficient estimates for the best-fit linear model predicting Fv/Fm at t=8 weeks as a function of treatment at t=8 weeks, treatment at t=4 weeks, Fv/Fm at t=4 and size at t=8. Asterisks indicate significant effects.....	236

Table C.S 19 Tukey Post hoc test estimates of Fv/Fm at t=8 considering comparisons between treatments at t=4 and treatment at t=8 weeks.	237
Table C.S 20 Summary statistics of the linear mixed effect models using Fv/Fm testing for acclimation at t=2, considering all treatment combinations.	239
Table C.S 21 List of statistical models predicting Fv/Fm at t=10 (all fragments under ambient treatment for 2 weeks) relative to the exposure to previous treatments at t=4 and t=8. The shaded area indicates the best-fit model.	242
Table C.S 22 Coefficient estimates for the best-fit linear model predicting Fv/Fm at t=10 as a function of treatment at t=4 and treatment at t=8 and size at t=8 weeks. Asterisks indicate significant effects.	242
Table C.S 23 Tukey Post hoc test estimates of all combinations of treatments testing significant differences on Fv/Fm at t=10 weeks.	243
Table C.S 24 List of statistical models predicting Fv/Fm at t=14 (fragments under heat stress or ambient treatment) relative to the exposure to previous treatments at t=4 and t=8 weeks. The shaded area indicates the best-fit model.	245
Table C.S 25 Coefficient estimates for the best-fit linear model predicting the linear growth at t=14 as a function of treatment at t=4 and treatment at t=8 and size at t=10 weeks. Asterisks indicate significant effects.	246
Table C.S 26 Tukey Post hoc test estimates of growth rate at t=14 weeks considering combinations of treatments.	247
Table C.S 27 Statistical results of the permutational multivariate analysis of variance (PERMANOVA) of Symbiodiniaceae composition using Bray-Curtis distance.	248
Table C.S 28 Coefficient estimates of the observed ASVs in adult coral fragments four weeks after transplantation, considering origin (t=4 weeks) and destination treatment (t=8 weeks).	250
Table C.S 29 Coefficient estimates of Chao1 index in adult coral fragments four weeks after transplantation, considering origin (t=4 weeks) and destination treatment (t=8 weeks).	252
Table C.S 30 Coefficient estimates of Shannon diversity index in adult coral fragments four weeks after transplantation, considering origin (t=4 weeks) and destination treatment (t=8 weeks).	254
Table C.S 31 Presence and absence of bacterial taxa (ASV level) on a rarefied data set. For each treatment history, a number '1' represents presence of a particular ASVs classified according to treatment history, genotype and sample ID, whereas '0' represents absence; total appearances among treatment histories included.	257

Table C.S 32 PERMANOVA test results (partial R^2 and p-values) for the effect of treatment on the relative composition of bacterial communities using Bray-Curtis similarity distance. Number of permutations=999	257
Table C.S 33 Permutation test for homogeneity of multivariate dispersions. Number of permutations=999	257
Table C.S 34 Indicator taxa for adult coral fragments four weeks after transplantation, considering origin (t=4) and destination treatment (t=8 weeks). Indval analysis done at the species level (ASV) and included alpha parameters of 0.05.....	258
Table C.S 35 Indicator taxa for adult coral fragments four weeks after transplantation, considering origin (t=4) and destination treatment (t=8 weeks). Indval analysis done at the family level and included alpha parameters of 0.05.	260
Table C.S 36 Individual models among bacterial families used to estimate difference in relative abundances from the top ten most abundant following a zero-inflated beta-regression. ...	261
Table C.S 37 Results from the posterior distribution of difference as the outcome for each model and bacterial family	261
Table C.S 38 Individual models among bacterial genera used to estimate difference in relative abundances from the top ten most abundant following a zero-inflated beta-regression.	266
Table C.S 39 Results from the posterior distribution of difference as the outcome for each model and bacterial genus (top 10 most abundant)	267
Table C.S 40 Estimates of differentially abundant bacteria (non-rarefied dataset) between origin and destination treatments. Only significantly different taxa displayed. Log ₂ FoldChange (x) values compare abundances found in particular treatment combinations, where a positive value favours treatment history 1 and a negative value means significantly higher abundance in treatment history 2. Its value represents magnitude of difference (2^x).....	271

List of Figures

- Figure 2. 1** Schematic representation of the experimental design. It includes two experiments: the primary experiment that aimed to evaluate recruit performance over time under three treatments, and a secondary experiment that aimed to evaluate response of larvae to heat stress..... 38
- Figure 2. 2** Kaplan-Meier curves showing survival probability over time for larvae exposed to two temperatures (27.5 and 35.5°C) at ambient $p\text{CO}_2$. Solid lines show survival of larvae exposed to acute heat stress at 35.5°C over a period of 144 hours, whereas dotted lines display survival of larvae exposed to the ambient temperature of 27.5 °C. Line colours represent the three rearing conditions being AMBIENT (blue), MID (black) and HIGH (red) temperature x $p\text{CO}_2$ 45
- Figure 2. 3** Survival probabilities of recruits in the three treatments at 2 weeks, 6 weeks and 10 weeks post settlement. Error bars show 95% confidence intervals. The size of the coloured circles represents the number of raw observations where the top circles show the number of survivors whereas the bottom circles show the number of dead recruits). 46
- Figure 2. 4** Mean basal growth of recruits for the different treatments (AMBIENT, MID, HIGH) in the first (a) and second (b) time intervals. Since basal growth was size-dependent, all predictions were corrected for size. Points show the fitted model mean and error bars are confidence intervals. The grey box plots show the data corrected for diameter. 47
- Figure 2. 5** Average composition of Symbiodiniaceae communities in 6-week old *A. loripes* recruits. Bar plots show the overall proportion of each type profile within each treatment (i.e., pooled across coral recruits within treatments)..... 48
- Figure 2. 6** NMDS of Symbiodiniaceae type profiles in 6-week old recruits across treatments. Values in axis represent Bray-Curtis distances between samples. The red lines show the ten Symbiodiniaceae type profiles that contributed most to the ordination, the remainder are represented by grey lines. Names in brackets represent SymPortal associated species to each of the type profiles..... 49
- Figure 2. 7** NMDS of bacterial communities in 6-week old recruits across treatments. The axes represent Bray-Curtis distances among samples..... 50
- Figure 2. 8** Relative abundance of the top 10 bacterial families (y-axis) among 6-week old recruits (x-axis) for each of the three treatments (AMBIENT, MID, HIGH); (n= 117 total families)..... 51
- Figure 2. 9** Relative abundance correlations among Symbiodiniaceae type profiles and bacterial families for 6-week old recruits. Correlation values based on the Spearman Rank correlation coefficient analysis. Significant correlations among pairs are shown inside the inside the matrix..... 52

- Figure 3. 1** Experimental design used to assess the potential for beneficial acclimation and thermal hardening in the early life stages of the coral *Acropora loripes*). Incubation times in weeks (t) and tissue sampling point (s) are also included. 64
- Figure 3. 2** Kaplan-Meier curves showing survival probability over time for 10-day old larvae exposed to two temperatures (27.5 and 35.5°C). Solid lines show survival of larvae exposed to acute heat stress at 35.5°C over a period of 144 hours, whereas dotted lines display survival of larvae exposed to AMBIENT water temperature (27.5 °C). Line colours represent the three rearing conditions being AMBIENT (blue), MID (black) and HIGH (red) temperature x pCO₂ scenarios..... 71
- Figure 3. 3** Settlement success of coral recruits from the three treatments shown as number of recruits per tank. Black circles show the fitted model and the error bars show standard errors. The grey boxplots show the distribution of the raw data. 72
- Figure 3. 4** Survival probabilities of recruits in the three treatments at 8, 16, 18 and 23 weeks post settlement and representing each of the treatment histories along the experimental stages. Error bars show 95% confidence intervals. The size of the black top circles represents the proportion of live recruits at a particular time point based on the number of raw observations..... 73
- Figure 3. 5** Panel a: Predicted proportional growth between 0 and 8 weeks by the best-fit model depending on treatment at t = 8 weeks. Number of observations: total=360. Panel b: Predicted proportional growth between 8 and 16 weeks by the best-fit model depending on the different treatments at t = 16 weeks. Symbols represent origin treatment whereas x-axis distribution represent destination treatments. Panel c: Predicted proportional growth between origin treatment at t = 8 in relation to linear extension at destination treatment at t=16 weeks. Grey lines represent variation for individual recruits within each group. Red lines used to observe potential negative growth, whereas asterisks represent significant differences on mean estimates..... 74
- Figure 3. 6** Differences in the posterior distributions of models predicting growth and Fv/Fm relative to experimental time points and treatment histories. Panel a: Difference between growth measured at t = 16 weeks and growth measured at t=8 weeks. Panel b: Difference between Fv/Fm at t=16 weeks and Fv/Fm at t=8 weeks. Panel c: Difference in growth at t=23 weeks between Ambient and heat stress treatment. Panel d: Difference in Fv/Fm at t=23 weeks between Ambient and heat stress treatment. 76
- Figure 3. 7** Predicted proportional growth between 18 and 23 weeks for heat stress and ambient treatment at t=23 weeks, considering each treatment history that followed transplantation. Box plots show the distribution of the raw data, grey crosses show the raw data and black points with error bars show the fitted model predictions with the associated standard errors. 77

Figure 3. 8 Panel a: Predicted Fv/Fm at t=8 weeks by the best-fit model depending on treatment at t=8 weeks. Number of observations: total=288. Panel b: Predicted Fv/Fm by the best-fit model at t=16 weeks for the different treatments. Symbols represent origin treatment whereas x-axis distribution represent destination treatments. Panel c: Predicted Fv/Fm between origin treatment at t = 8 in relation to Fv/Fm at destination treatment at t = 16 weeks. Grey lines represent variation for individual recruits within each group, whereas asterisks represent significant differences on mean estimates. 79

Figure 3. 9 Mean Fv/Fm at t=23 weeks for ambient and heat stress treatment, considering each treatment history that followed transplantation. Box plots show the distribution of the raw data, grey crosses show the raw data and black points with error bars show the fitted model predictions with the associated standard errors. 81

Figure 3. 10 Correlation between estimates from the best-fit models estimating yield and growth at t = 16 and t = 23 weeks. Panel a: Estimates of growth relative to Fv/Fm at t = 16 weeks. Panel b: Estimates of growth relative to Fv/Fm at t = 23 weeks. 82

Figure 4. 1 Experimental design used to assess the potential for beneficial acclimation via phenotypic plasticity in adult coral fragments and the possible enhanced thermal tolerance (hardening) in relation to treatment history. Incubation stages ('t') and sampling points (triangles) are also included within each experimental stage. 95

Figure 4. 2 Panel a: Proportional growth from t=0 to t=4 weeks by the best-fit model depending on treatment at t=4. Number of observations: total=378, number of genotypes=21. Panel b: Proportional growth by the best-fit model at t=8 weeks for the different treatments over 4 to 8 weeks. Symbols represent origin treatment whereas x-axis distribution represents the destination treatments. Number of observations: total=378, number of genotypes=21. Panel c: Proportional growth between origin treatment at t=4 weeks in relation to growth at the destination treatment at t=8. The solid black lines represent the fitted model and its predictions, whereas the dotted line is representative of no proportional change between time points. Grey lines represent variation for individual genotypes within each group. Red lines used to observe potential negative growth. Asterisk indicate significant differences in growth rate between timepoints. 101

Figure 4. 3 Proportional growth from t=10 to t=14 weeks for heat stress and ambient treatment, considering each treatment history over weeks 0 to 8. Box plots show the distribution of the raw data, grey crosses show the raw data and black points with error bars show the fitted model predictions with the associated standard errors. The asterisk indicates a statistically significant difference. 104

- Figure 4. 4** *Panel a*: Predicted Fv/Fm at t=4 weeks by the best-fit model depending on treatment at t=4. Number of observations: total=378, number of genotypes=21. *Panel b*: Predicted mean Fv/Fm by the best-fit model at t=8 weeks for the different treatments. Symbols represent origin treatment whereas x-axis distribution represent destination treatments. *Panel c*: Predicted mean Fv/Fm between origin treatment at t=4 weeks in relation to linear extension at destination treatment at t=8 weeks. Grey lines represent variation for individual genotypes within each group. 106
- Figure 4. 5** Predicted Fv/Fm at t=14 weeks for heat stress and ambient treatments, considering each treatment history over the period 1-8 weeks. Box plots show the distribution of the raw data, grey crosses show the raw data and black points with error bars show the fitted model predictions with the associated standard errors. 108
- Figure 4. 6** Correlation between the random effects estimates of genotype from the best-fit models estimating yield and growth at t=4 weeks and t=8 weeks. Panel a: Estimates showing growth at t=8 weeks relative to growth at t=8 weeks. Tendency line represents a positive correlation. Panel b: Estimates showing Fv/Fm at t=4 weeks relative to Fv/Fm at t=8 weeks. Panel c: Estimates showing growth at t=4 weeks relative to Fv/Fm at t=4 weeks. Panel d: Estimates showing growth at t=8 weeks relative to Fv/Fm at t=8 weeks. Correlation values based on the Spearman Rank correlation coefficient analysis. Significant correlations among pairs are shown inside the matrix. 109
- Figure 4. 7** Relative abundance of Symbiodiniaceae type profiles. Each block corresponds to fragments of the same genotype, belonging to different treatment histories. Each bar corresponds to a different fragment, each one labelled by two letters and a number: the first letter corresponds to treatment at t=4 weeks (A for 'AMBIENT', M for 'MID', and H for 'HIGH'), the second letter to treatment at t=8 weeks, and the number is the genotype. Different colours show different Symbiodiniaceae type profiles. 110
- Figure 4. 8** Relative abundance of the top 10 bacterial families (y-axis) among individual genotypes of coral fragments (x-axis) at t=8 weeks, across each of the nine treatment histories (n= 117 total families). 113
- Figure 4. 9** Correlation in relative abundance among Symbiodiniaceae types and bacterial families for adult coral fragments 4 weeks after transplantation (t=8 weeks). Correlation values based on the Spearman Rank correlation coefficient analysis. Significant correlations among pairs are shown inside the matrix. 114

Figure A.S 1 Settlement success of corals from the three treatments per plate. Black circles show the fitted model and the error bars show the 95% confidence intervals. The grey boxplots show the distribution of the raw data.	147
Figure A.S 2 Composition of Symbiodiniaceae communities in the 6-week old recruit <i>A. loripes</i> at the individual level in each of three treatments. Colours represent specific type profiles, where other background symbionts represent <10% relative abundance. Number of replicates: 18 recruits individually sampled per treatment (6 individuals per each of three tanks, with a total of 54 recruits across treatments).....	157
Figure A.S 3 Rarefaction curve corresponding to the relation of observed ASVs relative to sequencing depth (number of reads per sample).	158
Figure A.S 4 Venn diagram corresponding to number of ASVs on 6-week old recruit corals among treatments. Overlapping shades represent shared number of ASVs between treatments. Total number of ASVs: 10986.	158
Figure A.S 5 Alpha diversity of microbial communities in 6-week old recruit corals among treatments. Plots represent species richness (ASV counts=left) and species diversity index (Shannon=middle and Chao1=right).....	160
Figure A.S 6 Relative abundances of the top 15 bacterial families (y-axis) among 6-week old coral recruits across each of three treatments (ambient, mid, high) and the corresponding mesocosm system (x-axis).	168
Figure A.S 7 Relative abundances of the top 10 bacterial genera (y-axis) among 6-week old coral recruits across each of three treatments (ambient, mid, high) (x-axis).....	169
Figure A.S 8 DESeq2 estimates of differentially abundant bacterial families in 6-week old coral recruits, comparing mid:ambient (panel a), high:ambient (panel b) and mid:high (panel c). For each panel, values and magnitude of log ₂ FoldChange favour abundance of a family in the first treatment (negative) or in the second treatment (positive); separated by dotted blue line. Colours represent genus from each particular family.	173
Figure B.S 1 Mean basal growth for the history combinations of treatments at t=3 (18 weeks) after all fragments were moved to ambient conditions for a two-week period. Symbols represent origin treatment (at t=8 weeks) whereas x-axis distribution represent destination treatments (at t=16 weeks). Number of observations: total=358, tank=24, tray=62.	200
Figure B.S 2 Fv/Fm for the history combinations of treatments at t=3 (18 weeks) after all fragments were moved to ambient conditions for a two-week period. Symbols represent origin	

treatment (at t=8 weeks) whereas x-axis distribution represent destination treatments (at t=16 weeks). Number of observations: total=288, tank=24, tray=62. 215

Figure C.S 1 Residuals of the random intercept of the best-fit model predicting growth after transplantation. Grey line represents what is the expected change on linear extension in relation to the model, with values below this considered worse than the expected and with values above the line considered better than the expected. 226

Figure C.S 2 Mean linear growth for the history combinations of treatments at t=10 weeks after all fragments were moved to ambient conditions. Symbols represent origin treatment whereas x-axis distribution represent destination treatments. Number of observations: total=378, number of genotypes=21. 231

Figure C.S 3 Residuals of the random intercept of the best-fit model predicting linear growth during heat stress exposure. Grey line represents what is the expected change on linear extension in relation to the model, with values below this considered worse than the expected and with values above the line considered better than the expected. 234

Figure C.S 4 Residuals of the random intercept of the best-fit model predicting maximum quantum yield (Fv/Fm) after transplantation. Grey line represents what is the expected change on maximum quantum yield (Fv/Fm) in relation to the model, with values below this considered worse than the expected and with values above the line considered better than the expected. 239

Figure C.S 5 Mean Fv/Fm for the history combinations of treatments at t=3 after all fragments were moved to ambient conditions. Symbols represent origin treatment whereas x-axis distribution represent destination treatments. Number of observations: total=378, number of genotypes=21. 245

Figure C.S 6 Residuals of the random intercept of the best-fit model predicting maximum quantum yield [Fv/Fm] during the thermal stress exposure at t=14 weeks. Grey line represents what is the expected change on Fv/Fm in relation to the model, with values below this considered worse than the expected and with values above the line considered better than the expected. 248

Figure C.S 7 Overall relative abundance of each group of Symbiodiniaceae type profiles and associated species in all adult fragments 4 weeks after transplantation (i.e., all treatment histories combined). 249

Figure C.S 8 Rarefaction curves. 16S data analysis for bacterial communities. 250

Figure C.S 9 Alpha diversity of microbial communities in adult coral fragments four weeks after transplantation (t=8 weeks), considering origin (t=4 weeks) and destination treatment (t=8

weeks). Panel a: species richness (Observed ASV) Panel b: species diversity index (Chao 1) and panel c: Shannon index..... 256

Figure C.S 10 Venn diagram corresponding to number of ASVs in all adult fragments 4 weeks after transplantation (t=8 weeks). Overlapping shades represent shared number of ASVs between treatment histories. Total number of ASVs at the destination treatment was 456 (AMBIENT), 453 (MID), and 465 (HIGH). 256

Figure C.S 11 NMDS of bacterial communities in adult coral fragments four weeks after transplantation, considering origin (t=4 weeks) and destination treatment (t=8 weeks). Values in axis represent Bray-Curtis distances between samples. 258

Figure C.S 12 Relative abundance of the top 10 bacterial genera (y-axis) among individual genotypes of coral fragments (x-axis) at t=8 weeks, across each of the nine treatment histories (n= 1601 total genera). 266

Figure C.S 13 Estimates of differentially abundant bacteria (non-rarefied dataset) between origin and destination treatments. Only significantly different taxa displayed. Log₂FoldChange (x) values compare abundances found in particular treatment combinations, where a positive value favours treatment history 1 and a negative value means significantly higher abundance in treatment history 2. Its value represents magnitude of difference (2^x)..... 284

Chapter 1: General Introduction

Rapid warming of Earth's climate system is occurring, with many of the changes observed since 1950 considered unprecedented even over millennial time scales (IPCC, 2018). Accumulation of atmospheric greenhouse gases has caused an increase of $\sim 0.92^{\circ}\text{C}$ in the global mean surface temperature (GMST) between the average observed for the 1850 - 1900 period and the 2003 - 2017 period (IPCC, 2018); the sea surface temperature (SST) has increased 0.65°C over the same time (IPCC, 2019). Projections for the future suggest that ocean basins will continue to warm under both moderate (RCP4.5) to high (RCP8.5) emission trajectories. By the end of the century, SSTs are predicted to be approximately $1 - 2^{\circ}\text{C}$ higher under RCP4.5 and $2 - 4^{\circ}\text{C}$ higher under RCP8.5 (IPCC, 2019, Collins, 2013). Additional effects include a sharp increase in the frequency and intensity of extreme events (e.g., marine heat waves and cyclones) with the potential addition of 0.5°C of warming, on top of the 0.5°C to 1.0°C increase in GMST experienced between 1980 and 2018 (Hoegh-Guldberg et al., 2019, IPCC, 2019, Robinson and Shine, 2018, Thomson et al., 2011). This rapid warming is already impacting many marine ecosystems, pushing their thermal limits at different latitudes, and undermining their resilience (Tewksbury et al., 2008, Eakin et al. 2010, Hoegh-Guldberg et al., 2019).

Atmospheric greenhouse gases not only contribute to ocean warming, they also alter the chemical stability of the oceans. Uptake of carbon dioxide by the ocean has caused the pH of the ocean surface water to decrease by 0.1 since the industrial revolution. Ocean pH is projected to decline by approximately 0.14 to 0.15 (38 to 41%) for RCP4.5 and 0.30 to 0.32 (100 to 109%) for RCP8.5 over the same timeframe (IPCC, 2019). This is predicted to reduce the concentration of carbonate ions ($[\text{CO}_3^{2-}]$) in the seawater by $\sim 100 \mu\text{mol/kg}$ by 2100 (Doney et al., 2009, Hoegh-Guldberg et al., 2007, Meissner et al., 2012). As a consequence, it is forecast that the precipitation rate of aragonite would decrease by $\sim 48\%$ (Burton and Walter, 1987). Such projections raise concerns that calcifying organisms, like corals, could shift from a state of net carbonate accretion to net dissolution (i.e., lower extension and densification of skeletal growth) (Dove et al. 2013, Hoegh-Guldberg et al., 2007, Kleypas et al., 1999). Hence, understanding the response of organisms like corals to climate change conditions, requires the assessment of the response to simultaneous increases in temperature and $p\text{CO}_2$.

Coral reefs provide enormous benefits to the environment and economies of many tropical countries (Barlow et al., 2018, De Valck and Rolfe, 2019). These benefits are threatened by human-

induced rapid climate warming that is damaging coral reefs around the world (Hughes et al., 2017a). Since the 1970's, there has been an approximately 80 % decrease in coral cover in the Caribbean (Perry et al., 2013, Alvarez-Filip et al., 2009, Gardner et al., 2003) and an estimated 50% decline on Western Pacific reefs. The causes of decline in coral cover vary among geographic locations and include both local and global stressors. Coral cover has decreased drastically even in well-managed marine parks like the Great Barrier Reef (GBR) (Ortiz et al., 2018, Hughes et al., 2017a). Historically, the main drivers of coral mortality included cyclone and storm damage, diseases outbreaks and Crown-of-Thorns Starfish (CoTS) predation (Osborne et al., 2011, De'ath et al., 2012). More recently, the detrimental effects of ocean warming and acidification are threatening the persistence of coral reefs at a global scale (Hughes et al., 2018b). In the past five years, the GBR has experienced three major bleaching events, including two back-to-back mass bleaching (2016-2017) and a wide spread less intense bleaching event (2020), which have reduced GBR coral cover by 50% (Hughes et al., 2017a). Coral bleaching occurs when ocean heating above long-term averages accumulates over time, often expressed by the metric - degree heating weeks (DHW) (Heron et al., 2016, Donner et al., 2017). Most coral species will bleach with 2 - 6 DHW (van Hooidonk et al., 2014, McGowan and Theobald, 2017), although substantial variation can be observed across species (Hoogenboom et al., 2017, Hughes et al., 2018a). As coral bleaching events may be the norm in the coming few decades (Van Hooidonk et al., 2013, van Hooidonk et al., 2016) and ocean acidification may act synergistically with rising ocean temperature (Anthony et al., 2008, van Hooidonk et al., 2014), urgent research is needed to understand the capacity, limitations, and methods for enhancement of thermal tolerance in corals.

The environmental sensitivity of many coral species has raised concern about their capacity to persist under future environmental conditions (Chan and Conolly, 2013). Arguments for why corals might have low adaptability are commonly related to their long-generation times (Hoegh-Guldberg, 2012). While these generalisations may hold true for a subset of species, they do not apply to numerous others where high levels of genetic diversity, ecology and different life histories might facilitate a range of adaptive options (Maynard et al., 2008, Fuller et al., 2020, Matz et al., 2018). However, it is unknown if they can respond adaptively to the current rate of environmental change and frequency of bleaching events. Thus, it is essential to investigate coral physiological responses to chronic and acute environmental stress to better predict and protect the future of coral reefs.

Understanding coral resilience to current and projected rates of environmental change involves analysing the different pathways and intrinsic mechanisms of adaptation and acclimatisation

(Gates and Edmunds, 1999, Baker et al. 2004, Torda et al., 2017). Adaptation refers to changes in the distribution of phenotypes from one generation to the next within populations following natural selection. Adaptation is based on the existence of genetic polymorphism (i.e., allelic variation) and phenotypic changes are therefore evident as shifts in allele frequencies over time (Waddington, 2014). Acclimatisation via phenotypic plasticity (or acclimation if under controlled conditions) is a change in the phenotype that does not involve a genetic change (Bowler, 2005, Pigliucci et al., 2006). Acclimation can occur within the life span of an organism and is considered beneficial if the overall fitness is either sustained or enhanced when environmental conditions change (Via and Lande, 1985). Therefore, beneficial acclimation through phenotypic plasticity may provide an alternative coping mechanism for corals under current and predicted ocean warming and acidification. To gain insight into the potential of beneficial acclimation, comprehensive experimental work is needed to test for mechanisms of acclimation across different coral life stages.

Generally, three types of acclimation can be distinguished: developmental, reversible and transgenerational. Developmental acclimation occurs when organisms respond to particular environmental conditions (e.g., temperature) during one stage of the life cycle to enhance performance during a subsequent life-stage and these changes are usually irreversible (Scott and Johnston, 2012). Such developmental experiences can have lifelong and even transgenerational effects (Gibson and Wagner, 2000, Clarke and McKenzie, 1987, Parkash et al., 2014). In contrast, reversible plasticity refers to the capacity of an organism to reversibly change physiological processes to compensate for environmental variability (e.g., diurnal or seasonal changes) to maintain homeostasis despite fluctuations in environmental conditions (Bowler, 2005, Piersma and Drent, 2003, Wilson and Franklin, 2002, Little et al., 2013). Transgenerational acclimation occurs when parents respond to particular environmental conditions during their life, which enhances the performance of subsequent offspring in the same environment through nutritional, somatic, cytoplasmic, or epigenetic transfer between generations (Bonduriansky et al., 2012, Donelson and Munday, 2015). Overall, acclimation responses share some common properties: the detection of environmental signals, the transduction of this signal into a cellular response, and the activation of a molecular response through the activity of genes that cause a change in the phenotype (Wilson and Franklin, 2002). Hence, it is important to understand acclimation processes that occur in response to acute and chronic exposure to elevated temperature and CO₂, by applying long-term experimental designs encompassing reciprocal transplantation.

Hardening is a type of acclimation where the performance of an organism is enhanced following transient non-lethal environmental stress exposure (Packard et al., 2001). For example, brief exposure to extreme heat often increases short-term tolerance to thermal extremes in plants and animals (Hoffmann et al., 2003, Sinclair and Roberts, 2005). In corals, prior exposure to elevated temperature can increase the thermal tolerance under both field and laboratory conditions. For example, repeated bleaching events (i.e., similar temperature and solar radiation levels) revealed how some corals were capable of enhancing their temperature tolerance and reduced their bleaching susceptibility (Brown and Dunne, 2008, Castillo and Helmuth, 2005, Dove et al., 2006, Middlebrook et al., 2008). Coral mortality was lower in later events and the reduced bleaching susceptibility was attributed to acclimation or adaptation; although bleaching susceptibility varies across species in the field and laboratory conditions (Pratchett et al., 2020, Matsuda et al., 2020, McClanahan et al., 2007). Furthermore, corals exposed to high diel temperature variability often have higher heat tolerance and greater resistance to bleaching than nearby conspecifics in more stable regimes (Putnam and Edmunds, 2011, Schoepf et al., 2019, Schoepf et al., 2015a, Barshis et al., 2018). Therefore, the environmental history of individuals and populations plays a significant role in determining how they will respond to stress (Hughes et al., 2018c), and is likely driven by a combination of both acclimation via plasticity and adaptation (Bay and Palumbi, 2015, Kenkel and Matz, 2016, Palumbi et al., 2014, Matz et al., 2018). As heat stress events are likely to increase due to climate warming, studies that disentangle the role of prior exposure in the hardening response of corals will greatly advance our general understanding of thermal tolerance.

The coral animal lives in close association with a range of microbes that can have both positive and negative impacts on their health and fitness (Vanwonderghem and Webster, 2020, Bourne et al., 2016). Healthy corals have mutualistic associations with a wide diversity of microorganisms including dinoflagellate photosymbionts in the family Symbiodiniaceae (formerly genus *Symbiodinium*), prokaryotes, fungi and viruses (Blackall et al., 2015). These associations are referred to as the coral holobiont (Thompson et al., 2014, Rohwer et al., 2002). Symbiodiniaceae form an obligate symbiosis with the coral host and can provide up to 95% of its nutritional requirements (Pearse and Muscatine, 1971, Muscatine, 1990). Prokaryotes (bacteria and archaea) can play roles in nitrogen fixation, sulphur cycling, vitamin provisioning and immunity (Kimes et al., 2010, Raina et al., 2009, Ritchie, 2006, Rohwer and Kelley, 2004, Robbins et al., 2019) and thus provide corals with essential compounds and metabolic pathways for health and fitness. However, dysbiosis in the coral microbiome can occur during environmental stress, which could have important implications for the overall fitness of the coral. In particular, novel microorganisms including opportunistic pathogens can proliferate when corals are

under stress and the natural beneficial symbiont population can become destabilised (Bourne et al., 2008, Bourne et al., 2009, Rosenberg et al., 2007).

Changes in microbial communities could provide a rapid mechanism for acclimation and the potential rapid evolution of corals under climate change (Peixoto et al., 2017, Webster and Reusch, 2017, Vanwonderghem and Webster, 2020, Rosado et al., 2019, Quigley et al., 2018). For instance, variations in Symbiodiniaceae abundance and diversity are known to play an important role in the tolerance of corals to stress from light, temperature and other perturbations (Berkelmans and van Oppen, 2006, Robison and Warner, 2006, Rouze et al., 2019, Lawson et al., 2019). Acclimation of the coral holobiont based on Symbiodiniaceae associations can occur through different mechanisms. First, changes in coral phenotypes may occur as a result of changes in physiological and biochemical traits of Symbiodiniaceae (Brown et al., 2002a, Brown et al., 2002b, Brown and Dunne, 2008, Brown et al., 2000b, Salih et al., 2000). Second, phenotypic changes may occur due to the replacement of susceptible Symbiodiniaceae by tolerant and genetically distinct Symbiodiniaceae through a process called switching (i.e., changes in genetically distinct symbiont) (Baker et al., 2004, Rowan, 2004, Boulotte et al., 2016, Pettay et al., 2015). Third, phenotypic changes resulting from shifts in the relative abundance of members of Symbiodiniaceae populations in corals through a process called shuffling (Berkelmans and van Oppen, 2006, Jones et al., 2008, Baker, 2003). Despite the current progress on how Symbiodiniaceae may respond to environmental fluctuations, it is still unclear how fast these mechanisms of switching, shuffling or even intrinsic acclimatory responses (e.g., physiological adjustment of the Photosystem II) can occur, nor how variable these responses would be across different life stages of coral.

While coral-associated prokaryote communities can also change under stress to affect holobiont function and fitness, they are much less understood compared to Symbiodiniaceae, (Webster and Reusch, 2017). Like Symbiodiniaceae, bacterial communities can undertake processes of switching and shuffling in response to environmental change (Sweet et al., 2017). For example, transplantation experiments have demonstrated that bacterial communities shift when corals are introduced to new and non-native habitats, suggesting microbiome alteration as an acclimatization strategy to improve holobiont physiology in response to changing environmental conditions such as salinity, nutrients, and water temperature (Ziegler et al., 2017, Ziegler et al., 2019, Röthig et al., 2016). Moreover, prokaryotic communities have been found to differ in corals located at carbon dioxide seep sites (i.e., higher concentrations of pCO₂) (Morrow et al., 2015), suggesting a potential role for

prokaryotes in the acclimation of corals to ocean acidification (Webster et al., 2013, Torda et al., 2017). However, the response of the coral-associated microbial community to environmental perturbation can also involve growth of pathogens or opportunistic microorganisms, with cascading adverse effects on holobiont function (Thompson et al., 2014). The coral microbiome can vary not only with environmental conditions, but also amongst different life stages due to the processes of recognition, winnowing and retention of symbionts during development (Williams et al., 2015, Bernasconi et al., 2019). Indeed, early life stages tend to harbour a higher diversity of bacterial taxa relative to their adult counterparts, suggesting that the environment is a reservoir of bacterial symbionts during development (Lema et al., 2014, Littman et al., 2009a, Littman et al., 2009b, Sharp et al., 2012). Although the main uptake source for microbial symbionts is thought to be the water column, there is also evidence that sediment can act as an important seedstock of coral microbes (Apprill et al., 2009, Apprill et al., 2012, Carlos et al., 2013, Schöttner et al., 2013). While our understanding of the variability in coral microbiomes has increased dramatically over the past decade (van Oppen and Blackall, 2019), it is still unknown how the community of microbes changes through life history stages of corals exposed to ocean warming and acidification.

The overarching goal of this thesis was to quantify the extent to which phenotypic plasticity could support beneficial acclimation in a common species of coral from the GBR when exposed to predicted climate change conditions. In addition, I assessed if stress-hardening could enhance thermal tolerance via exposure of corals to two levels of combined warming and acidification conditions with both acute and longer-term heat stress exposure experiments. I measured four phenotypic traits to assess the response of the coral host (larval settlement, growth and survival) and the Symbiodiniaceae (photochemical efficiency). I also compared the Symbiodiniaceae and bacterial community structure among treatments to determine if symbiont switching or shuffling had occurred. Three major objectives were addressed in individual data chapters and the thesis includes a final chapter that synthesises the major findings and discusses the implications of these results.

Specifically, in Chapter 2 I measured:

The response of coral early life stages to two different levels of elevated temperature and $p\text{CO}_2$ for a period of 10 weeks following fertilization, relative to their performance under ambient conditions

In this chapter I quantified the response of the coral host including settlement success, growth and survival under elevated temperature and $p\text{CO}_2$. A thermal shock experiment tested for potential

thermal hardening of larvae. Comparisons of Symbiodiniaceae and bacterial communities across treatment conditions was carried out to assess how simulated ocean warming and acidification affected the diversity and relative abundance of symbionts in coral early life stages.

In Chapter 3, I extended the research to:

Evaluate if exposure of coral larvae to simulated climate change conditions can have lasting effects on growth, survival and stress tolerance across development.

In this chapter I tested the potential for beneficial acclimation and stress-hardening in early life stages of coral. This included a reciprocal transplantation experimental design across three levels of combined temperature and $p\text{CO}_2$. I compared host and symbiont traits (e.g., growth rate and photochemical efficiency) before/after transplantation. I tested for hardening with an acute heat stress assay on larvae and a chronic ramp-and-hold bleaching experiment for the juvenile stage.

In the final data Chapter 4 I:

Quantified the patterns of acclimation in adult coral fragments to predicted future temperature and ocean acidification conditions.

In this chapter I again followed a reciprocal transplantation experimental approach to test for beneficial acclimation and stress-hardening in the adult life stage of coral using clonal fragments. In addition to the assessment of phenotypic traits from the coral host, this chapter also included evaluation of the Symbiodiniaceae and bacterial communities, to determine if any observed acclimation was associated with a shift in the symbiont communities.

The general discussion in Chapter 5:

Provides a summary of findings and implications from my research. In this chapter, I focus on the additional questions that my study generated. For example, I explore the potential mechanisms explaining the observed beneficial acclimation and thermal hardening (e.g., gene expression, epigenetic markers). Furthermore, I consider the role of preconditioning timeframes on shaping or triggering the phenotypic responses. Finally, I highlight the relevance of my findings in the context of coral restoration approaches.

My thesis concludes that hardening and beneficial acclimation can be induced in corals and thus could be considered in coral breeding and aquaculture programs. My analyses provide new insights into the variation in coral holobiont partners under climate change conditions and highlights the importance of exploring the response of the coral holobiont (i.e. host and symbionts) across multiple life stages. Furthermore, it highlights the importance of studies into phenotypic plasticity, by showing that acclimation of corals to dynamic environments may be beneficial for inducing more temperature resilient phenotypes, and is thus of relevance to proposed reef restoration and adaptation approaches.

Chapter 2: Thermal preconditioning of coral larvae increases their tolerance to heat waves and affects phenotypic traits of the recruit

2.1 Abstract

Rapid climate change poses a serious threat to coral reefs worldwide. Coral responses to environmental change can be driven by the coral host and its associated photosynthetic algal and/or bacterial communities. To test how the thermal tolerance and development of coral early life stages are affected by predicted future ocean conditions, I fertilised *Acropora loripes* gametes, reared larvae for 10 days and the subsequent recruits for 10 weeks at: 1) current-day ambient conditions (AMBIENT: 27.5°C, 410 $\mu\text{atm pCO}_2$) and two different treatments consistent with projected future temperature and acidification conditions under MID (AMBIENT +1.0°C, 670 $\mu\text{atm pCO}_2$) and HIGH (AMBIENT +2.0°C, 900 $\mu\text{atm pCO}_2$) CO₂ emissions trajectories. I assessed how these different treatment conditions affected larval tolerance to acute heat stress (35.5 °C, 144 hours), as well as settlement, survival and growth rate, and the associated symbionts of *A. loripes* recruits. Larval survival under acute heat stress differed among rearing conditions, with larvae from the HIGH treatment surviving longer than those reared under MID and AMBIENT conditions. Settlement rates were similar among rearing treatments, but recruit survivorship was greater in the HIGH treatment. Treatment was found to have a significant effect on growth rate after six and ten weeks of treatment, but the effect size was small (< 11 % difference in growth rate for MID and HIGH relative to AMBIENT) and post-hoc testing could not detect a significant difference between pairs of treatments. Symbiodiniaceae and bacterial communities in 6-week old coral recruits significantly differed among treatments, with treatment explaining 25 and 6% of the variation, respectively. My results suggest that preconditioning of aposymbiotic larvae to future ocean conditions can increase their tolerance to extreme thermal events, without reducing short-term survival or growth of recruits post settlement. Larval preconditioning may thus be an option to increase fitness of coral recruits and the success of coral restoration in a rapidly warming and acidifying ocean. These findings provide valuable insights into the effects of future climate scenarios on the performance of coral early life history stages, and their ability to withstand acute thermal stress, to better inform predictions of future reef states.

Keywords: Acute stress, chronic stress, larval preconditioning, Symbiodiniaceae, bacteria, growth, survival, climate change.

2.2 Introduction

The sensitivity of most coral species to summer heat waves, and the increased frequency at which such events are now occurring, have raised concerns about whether corals possess mechanisms (genetic and non-genetic) that could help them cope with ocean conditions predicted under rapid climate change. Corals generally bleach when experiencing >4-degree heating weeks (Baird et al., 2009, Jones, 2008), with changes to the symbiont cell morphology and cell division rates recorded from as little as two DHW (Gierz et al., 2020). Coral populations may become more tolerant to higher temperature over time as natural selection increases the frequency of individuals with thermally tolerant gene variants (i.e., alleles) (Waddington, 2014, Kenkel and Matz, 2016), or of thermally tolerant microbial partners (Howells et al., 2012, Silverstein et al., 2015, Webster and Reusch, 2017, Ziegler et al., 2017). Alternatively, phenotypic plasticity could maintain the performance of the organism without involving a genetic change (Pigliucci et al., 2006, Via and Lande, 1985, Torda et al., 2017).

Acclimation can occur at different life stages in response to exposure to different types, durations and intensities of environmental stress (Angilletta, 2009, Fox et al., 2019). Transient non-lethal stress exposure may lead to acclimation responses that enhance performance (Packard et al., 2001). For example, brief exposure to mild heat often increases short-term tolerance to thermal extremes in plants and animals (Hoffmann et al., 2003, Sinclair and Roberts, 2005), a process known as hardening (Bowler, 2005). Further, prolonged exposure to moderate temperatures can trigger lasting changes in thermoregulation and thermosensitivity (Angilletta, 2009). Generally, organismal responses to both short-term and prolonged exposure to temperature can be reversible, although some remain fixed (Johnston and Wilson, 2006). In corals, prior exposure to elevated temperature has been shown to increase the thermal bleaching tolerance in both the field and the laboratory (Brown and Dunne, 2008, Castillo and Helmuth, 2005, Dove et al., 2006, Middlebrook et al., 2008). The mechanisms underpinning such increases in temperature tolerance likely include coral host epigenetics and microbial interactions (Torda et al., 2017), but the way they operate, and at which lifestages, are currently not known.

The health and fitness of reef-building scleractinian corals depends on stable associations between the cnidarian host and its microbial community or 'microbiome', particularly photosynthetic

endosymbionts (family Symbiodiniaceae, formerly genus *Symbiodinium*; (LaJeunesse et al., 2018)). Environmental stressors, however, can compromise the benefits of symbiosis, with potential adverse impacts on the coral holobiont. For example, high temperature disrupts the functioning of algal photosystem II, which results in oxidative stress that breaks down the Symbiodiniaceae-coral symbiotic association. Additional stressors including exposure to light or unbalanced nutrient availability may act synergically with heat (Warner et al., 1999, Brown et al., 2000b). It has been suggested that, prior to complete dysbiosis, corals may attempt to restructure their symbiont community to maintain their health and fitness, since eukaryotic and prokaryotic symbionts of corals can vary in their tolerance to environmental stress (Webster and Reusch, 2017, Blackall et al., 2015).

Thermo-tolerant Symbiodiniaceae taxa have been linked to better coral performance and recovery under elevated temperatures (Bay et al., 2016, Oliver and Palumbi, 2009, Smith et al., 2017). Further, changes in the community composition of Symbiodiniaceae can play an important role in the tolerance of corals to stress from light, temperature and other perturbations, thus contributing to broad disparities in thermal tolerance among individual host colonies, life stages and species (Berkelmans and van Oppen, 2006, Robison and Warner, 2006, Baker, 2001). The diversity and dynamics of Symbiodiniaceae communities in response to environmental change is well described in adult corals, but little is known about these dynamics in coral recruits. This is likely due to the higher diversity of Symbiodiniaceae within young corals and the dynamic sorting processes that occur during early development (Abrego et al., 2008, Quigley et al., 2016, Chan et al., 2019). Evaluating the community composition of Symbiodiniaceae in early life stages of coral, and how this correlates with the coral response to rapid environmental change, is important for assessing their potential role in thermal plasticity of the coral holobiont.

Compared to Symbiodiniaceae associations, much less is known about how coral-associated prokaryote communities (bacteria and archaea) affect coral holobiont function and fitness (Webster and Reusch, 2017, van Oppen and Blackall, 2019), as most evidence is based on correlations between community composition and holobiont phenotypes. However, it is clear that coral bacterial associations contribute to various aspects of coral fitness, including nutrition, defence, growth, and survival (Bourne et al., 2016, Rosenberg et al., 2007) with recent analysis showing that some coral-associated bacterial genomes encode motifs that have a crucial role in maintaining symbiosis as well as in supplying fixed carbon, B-vitamins and amino acids to their symbiotic partners (Robbins et al.,

2019). It has also been postulated that coral-associated bacteria facilitate acclimation and stress resistance through rapid community restructuring (Gardner et al., 2019, Thompson et al., 2014, Ziegler et al., 2017, Bourne et al., 2008). For example, prokaryotic communities have been found to differ in corals located at natural carbon dioxide seeps (Morrow et al., 2015), which suggests a potential role in the acclimation of corals to high CO₂ environments. Particular bacterial community profiles have also been linked to different bleaching susceptibility among corals, although functional roles of specific taxa remain largely unknown (Gardner et al., 2019, Ziegler et al., 2017). Nevertheless, environmental stress can lead to the growth of bacterial pathogens or other opportunistic microorganisms, with negative effects on holobiont health (Thompson et al., 2014). Understanding how bacterial communities vary in relation to environmental change is important when assessing their role in the performance and survival of corals, particularly in early life history stages when corals commonly display increased sensitivity to environmental stressors (Wilson and Harrison, 2005).

As ocean warming and acidification are predicted to worsen over coming decades, the ability of corals to survive and grow could reach its physiological limits. It is unclear if genetic adaptation can keep pace with the rapid speed at which the environment is changing (Lough et al., 2018). Thus, corals may need to rely on acclimatory responses from phenotypic plasticity to persist under rapid environmental change (Torda et al. 2017). Here, I experimentally investigated how coral early life stages responded to two different levels of elevated temperature and pCO₂ for a period of 10 weeks following fertilization, relative to their performance in simulated current-day reef conditions. The two treatments were consistent with climate change projects under a moderate (+1.0°C, 670 µatm pCO₂) and high (+2.0°C, 900 µatm pCO₂) CO₂ emissions trajectory (IPCC, 2019). Coral responses to these treatments included the assessment of settlement success, growth rate and survivorship. Moreover, because of the predicted role of coral symbionts in the coral holobiont response to climate change, I compared the diversity and composition of Symbiodiniaceae and bacterial communities after six weeks of exposure to each treatment. In addition, I used the principle of hardening to test if fertilisation of coral gametes and rearing of larvae under each treatment influenced the survivorship of larvae exposed to acute thermal stress. This approach allowed us to examine the potential for acclimatory response of early life stages to chronic and acute warming and acidification stress, including its influence on the community structure of symbionts. My findings, which show that larval preconditioning may be an option to increase fitness of coral recruits, provide new insights into the effects of future climate scenarios on the performance of coral early life history stages, and their ability

to withstand acute thermal stress. These results should improve predictions of future reef states and contribute to the success of coral restoration in a rapid warming and acidifying ocean.

2.3 Material and Methods

2.3.1 Study species collection

The coral species *Acropora loripes* was used in this study due to its common and widespread distribution, ease of identification and suitability for maintenance in aquaria. Twelve gravid colonies (<25 cm in diameter) were collected at about 6 m depth from Davies Reef in the Central Great Barrier Reef (18.83S; 147.63E) under GBRMPA permit G11/3471.1. Collection occurred from 11 - 14th November 2016, immediately prior to mass spawning at this reef. After collection, the coral colonies were transported to the National Sea Simulator (SeaSim) at the Australian Institute of Marine Science (AIMS) and housed in flow-through AMBIENT conditions (27.5 °C; 415 $\mu\text{atm } p\text{CO}_2$) which simulated the environmental conditions at Davies Reef.

2.3.2 Experimental parameters and coral spawning

To evaluate performance of coral larvae and recruits under simulated climate change scenarios, this study used three levels of combined temperature and $p\text{CO}_2$ under control conditions, described in upper case: 1) AMBIENT (27.5°C, 410 $\mu\text{atm } p\text{CO}_2$), 2) MID (AMBIENT +1.0°C, 670 $\mu\text{atm } p\text{CO}_2$) and 3) HIGH (AMBIENT +2.0°C, 900 $\mu\text{atm } p\text{CO}_2$) (Fig 2.1); 'ambient' in lower case is used in some instances to compare treatment with natural ambient conditions. The experimental systems were monitored in real time for temperature and $p\text{CO}_2$. All inputs were integrated by the Control System in the *Model Predictive Control* logic to manage experimental parameters. See (Uthicke et al., 2020) for further details on how temperature and $p\text{CO}_2$ are monitored and controlled at the SeaSim facility. Manipulations mirrored seasonal and daily variation in both temperature and $p\text{CO}_2$ based on reference field measurements from Davies reef with offsets being applied to simulate treatment conditions.

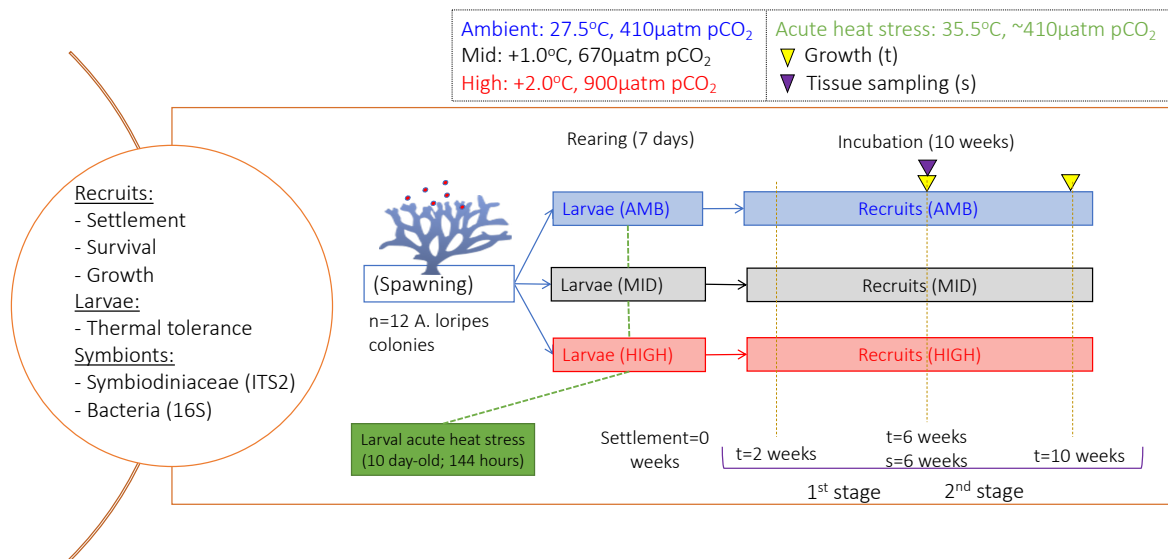


Figure 2. 1 Schematic representation of the experimental design. It includes two experiments: the primary experiment that aimed to evaluate recruit performance over time under three treatments, and a secondary experiment that aimed to evaluate response of larvae to heat stress.

On the night of spawning, colonies were isolated in individual tanks in the dark without water flow. After spawning, the positively buoyant gamete bundles were collected from the water surface and eggs and sperm from each colony were separated using filtration (120 µm mesh size) and gentle agitation. Equal proportions of eggs and sperm from all twelve spawning colonies were mixed to produce two individual batch cultures for each of the treatments (i.e. fertilised using water from the corresponding treatment). Each batch fertilisation contained approximately 75,000 eggs in 6.5 L volume and a sperm density of 10⁶ per ml (Willis et al., 1997). After one hour (just prior to or at the time of first cleavage) each batch fertilisation was thrice rinsed in treatment specific filtered sea water (FSW) then stocked at 1 larva/mL in two replicate 65 L rearing tanks in each of the three treatment conditions. Rearing tanks received water-flow of 2.5 L/min FSW, an outflow covered by a 60 µm filter and constant airflow, which was added after the first 24h. Importantly, it is possible that individual treatment conditions (temperature, pH) may have incur selection on the gamete pool considering the significant influence and synergy of multi stressors during early ontogenetic stages (from gametes to larvae) on different marine taxa (Przeslawski et al., 2015) despite the fact that each batch culture was treated similarly. Overall, densities of larvae in each batch culture remained similar, but concentrating

larvae to normalised levels prior to settlement was a step that was done. Larvae reared under each treatment were used for two separate experiments, as described below.

2.3.3 Larval acute heat stress experiment

After ten days of rearing, twenty haphazardly sampled swimming larvae from each treatment were placed in each of 24 replicate mesh-bottomed containers (net-wells) (i.e., 480 larvae per treatment x 3 treatments, n=72 net-wells total). Larvae were aposymbiotic. The wells were assigned to four 50 L tanks, each with three holding trays. Two wells from each treatment were floated in each holding-tray (i.e., n=6 wells in total for each holding tray in each tank). Tanks had a turnover flow of FSW of 0.8 L/min. All larvae were first acclimated to AMBIENT conditions (27.5 °C) for one hour in all tanks. The temperature was then increased in two tanks by 1°C per hour over eight hours until 35.5°C was reached. The AMBIENT temperature of 27.5 °C was maintained in the other two tanks. The $p\text{CO}_2$ level was maintained at ~450-500 $\mu\text{atm CO}_2$ in all four tanks. Survival was measured from repeated visual counts of remaining larvae every 12 hours for five days.

2.3.4 Recruit performance experiment

At seven days post fertilization approximately 1500 larvae per larval treatment (i.e., similar density generated from each batch culture per treatment) were settled onto acrylic plates (10 cm x 20 cm) in each of nine 50 L tanks (i.e., six plates per tank, three tanks per treatment) overnight under static conditions. Approximately 1 g of crushed crustose coralline algae (CCA) was sprinkled onto the settlement plates as a cue to induce larval settlement. After three days, the plates were moved to outdoor mesocosm systems maintained under the three experimental conditions (three mesocosms per treatment) where a total of 18 plates per treatment (six per mesocosm) were held for 10 weeks. Within the mesocosms, coral recruits were exposed to adult *A. loripes* colonies and other reef organisms and substrata (e.g., sponges, sea urchins, seagrass, sediment) that had been established within the systems under each of the treatment conditions for > 18 months, to allow for horizontal transmission of symbionts.

Settlement was estimated by counting the number of settled coral recruits on each plate after two weeks and settlement success was estimated as the number of recruits at two weeks compared with the 4500 larvae stocked in each treatment.

Measurements of the change in live tissue surface area (basal growth) of recruits were obtained from photographs taken two, six and ten weeks after settlement, using a frame mounted NIKON D810 camera. A total of 22 recruits per plate per treatment were haphazardly selected and labelled at the first time point (two weeks). Two four-week time intervals were used to assess growth rates. Each recruit was manually traced using the straight-freehand line tool on IMAGEJ (version: 1.50i) (Rasband, 2012). Three replicate measures of the diameter (d) were traced and their average used to predict changes in basal growth among treatments over time (Pratchett et al., 2015). A numeric scale was included in each photo to transform number of pixels to mm. The basal growth rate was quantified by calculating the proportional change in diameter of live recruits between timepoints ($\log_{10} \left(\frac{d_{t+1}}{d_t} \right)$). This resulted in two basal growth measurements: interval 1 was 2 – 6 weeks and interval 2 was 6 - 10 weeks. In addition, photographs were used to estimate survival rates of recruit corals over time for each treatment.

2.3.5 DNA extraction, Amplification and Sequencing Protocol

For the analysis of symbiotic communities, 18 recruits were sub-sampled from each treatment (six per tank, 54 total) at the 6-week sampling timepoint. Recruits were immediately placed in liquid nitrogen and stored at - 80°C. Total DNA was extracted from recruits using DNeasy® UltraClean® Microbial Kit (QIAGEN) following the Manufacturer's protocol with some modifications. Individually frozen whole recruits (~15 mg) were transferred to power bead tubes containing the lysis solution. Tubes were incubated at 65°C for 10 min and homogenised using the MP Biomedicals™ BeadBeater (FastPrep-24 5G) for 40 sec at 4m/s. Tubes were centrifuged (1000 g, 30 sec) and supernatant was transferred to IRS solution. After elution, total DNA (50µl volume) was quantified using Thermo Scientific NanoDrop™ NanoDrop 2000/2000c series Spectrophotometer and PicoGreen measurements following the manufacturer's protocol. A 0.8% agarose 5X TAE electrophoresis gel was run for a subset of samples (90 V, 45 min) against a 1 kb ladder to visually assess DNA quality and potential degradation. Extracted DNA was stored at -20°C before PCR amplification and sequencing. To test for potential kit contamination, two separate DNA extractions were performed using all kit reagents but excluding coral tissue. These blank samples were PCR-amplified with the corresponding primers, pooled as one blank sample and then sent for sequencing; this process was done independently for ITS2 and 16S rRNA gene analysis. Positive and negative PCR controls were included in the PCR amplification but only used to confirm functionality of primers and purity of master mix.

2.3.5.1 Preparation of ITS2 and 16S libraries for sequencing

To amplify bacterial 16S rRNA gene amplicons, primers 27F (Lane 1991) and 519R (Lane et al. 1993) (v1-v3 region; ~530bp) (Caporaso et al., 2012), including MiSeq adaptors, were used in a 30-cycle PCR using AmpliTaq Gold® 360 Master Mix (Applied Biosystems). PCR cycling conditions included: 95°C for 10 min, followed by 30 cycles of 95°C for 30s, 55°C for 30s, and 72°C for 90s, a final elongation of 72°C for 7 min. Three replicate (10 ul) PCR reactions were pooled into a ~25 ul volume prior to sequencing. The strategy of pooling PCR products was carried out to capture the majority of taxa, although previous work has shown non-significant differences in the communities obtained from two sets of independent PCRs carried out via clone libraries from the same sample, even with different number of cycles (Acinas et al., 2005, Bonk et al., 2018). PCR products were sequenced at the Ramaciotti Centre for Genomics (RCG, University of New South Wales) with a MiSeq v3 2x300bp sequencing run (including PhiX spike-in). PCR clean-up and DNA library preparation were performed by RCG. The same approach was carried out for the ribosomal DNA internal transcribed spacer 2 (ITS2) region of the family Symbiodiniaceae using the primers Sym_VAR_5.8S2 forward and Sym_VAR_REV reverse (Hume et al., 2016).

2.3.5.2 Metabarcoding analyses

For the Symbiodiniaceae community analysis, data was processed following the standardized remote analysis of the SymPortal analytical framework (symportal.org, github.com/SymPortal) in order to predict putative Symbiodiniaceae taxa (Hume et al., 2019). This framework can resolve genetically differentiated taxa by taking into consideration intragenomic sequence diversity which occurs due to the multicopy nature of the ITS2 rDNA region within Symbiodiniaceae genomes. Demultiplexed and paired forward and reverse fastq.gz files outputted from Illumina sequencing were submitted remotely to SymPortal. Sequence quality control and filtering steps were conducted as part of the SymPortal pipeline using Mothur 1.39.5 (Schloss et al., 2009), the BLAST + suite of executables (Camacho et al., 2009), and minimum entropy decomposition (MED) (Eren et al., 2015). The nomenclature of Gardner et al (2019) (Gardner et al., 2019) was used to define either a putative or defined taxon.

16S rRNA gene sequence data was processed using the open-source software Quantitative Insights Into Microbial Ecology (QIIME2, version 2019.7) (Caporaso et al., 2010). Filtering and denoising steps were carried out using DADA2 (Callahan et al., 2016), with F290 and R240 truncation parameters, and trimming of forward and reverse primers. Values for expected errors for forward reads were kept as default and increased to 4 on the reverse reads to increase number of merged reads. A total of

2,000,000 reads were allocated for the dada2 algorithm when training the error model. Chimeric sequences were identified and removed using the 'consensus' method within the DADA2 platform and only sequences with a minimum quality score of 20 were used in the analysis. A Naïve Bayes classifier was used against a curated SILVA database version 132 (Quast et al., 2013) and clustered at 99% similarity level to assign taxonomy to amplicon sequencing variants (ASVs). Chloroplast and mitochondria ASVs were removed from resulting biom tables using the phyloseq package (McMurdie and Holmes, 2013) in R (Team, 2013). Further steps included removal of ASVs not observed in any recruit sample, low-abundance samples ($<1e-5$) and contaminants. Contaminants were identified using a similar method to that outlined in Lee et al. (2015); as contaminant taxa are expected to have high relative abundance in negatives and low relative abundance in samples, any ASV that exhibited a relative abundance of one or more orders of magnitude higher in negatives compared with coral samples were removed. Remaining data were rarefied to an even depth of 6467 reads per sample and transformed to relative abundances using phyloseq.

2.3.6 Statistical analysis

2.3.6.1 Larval heat tolerance, settlement and basal growth

Kaplan-Meier (K-M) survival analysis was used to estimate survival rates of larvae through time by grouping all survivors at the treatment level for each timepoint. Rearing treatment (AMBIENT, MID, High) and acute heat stress conditions (27.5 or 35.5°C) were fixed effects. Data was analysed with the *survfit* function in the R package 'survival' (Therneau and Lumley, 2014).

Variation in settlement success was evaluated with a generalised linear mixed effect model with the function *glmer*, with tank as a random effect and treatment as a fixed effect. The number of recruits were \log_{10} -transformed to meet the normality assumption. Bootstrapping techniques were used to generate the 95% confidence intervals.

To compare basal growth rates, a set of linear mixed effect models were fitted with different combinations of fixed (treatment, diameter and time) and random effects (individual nested in plate and tank). All models included the three fixed effects, but had different interactions among them. The interaction between diameter and time was not included in any of the models because diameters were

generally larger during the second time interval. Model selection was performed using AIC. A Levene's Test was used to confirm homogeneity of variance ($p > 0.05$) for settlement and growth data.

A generalised linear mixed effects model with a binomial error structure was fitted to predict the survival of recruits among treatments at the different time intervals. The model included time, treatment and their interaction as fixed effects, and plate number as a random intercept. The model was fitted using the function *glmer* from the R package 'lme4' (Doran et al., 2007). All analyses were performed in R version 3.6 (Team, 2013)

2.3.6.2 Symbiont associations

Symbiodiniaceae and bacterial diversity analysis was performed using the relative abundance of the ITS2 type profile and 16S rRNA gene ASVs data obtained from either SymPortal or QIIME2/Phyloseq. The effects of treatment and tank on community composition were tested with a permutational multivariate analysis of variance (PERMANOVA) using Bray-Curtis similarity distance with the function *adonis* from the R package 'vegan' (Oksanen et al., 2013) with the additional NMDS to visualise the effects of treatment.

For the bacterial communities, variations in alpha diversity were evaluated through species richness (number of ASVs) and species diversity (Chao1 and Shannon index). Each measure of alpha diversity was analysed with a linear mixed effect model with treatment as a fixed effect and tank as random intercept. Chao1 estimates were \log_{10} transformed to meet the normality assumption. Differences in beta diversity were analysed using PERMANOVA with 999 permutations. Pairwise comparisons were performed using the function *pairwise.perm.manova* (with 999 permutations and BH method) from the package *RVAideMemoire* (Hervé and Hervé, 2019). Differences in beta diversity were visualised using an NMDS fit with Bray-Curtis distances. Bacterial indicator taxa analysis (i.e., indicative of a specific treatment) was performed using a multi-level pattern analysis with 999 permutations with the function *IndVal-multipatt* from the package *indicspecies* (De Cáceres, 2013, De Cáceres and Legendre, 2009). This analysis was carried out at three separate levels including family, genus and species with $\alpha = 0.05$.

To compare differences in the relative abundance of bacterial families among treatments, a linear model with treatment as a fixed effect was fitted to the ten most abundant families in the rarefied dataset using the Bayesian package 'brms' (Bürkner, 2017). A zero-inflated beta distribution was used for all families except Rhodobacteraceae, where a beta distribution model was used as all samples had relative abundances larger than zero. To quantify differences in the predicted relative abundance of each family among treatments, the 95% credible interval of the posterior distribution of the difference between relative abundances of each pair of treatments was calculated. When the 95% credible interval overlapped with zero, it was assumed that the relative abundances were not different. To identify differences in relative abundances of particular families differentially abundant among treatment combinations (i.e., in a non-rarefied dataset), a differential expression analysis based on a negative binomial distribution was performed using the function DESeq (Wald test) from the package DESeq2 (Love et al., 2014), which has been previously used in microbial community analysis due to its increased sensitivity, particularly on smaller datasets (Weiss et al., 2017). Log2FoldChange values were used to compare significant differences among treatment combinations, to identify not only the order of magnitude in relative abundances between treatments but also which treatment favoured the abundance of each taxa.

To investigate associations between pairs of bacterial families or Symbiodiniaceae types, a Spearman rank correlation test was computed for each pair of bacterial family and Symbiodiniaceae type profiles that were present in at least ten samples. To compensate for the lack of replication at the genotype level, a Mantel test was used to evaluate potential relationships between Symbiodiniaceae and bacterial communities.

2.4 Results

2.4.1 Phenotypic performance

2.4.1.1 Larval heat stress survival

Rearing condition had a significant effect on survival probability when larvae were exposed to an acute thermal event of 35.5 °C at ambient $p\text{CO}_2$ ($p < 0.001$, method: Log-rank). Larvae reared in the HIGH treatment had the highest probability of survival during acute heat stress, at least for the first 120 hours, followed by MID treatment, then AMBIENT, with the last two treatments showing more similar survival rates through time (Fig. 2.2). Larvae from each rearing treatment that were maintained under AMBIENT temperature conditions had survival probabilities close to one and survival did not differ among treatments ($p = 0.73$, method: Log-rank).

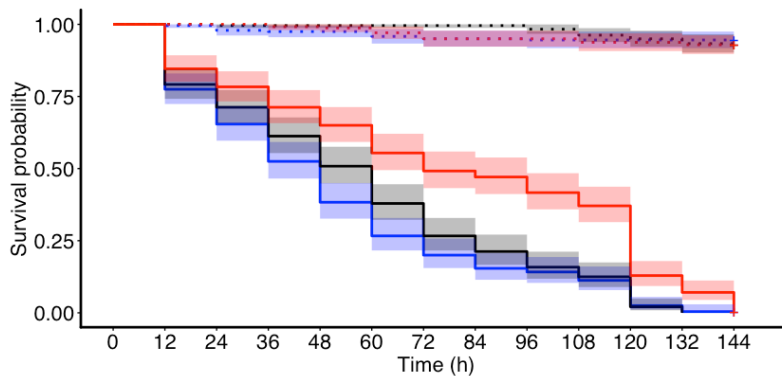


Figure 2. 2 Kaplan-Meier curves showing survival probability over time for larvae exposed to two temperatures (27.5 and 35.5°C) at ambient $p\text{CO}_2$. Solid lines show survival of larvae exposed to acute heat stress at 35.5°C over a period of 144 hours, whereas dotted lines display survival of larvae exposed to the ambient temperature of 27.5°C. Line colours represent the three rearing conditions being AMBIENT (blue), MID (black) and HIGH (red) temperature x $p\text{CO}_2$.

2.4.1.2 Settlement success and survival of recruits over time

Settlement did not differ among treatments ($p > 0.05$, Table A.S1), with a total of 2359, 2517 and 2329 settled recruits in the AMBIENT, MID and HIGH treatments, respectively. The number of recruits on plates in the MID treatment showed less variation compared to AMBIENT and HIGH (Fig. A.S2).

Survival of recruits significantly decreased over time and differed among treatments, but there was no significant interaction between time and treatment (Table 2.1, Fig. 2.3). Overall, recruits from the AMBIENT (as the contrast 'intercept' variable) treatment had significantly lower survival compared with recruits from the MID and HIGH treatments. For the first time interval (2 to 6 weeks), recruits from the MID treatment had the highest survival followed by recruits from the HIGH treatment, both displaying survival $> 75\%$. In contrast, recruits from AMBIENT showed close to 75% survival. A similar pattern was observed at the second time interval (6 to 10 weeks), although the overall survival was lower for all treatments. In this interval, average survival was highest for recruits from MID ($\sim 65\%$), followed closely by recruits from HIGH ($\sim 50\%$), while recruits from the AMBIENT treatment had $\sim 25\%$ survival.

Table 2. 1 Coefficient estimates for survival of recruits among treatments corresponding to all time intervals over a total period of 8 weeks (2 to 10 weeks).

	Estimate	Std. Error	z value	Pr(> z)
(Intercept) AMBIENT	2.745	0.307	8.95	<0.0001
Time	-1.943	0.119	-16.35	<0.0001
Treatment HIGH	2.466	0.53	4.66	<0.0001
Treatment MID	1.222	0.464	2.63	0.0085
Time:Treatment HIGH	-0.443	0.228	-1.94	0.0518
Time:Treatment MID	-0.144	0.185	-0.078	0.4373

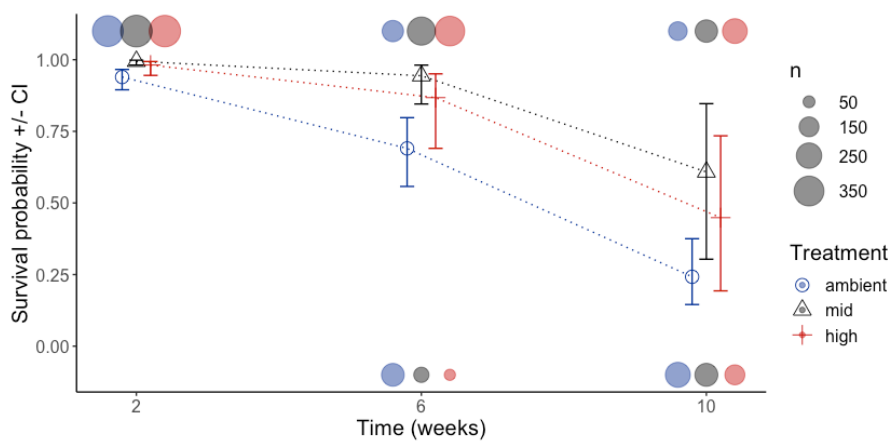


Figure 2. 3 Survival probabilities of recruits in the three treatments at 2 weeks, 6 weeks and 10 weeks post settlement. Error bars show 95% confidence intervals. The size of the coloured circles represents the number of raw observations where the top circles show the number of survivors whereas the bottom circles show the number of dead recruits). Detailed information on the multiple significant interaction can be found on Table2.1'

2.4.1.3 Recruit basal growth over time

The best-fit model for estimating basal growth included treatment, diameter, and time as additive fixed effects, and individual nested within plate as random intercept (Table A.S2). Basal

growth significantly decreased with increasing diameter and differed among treatments (Table A.S3). However, posthoc comparisons did not find significant differences among specific pairs of treatments (Table A.S4) and the effect size was small. The mean growth of coral recruits in the MID and HIGH treatments was only 10.9 and 9.7 % less than in AMBIENT for the first time interval, respectively and 11.6 and 10.3 % for the second time interval. Recruits grew less during the second time interval relative to the first time interval, although the difference was small (Fig. 2.4).

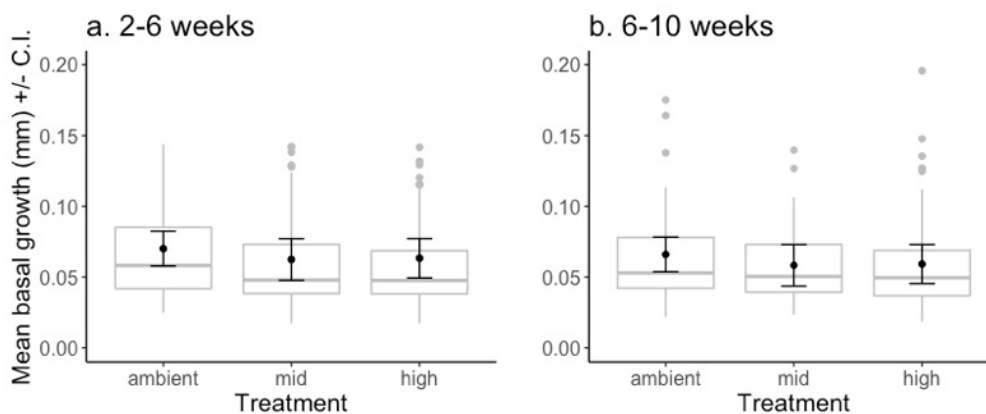


Figure 2. 4 Mean basal growth of recruits for the different treatments (AMBIENT, MID, HIGH) in the first (a) and second (b) time intervals. Since basal growth was size-dependent, all predictions were corrected for size. Points show the fitted model mean and error bars are confidence intervals. The grey box plots show the data corrected for diameter.

2.4.2 Symbiotic associations

2.4.2.1 Symbiodiniaceae communities of 6-week-old recruits

A total of 2,727,278 raw reads were obtained from the 54 samples across all treatments, ranging from 22,6006 to 79,829 reads per sample. An average number of 50,511 pair-end reads were obtained per sample, with downstream filtering steps reducing this to 33,119 reads. A total of 350 filtered reads were found in the blank sample, however, no ITS2 profiles were predicted by SymPortal.

Treatment had a significant effect on Symbiodiniaceae type profiles in 6-week-old recruits, explaining ~25% of the variance ($R^2=0.25$, Table A.S5). Tank did not have a significant effect on the Symbiodiniaceae associations, although it explained ~15% of the variance ($R^2=0.15$, Table A.S5). The

remaining ~60% variance remained unexplained. Individuals from the AMBIENT treatment were dominated by types where ~62% of reads matched D1.D4.D6.D2.D1c.D4c (*Durusdinium glynnii*, *D. trenchii*), followed by ~17% of reads matching C50c.C50a.C3.C21.C50f.C3b (no associated species). The remaining 21% of reads matched less abundant type profiles (Table A.S6, Fig. 2.5). Almost half of the individuals from the MID treatment (~45%) matched C1.C1b.C1c.C42.2.C1bh.C1br (*C. goreau*), ~30% matched D1.D4.D6.D2.D1c.D4c (*D. glynnii*, *D. trenchii*), ~13% matched D1.D4.D17c.D17d.D1r.D17e.D4c.D17k.D17j.D17l (*D. trenchii*), with other type profiles sharing the remaining ~12% (Table A.S4, Fig. 2.5). Over half of the individuals from the HIGH treatment (~53%) were dominated by type profile D1.D4.D6.D2.D1c.D4c (*D. glynnii*, *D. trenchii*), followed by C1.C1b.C1c.C42.2.C1bh.C1br (*Cladocopium goreau*) (~23%) and then C1.C1c.C1b.C1ao.C1am.C1an.C3cm (*C. goreau*) (~12%), with less abundant types accounting for the remaining ~12% (Table A.S6, Fig. 2.5). A total of 12 different Symbiodiniaceae type profiles were detected in 6-week-old recruits from the AMBIENT treatment, whereas 18 and 14 different type profiles were detected in the MID and HIGH treatments, respectively. More detailed information (i.e., dominant vs. rare profiles detected) at the individual recruit level from each treatment can be found in the supplementary material (Tables A.S7 to A.S9, Fig. A.S2).

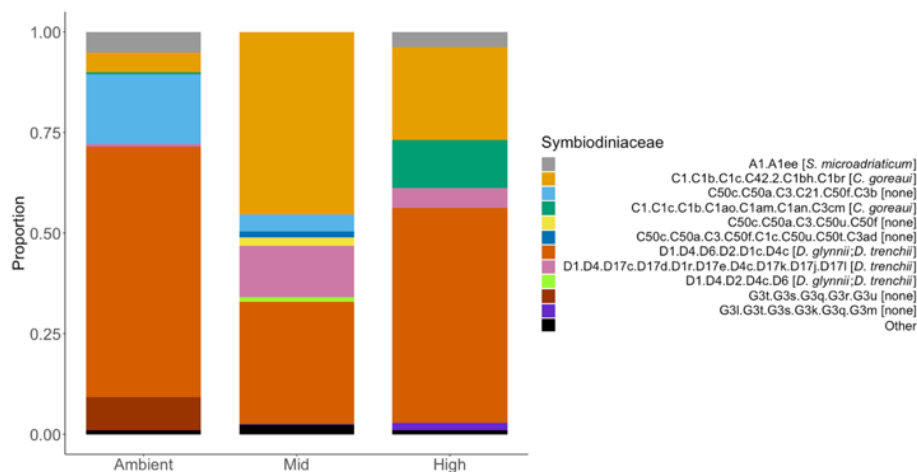


Figure 2. 5 Average composition of Symbiodiniaceae communities in 6-week-old *A. loripes* recruits. Bar plots show the overall proportion of each type profile within each treatment (i.e., pooled across coral recruits within treatments).

NMDS revealed a weak segregation of recruits according to treatment (Fig. 2.6a). Despite this weak clustering, pairwise PERMANOVA comparisons confirmed significant differences among treatment groups (AMBIENT - MID: $p < 0.05$; AMBIENT - HIGH: $p < 0.05$; MID - HIGH: $p < 0.05$). Moreover, from the type profiles that have known associated species, the vectors driving the separation did not necessarily have the same associated species (Fig.2.6b). For example, type profiles C1.C1c.C1b.C1ao.C1am.C1an.C3cm and A1 pulled the ordination in the same direction, yet one is associated with *C. goreau* and the other one with *S. microadriaticum*.

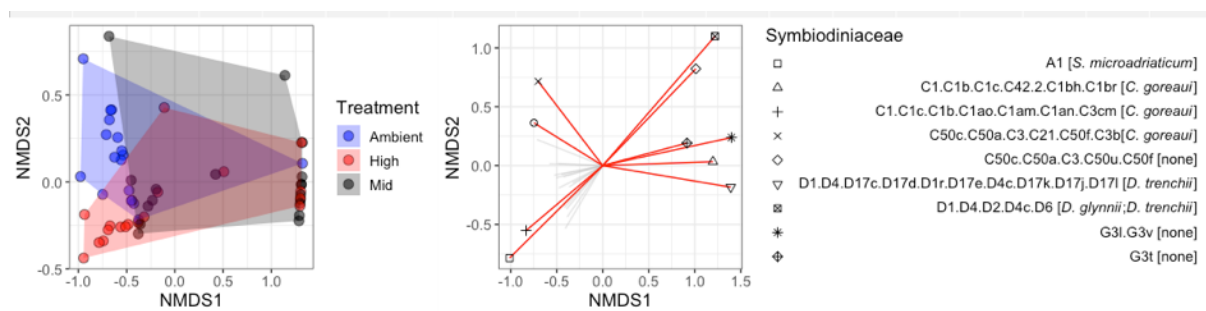


Figure 2. 6 NMDS of Symbiodiniaceae type profiles in 6-week-old recruits across treatments. Values in axis represent Bray-Curtis distances between samples. The red lines show the ten Symbiodiniaceae type profiles that contributed most to the ordination, the remainder are represented by grey lines. Names in brackets represent SymPortal associated species to each of the type profiles.

2.4.2.2 Bacterial communities for 6-week old recruits

A total of 3,513,801 bacterial sequences were retrieved from the 6-week-old recruits (N=54) sampled across all treatments, corresponding to 1,282 unique ASVs. The number of reads per sample ranged from 37,543 to 104,262. On average, 65,070 pair-end reads were obtained per sample after sequencing with downstream filtering steps reducing this to 41,602 reads. The number of ASVs per sample ranged from 4,251 to 20,245. Rarefaction analysis showed curve asymptotes at ~5,000 reads (Fig. A.S3), thus the dataset was rarefied to even depth of 4,251. All samples were retained in the analysis, and a total of 1282 taxa were retrieved following rarefaction. A total of 280 merged non-chimeric reads were recovered from the blank sample (i.e., DNA extraction control) and clustered into two ASVs, however these ASVs did not have any bacterial taxonomic affiliation and were not present in any of the 54 coral recruit samples.

The number of shared ASVs varied according to treatment (Fig. S4). A total of 197 taxa were found in AMBIENT, 212 in MID and 209 in HIGH, with some taxa occurring under different treatments. For example, the HIGH treatment had 123 unique ASVs, followed by the MID and AMBIENT treatments with 119 and 111, respectively. Samples from the HIGH and MID treatments shared 26 ASVs and samples from the MID and AMBIENT treatments also shared 26 ASVs (one-level of difference in treatment conditions). This contrasts with only 19 ASVs shared between HIGH and AMBIENT (two-level of treatment conditions difference).

Alpha diversity was not significantly different among treatment combinations (AMBIENT-MID, AMBIENT-HIGH, MID-HIGH) ($p > 0.05$; Tables A.S8- A.S10). Species richness was also not significantly different among treatments (Fig. A.S5). By contrast, beta diversity varied depending on treatment and Bray-Curtis dissimilarity matrices showed that treatment had a significant effect on bacterial community composition, although it explained only 6% of the variance in relative abundances ($p < 0.01$, $R^2 = 0.06$, Tables A.S11 - A.S12). Tank did not have a significant effect on the bacterial communities, explaining only 2% of the variation ($p > 0.01$, $R^2 = 0.021$, Table A.S11). The remaining ~92% variance remained unexplained. Although a weak segregation was observed among treatments (Fig. 2.7), pairwise PERMANOVA confirmed significant differences among treatments pairs (AMBIENT : MID < 0.01 ; AMBIENT : HIGH < 0.01 ; MID : HIGH < 0.01).

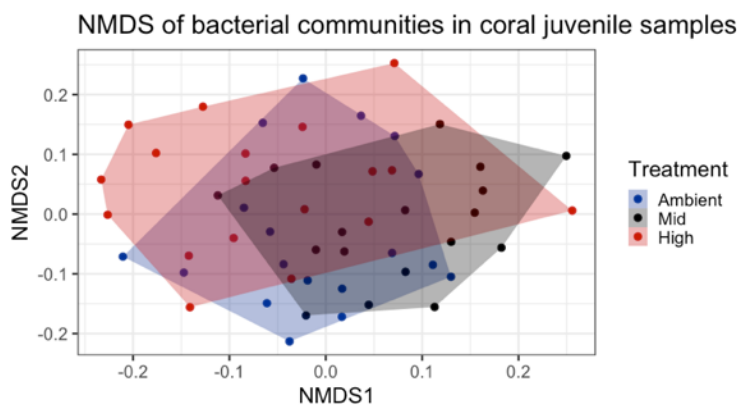


Figure 2. 7 NMDS of bacterial communities in 6-week-old recruits across treatments. The axes represent Bray-Curtis distances among samples.

At the species level, a total of five indicator taxa were identified across all treatments (Table A.S13, $\alpha = 0.05$, $p\text{-value} < 0.05$), all from the phylum cyanobacteria. However, most fidelity values ranged from 20 - 50% and consequently, none of these species was considered as an indicator for any particular treatment. A similar result and conclusion were found at the genus (Table A.S14) and family (Table A.S15) levels.

Based on the rarefied dataset, relative abundances of the top 10 most abundant bacterial families did not vary among treatments (Fig. 2.8, Tables A.S16- A.S17). The most abundant bacterial family across all treatments was Rhodobacteraceae. When including the top 15 families, other common coral-associated bacterial families like Endozocoimonadaceae were also detected, although they were not present in all samples within each treatment (Fig. A.S6). At the genus level, the top ten bacterial genera did not vary among treatments (Fig A.S7, Tables A.S18- A.S19). In addition, analysis of the non-rarefied dataset revealed significant differences among particular bacterial families between pairs of treatments, with $\log_2\text{FoldChange}$ values favouring the abundance of some taxa under HIGH treatment (Fig A.S8, Tables A.S20- A.S22).

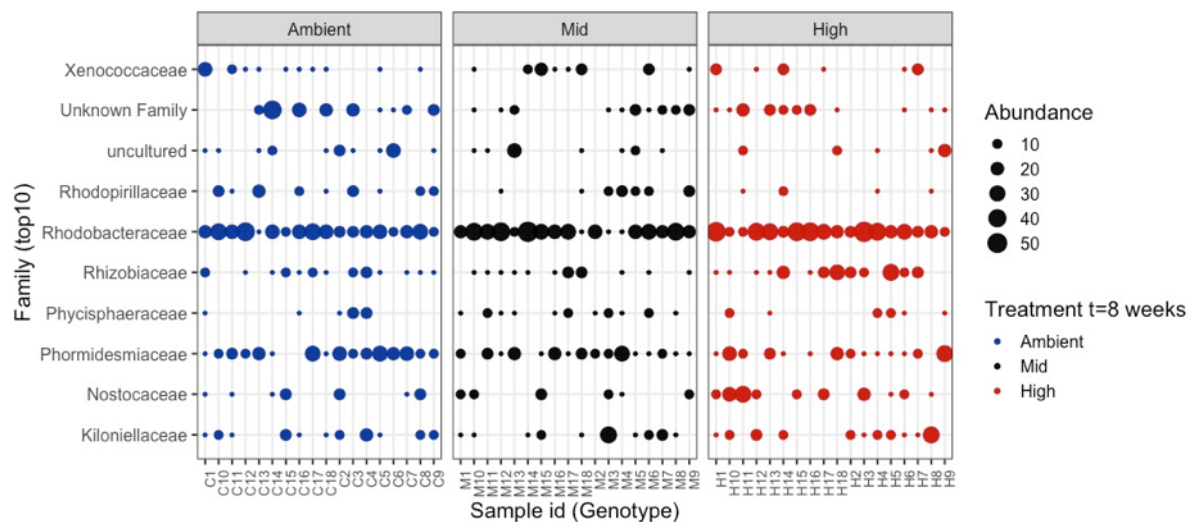


Figure 2. 8 Relative abundance of the top 10 bacterial families (y-axis) among 6-week-old recruits (x-axis) for each of the three treatments (AMBIENT, MID, HIGH); (n= 117 total families).

2.4.2.3 Correlation of relative abundances across symbiont members

Spearman Rank correlation coefficients revealed only weak correlations in relative abundances between pairs of the top 10 most abundant bacterial families, but stronger associations between Symbiodiniaceae type profiles (Fig. 2.9). For example, there was a strong negative correlation between D1.D4.D6.D2.D1c.D4c (*D. glynnii*/*D. trenchii*) and D1.D4.D17c.D17d.D1r.D17e.D4c.D17k.D17j.D17l (*S. trenchii*), and a strong positive correlation between the latter (*D. trenchii*) and C1.C1b.C1c.C42.2.C1bh.C1br (*C. goreau*). In addition, the Mantel test showed that the Symbiodiniaceae community did not have a significant relationship with the bacterial community (Mantel statistics $R = 0.019$, $p = 0.289$) at the genotype level. In other words, samples that had similar bacterial families, did not necessarily have similar Symbiodiniaceae type profiles.

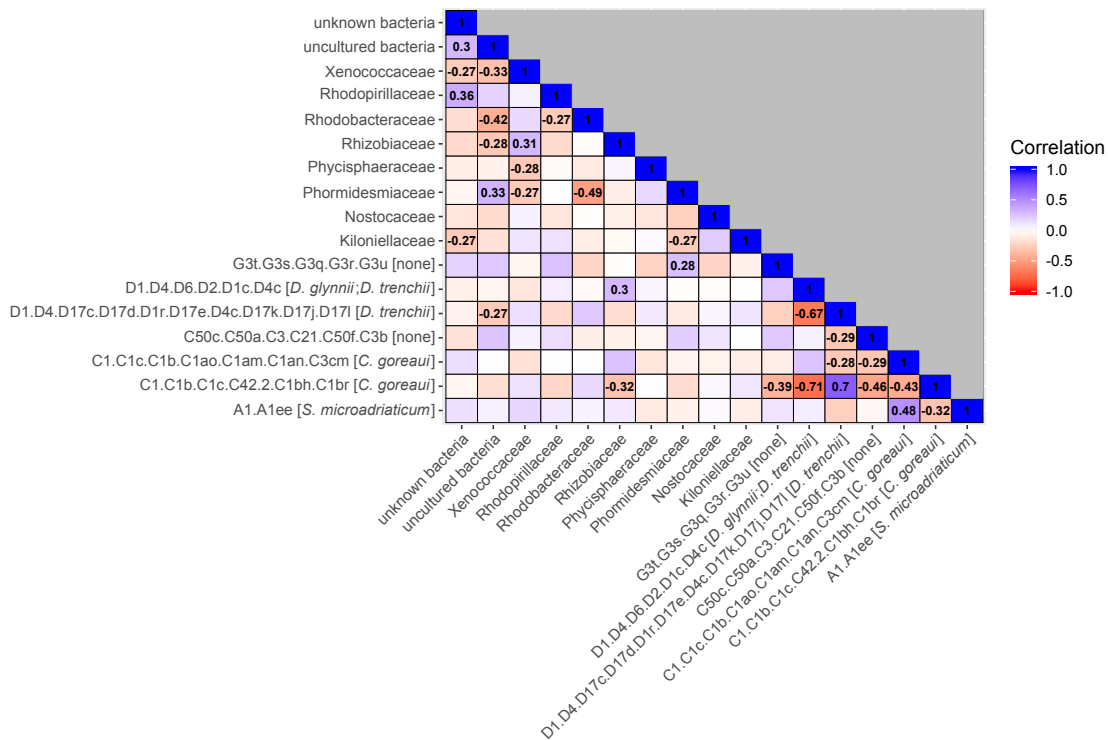


Figure 2. 9 Relative abundance correlations among Symbiodiniaceae type profiles and bacterial families for 6-week-old recruits. Correlation values based on the Spearman Rank correlation coefficient analysis. Significant correlations among pairs are shown inside the inside the matrix.

2.5 Discussion

My results provide insights into the effects of elevated temperature and $p\text{CO}_2$ on the performance of coral early life stages and their microbial associations. Importantly, I observed increased thermal tolerance of coral larvae following a short rearing period of combined elevated temperature and $p\text{CO}_2$. Rearing under simulated future climate conditions influenced growth rate and survival of recruits, but had subtle effect on symbiotic community structure. Hence, suggesting that the coral host plays a major role, relative to the community composition of their symbionts, in the observed differences in thermal tolerance of larvae and growth and survival of *A. loripes* recruits.

2.5.1 Larval and recruit survival

Exposure to stressful, but non-lethal, environmental conditions, can induce stress-hardening responses that increases survival probability in similar or even more extreme conditions (Bowler, 2005, Sinclair and Roberts, 2005). This study demonstrated that rearing treatment conditions served as a physiological preparation by significantly influencing survival probabilities of 10-day old coral larvae exposed to a temperature treatment 8 °C above the AMBIENT baseline. Coral larvae that had been reared at elevated temperature and $p\text{CO}_2$ conditions (+2.0°C and 900 $\mu\text{atm } p\text{CO}_2$) exhibited increased survivorship during 120 hours of thermal stress, which suggests a hardening response from pre-exposure to elevated temperature and/or $p\text{CO}_2$. It is possible that increased survivorship of coral larvae from the HIGH treatment when acutely exposed to thermal stress (35.5°C) was a consequence of treatment conditions differentially affecting early larval development, since rates of embryogenesis are temperature-dependent (i.e., due to the possibility that larvae from HIGH treatment were more developed relative to AMBIENT and MID larvae during the same 10-day rearing period). For example, warm temperatures have been shown to accelerate development in several species including acroporids and mussids (Negri et al., 2007, Heyward and Negri, 2010, Chua et al., 2013b). However, elevated temperatures can also be linked to an increased likelihood of embryonic abnormalities that leads to higher mortality rates (Keshavmurthy et al., 2014, Randall and Szmant, 2009b). In fact, studies in other *Acropora* spp. have recorded decreased larval survival by ~60% following a 4 °C increase in temperature, with most losses occurring during the process of gastrulation (Randall and Szmant, 2009a). Here, I allowed sufficient time for larvae to be fully developed in all three treatments prior to applying the acute heat stress, and only recorded between a 20-25% decrease in larval survival for the first 12 hours of acute heat stress across all treatments. Such differences in survival rates are more likely linked to molecular responses triggering enhanced thermal tolerance in larvae that experienced higher thermal stress during the rearing period. The increased survivorship of larvae under acute heat

stress is clear evidence of rapid stress-hardening responses triggered by HIGH treatment conditions. However, it is important to recognise that my experimental design precludes determination of whether hardening was triggered by preexposure to elevated temperature only, $p\text{CO}_2$ only, or their combination. Future experiments should consider implementing fully orthogonal experimental designs to tease apart factors underpinning stress-hardening and also consider using individual crosses of parental colonies to be able to assess how genetic diversity may be partitioned across larvae, or recruits, due to treatment conditions.

The transcriptional response of corals exposed to acute thermal stress has been shown to include a rapid increase in heat-shock proteins but also a decreased expression of particular proteins (e.g., mannose-binding C-type lectin) that can potentially compromise the host immune response (Rodriguez-Lanetty et al., 2009). Moreover, a rapid depletion of larval energy stores due to compromised enzymes involved in the glyoxylate cycle and negative effects to cytoskeletal structure have also been linked to altered transcriptional responses associated with hyperthermal stress (Polato et al., 2013). In my study, I allowed a resetting period to AMBIENT conditions prior to acute thermal stress. I therefore hypothesise that higher survival rates observed in larvae from HIGH treatment is a stress-hardening response related to particular molecular mechanisms of thermal tolerance established during the rearing period, which could have been retained via epigenetic mechanisms (e.g., DNA methylation) (Dimond and Roberts, 2016, Liew et al., 2018, Putnam et al., 2016). However, the mechanisms responsible for this apparent thermal hardening in my study remain unknown. If the assumption is that a consistent genetic pool was maintained across batch cultures, it is possible that increased survivorship in the HIGH treatment is the result of thermal hardening. For instance, it is important to consider that thermal tolerance arises primarily through mechanisms of acclimation and adaptation (Chevin et al. 2010, Foo and Byrne, 2016). Therefore, acknowledge that different rearing conditions may have selected for different genotypes, resulting in genetic differences in the larval pools of the three treatments. I also assumed that all larvae were aposymbiotic and thus the increased survivorship was not due to differential effects of treatments on the Symbiodiniaceae communities. Future studies should investigate how alleles can be selected due to elevated treatment conditions, as well as the cellular response of the larvae (Meyer et al., 2011a) and determine whether survival rates can be modified when larvae have been infected with Symbiodiniaceae (e.g., vertical symbiont transmission), since some taxa are known to enhance thermal tolerance (Kenkel and Bay, 2016, Quigley et al., 2016, Robison and Warner, 2006).

Regardless of the exact mechanism/s responsible, increased survivorship under acute thermal stress due to hardening could be beneficial to coral larvae under future climate conditions. Water temperatures can become elevated over shallow reefs during the day, and such conditions can increase in intensity as sea surface temperatures rise, therefore thermally hardened coral larvae would have an increased probability of survival under these conditions, particularly due to the possibility that future marine heat waves (i.e., referring to thermal anomalies causing coral bleaching events due to increased temperatures) may extend beyond the peak of summer seasons due to rapid climate change (e.g., including periods of mass spawning events) (Oliver et al., 2019); . Although it is not possible to conclude whether this stress-hardening will remain a fixed trait during subsequent stages of development (i.e., developmental acclimation), it is important to note that I did not observe negative consequences (trade-offs) to the overall fitness, including settlement success, post-settlement growth and survival. This suggests that the upper thermal limits of coral larvae can be enhanced when fertilisation of gametes and larval rearing is carried out under HIGH treatment conditions. Inducing thermal hardening by exposure of developing larvae to elevated temperature and $p\text{CO}_2$ might therefore be a strategy to enhance the success of coral restoration projects.

Coral larval settlement can be affected by a range of environmental factors, including variation in water temperature, water quality and substratum availability (Erftemeijer et al., 2012, Richmond et al., 2018). In this experiment, settlement success was not significantly influenced by treatment conditions, thus contrasting with previous studies that have recorded reduction in recruitment due to elevated temperatures or low and variable pH (Viyakarn et al., 2015, Randall and Szmant, 2009b, Caroselli et al., 2018). It is possible that such contrasting result can be explained by the different species of corals used and their sampling regions, since a study with three *Acropora* species from the GBR found that none of the early life-history stages tested were consistently affected by reduced pH (Chua et al., 2013a).

Post-settlement success is influenced by many environmental factors that induce increased mortality over time (Ferrier-Pages et al., 2000, Trapon, 2013). Indeed, coral mortality in the first year can be extremely high in nature (>30-99%) (Wilson and Harrison, 2005, Suzuki et al., 2018). Drivers of post settlement mortality have been shown to shift with life stage and size, with survival rates of 30% at 8 weeks post-settlement, and as low as 5% after 5 months, with little variation thereafter (Cruz and

Harrison, 2017). This may be linked to small recruits (1-2 mo. Old) being more susceptible to accidental grazing (Traçon et al., 2013) compared with larger (10-14 mo. Old) recruits (Davies et al., 2013). By contrast, I found survivorship was greater between 2 - 6 weeks post settlement compared with 6 - 10 weeks post-settlement. It is possible that the higher mortality (~65%) observed after ten weeks compared to the first 4 weeks (~25%) is the result of cumulative stress due to laboratory rearing conditions for all treatment levels. Although this temporal pattern in mortality was observed for recruits in all treatments, corals in the MID treatment had higher survivorship relative to corals in HIGH and AMBIENT. In this context, the effect of elevated temperature can also determine post-settlement success as it can promote larval development in corals and other marine invertebrates (Edmunds et al., 2001, Pineda et al., 2002), which results in an increased settlement success and lowered post-settlement mortality. However, other studies have reported reduced settlement and survival associated with thermal stress (Nozawa and Harrison, 2008). In *A. loripes*, I recorded no variation in settlement success across treatments, but recruits in the MID treatment had the highest survivorship in both periods, suggesting that the MID treatment provided more suitable conditions relative to AMBIENT or HIGH.

In the wild, mortality pressures are most evident in coral recruits until they reach a size refuge, estimated to be around 5 mm or 3-9 months old (Babcock and Mundy, 1996, Doropoulos et al., 2012a), with growth in the first weeks being considered the most crucial for further survival. A two-fold increase in diameter of recruits 12 weeks post-settlement and an eight-fold increase over 12 months, has been reported for recruits settled on either recruitment tiles or natural substrata (Cruz and Harrison, 2017). Here, in a laboratory-based experiment, I found an important effect of size, with overall growth rates decreasing with increasing diameter of the recruits across all treatments over a 10-week period, potentially explaining the slightly lower growth rate recorded between 6-10 weeks relative to 2-6 weeks. While a negative effect of elevated temperature and $p\text{CO}_2$ on growth rate has been reported in other *Acropora* spp. (Yuan et al., 2018), in *A. loripes* I detected no substantive differences in growth rates across treatments.

2.5.2 Symbiodiniaceae diversity and community structure

Investigating the diversity and abundance of Symbiodiniaceae can provide insights into the response of corals to changing environmental conditions (Oliver and Palumbi, 2011, Davies et al., 2019, Ulstrup et al., 2008, Stat et al., 2011). Here, Symbiodiniaceae infection occurred naturally from

exposure to other organisms (e.g., adult corals) and sediments within the treatment mesocosm systems. Overall, treatment significantly influenced Symbiodiniaceae communities, explaining 25% of the total variation. The remaining 60% of variation, could be contributed by specific host-Symbiodiniaceae associations effects. It is possible that treatment conditions were not sufficiently challenging to trigger changes in the community structure of Symbiodiniaceae or also, that the continuous winnowing process of the recruits did not allowed a clear delineation of treatment-specific effects.

I found evidence for a strong correlation among particular Symbiodiniaceae type profiles (ranging from -0.71 to 0.70). The positive correlations between *C. goreau* and *D. trenchii*, and *S. microadriaticum* with *C. goreau*, are of particular interest considering that previous studies have only recorded positive correlations among Symbiodiniaceae members from the same lineage (Bonthond et al., 2018). Strong negative correlations were also observed, but no clear comparisons were possible due to the double species ID assigned to the type profile that displayed negative correlation with *D. trenchii* and *C. goreau*. Such information is valuable to improve our understanding on how Symbiodiniaceae communities potentially interact *in hospite* (Tonk et al., 2013).

2.5.3 Bacterial diversity and community structure

Bacterial community composition in 6-week old recruits differed significantly among treatments, despite treatment explaining only a small proportion of the variation. It is possible that differences in the intensity of treatment conditions were not sufficient to induce major changes in relative abundances (i.e., differences in the degree to which coral microbiomes vary over environmental gradients or experimental treatments) (Grottoli et al., 2018, Hernandez-Agreda et al., 2016, van de Water et al., 2017), and that the composition observed was similar due to contrasting effects of the stochasticity produced by treatment conditions (i.e., deterministic changes due to treatment producing similar beta diversity dispersion among them) (Zaneveld et al., 2017). These findings were further supported by the low values for indicator specificity, which precluded their assignment as robust indicators for treatment conditions.

In addition, the most distinct negative correlation was found between Rhodobacteraceae and Phormidesmiaceae, with the majority of taxa displaying only weak or moderate correlations. However,

the reasons behind such negative associations are unknown. Some co-occurrences were also found but corresponded to unknown or uncultured bacteria, thus limiting interpretation of these results. Future studies should consider increasing the temporal scale of sampling points as the rate of change in coral bacterial communities in responses to environmental stress is unknown.

2.5.4 Conclusions

Here I showed that early coral life stages can increase their thermal tolerance to acute high temperature events via short-term exposure to elevated temperature and/or $p\text{CO}_2$ conditions predicted to occur this century (i.e., evidence of phenotypic plasticity). I further showed that survival of coral recruits was greatest under elevated temperature and $p\text{CO}_2$ conditions, contrasting with previous laboratory and field-based findings. Further, larval settlement and growth of recruits were not affected by MID and HIGH treatment conditions. Thus, inducing stress-hardening during *A. loripes* larval stages did not involve trade-offs with other fitness traits at the recruit stage. This research provides a platform for future work to elucidate the molecular mechanisms (including epigenetic markers) underpinning acclimation responses.

Chapter 3: An experimental test of beneficial acclimation and thermal hardening to climate change conditions in coral early life stages

3.1 Abstract

Multiple climate change stressors, like the combination of ocean warming and acidification, will continue challenging the resilience of corals. Acclimation and hardening of corals via phenotypic plasticity could enable them to overcome rapid climate change. To better understand how the early life stages of coral will respond to predicted future climate change conditions, I reared larvae and recruits of *Acropora loripes* under three different combinations of water temperature and acidification, simulating current-day and future climate change scenarios. Gametes from 14 wild-collected colonies of *A. loripes* were cross fertilized in ambient (27.5°C, 410 $\mu\text{atm } p\text{CO}_2$), mid (AMBIENT +1.0°C, 670 $\mu\text{atm } p\text{CO}_2$) and high (AMBIENT +2.0°C, 900 $\mu\text{atm } p\text{CO}_2$) treatments. Larvae and recruits were subsequently reared under the three treatment conditions for a period of 23 weeks, including a full reciprocal transplant across treatments at 8 weeks of age, and a thermal stress experiment after 16 weeks of age. I observed evidence for thermal hardening in larvae, which displayed enhanced tolerance to extreme temperature (35.5 °C) after 10-days preconditioning under elevated conditions. There was subtle evidence for beneficial acclimation in the maximum photochemical efficiency (Fv/Fm) of 16-week old recruits following the reciprocal transplantation across treatment combinations. Recruits with prior exposure to elevated treatment conditions exhibited higher Fv/Fm under elevated treatments compared with recruits that did not experience elevated treatment conditions prior to reciprocal transplantation. Furthermore, acclimation was reversible, with Fv/Fm returning to ambient levels in recruits returned to ambient conditions after reciprocal transplantation. Finally, the negative effect of heat stress (31°C) on Fv/Fm was buffered in recruits that had experienced elevated conditions during the reciprocal transplantation stage, providing evidence for thermal hardening. Treatment conditions had no clear effect on the growth of recruits during transplantation or heat stress. My findings suggest that corals with past exposure to climate change conditions may have more tolerant phenotypes under acute heat stress conditions. The cost, benefit and risk of stress hardening should be considered in the context of the propagation of corals for restoration and adaptation.

Keywords: global warming, ocean acidification, coral, thermal acclimation, phenotypic plasticity, restoration, adaptation.

3.2 Introduction

Anthropogenic climate change is challenging the stress tolerance of scleractinian corals. Corals have adapted and evolved to a variety of climates over tens of thousands of years (Stanley, 2003), with populations thriving at different geographic locations, even under extreme conditions of thermal and acidification stress (e.g., upwelling and CO₂ vent sites) (Palumbi et al., 2014, Schoepf et al., 2015b, Fabricius et al., 2011). However, the current rate of climate change is considered unprecedented on millennial scales, raising the question of whether corals will be able to adapt to the current rate of change (Hoegh-Guldberg, 2012). Indeed, current predictions suggest that even under greenhouse gas mitigation scenarios, ocean temperatures are on track for at least 1°C warming, which may exacerbate the frequency and intensity of acute thermal-stress events like coral bleaching (Cai et al., 2014, Ainsworth et al., 2016, IPCC, 2019, Hoegh-Guldberg et al., 2019), which is considered the main source of coral cover decline in many regions around the globe (Perry and Morgan, 2017, Wilson et al., 2019, Hughes et al., 2017a). Despite the uncertainty around the future of corals in a rapidly changing climate, there are adaptive pathways that could potentially help corals adjust to these altered environmental conditions.

Environmental changes are constantly challenging the resilience capacity of organisms and their populations. In corals, the detrimental effect of long and short-term environmental stress can be overcome via organismal adaptation and/or acclimation, and also facilitated through their co-evolved symbiotic associations (Fox et al., 2019, Torda et al., 2017, Adjeroud et al., 2018). If there is sufficient standing genetic variation among populations with different environmental histories then local adaptation can occur (Kenkel et al., 2018, Howells et al., 2013, van Oppen et al., 2018, Quigley et al., 2019). Under this scenario adaptive alleles from populations on warmer reefs can disperse to other reefs and more heat tolerant populations would be expected to evolve. It is still unclear however, how fast those alleles would be fixed considering the long generation times for some coral species and other factors limiting the spread of alleles among populations (Palumbi et al., 2011, Quigley et al., 2019). Thus, it is also important to assess other adaptive strategies and mechanisms occurring within the lifespan of the organism, which may or may not be transferred to subsequent generations.

Phenotypic plasticity is a mechanism by which organisms can rapidly respond to short term environmental changes to sustain homeostasis and fitness. Beneficial acclimation through phenotypic plasticity can occur within life stages (e.g., developmental and reversible acclimation) and can potentially be transmitted between generations (e.g., transgenerational acclimation) (Munday et al.,

2013, Torda et al., 2017). Both, *in situ* and *vitro* transplantation experiments have shown that corals can acclimatise to new physicochemical conditions (Bongaerts et al., 2011). The acclimation response has been attributed to the role of the host (i.e., cellular response linked to particular gene and protein expression profiles) and the role of symbionts (i.e., more tolerant Symbiodiniaceae and bacteria) (Webster and Reusch, 2017, Blackall et al., 2015, van Oppen and Blackall, 2019). It can also be regulated through epigenetic mechanisms (Liew et al., 2020, Dimond and Roberts, 2016). Moreover, the induction of plastic responses can occur through hardening, where a brief exposure to a non-lethal condition triggers changes that can increase an organism's tolerance of subsequent more extreme conditions (Wilson and Franklin, 2002). Indeed, corals that have been exposed to stressful conditions may perform better under more extreme environmental conditions (e.g., reduced bleaching susceptibility) (Hoffmann et al., 2003, Sinclair and Roberts, 2005). Therefore, as ocean warming and acidification conditions continue to worsen, it is not only important to explore the mechanisms underpinning acclimation responses and their limitations in face of rapid climate change, but also what alternatives can be implemented to enhance survival probabilities of early life stages of corals.

Early life stages of coral are crucial for sustaining populations and maintaining genetic diversity. Despite the immense amount of sexually produced offspring that can be generated by spawning corals every year (Harrison et al., 1984), only a small number of larvae will settle and develop into juvenile or adult corals. Although survival rates stabilise after a few months, mortality can be as high as 80% post-settlement, even under controlled environments (Wilson and Harrison, 2005, Davies et al., 2013, Suzuki et al., 2018). Various physical, biological, and chemical factors influence the mortality rate of coral larvae and recruits, including the availability of adequate substratum or biofilms for settlement, sediments or pollutants, predation, water temperature and carbonate saturation state (Davies et al., 2013, Traçon et al., 2013, Mumby, 1999, Humanes et al., 2016). Importantly, extreme environmental conditions that can dramatically affect mortality rates are predicted to increase in the future. For example, the frequency and intensity of heat waves are predicted to increase as the climate warms and are no longer constrained to years with extreme El Niño-Southern Oscillation (ENSO) conditions (Hughes et al., 2018b, Hoegh-Guldberg et al., 2019). Consequently, it is important to consider the capacity of coral early life stages to acclimate to warmer conditions, especially as early development takes place during summer (southern hemisphere) when heatwaves are most likely to occur.

In addition, rising temperatures may force early life stages of corals to undertake shuffling or switching of symbionts (i.e., in addition to their vertically transmitted microorganisms), giving priority to more thermally tolerant symbiotic associates. However, there could also be trade-offs associated with shuffling or shifting of symbionts, including reduced nutritional uptake (Yorifuji et al., 2017, Abrego et al., 2012), and even proliferation of potential pathogens (Bourne et al., 2009, van Oppen and Blackall, 2019, Webster et al., 2016), with implications for growth, development and the time needed to reach sexual maturity. Current studies exploring the response of corals, and their symbionts, to environmental stress usually rely on short-term exposure to stressors (e.g., temperature), but do not necessarily explore the long-term consequences, nor if acclimation is beneficial when the intensity of the stress changes, or if preconditioning during early life stage could shape the response to more extreme events. Thus, it is important to explore how climate change conditions affect the phenotypic traits of the early coral host and its symbionts, and determine if acclimation can be maintained or drive the appearance of more tolerant phenotypes.

In this context, generating more tolerant phenotypes with high genetic diversity could be an alternative pathway to increase the success of current coral reef restoration initiatives. Current strategies mostly focus on adult life stages (e.g., via clonal propagation), which has serious limitations for both scaling up and genetic diversity (Lirman and Schopmeyer, 2016, Young et al., 2012, Forsman et al., 2015). More recently, reef restoration efforts have been exploring a range of alternatives at different life stages, with a particular focus on sexually produced individuals, targeting the intrinsic resilient capacity of the various members of the coral holobiont and determining limits to their environmental tolerance (van Oppen et al., 2017, Randall et al., 2020, Bostrom-Einarsson et al., 2020). Although a long-term global commitment is needed to tackle greenhouse emissions and help coral reefs survive, it is also important to consider the potential of small but scalable options via exploring the intrinsic mechanisms of coral resilience to environmental stress. Hence, it is important to evaluate whether early life stages of coral could endure predicted climate change conditions through rapid adaptive mechanisms, but also if such tolerance can be sustained if physicochemical conditions change or worsen.

The aim of this study was to evaluate if preconditioning of coral larvae to controlled climate change conditions can have lasting effects on coral recruit development. In particular, I was interested in testing whether beneficial acclimation to climate change stressors can occur during early life stages of the coral. Specifically, I tested for acclimation capacity by using a common garden experiment (i.e.,

reciprocal transplantation) that exposed coral recruits to an arrangement of three levels of combined temperature and $p\text{CO}_2$ and compared host and symbiont traits (e.g., growth rate and photosynthetic efficiency) before/after transplantation. If beneficial acclimation was occurring, individual performance should improve after a period of exposure to altered environmental conditions compared with performance following acute or short-term exposure to the same environmental conditions (Angilletta, 2009). After a resetting to ambient / control conditions, I exposed the surviving recruits to heat stress and tested for thermal hardening induced by previous exposure to the different experimental treatment combinations during the common garden experiment. Furthermore, after a resetting to ambient / control conditions, I separately exposed a subsample of pre-conditioned larvae from each of the original treatment levels to an acute heat stress, aiming to test for a thermal hardening response that could improve survivorship during extreme temperature events, such as heatwaves. The objective of this study was to improve our understanding of the challenges faced by early life stages by taking into account the detrimental effects of predicted climate change and the corals capacity for thermal acclimation (including hardening).

3.3 Material and Methods

3.3.1 Study species and coral collection

Acropora loripes was chosen as the focal species for several reasons, including its high local abundance and widespread distribution, ease of identification and amenability to cultivation in the laboratory. Fourteen gravid colonies (<25 cm in diameter and assumed to represent distinct genotypes) were collected at about 6 m depth at Davies Reef in the Central Great Barrier Reef (18.83S; 147.63E) under GBRMPA permit G11/3471.1. Collection occurred on 17 - 20th October 2017, immediately prior to the predicted major mass spawning event at this reef. After collection, the corals were transported to the National Sea Simulator (SeaSim) at the Australian Institute of Marine Science (AIMS) and housed in flow-through aquaria under ambient conditions (27.5 °C; 410 $\mu\text{atm CO}_2$) simulating the environmental conditions at Davies Reef.

3.3.2 Experimental parameters and coral spawning

To evaluate performance of coral larvae and recruits under simulated climate change scenarios, this study used three levels of combined temperature and $p\text{CO}_2$: 1) AMBIENT (27.5°C, 410 $\mu\text{atm pCO}_2$), 2) MID (ambient +1.0°C, 670 $\mu\text{atm pCO}_2$) and 3) HIGH (ambient +2.0°C, 900 $\mu\text{atm pCO}_2$). The experimental systems were monitored in real time for temperature and $p\text{CO}_2$ and all inputs were integrated by the Control System in the *Model Predictive Control* logic to manage experimental

parameters. The experimental manipulations mirrored seasonal and daily variation in both temperature and pCO₂ based on reference field measurements from Davies reef with offsets being applied to simulate treatment conditions. See (Uthicke et al., 2020) for further details on the monitoring of temperature and pCO₂ at the SeaSim facility. Additional treatment conditions included acute exposure of larvae to 35.5°C for five days and heat exposure of recruits to 31°C for up to 35 days to assess the potential for thermal hardening of larvae and recruits, respectively, induced by previous experimental treatments during the rearing period or the transplantation phase (Fig. 3.1).

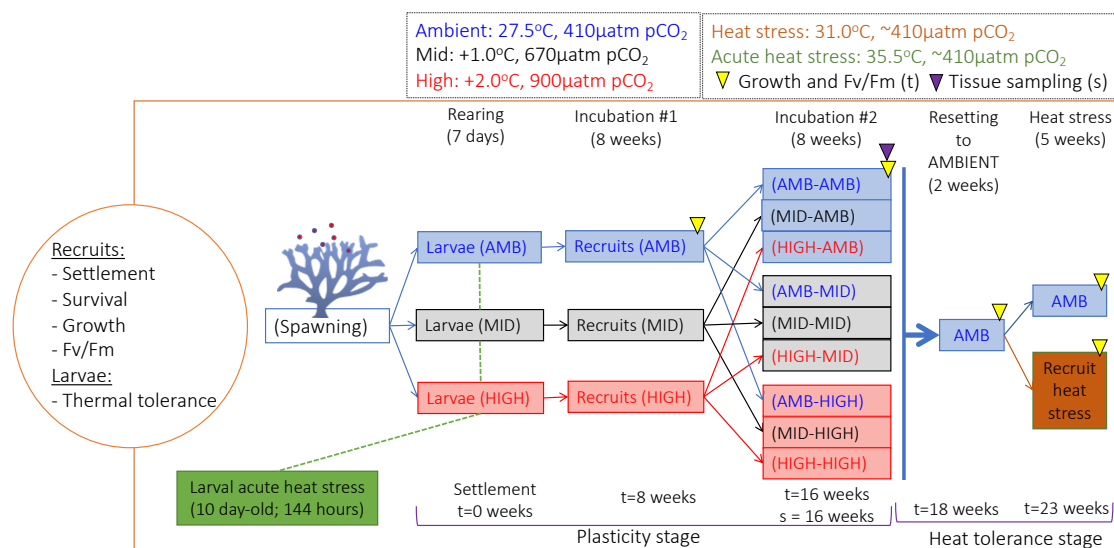


Figure 3. 1 Experimental design used to assess the potential for beneficial acclimation and thermal hardening in the early life stages of the coral *Acropora loripes*. Incubation times in weeks (t) and tissue sampling point (s) are also included.

Colonies were isolated in individual tanks in the dark without water flow on the night of spawning. After spawning, the positively buoyant gamete bundles were collected from the water surface and eggs and sperm from each colony were separated using filtration (120 µm mesh size) and gentle agitation. Equal proportions of eggs and sperm from all fourteen spawning colonies were mixed to produce two individual batch cultures for each of the treatments (i.e. fertilised using water from the corresponding treatment). Each batch fertilisation contained approximately 75,000 eggs in 6.5 L volume and a sperm density of 10⁶ per ml (Willis et al., 1997). After one hour (just prior to or at the time of first cleavage) each batch fertilisation was thrice rinsed in treatment specific FSW then stocked

at 1 larva/mL in two replicate 65 L rearing tanks in each of the three treatment conditions. Rearing tanks received water-flow of 2.5 L/min FSW, an outflow covered by a 60 μm filter and constant airflow, which was started 24h post-fertilisation. Although these batch cultures were treated similarly, it is important to acknowledge that differences in temperature and $p\text{CO}_2$ conditions may have selected for different genotypes, resulting in genetic differences in the larval pools of the three treatments. Larvae reared under each treatment were used for two separate experiments, as described below.

3.3.3 Acute heat tolerance of coral larvae

After ten days of rearing, swimming larvae were haphazardly sampled from each treatment. Twenty larvae per treatment were placed in 24 replicate mesh bottomed containers (net-wells) (i.e. larvae = 480, n=72 net-wells total). Larvae were assumed to be aposymbiotic. The wells were floated on four 50 L tanks (i.e., with turnover flow of FSW of 0.8 L/min) in an arrangement of six wells per holding-tray containing two wells from each treatment (n = 3 holding-trays per tank). All larvae were first acclimated to AMBIENT conditions for one hour in all tanks. After the short acclimation, the temperature was increased in two tanks by 1°C per hour over eight hours until 35.5°C was reached, whereas AMBIENT temperature of 27.5 °C was maintained in the other two tanks. The $p\text{CO}_2$ level was maintained at ~450-500 μatm CO_2 in all four tanks. Survival was measured from repeated visual counts of remaining larvae every 12 hours for five days.

3.3.4 Settlement and follow up of recruit development

At seven days post fertilization approximately 1500 larvae were settled onto wax-coated ceramic plugs (1.2 cm in diameter) contained within trays (i.e., one tray per 50 L tank, 12 tanks per treatment, 36 trays). Prior to settlement, full trays were deployed at the bottom of 50 L acrylic tanks whereas approximately 1 g of crushed crustose coralline algae (CCA) was both sprinkled and embedded on all plugs as a cue to induce larval settlement; each tray had three subsections with a total of 195 plugs to allow for reciprocal transplantation movements. Pumps were turned on 24 hours post settlement to allow for adequate FSW circulation. A total of six *A. loripes* adult coral fragments, previously acclimatised to each treatment conditions (i.e., sourced from chapter 4, >6 months), were deployed into each tank according to treatment to allow for the new recruits to gain photosynthetic algae and bacteria via horizontal transmission in addition to maternal transfer. Settlement was estimated by counting the total number of coral-settled recruits on each tray after one week when attachment of settlers was stronger. Recruits were grown for a 23-week period that included two experimental stages.

In brief, to evaluate the potential for beneficial acclimation via phenotypic plasticity of coral early life stages under simulated climate scenarios, recruits were first incubated under the same chronic conditions: AMBIENT, MID, or HIGH in accordance with rearing condition (Fig 3.1; Incubation #1). All these treatments were then reciprocally transplanted, which resulted in nine treatment histories (e.g., HIGH-AMBIENT) (Fig. 3.1; Incubation #2). After 16 weeks all recruits were returned to ambient conditions for a period of two weeks. To evaluate if hardening of heat tolerance occurred, recruits from each of the treatment histories were then exposed to heat stress (31 °C) for five weeks (Fig. 3.1, heat stress). Performance of recruits under heat stress was compared to their replicated counterparts maintained under AMBIENT for the duration of the heat stress experiment. The experimental set-up consisted of 36 (50 L) indoor tanks (3 treatments x 12 replicate tanks) receiving water-flow of 0.8 L/min FSW, artificial light (150-260 $\mu\text{E m}^{-2} \text{s}^{-1}$) and daily feeds with an *Artemia* density of 0.5 nauplii/ml. The acute heat stress stage used 36 x 50 L indoor tanks (2 treatments x 18 replicate tanks) receiving a flow of FSW of 0.8 L/min, and similar artificial light spectrum and feeding regimes.

3.3.5 Recruit performance under chronic conditions

A common garden experiment was used to assess the response of corals to treatments, before and after transplantation (Fig. 3.1). Changes in growth rate and photosynthetic efficiency were recorded eight and 16 weeks after settlement ($t = 0$ weeks). For the first eight weeks ($t = 8$ weeks; incubation #1), each treatment was represented by 12 trays that could be further split into three smaller trays (i.e., third trays). For the second eight weeks ($t = 16$ weeks; incubation #2) each one of the 1/3rd trays was distributed into the other two conditions resulting in nine treatment histories, each represented by duplicated 1/3 trays with replicate 55 plugs. In addition, ten individual recruits per treatment history per 1/3 tray were snap-frozen with LN₂ at the end of incubation post transplantation ($t = 16$ weeks) for metabarcoding analysis (i.e., symbiont communities) to be conducted.

Basal growth was measured by the change in live tissue surface area of individual recruits and was obtained from photographs taken at $t = 0, 8$ and 16 weeks after settlement, using a frame mounted NIKON D810 camera. A total of 10 recruits per tray per treatment (12 trays by 3 treatments = 360 total) were haphazardly selected and labelled at the first time point ($t = 0$ weeks). Two eight-week time intervals were used to assess growth rates. Each recruit was manually traced using the straight-freehand line tool on IMAGEJ (version: 1.50i) (Rasband, 2012). Three replicate measures of the diameter (d) were traced and their average used to predict changes in basal growth among treatment histories over time (Pratchett et al., 2015). A numeric scale was included on each photo to transform number of pixels to mm. The basal growth rate was quantified by calculating the proportional change

in diameter of live recruits between timepoints ($\log_{10} \left(\frac{d_{t+1}}{d_t} \right)$). This resulted in two basal growth measurements: interval 1 was 0 – 8 weeks and interval 2 was 8 - 16 weeks).

In addition, photographs were used to estimate survival rates of recruits over time for each treatment. The total number of live individual recruits was recorded by visual counts at $t = 0$, and used as a baseline to estimate survival rate over time across treatment histories and experimental stages.

Photochemical performance of Symbiodiniaceae was assessed in coral recruits with Imaging Pulse Amplitude Modulated (iPAM) fluorometry and its affiliated software (Walz, Effeltrich, Germany). Measurements were obtained at the same time points as the estimates of basal growth. A total of 8 recruits per tray per treatment ($n = 288$ total, 12 trays, 3 treatments) were haphazardly selected and labelled at the first time point ($t = 0$ weeks). The iPAM can resolve at a scale of $100 \mu\text{m}$, thus allowing for accurate photosynthetic measures even for small areas of tissue (Ulstrup et al., 2008). The actinic light was calibrated with an Apogee quantum sensor (Model MQ-200, UT, USA) with the following settings: measuring intensity = 4, saturation pulse intensity = 7, gain = 1, damping = 2. Maximum quantum yield (ratio of variable to maximum fluorescence: F_v/F_m) was measured two hours after dark. Yields were calculated from the area of interest at the different time points (i.e., using the total area of live tissue), by orientating the recruits to a fixed angle in a plastic mount built for the iPAM. This methodology has been used to determine photosynthetic productivity in studies of plant physiology (Maxwell and Johnson, 2000); it reflects the efficiency of photosystem II (Krause and Weis, 1991), and is a widely accepted indicator of stress in corals (Jones and Hoegh-Guldberg, 2001).

A second experimental stage investigated the potential for enhanced thermal tolerance in 23-week old coral recruits due to stress-hardening triggered by the previous treatment history. This stage started with a 2-week pre-acclimation period ($t = 16$ to 18 weeks) where all recruits (i.e., 8 small trays, 9 treatment histories, $n = 288$) were incubated at Ambient conditions prior to the ACUTE heat stress. This procedure ensured that all recruits started from the same baseline temperature in the hardening experiment, regardless of their prior treatments. For the acute heat stress experiment ($t = 18$ to 23 weeks), half of the small trays from each treatment history were exposed to a temperature ramping of $+0.4^\circ\text{C}$ per day until 31°C was reached, and then incubated for a maximum of 35 days at which point maximum quantum yield (F_v/F_m) values declined to ≤ 0.3 . The remaining small trays from each treatment history were kept at ambient conditions for the total duration of the experiment (i.e., 4

third-trays, 18 treatment histories). Growth and Fv/Fm measurements were obtained at the end of the acclimation to ambient conditions (t = 10 weeks) and also at the end of the heat stress experiment (t=23 weeks), using the same approach as in the first experimental stage. In addition, ten individual recruits per treatment history per tray were snap-frozen with LN2 at the end of the heat stress stage (t=23 weeks) for future metabarcoding analysis (i.e., symbiont communities), but not included within this chapter.

3.3.6 Statistical analysis

3.3.6.1 Larval survival under acute heat stress

Kaplan-Meier (K-M) survival analysis was used to estimate survival rates of larvae through time by grouping all survivors at the treatment level for each timepoint. Rearing treatment (AMBIENT, MID, HIGH) and treatment during the acute heat stress (AMBIENT, ACUTE) were fixed effects. Data was analysed with the *survfit* function in the R package 'survival' (Therneau and Lumley, 2014).

3.3.6.2 Settlement and survival of coral recruits

Variation in settlement success was evaluated with a set of generalised linear mixed effect models with the function *glmmadmb* from the R package 'glmmADMB' (Fournier et al., 2012), with tank as random effect and treatment as a fixed effect. The number of recruits were log₁₀-transformed to meet the normality assumption. Bootstrapping techniques were used to generate the 95% confidence intervals.

A generalised linear mixed effects model with a binomial error structure was fitted to predict the survival of recruits among treatments at the different time intervals. The models included time, treatment and their interaction as fixed effects, and tank as a random intercept. The models were fitted using the function *glmmadmb* from the R package 'glmmADMB' (Fournier et al., 2012). All analyses were performed in R version 3.6 (Team, 2013).

3.3.6.3 Basal growth of coral recruits

Sets of linear statistical models were compared to quantify the response of proportional basal growth to treatment conditions at the different time points. Models were fitted using the function 'glmmadmb' from the package glmmADMB (Fournier et al., 2012). A second order Akaike Information

Criterion (AICc) was used to identify the best-fit model. All analyses were performed in R version 3.6 (Team, 2013). A Levene's Test was used to confirm homogeneity of variance ($p > 0.05$) for settlement and growth data.

For the beneficial acclimation data, the analysis of growth for the first 8 weeks, prior to transplantation ($t = 8$ weeks), included three models with treatment as a fixed effect and different combinations of: recruit area (log-scale) as a fixed effect, and tray or tank as random intercept. Growth during the second 8-week period was measured in all treatment combinations at $t = 8$ and 16 weeks (i.e. nine treatment histories in total) with growth as the response variable, size as a fixed factor, and tank as a random intercept. If growth at the second time point was significantly lower than at the first time point, acclimation was assumed not to have occurred. In addition, a second model was built to predict how linear growth in treatment at $t = 16$ weeks was influenced by the previous treatment ($t = 8$ weeks) and included growth at $t = 16$ as the response variable, an interaction between treatment at $t = 8$ and treatment at $t = 16$ and fragment size (log scale) as fixed effects and tank as a random intercept. A Tukey post hoc test was used to contrast the growth between different combinations of treatments at $t = 8$ and $t = 16$.

For the heat stress data, a series of models were fitted and compared to test whether acclimation to AMBIENT conditions ($t = 18$ weeks) was reached in corals from all treatment histories prior to the heat stress experiment. The models included combinations of the following variables: interaction between treatments at $t = 8$ and $t = 16$, and recruit size as possible fixed effects, plus tray nested in tank, and tank as a random intercept. For the best fit model, a Tukey *post hoc* test was used to compare growth among treatment histories. For the acute heat stress exposure $t = 23$, three statistical models were used to test for the effect of treatment at $t = 8, 16, 23$ on fragment growth at $t = 23$ weeks (i.e. HEAT STRESS vs. AMBIENT in relation to treatment history). The most complex model included a three-way interaction (as fixed effects) among treatments at $t = 8, 16, 23$, recruit size (as a fixed effect) and tray nested in tank as random intercepts. Subsequent models were a subset of this model.

To compare differences in the change in growth rates between $t = 8$ and 16 weeks among the different treatments, two models (one for each time point) were fitted in a Bayesian framework using the package 'brms' (Bürkner, 2017). The model predicting growth at 8 weeks had treatment and recruit

size (log-scale) as fixed effects and tank as a random effect. The model predicting growth at $t = 16$ weeks had treatment at 8 weeks, treatment at $t = 18$ weeks, as well as their interaction and recruit size as fixed effects, and tank as a random effect. Using these two models, I predicted growth standardised for recruit size (i.e., using the mean recruit size at $t = 16$ weeks) at each time point for each treatment history. Then, I drew samples from the posterior predictive distribution of growth at each time point and estimated the distribution of differences between time points. In brief, overlapping of the 95% credible intervals of the posterior distributions of the difference in growth between time points implied that the change in growth was not different among treatment histories. Similarly, to compare differences in growth during the acute heat stress among treatment histories, I fitted a Bayesian model predicting growth at $t = 23$ weeks with treatment at each time point ($t = 8, 16,$ and 23 weeks) and their three-way interaction, as well as recruit size (log-scale) as fixed effects, tank was included as a random effect. For each treatment history, the analysis predicted growth (with mean recruit size at $t = 18$ weeks) for the acute and control treatments at $t = 23$ weeks, and estimated the distribution of the difference in the posterior predictive distributions.

3.3.6.4 Maximum quantum yield (Fv/Fm)

A similar statistical approach to that of basal growth was used to estimate changes in maximum quantum yield (Fv/Fm) for the same experimental time points. Moreover, size and Fv/Fm were also included as fixed effects. The response variable was: $\left(\frac{Fv}{Fm}\right)_{t+1} = \log_{10}\left(\frac{Yield_{t+1}}{Yield_t}\right)$

3.3.6.5 Correlation of traits

Using the best fit models for growth and yield at week 16, I predicted the response of both traits to treatment history, standardising for recruit size and yield at the previous time point. Using the predictions, I tested for a correlation between growth and yield performance with a Spearman rank correlation. I repeated the same process to investigate correlations of the same traits during the acute heat stress stage.

3.4 Results

3.4.1 Larvae survival during acute heat stress

Rearing treatment conditions significantly influenced the survival of 10-day old larvae during a 144-hour period of exposure to 35.5°C ($p < 0.0001$, method: Log-rank). Overall, larvae reared under HIGH treatment had the highest survival probability relative to MID and AMBIENT (Fig. 3.2). Larvae from the MID and AMBIENT passed the 50% mortality threshold within 72 hours whereas with larvae from HIGH reached 50% mortality after 120 hours. Survival of larvae that were maintained under

AMBIENT was very high for all treatments and did not vary over the experiment ($p = 0.81$, method: Log-rank).

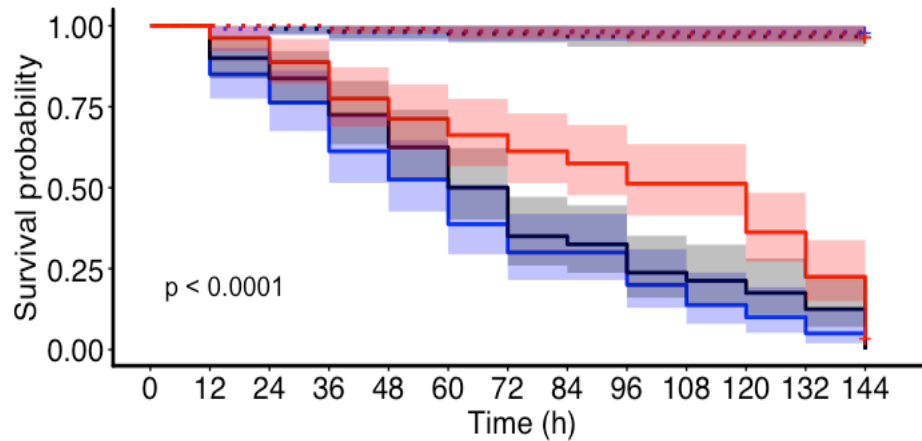


Figure 3. 2 Kaplan-Meier curves showing survival probability over time for 10-day old larvae exposed to two temperatures (27.5 and 35.5°C). Solid lines show survival of larvae exposed to acute heat stress at 35.5°C over a period of 144 hours, whereas dotted lines display survival of larvae exposed to AMBIENT water temperature (27.5 °C). Line colours represent the three rearing conditions being AMBIENT (blue), MID (black) and HIGH (red) temperature x pCO₂ scenarios.

3.4.2 Settlement success of recruits

The best-fit model included treatment at $t = 0$ and excluded tank as a random intercept (Table B.S1). There was a significant effect of treatment on recruit settlement rates ($p < 0.001$; Table B.S2; Fig. 3.3) with a total of 4600, 4865 and 6542 settled recruits in the AMBIENT, MID and HIGH treatments, respectively. Pairwise comparisons based on Tukey post hoc tests confirmed significant differences between HIGH and the AMBIENT and MID treatments ($p < 0.001$; Table B.S2), whereas the latter two did not differ (Table B.S2).

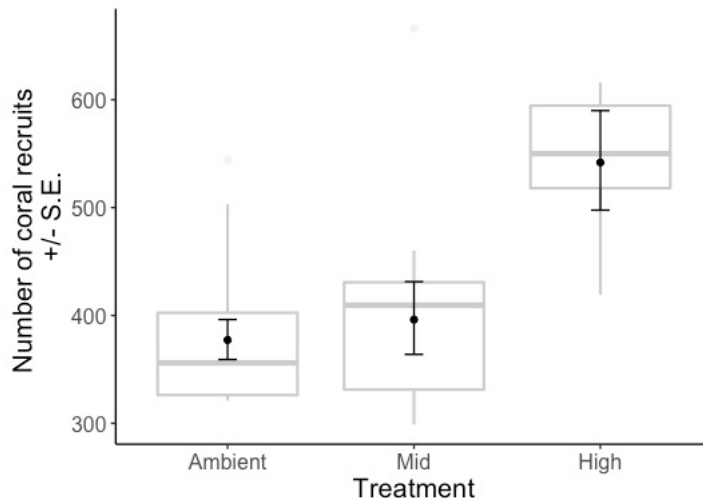


Figure 3. 3 Settlement success of coral recruits from the three treatments shown as number of recruits per tank. Black circles show the fitted model and the error bars show standard errors. The grey boxplots show the distribution of the raw data.

3.4.3 Coral recruit survival

Survival probability of coral recruits declined with increasing age of the individual (Fig. 3.4). However, the magnitude of change was found to be different at particular time points due to treatment effects. Prior to transplantation (8-week old recruits), the best fit model revealed that there was a significant effect of treatment on survival rates, with the MID treatment displaying a significantly lower survival rate (~50%) relative to AMBIENT (~60) following pairwise comparisons (Table B.S4 - B.S6). Post transplantation (16-week old recruits), the best fit model showed a significant interaction of both treatment periods on survival rates, without significant differences among any of the pairwise comparisons of treatment histories (Table B.S7- B.S9). Survival rates ranged between ~25 - 40% for all treatment histories (Fig 3.4, 8 – 16 week period). During the resetting to ambient conditions (18-week old recruits), the best fit model confirmed that survival rates depended upon treatment history (Table B.S10 - B.S12). Survivorship at this stage was approximately 30% if the previous treatment (t=16 weeks) was either AMBIENT or HIGH, and 25% if MID was experienced. During the heat stress stage (23-week old recruits), the best fit model revealed that treatment history had a significant effect on survival probability (Table B.S13 - B.S15); however, the observed survival rate ranged from 10-25% across all treatment histories, which were not significantly different relative to AMBIENT in pairwise comparisons.

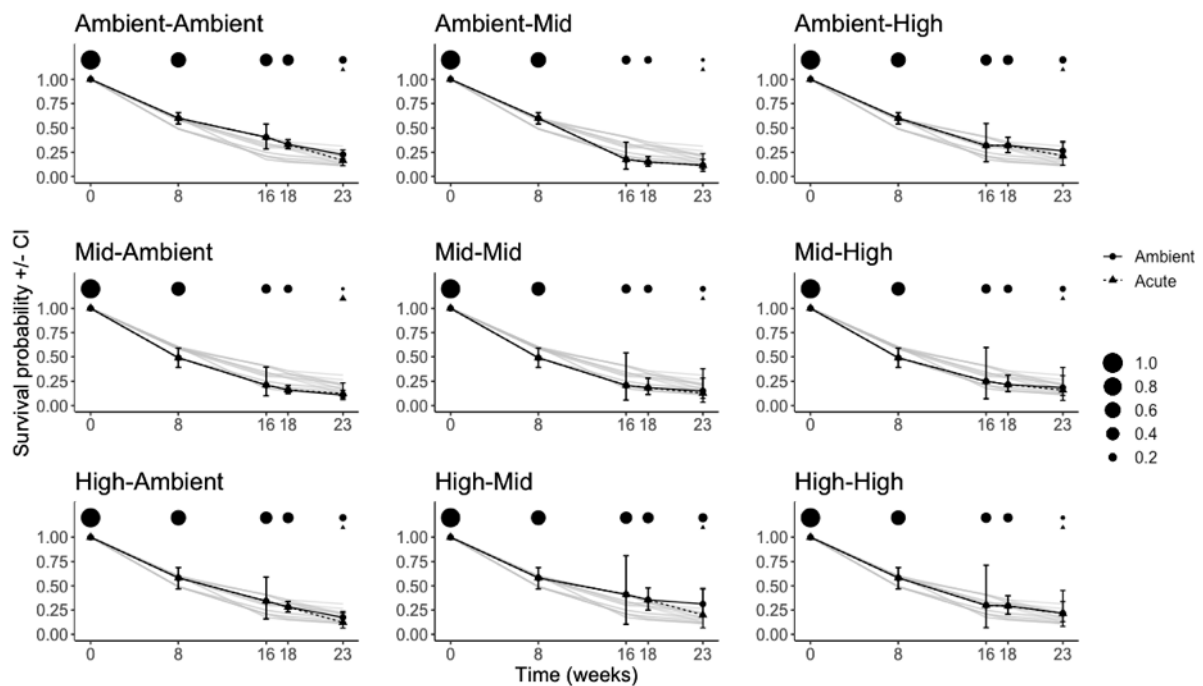


Figure 3. 4 Survival probabilities of recruits in the three treatments at 8, 16, 18 and 23 weeks post settlement and representing each of the treatment histories along the experimental stages. Error bars show 95% confidence intervals. The size of the black top circles represents the proportion of live recruits at a particular time point based on the number of raw observations. Grey lines represent raw data, whereas the black ‘decreasing lines’ is a representation of the magnitude of change between time points.

3.4.4 Coral recruit growth

3.4.4.1 Growth before and after transplantation

Growth gradually increased with age but no clear effect of treatment was detected (Fig 3.5). Prior to transplantation, the best-fit model included treatment (at $t = 8$ weeks) and size (at $t = 0$ weeks) and tank as a random effect (Table B.S16). At this experimental stage, growth was evident for all treatments with slightly higher values for HIGH treatment, however, no significant differences were observed among treatments based on pairwise comparisons. Additionally, there was a significant effect of initial size (at $t = 0$ weeks), suggesting a lower growth with increased recruit size (Fig. 3.5a, Table B.S17- B.S18).

After transplantation, the best-fit model included the interaction of treatment before (at $t = 8$ weeks) and after transplantation (at $t = 16$ weeks), and size (at $t = 8$ weeks) and tank as a random effect (Table B.S19). Growth was recorded after transplantation for all possible treatment combinations although their interaction was not significant; there was a significant effect of size (at $t = 8$ weeks) suggesting a lower growth with increased recruit size (Fig. 3.5b, Table B.S20- B.S21). Moreover, pairwise comparisons confirmed no significant differences among all possible treatment combinations despite recruits coming from MID performing slightly better across treatment histories.

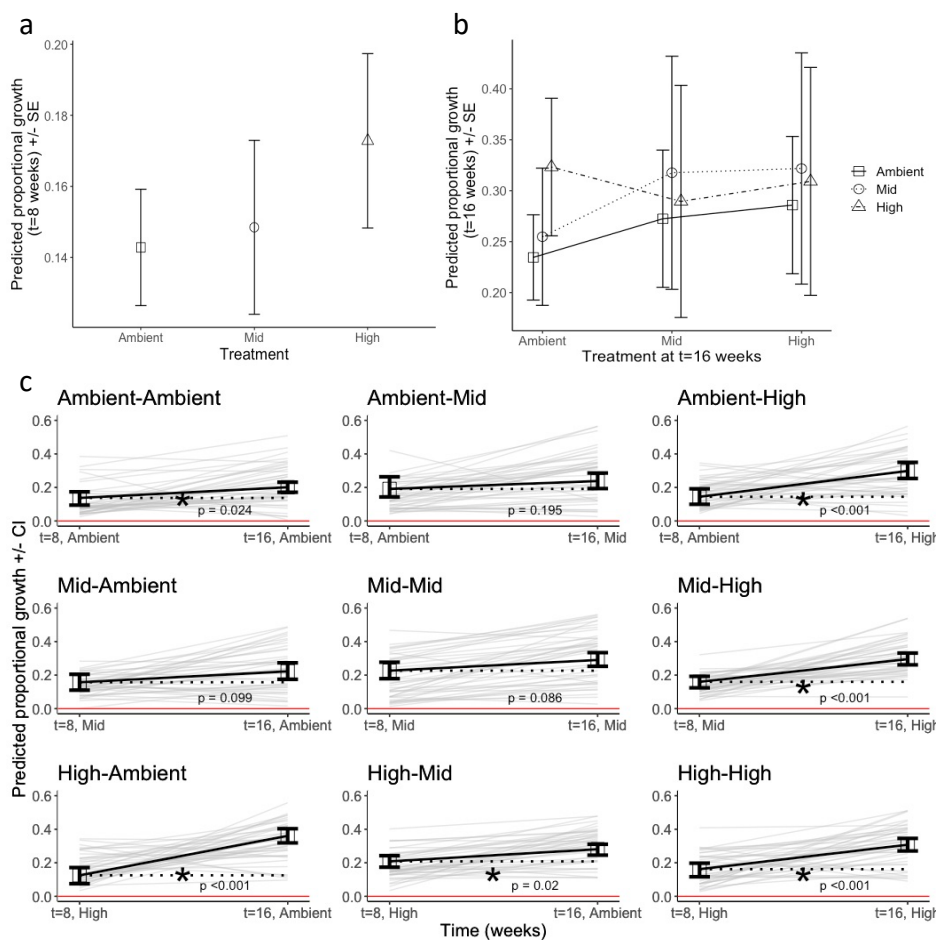


Figure 3. 5 Panel a: Predicted proportional growth between 0 and 8 weeks by the best-fit model depending on treatment at $t = 8$ weeks. Number of observations: total=360. Panel b: Predicted proportional growth between 8 and 16 weeks by the best-fit model depending on the different treatments at $t = 16$ weeks. Symbols represent origin treatment whereas x-axis distribution represent destination treatments. Panel c: Predicted proportional growth between origin treatment at $t = 8$ in relation to linear extension at destination treatment at $t=16$ weeks. Grey lines represent variation for

individual recruits within each group. Red lines used to observe potential negative growth, whereas asterisks represent significant differences on mean estimates.

Individual models (i.e., based on best-fit), found that 16-week old recruits could sustain or enhance their growth rate after transplantation (Fig. 3.5c). However, there was not a clear effect of treatment on growth. Consequently, it was not possible to detect a consistent pattern of phenotypic plasticity underpinning a beneficial response. For example, even under the most challenging destination treatment (i.e., HIGH at $t = 16$ weeks), recruits coming from MID and AMBIENT showed similar growth rates to recruits that previously experienced HIGH treatment (at $t = 8$ weeks), and all of them grew more relative to the previous experimental interval. Growth data also revealed that growth increases with increasing treatment conditions following transplantation. In fact, the baseline treatment history (AMB-AMB) had proportional growth around 0.019 and 0.025 mm week^{-1} for 8 and 16-week old recruits (0.975 and 1.3 mm yr^{-1} , respectively), but growth had the potential to double, up to around 0.05 mm week^{-1} (2.6 mm yr^{-1}), when recruits experienced higher temperatures in combination with CO_2 (e.g., AMB-HIGH). Nevertheless, this is more likely evidence of a carryover effect, where corals initially in the HIGH treatment grew better in AMBIENT during the second time interval (HIGH-AMB) than corals staying in AMBIENT conditions (AMB-AMB). Overall, there was no significant influence of elevated treatment conditions in growth, despite the tendency observed around higher temperatures promoting growth. Indeed, the Bayesian analysis performed using differences in posterior distribution of growth rate estimates between destination ($t = 16$ weeks) and origin ($t = 8$ weeks) treatment, confirmed little evidence for plasticity and no evidence of beneficial acclimation due to the large degree of overlap observed across treatment histories (Fig. 3.6a). In other words, growth rate tended to increase after transplantation, but the confidence was low to moderate. Hence, changes in treatment conditions due to transplantation of recruits did not generate enough effects on growth to provide a clear signal of plasticity.

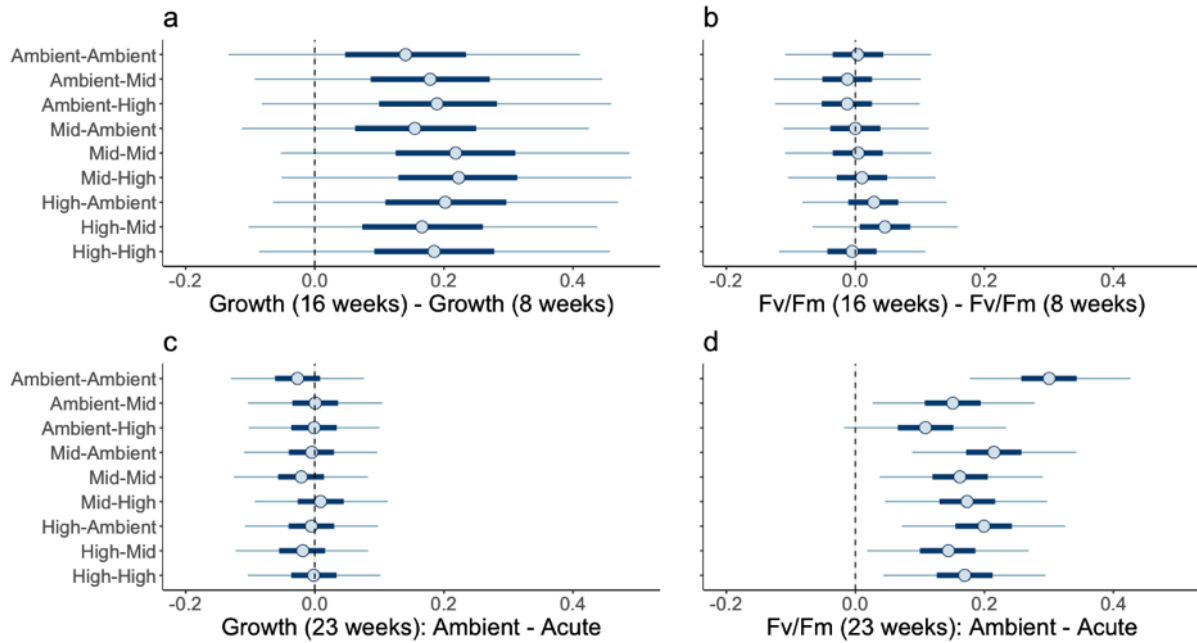


Figure 3. 6 Differences in the posterior distributions of models predicting growth and Fv/Fm relative to experimental time points and treatment histories. Panel a: Difference between growth measured at $t = 16$ weeks and growth measured at $t=8$ weeks. Panel b: Difference between Fv/Fm at $t=16$ weeks and Fv/Fm at $t=8$ weeks. Panel c: Difference in growth at $t=23$ weeks between Ambient and heat stress treatment. Panel d: Difference in Fv/Fm at $t=23$ weeks between Ambient and heat stress treatment.

3.4.4.2 Growth during heat stress exposure

Growth rates of 18-week old coral recruits were similar during the two-week resetting period to ambient conditions before the heat stress stage (Fig. B.S1). The best fit model included the interaction of treatment at $t = 8$ and 16 weeks, and size at $t = 16$ weeks, plus tray nested in tank as a random effect (Table B.S22). The interaction of origin and destination treatments (i.e., treatment history) did not have a significant effect on the growth rate observed during the resetting period and no significant differences were found in any of the pairwise comparisons (Fig. B.S1, Table B.S23- B.S24). Size (at $t = 16$ weeks) had a significant effect on growth during the resetting, with lower rates observed for larger recruits.

Growth rate was not significantly different between ambient and heat stress conditions in 23-week old recruits (Fig. 3.7). The best fit model included the interaction of previous treatments ($t = 8,$

16 weeks) with treatment at $t = 23$ weeks, and size (at $t = 18$ weeks), and also tank as a random effect. The interaction of previous treatments was not significant, although size (at $t = 18$ weeks) had a significant effect on growth rate, with lower rates observed for larger recruits. Estimates of pairwise comparisons confirmed no significant differences among any of the relevant treatment history combinations, averaging a growth rate of ~ 0.1 mm for all of them (Fig. 3.7, Table B.S26- B.S27). Finally, differences in posterior distribution of growth rate estimates between destination ($t = 16$ weeks) and origin ($t = 8$ weeks) treatment, confirmed that recruits were likely to maintain similar growth rates under heat stress relative to ambient conditions, without particular treatment histories performing significantly better than others (Fig. 3.6c). Hence, there was no evidence of a clear effect of treatment on growth even under intensified thermal stress, suggesting that heat stress conditions did not impair the growth performance of 23-week old recruits, but also limiting the detection of plasticity and the potential for beneficial acclimation.

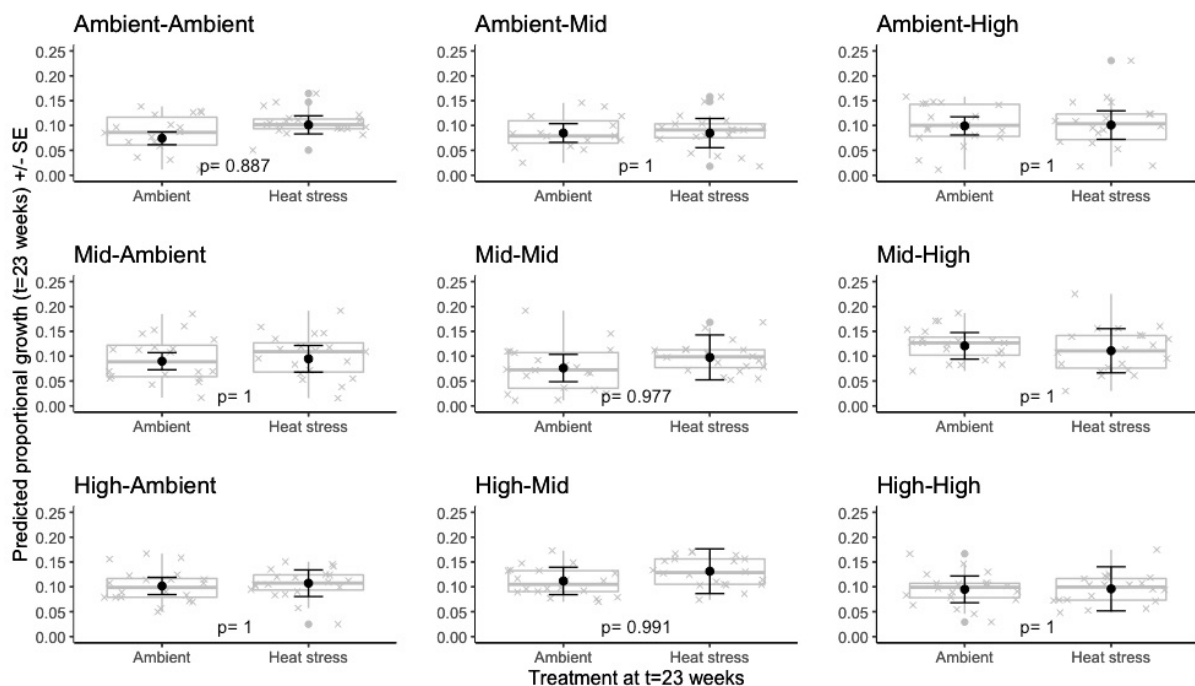


Figure 3. 7 Predicted proportional growth between 18 and 23 weeks for heat stress and ambient treatment at $t=23$ weeks, considering each treatment history that followed transplantation. Box plots show the distribution of the raw data, grey crosses show the raw data and black points with error bars show the fitted model predictions with the associated standard errors.

3.4.5 Photochemical efficiency (F_v/F_m) across experimental stages

3.4.5.1 F_v/F_m before and after transplantation

Differences in F_v/F_m of coral recruits, although subtle, were only evident at the treatment level following transplantation. Prior to transplantation the 8-week old recruits displayed similar F_v/F_m (Fig. 3.8a), based on the best-fit model that included treatment (at $t = 8$ weeks) and yield (at $t=0$ weeks), plus tank as a random effect (Table B.S28). The best-fit model revealed that treatment did not have a significant effect on the yield at $t = 8$ weeks, which was confirmed by no significant differences found for any of the treatments in pairwise comparisons (Table B.S29- B.S30). Moreover, there was a significant effect of F_v/F_m recorded at $t = 0$ weeks over the F_v/F_m measured at $t = 8$ weeks.

Following transplantation, the 16-week old recruits displayed similar yield values irrespective of treatment history (Fig. 3.8b). Here, the best-fit model included the interaction of treatments at $t = 8$ weeks and $t = 16$ weeks, plus tank as a random effect (Table B.S31). The model revealed that the interaction was not significant, and that the majority of treatment combinations were not significantly different following a pairwise comparison (Table B.S32- B.S33); the exception was a significantly different yield between HIGH-MID vs. HIGH-HIGH. Moreover, there was a significant effect of F_v/F_m observed prior to transplantation, as higher F_v/F_m was likely to occur at $t = 16$ weeks if F_v/F_m was already higher at $t = 8$ weeks. Interestingly, recruits coming from MID treatment had a slightly higher yield relative to any of the possible treatment combinations generated post transplantation, particularly with HIGH as the destination treatment.

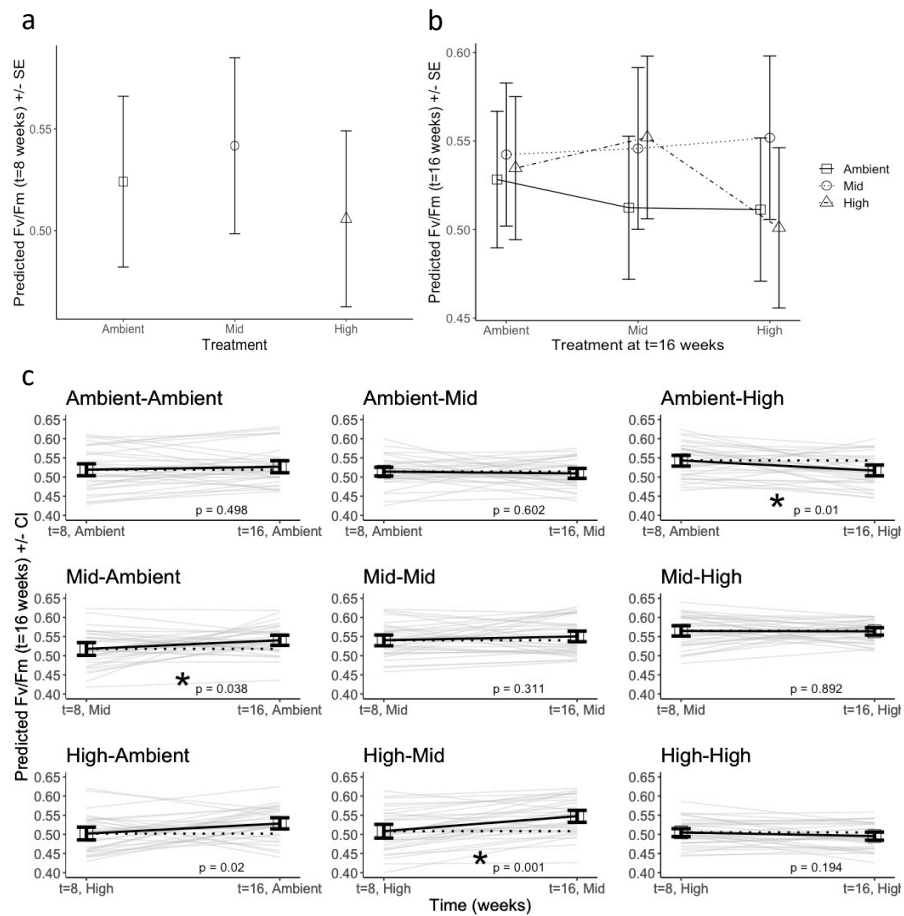


Figure 3. 8 Panel a: Predicted Fv/Fm at t=8 weeks by the best-fit model depending on treatment at t=8 weeks. Number of observations: total=288. Panel b: Predicted Fv/Fm by the best-fit model at t=16 weeks for the different treatments. Symbols represent origin treatment whereas x-axis distribution represent destination treatments. Panel c: Predicted Fv/Fm between origin treatment at t = 8 in relation to Fv/Fm at destination treatment at t = 16 weeks. Grey lines represent variation for individual recruits within each group, whereas asterisks represent significant differences on mean estimates. Dotted lines represent a graphic extension of the Fv/Fm values observed during t=8.

Subtle evidence for beneficial acclimation was detected following a more detailed analysis of Fv/Fm data, including individual treatment histories. Individual models (i.e., based on the best-fit model), showed that Fv/Fm from 16-week old recruits was not necessarily sustained or enhanced after transplantation, and in fact treatment history played an important role (Fig. 3.8c). Indeed, a significantly lower Fv/Fm was observed after transplantation when recruits were moved from Ambient to higher levels of stress under treatment conditions (AMBIENT-HIGH). For example, an increasing negative slope was detected with increasing treatment conditions (i.e., AMB-HIGH>AMB-MID>AMB-

AMB). However, the negative slope became neutral if recruits had a prior exposure to elevated treatment conditions (MID or HIGH), with the resulting Fv/Fm values displaying similarities with what would be expected for the treatment history acting as a control (AMB-AMB). Moreover, it was also possible to detect subtle evidence of reversibility of the acclimatory response, due to the positive slope observed when transplantation occurred from more to less intense treatment conditions (e.g., HIGH-AMB). In addition, differences in posterior distribution of Fv/Fm estimates between destination (t = 16 weeks) and origin (t=8 weeks) treatment, confirmed that recruits were likely to maintain their photosynthetic efficiency over time under the same treatment, and that the yield can be expected to be lower or higher depending on whether treatment conditions worsen or improve, respectively (Fig. 3.6b). Hence, changes in treatment conditions following transplantation allowed the detection of plasticity in Fv/Fm, although the evidence for beneficial acclimation and its reversibility was only subtle.

3.4.5.2 Fv/Fm during heat stress exposure

Fv/Fm values were similar for 18-week-old juveniles by the end of the two-week resetting period to AMBIENT conditions (Fig. B.S3). The best fit model included the interaction of treatment at t = 1 (8 weeks) and treatment at t = 2 (16 weeks), and size at t = 2 (16 weeks) as fixed effects, plus tray nested in tank as a random effect (Table B.S34). The interaction of treatments before and after transplantation was not significant, and none of the treatment combinations had significant differences following a pairwise comparison (Table B.S35- B.S36); Fv/Fm at the previous time point (t = 16 weeks) had a significant effect over the Fv/Fm observed during the resetting period, although the effect applied for all treatment histories.

Following heat stress exposure, the 23-week old recruits displayed a significant lower Fv/Fm relative to AMBIENT, irrespective of their treatment histories (Fig. 3.9). The best fit model included the interaction of previous treatments (t = 8, 16 weeks) with treatment at t = 23 weeks), and size (at t = 18 weeks) as fixed effects, plus tank as random effect (Table B.S37). The best-fit model revealed that the interaction of treatments (i.e., treatment history) had a significant effect on Fv/Fm at t = 23 weeks. Pairwise comparisons confirmed significant differences between Fv/Fm of recruits under heat stress vs. AMBIENT coming from the same treatment history (Table B.S38- B.S39). Moreover, yield at the previous stage (t = 18 weeks) had a significant effect on the Fv/Fm at t = 23 weeks. Overall, 23-week old recruits under AMBIENT showed Fv/Fm values ranging from 0.5 to 0.6, whereas Fv/Fm for recruits

under heat stress ranged from 0.2 to 0.45. Finally, differences in posterior distribution of growth rate estimates between the second ($t = 16$ weeks) and the first ($t = 8$ weeks) treatment period, confirmed that recruits were likely to reduce their performance based on Fv/Fm estimates under heat stress, with particular treatment histories performing significantly better than others (Fig. 3.6d). Recruits from treatment histories which included more challenging treatment conditions (e., MID, HIGH) performed similar under heat stress treatment, although they were all significantly different to recruits with an AMBIENT-AMBIENT treatment history, which displayed the lowest values of Fv/Fm by the end of the heat stress exposure. Hence, past exposure to MID and HIGH treatments, before or especially after transplantation, improved Fv/Fm performance compared with control corals (AMB-AMB) exposed to heat stress, which is evidence of a hardening response triggered by prior exposure to more intense treatment conditions earlier in the experiment.

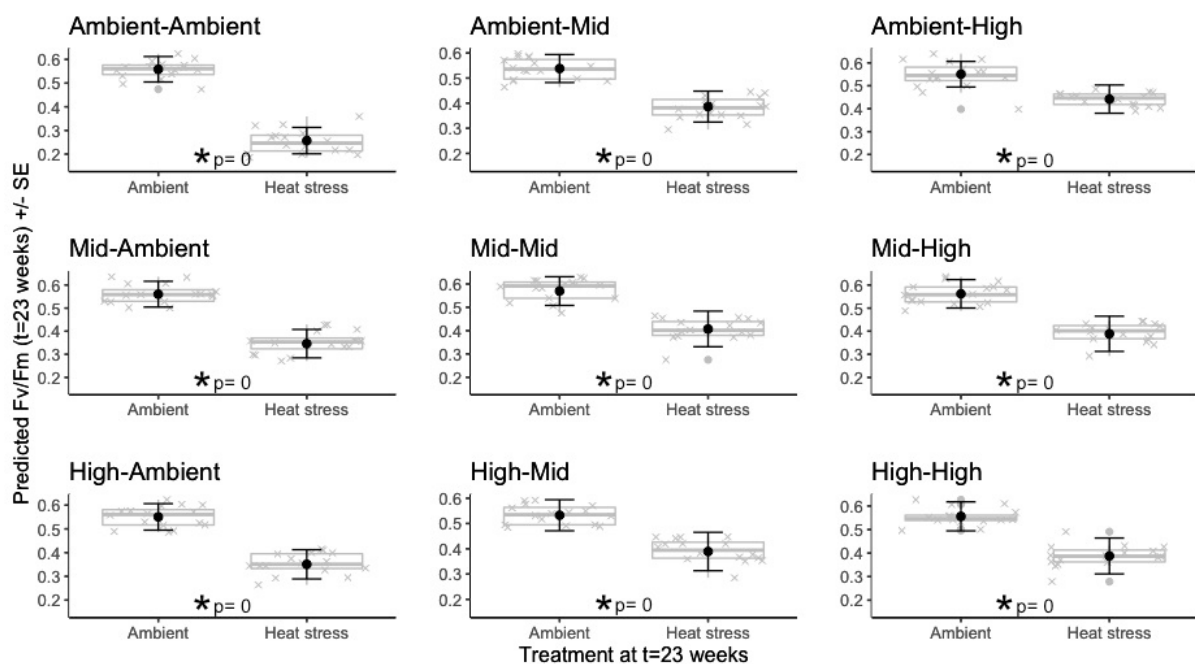


Figure 3. 9 Mean Fv/Fm at t=23 weeks for ambient and heat stress treatment, considering each treatment history that followed transplantation. Box plots show the distribution of the raw data, grey crosses show the raw data and black points with error bars show the fitted model predictions with the associated standard errors.

3.4.6 Correlation between growth and Fv/Fm

No correlation was found between growth and Fv/Fm during the heat stress exposure (Fig.3.10b). Nevertheless, it is important to consider that growth and Fv/Fm measures were not necessarily generated from the same recruit. Similarly, the growth rate observed in 16-week old recruits was not correlated to Fv/Fm values recorded after transplantation occurred (Fig. 3.10a).

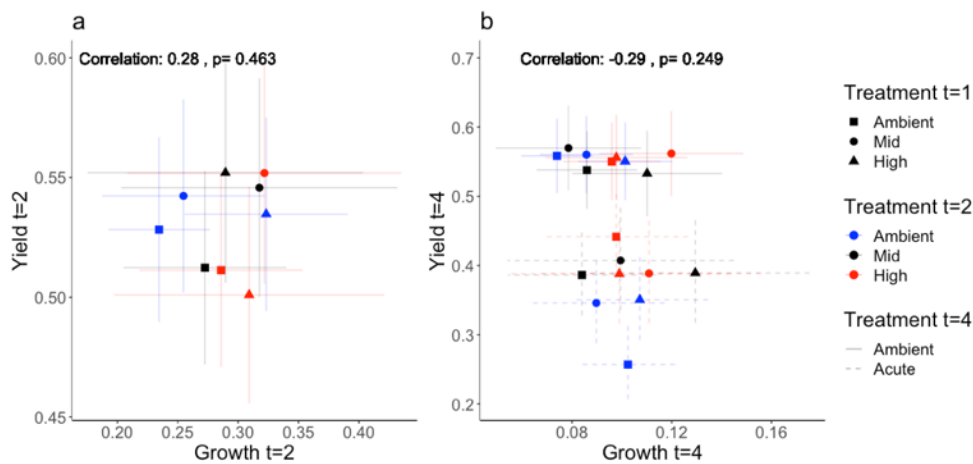


Figure 3. 10 Correlation between estimates from the best-fit models estimating yield and growth at t = 16 and t = 23 weeks. Panel a: Estimates of growth relative to Fv/Fm at t = 16 weeks. Panel b: Estimates of growth relative to Fv/Fm at t = 23 weeks.

3.5 Discussion

Phenotypic responses of early life stages of coral to a combination of elevated temperature and $p\text{CO}_2$ were assessed under controlled laboratory conditions. Enhanced thermal tolerance was detected in larvae under acute heat stress, whereas chronic exposure to elevated treatment conditions did not affect post-settlement survival rates. Subtle evidence of beneficial acclimation was detected in Fv/Fm, in addition to the greater tolerance to heat stress due to prior exposure to elevated treatment conditions (i.e., hardening). There was no clear effect of treatment on the growth of recruits, even under heat stress conditions.

3.5.1 Thermal tolerance of larvae under heat stress

The effectiveness of the larval heat stress experiment in my study was demonstrated by the significant mortality observed relative to AMBIENT conditions. Survival rates of larvae under heat stress also differed among treatments. Indeed, exposing larvae to elevated climate change conditions

provided some level of preparation – physiological or genetic - that allowed larvae from HIGH to display a 50% survival at 120 hours of exposure relative to 48h in the larvae from the AMBIENT treatment. This is likely a stress-hardening response where prior exposure of an organism to similar non-lethal environmental conditions, can induce increase tolerance to that stress, leading to enhanced performance when subsequently facing similar or even more extreme conditions (Bowler, 2005, Sinclair and Roberts, 2005). Since larvae were assumed to be aposymbiotic (i.e., lack of external inoculation) and each of the batch cultures were obtained from the same parental colonies following the same breeding protocol, I infer that the stress-hardening comes from the host. Indeed, the host could have relied on the differential expression of beneficial genes during heat stress, from which a higher heat tolerance has been attributed to ‘frontloaded’ genes (i.e., elevated baseline expression of stress response genes primes the organisms for stress) (Barshis et al., 2013, Dixon et al., 2015), and consequently promoting the production of heat shock proteins or antioxidant enzymes (Rodriguez-Lanetty et al., 2009), although the exact nature of the underpinning mechanisms remain unclear.

Despite larvae from all treatments being reared for the same period of time prior to heat exposure, it is also possible that the increased water temperature during rearing had a positive effect by accelerating the development of larvae as observed in other acroporids (Negri et al., 2007, Heyward and Negri, 2010, Chua et al., 2013b); for instance, increasing the likelihood of finding stronger phenotypes when subsampling larvae for the heat stress experiment. In contrast, studies have also found negative effects of increased temperature in fertilization rates (Albright and Mason, 2013) and an increased rate of embryonic abnormalities, leading to higher mortality rates (Keshavmurthy et al., 2014, Randall and Szmant, 2009b). Indeed, studies in other *Acropora* spp. have shown that a 4 °C increase in temperature can decrease larval survival by ~60% (Randall and Szmant, 2009a). Despite using 8 °C above the ambient baseline temperature, a similar mortality rate was observed after five days under thermal stress on larvae from the HIGH treatment and after three days for AMBIENT, suggesting that differences in survival probabilities were a function of treatment and not necessarily due to larvae failing to properly develop. In addition, I also confirmed that reduction in $p\text{CO}_2$ did not have a significant effect on survival of larvae, as corresponding individuals from the different treatments maintained under AMBIENT were not affected for the duration of the experiment. Hence, stress-hardening can be induced in coral larvae after a short rearing period to enhance thermal tolerance. Although the mechanisms involved remain unclear, it would be interesting to explore how this can be used to increase the survival probabilities of larvae facing heat waves following spawning events, particularly due to the importance of vertically transmitted thermo-tolerant Symbiodiniaceae (Kenkel and Bay, 2016, Quigley et al., 2016, Robison and Warner, 2006), and epigenetic mechanisms

like DNA methylation that can play a role in transcriptional plasticity promoting stress hardening (Dimond and Roberts, 2016, Liew et al., 2018, Putnam et al., 2016). Importantly, it is possible that individual treatment conditions (temperature, pH) may have induced selection on the gamete pool (Przeslawski et al., 2015). Hence, future studies should investigate if alleles might have been selected due to elevated treatment conditions during the larval rearing period. In this context, the spare larval samples obtained during the rearing period with 12-hour intervals could potentially be used for an analysis of SNPs to investigate if there was differential selection on genotypes among treatments.

3.5.2 Settlement, survival, growth and Fv/Fm of coral recruits

Higher rearing temperature increased settlement success of larvae whereas survival rates of recruits were not affected by transplantation history among treatment, nor impaired during the heat stress stage. Temperature is one of the factors that can influence settlement success of coral larvae, acting in some instances synergistically with other stressors like low water quality and a lack of appropriate substratum availability (Erftemeijer et al., 2012, Richmond et al., 2018). Although elevated temperatures and low or variable pH has been linked to reduced recruitment (Viyakorn et al., 2015, Randall and Szmant, 2009b, Caroselli et al., 2018), in other cases, settlement of *Acropora* species was not impaired by stressors like low pH (Chua et al., 2013a). Despite controlling treatment parameters in the aquaria, it is possible that there were differences in the bacterial biofilms (i.e., chemical inducers) rapidly generated under each treatment condition, which could have inhibited or promoted settlement (Sharp et al., 2015, Tran and Hadfield, 2011, Webster et al., 2004), although my set-up and methodology was consistently similar among treatment conditions. Hence, the current results suggest that elevated temperature and $p\text{CO}_2$ can increase settlement rates, but additional steps including an assessment of healthy larval development and biofilm sampling should be undertaken to further support this conclusion. Settlement rates were different from chapter 2, where all treatments performed similarly, however, chapter 3 was based on a different batch of parental colonies and with higher level of replication to account for additional factors influencing settlement success.

Following the survival of recruits over time revealed that mortality rates were not different among treatments or treatment histories. Post-settlement is one of the most critical and challenging stages for coral recruits with a range of biotic and abiotic stressors influencing their survival (Ferrier-Pages et al., 2000, Traçon, 2013). In this study, additional stressors that can increase mortality rates post settlement (e.g., sediments, overgrown algae or grazing) were controlled for and the mortality rate declined over time. Indeed, 8-week old recruits from all treatment conditions and combinations

had a survival rate of 50 - 60%, whereas the survival probability for 16-week old recruits ranged from 25 - 40%. These estimates are within similar ranges reported in previous studies: survival rates of 30% in 8-week old recruits and a stable 5% survival rate 5 months post-settlement *in situ* (Cruz and Harrison, 2017), or as high as 95% survival rate in 5-day old recruits under *in vitro* ambient temperature of 26°C (Nozawa and Harrison, 2007). Survival rates shifting with life stage and size could be due to smaller recruits being more susceptible to accidental grazing relative to recruits that managed to reach a juvenile stage after a few months (Traçon, 2013, Davies et al., 2013). However, my results suggest that survival rates steadily decline over time, even when other factors were removed, and most importantly, that the rates are not influenced by exposure to elevated levels of ocean warming and acidification. Remarkably, survival rates of 23-week old recruits under ACUTE heat stress (i.e., 4°C above ambient conditions and accumulated 4.97 DHW, assuming a bleaching threshold of 29.8°C at Davis Reef) were similar (10 - 25%) to AMBIENT, and that was true for all possible treatment histories. My results are consistent with other studies that show limited survival of recruits (5%) when they were exposed to temperatures +6°C above their ambient, or as high as 80% at 31°C (Nozawa and Harrison, 2007), although the species and the actual DHW from each location played an important role. Thus, survival rates of coral recruits can be sustained even under elevated temperature and $p\text{CO}_2$ relative to ambient conditions, suggesting that selection of genotypes is likely occurring during development at a similar rate among treatment histories.

In addition to settlement success and survival, growth is a commonly used trait to assess reef population dynamics and determine how it correlates with recovery capacity following disturbances (Edmunds and Elahi, 2007, Hughes et al., 2003, Babcock, 1991). As many factors can influence coral recruit growth (Traçon, 2013, Wilson and Harrison, 2005), it is important to understand how the combination of elevated temperature and acidification will affect growth and development in newly settled recruits (Edmunds, 2007). Previous studies have shown that elevated temperature and $p\text{CO}_2$ can have a negative effect on growth rate, from which elevated $p\text{CO}_2$ has been shown to delay early development in other *Acropora* spp. (Yuan et al., 2018). However, in this study growth rate of recruits was similar before and after transplantation, with higher temperature acting as a promoter of growth especially during the first four weeks. Yet, treatment conditions and their combinations that followed transplantation, did not have a significant effect on growth to allow a clear detection of plasticity, therefore limiting the detection of beneficial acclimation. This suggests that the observed patterns of growth are more likely related to a basic physiological response due to the stimulus triggered by increased temperature (i.e., as per environmental gradients) (Anderson, 2016). In fact, weekly growth rates were up to twice the magnitude when recruits from higher temperature and $p\text{CO}_2$ conditions

prior to transplantation were transplanted to ambient conditions. These results are similar to the increased growth rate observed in early life stages of some species of coral following sub-lethal increases in temperature (Edmunds, 2005). The growth rate that I observed for AMBIENT is lower compared to the rate of 3 mm yr⁻¹ recorded in other studies (Edmunds, 2007), highlighting large variation among species and environments (Conlan et al., 2017). Importantly, it is also possible that current ambient conditions are becoming more challenging for coral recruits to develop, and if growth rates are declining due to the challenges presented by ongoing rapid climate change, the consequences could include populations failing to sustain genetic diversity (i.e., less colonies managing to reach sexual maturity) (Doropoulos et al., 2012b). Finally, the growth rate of 23-week old coral under acute heat stress did not differ from ambient, which could, to some extent, be explained by enhanced thermal tolerance in the coral host via molecular mechanisms (Mayfield et al., 2014, Mayfield et al., 2012). While the full extent of mechanisms contributing to host tolerance remain unclear, the host genotype is likely playing a primary role in sustaining growth in spite of challenging temperature and pCO₂ conditions. However, as recruits continue to growth it will also be important to recognise the importance and role of their symbiotic associations.

Photochemical efficiency (Fv/Fm) is likely to be modified when temperature changes (Jones and Hoegh-Guldberg, 2001). Such change can be a reflection of changes in the community structure towards more tolerant Symbiodiniaceae or increased oxidative stress due to thermal stress (Karim et al., 2015). When evaluating photochemical efficiency of Symbiodiniaceae in coral recruits, I found subtle evidence of plasticity underpinning beneficial acclimation. Fv/Fm values decreased with increasing treatment conditions that followed transplantation, represented by subtle increase in the negative slope when comparing before and after Fv/Fm values. However, prior exposure to elevated treatment conditions dampened the negative effect of treatment, such that even under the most intensified treatment conditions, the slope was found to be neutral and in accordance to expected Fv/Fm for ambient conditions. These results suggest that previous exposure to similar stress levels of temperature and pCO₂ improved the Fv/Fm following transplantation and is considered evidence, although subtle, of beneficial acclimation. Moreover, Fv/Fm increased when recruits from elevated treatment conditions were transplanted to less intense conditions, which suggests that the beneficial acclimation pattern can be reversed. It is possible that the underpinning mechanisms of beneficial acclimation detected in Fv/Fm of recruits are related to particular spatial-temporal changes in Symbiodiniaceae types (i.e., switching and/or shuffling) (Yorifuji et al., 2017), but could also be due to intrinsic acclimatory responses that follow the physiological adjustment of the PSII (e.g., antioxidant activity, membrane modifications) (Díaz-Almeyda et al., 2010). The lack of a strong signal of beneficial

acclimation may be explained by the continuous winnowing process of symbionts that occur in early life stages of coral, relative to a more established community in their adult counterparts (reviewed by (Thornhill et al., 2017)).

Interestingly, the reduction in Fv/Fm under heat stress depended on previous treatment exposure. Even though I expected lower Fv/Fm values under heat stress relative to ambient treatment, due to temperature-mediated damage to the photosynthetic machinery (Lesser, 1997, Jones et al., 1998, Warner et al., 1999), the extent to which photochemical efficiency was affected varied depending on treatment history. Overall, if recruits experienced any sort of exposure to higher temperature, their Fv/Fm mean values were lowered but not with the same intensity as for recruits with constant exposure to ambient conditions. This is evidence of a hardening response that enhances heat tolerance of the phenotypes (i.e., environmental history influencing the response of corals to physiological stress) (Brown et al., 2002b, Ainsworth et al., 2016). Thus, it is possible that prior exposure to elevated treatment conditions allowed the recruits to enhance their thermal tolerance due to mechanisms including the particular Symbiodiniaceae gained or augmented during the transplantation period, acclimation of the PSII machinery, beneficial bacteria facilitating acclimation, particular expression of proteins from the host, or a combination of all these mechanisms. Indeed, although the beneficial acclimation patterns are only subtle, these findings suggest that exposure to different levels of stress promotes enhanced thermal tolerance, a process of photoacclimation that could be linked to various properties of Symbiodiniaceae photomachinery and rates of electron transport (Warner et al., 2010).

3.5.3 Conclusions

The resilience of corals will continue to be challenged by rapid climate change, particularly since early life stages need to overcome additional stressors during larval and recruit stage. This study showed that preconditioning of larvae to a combination of elevated temperature and $p\text{CO}_2$ conditions, resulted in a rapid hardening response to underpin enhanced tolerance to acute heat stress. In addition, it is shown that recruits can sustain or enhance their growth rate when conditions change, but the signals generated did not allow the clear detection of plasticity nor beneficial acclimation patterns. In contrast, a more consistent effect of treatment was detected in Fv/Fm, which allowed the recognition of plasticity and the likelihood of beneficial acclimation; something that became more evident after confirming that prior exposure to elevated temperature and $p\text{CO}_2$ reduced the detrimental effect of heat stress over Fv/Fm (i.e., stress-hardening response). It is possible that genetic

selection may have occurred and/or that acclimation responses were possible due to particular symbiont associations. The current results indicate the limitations in detecting a clear signal of beneficial acclimation, potentially due to ongoing processes of recognition, winnowing and retention of symbionts during development. Finally, although transplantation seems to generate a more tolerant phenotype when recruits face heat stress events, further exploration needs to occur to assess the role of the host (e.g., gene expression profiles), together with their symbiont communities.

Chapter 4: Beneficial acclimation through preconditioning may enhance coral tolerance to acute heat

4.1 Abstract

As oceans continue to warm and acidify at an increasing rate, the survival of scleractinian corals is becoming compromised. A considerable body of research has attempted to determine how corals will respond to rapid climate change, although few studies have holistically assessed the performance of all members of the coral holobiont. Here I collected 21 genotypes (n=651 fragments) of *Acropora loripes* from Davies Reef (GBR, Australia) and established a two-stage experimental framework over a 14-week period. Firstly, I acclimated fragments of all genotypes to three environmental treatments AMBIENT (27.5°C, 410 $\mu\text{atm } p\text{CO}_2$), MID (28.5°C, 670 $\mu\text{atm } p\text{CO}_2$), and HIGH (29.5°C, 900 $\mu\text{atm } p\text{CO}_2$) for four weeks, followed by a reciprocal transplant of all acclimated fragments to all three conditions for another four weeks to evaluate the capacity for beneficial acclimation using the following traits: i) growth, ii) maximum photochemical efficiency Fv/Fm, iii) community structure of coral-associated algal symbionts (Symbiodiniaceae) and iv) community structure of the bacterial microbiome. Secondly, I explored whether treatment history influenced the thermal tolerance of *A. loripes* when exposed to four weeks of elevated temperature (31°C) after a 2-week pre-acclimation to ambient conditions. Reciprocal transplantation results showed that growth can be sustained or even enhanced during exposure to altered temperature and $p\text{CO}_2$ conditions, but the effect of treatment on growth was not strong enough to establish that beneficial acclimation occurred. Further, growth rates were not reduced at 31°C relative to ambient conditions, with treatment history AMBIENT-HIGH being the only exception, suggesting a lack of short-term sensitivity of growth to high temperature. In contrast, Fv/Fm data from the transplantation experiment showed clear evidence of beneficial acclimation, as Fv/Fm decreased with increasingly severe treatment conditions but this effect was dampened in fragments that experienced MID or HIGH conditions prior to transplantation. Fv/Fm values were significantly lower at 31°C, but this reduction was buffered in fragments that had experienced changes in treatment conditions following transplantation, confirming that the response was indeed beneficial. No significant effect of treatment history was evident in the community structure of Symbiodiniaceae or bacteria. Host genotype had the greatest effect on Symbiodiniaceae and bacterial community structure, explaining 55% and 15% of the variation, respectively. In the context of reef restoration, these results show that acclimation of corals under dynamic but controlled

environments prior to field deployment may be beneficial for inducing more temperature resilient phenotypes.

Keywords: Thermal tolerance, hardening, phenotypic plasticity, Symbiodiniaceae, bacteria, climate change.

4.2 Introduction

Marine ecosystems like coral reefs provide a range of ecological and economic benefits (Chen et al., 2015), but human-induced rapid climate warming is challenging their future (Hughes et al., 2017a). Accumulation of greenhouse gases in the atmosphere has led to increases in sea surface temperatures (0.65°C), and a pH reduction (0.1) in the ocean surface water (IPCC, 2019), with modelling suggesting that ocean basins will continue to warm and acidify under moderate (RCP4.5: 1-2°C higher, pH 0.14 to 0.15 lower) to high (RCP8.5: 2-4°C higher, pH 0.30 to 0.32 lower) emission trajectories (IPCC, 2019, Collins, 2013). Continued emissions increase the risk of more intense extreme events (e.g., marine heat waves or warmer seasons) and challenge the upper thermal limits of coral reefs (Hoegh-Guldberg et al., 2019, Fitt et al., 2001), raising concern about their future.

Scleractinian corals rely on associations with a diverse microbial community or ‘microbiome’, particularly the photosynthetic endosymbionts (family Symbiodiniaceae, formerly genus *Symbiodinium*; (LaJeunesse et al., 2018)) for their survival. However, corals are sensitive to environmental perturbations and frequently expel their photosymbionts (bleaching) when they experience water temperatures 1 - 2°C higher than the long-term average summer maximum. High temperature damages the algal photosystem II functioning, leading to oxidative stress that breaks down the Symbiodiniaceae-coral symbiosis (Warner et al., 1999, Van Oppen and Lough, 2009, Brown et al., 2000b, Baird et al., 2009, Jones et al., 2008). As a result of successive mass coral bleaching events in recent years, there has been a drastic decline in coral cover in many ocean basins, even in well-managed marine parks like the Great Barrier Reef (GRB) (De'ath et al., 2012) (Hughes et al., 2017b). Indeed, coral bleaching events driven by summer heat waves may be the norm in the coming few decades (Van Hooidonk et al., 2013, van Hooidonk et al., 2016) and ocean acidification may act synergistically with rising ocean temperatures (Anthony et al., 2008, van Hooidonk et al., 2014). Although coral communities can recover from natural disturbances when given sufficient time (Adjeroud et al., 2018, Gilmour et al., 2013), it is unlikely that genetic adaptation can keep up with the current rate of environmental change.

Acclimation through phenotypic plasticity could potentially assist corals to cope with rapid environmental changes in the short-term, while genetic adaptive processes occur over the longer term (Torda et al., 2017). Transient non-lethal stress exposure can lead to acclimation responses that enhance performance (Packard et al., 2001), for example, the enhanced thermal tolerance of plants and animals under extreme temperatures due to their prior exposure to moderately elevated temperatures (Hoffmann et al., 2003, Sinclair and Roberts, 2005), a process known as hardening. Further, prolonged exposure to moderate temperatures could trigger lasting changes in thermosensitivity (Angilletta, 2009). Reversible plasticity is the capacity of an organism to reversibly change physiological processes to compensate for environmental variability (e.g., diurnal or seasonal changes) to maintain homeostasis (Bowler, 2005, Piersma and Drent, 2003, Wilson and Franklin, 2002). Prior exposure to elevated temperatures has been shown to increase the thermal tolerance of corals in some instances. For example, repeated bleaching events caused by similar temperature and solar radiation levels have revealed how some corals are capable of enhancing their temperature tolerance and reducing their bleaching susceptibility (Brown and Dunne, 2008, Castillo and Helmuth, 2005, Dove et al., 2006, Middlebrook et al., 2008, Guest et al., 2012, Ainsworth et al., 2016). The mechanisms underpinning such increases in temperature tolerance can include coral host epigenetics and/ or changes in the associated microbiome (Torda et al., 2017).

The eukaryotic and prokaryotic symbionts of corals can vary under a range of environmental conditions and can respond rapidly to environmental change (Webster and Reusch, 2017, Blackall et al., 2015, van Oppen and Blackall, 2019). Changes in the community composition of Symbiodiniaceae can play an important role in the tolerance of corals to stress from light, temperature and other factors, thus contributing to broad disparities in thermal tolerance among conspecific host colonies, life stages and species (Berkelmans and van Oppen, 2006, Robison and Warner, 2006, Baker, 2001). For adult corals in particular, thermo-tolerant Symbiodiniaceae taxa have been linked to better coral performance and recovery under elevated temperatures (Bay et al., 2016, Oliver and Palumbi, 2009, Smith et al., 2017), confirming physiological and transcriptional responses observed in thermo-tolerant cultured Symbiodiniaceae (Levin et al., 2016). Coral-associated prokaryote communities (bacteria and archaea) have also been linked to coral holobiont function and coral fitness, as shown by correlations between bacterial community composition and holobiont phenotypes (Webster and Reusch, 2017, van Oppen and Blackall, 2019), including aspects of nutrition, defence, growth, survival and overall health (Bourne et al., 2016, Rosenberg et al., 2007); however, the functions of most coral associated bacteria

remain unknown. For example, prokaryotic communities have been found to differ in corals located at natural carbon dioxide seeps compared to those in nearby corals not influenced by the seep high CO₂ levels (Morrow et al., 2015), which suggest a potential role in the acclimation of corals to high CO₂ environments. Particular bacterial community profiles have also been linked to different bleaching susceptibility among corals, although functional roles of particular taxa remain unknown (Gardner et al., 2019, Ziegler et al., 2017). In addition, a comparative genomic study revealed that many bacterial genomes found in corals encode motifs that may have a crucial role in maintaining symbiosis and providing nutrient acquisition for the host and their eukaryotic partners (Robbins et al., 2019). And most recently, it has been hypothesized that bacteria-Symbiodiniaceae-coral relationships underpin the coral holobiont's nutrition and stress tolerance (Matthews et al., 2020). Hence, it is important that the assessment of beneficial acclimation in adult corals investigates how the various members of the coral holobiont contribute or change following exposure to climate change conditions.

The aim of this study was to test for beneficial acclimation of adult coral fragments to predicted future temperature and ocean acidification conditions. Specifically, I investigated if adult coral fragments sustained or modified their performance (i.e., plasticity promoting beneficial acclimation) by using a common garden experiment that exposed replicated fragments from each of 21 individual genotypes to all combinations of three treatment conditions. I also investigated if plasticity is reversible when elevated treatment conditions are removed, and most importantly, if the magnitude of response to extreme heat stress (31°C) was influenced by the prior exposure to a particular treatment. Plasticity was measured for a host and symbiont trait (e.g., growth rate and photosynthetic efficiency), and correlated to the Symbiodiniaceae and bacterial community composition. This comprehensive approach contributes to our understanding of the acclimation capabilities and hardening responses of adult coral fragments under simulated future climate scenarios to inform and improve predictions of future reef states, and also to enhance the potential success of coral reef restoration based on fragmentation and propagation strategies.

4.3 Material and Methods

4.3.1 Study species collection

The coral species *Acropora loripes* was selected for this study due to its common and widespread distribution, ease of identification and maintenance in aquaria. Adult colonies (21 total, <25 cm in diameter and assumed to represent distinct genotypes) were collected mid-April 2017 at 6 m depth at Davies Reef in the central Great Barrier Reef (18.83S; 147.63E) (GBRMPA permit

G11/3471.1). After collection, corals were transported to the National Sea Simulator (SeaSim) at the Australian Institute of Marine Science (AIMS) and housed in aquaria with flow-through seawater (27.5 °C; 415 $\mu\text{atm CO}_2$) simulating the environmental conditions at Davies Reef. Corals underwent a quarantine period of 4 weeks at ambient conditions prior to fragmentation. Pest screening included visual inspection and counts of *Acropora*-eating flat worms in low-pressure filtered-sea-water washes.

4.3.2 Coral propagation and experimental parameters

Each coral colony was fragmented to make 31 individual nubbins (fragments were 2 – 5 cm each; $n = 651$) using a diamond-blade band saw. The cut base was glued onto large aragonite plugs that were labelled and marked to track orientation (for photography) and genotype. This replication facilitated a statistical design where all genotypes were present in all treatments for the experiment.

To evaluate the potential for beneficial acclimation of adult coral fragments under simulated climate scenarios (i.e., *plasticity stage*), this study initially used three levels of combined temperature and $p\text{CO}_2$: 1) AMBIENT (27.5°C, 410 $\mu\text{atm } p\text{CO}_2$), 2) MID (ambient +1.0°C, 670 $\mu\text{atm } p\text{CO}_2$) and 3) HIGH (ambient +2.0°C, 900 $\mu\text{atm } p\text{CO}_2$) (Fig. 1), which resulted in nine treatment histories after reciprocal transplantation (e.g., AMBIENT-HIGH). The MID and HIGH treatments matched climate change predictions for tropical oceans for moderate and high CO_2 emissions scenarios by year 2100 (IPCC, 2019). To determine if any observed plasticity was reversible, all treatments were reset to AMBIENT conditions at the end of the reciprocal transplantation stage. Resetting to ambient conditions also ensured that all fragment started from the same temperature and $p\text{CO}_2$ conditions in the subsequent test of heat tolerance. To evaluate heat tolerance as a consequence of treatment history (i.e. thermal hardening response; *heat tolerance stage*), coral fragments were then exposed to either ambient temperature (27.5°C) or high temperature (31.0°C) at $\sim 410 \mu\text{atm } p\text{CO}_2$ (Fig. 4.1).

The plasticity stage set-up consisted of nine 1200 L outdoor aquaria (3 treatments x 3 replicate aquaria) receiving water flow of 2.5 L/min FSW, natural light (150-400 $\mu\text{E m}^{-2} \text{ s}^{-1}$) and daily feeds with an *Artemia* density of 0.5 nauplii/ml. The heat tolerance stage included 12 x 50 L indoor aquaria (2 treatments x 6 replicate aquaria) receiving a flow of FSW at 0.8 L/min, and similar artificial light spectrum and feeding regimes. The experimental systems were monitored in real time for temperature and $p\text{CO}_2$. All inputs were integrated by the Control System in the *Model Predictive Control* logic to manage experimental parameters. See (Uthicke et al., 2020) for further details of the how temperature

and $p\text{CO}_2$ are monitored and controlled at the SeaSim facility. Treatments mirrored seasonal and daily variation in both temperature and $p\text{CO}_2$ based on reference field measurements from Davies reef with offsets being applied to simulate treatment conditions.

4.3.3 Experimental design and trait assessment

The *plasticity stage* investigated whether adult corals have the capacity for beneficial acclimation via phenotypic plasticity. If so, their performance should be either maintained or improved following an extended period in altered treatment conditions (Angilletta, 2009). In the context of the current experiment, beneficial acclimation would be evident if prior exposure to MID or HIGH treatments enables coral fragments to maintain their performance in these conditions, whereas coral fragments without prior exposure to MID and HIGH treatments exhibit decreased performance in these conditions. A common garden experiment was used to assess the response of corals to specific treatments, before and after transplantation. The experimental design is shown in Figure 4.1. Changes in growth rate and photosynthetic efficiency were recorded at four and eight weeks after the end of the quarantine period ($t=0$ weeks). For the first four weeks ($t=4$ weeks), each genotype was represented by 9 fragments per treatment (i.e., haphazardly split into groups of 3 fragments per aquarium). For the second four weeks ($t=8$ weeks), groups were transplanted to account for all possible combinations of treatments (e.g., ambient-ambient, ambient-mid, ambient-high), meaning that each genotype had the same level of replication. In addition, one fragment per genotype per treatment combination was snap-frozen with liquid nitrogen (LN_2) at the end of incubation post transplantation for metabarcoding analyses ($t=8$ weeks).

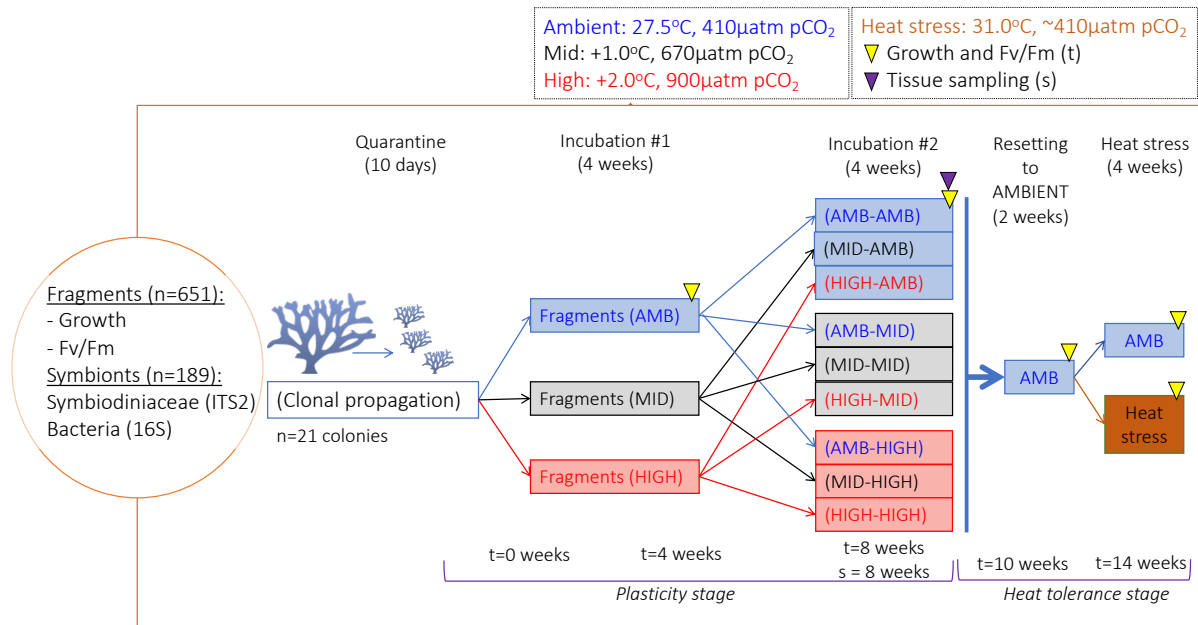


Figure 4. 1 Experimental design used to assess the potential for beneficial acclimation via phenotypic plasticity in adult coral fragments and the possible enhanced thermal tolerance (hardening) in relation to treatment history. Incubation stages ('t') and sampling points (triangles) are also included within each experimental stage.

Linear growth measurements of the change in live tissue surface area were obtained from photographs taken at the end of quarantine (t = 0), just before transplantation (t = 4) and four weeks post transplantation (t = 8), using an OLYMPUS TG-60 camera with default setting on microscope mode. Fragments were orientated in the same position by using a marked reference on the aragonite plug. Each photograph was manually traced using the straight-freehand line tool in IMAGEJ (version: 1.50i) (Rasband, 2012). A numeric scale was included on each photo to transform number of pixels to mm. Linear growth rate was quantified by calculating the proportional change in area (cm²) of live tissue between timepoints: $(\log_{10} \left(\frac{Area_{t=1}}{Area_{t=0}} \right))$. This resulted in two linear growth measurements: interval 1 was 0 – 4 weeks and interval 2 was 4 – 8 weeks. In addition, photographs were used to estimate survival rates of coral fragments over time for each treatment.

Photochemical performance of Symbiodiniaceae was assessed in coral fragments with Imaging Pulse Amplitude Modulated (iPAM) fluorometry and its affiliated software (Walz, Effeltrich, Germany). Measurements were obtained at the same time points as linear growth. The iPAM can resolve at a

scale of 100 μm , thus allowing for accurate photosynthetic measurement of small areas of tissue (Hill and Ulstrup, 2005). The actinic light was calibrated with an Apogee quantum sensor (Model MQ-200, UT, USA) with the following settings: measuring intensity=1, saturation pulse intensity=9, gain=2. Maximum quantum yield (ratio of variable to maximum fluorescence: F_v/F_m) was measured two hours after dusk. Yields were calculated from the same area of interest at the different time points (i.e., using nine different 2 mm^2 positions to account for top, middle and bottom of the fragment and also core and edges of the fragment), by orientating the fragments to a fixed angle in a plastic mount built for the iPAM. This methodology has been used to determine photosynthetic productivity in studies of plant physiology (Maxwell & Johnson 2000); it reflects the efficiency of photosystem II (Krause and Weis 1991), and is a widely accepted indicator of stress in corals (Jones et al. 1999).

The following experimental stages investigated whether treatment-specific phenotypic responses are reversible and also if particular treatment combinations experienced during stage one could trigger a thermal hardening response. These experimental stages started with a 2-week pre-acclimation period (t=8 to 10 weeks) where all fragments (i.e., 2 fragments x 21 genotypes x 9 treatment combinations) were incubated under ambient conditions prior to heat stress exposure. This not only allowed testing for reversible plasticity but also ensured that all fragments, regardless of past history, started from the same temperature in the heat stress experiment. For the heat stress experiment (t=10 to 14 weeks), one fragment from each genotype from each treatment history was exposed to a temperature ramping of $+0.4^\circ\text{C}$ per day until 31°C was reached (~ 10 days), and then incubated until the maximum quantum yield (F_v/F_m) reached values of ≤ 0.3 (~ 26 days). The remaining fragment was kept at ambient conditions for the total duration of the experiment. All fragments were snap-frozen with LN_2 at the end of the heat stress experiment (t=14 weeks); although these were not used in this study. Both, linear growth and F_v/F_m measurements were obtained at the end of the acclimation to ambient conditions (t=10 weeks) and also at the end of the heat stress experiment (t=14 weeks), using the same approach as described for the first experimental stage.

4.3.4 DNA extraction, Amplification and Sequencing Protocol

One adult coral fragment was sub-sampled from each treatment post transplantation (t=8 weeks; 21 genotypes x 9 treatments, 189 total) for microbiome analysis.

Frozen coral fragments were crushed using a cold stainless-steel mortar and pestle adapted to work in a French press (i.e., hydraulic system). Fragments were placed into the mortar with ~10 ml of LN₂, with the pestle positioned on top to carefully crush the fragment with a maximum pressure of 70,000 Newtons. After removing pressure and the steel pestle, an additional hand crushing was performed using a small ceramic pestle to obtain homogeneous coral powder. Coral powder was distributed across two clean 2 ml plastic tubes which were stored at -80 °C. Mortars and pestles were carefully cleaned between samples using chlorine solution, ethanol 80% and ultra-pure water.

Total DNA was extracted from the coral powder (0.5 g) using the DNeasy® UltraClean® Microbial Kit (QIAGEN) following the Manufacturer's protocol with some modifications as described in chapter 2.

4.3.4.1 Preparation of ITS2 and 16S libraries for sequencing

Bacterial 16S rRNA gene amplicons were amplified using primers 27F (Lane 1991) and 519R (Lane et al. 1993) to which MiSeq adaptors were added (v1-v3 region; ~530 bp) (Caporaso et al., 2012), with a 30-cycle PCR using AmpliTaq Gold® 360 Master Mix (Applied Biosystems). PCR cycling conditions and following steps were performed as described in chapter 2.

4.3.4.2 Metabarcoding analyses

For the Symbiodiniaceae community analysis, data was processed as described in chapter 2 following the standardized remote analysis of the SymPortal analytical framework (symportal.org, github.com/SymPortal) in order to predict putative Symbiodiniaceae taxa (Hume et al., 2019).

Sequencing data for the 16S rRNA gene was processed as described in chapter 1 using the open-source software Quantitative Insights Into Microbial Ecology (QIIME2, version 2019.7) (Caporaso et al., 2010).

4.3.5 Statistical analysis – phenotypic and physiological measurements

4.3.5.1 Growth

Sets of linear statistical models were compared to quantify the response of proportional linear growth to treatment conditions at the different time points. Models were fitted using the function

'glmmadmb' from the package glmmADMB (Fournier et al., 2012). A second order Akaike Information Criterion (AICc) was used to identify the best-fit model. All analyses were performed in R version 3.6 (Team, 2013).

For the plasticity stage, analysis of growth for the first 4 weeks prior to transplantation (t=4 weeks), included five models with treatment as a fixed effect and different combinations of: fragment area (log-scale) as a fixed effect, genotype as a random intercept or as a random slope, and tank as a random intercept. The potential for beneficial plasticity (i.e., second-4-week period) was tested for each combination of treatments at times 4 and 8 (i.e. nine treatment histories in total) with growth as the response variable, time as a fixed factor, and genotype as a random intercept and slope. In addition, to predict how linear growth during each treatment at t=8 was influenced by treatment history (t=4), a model was built including growth at t=8 as the response variable, an interaction between treatment at t=4 and treatment at t=8 and fragment size (log scale) as fixed effects and genotype as a random intercept. A Tukey post hoc test was used to contrast growth between different combinations of treatments at t=4 and t=8. Overall, genotype as a random intercept was included to account for potential constant differences in growth rates among genotypes under the different treatments (e.g. genotype A grows more rapidly than B in all treatments). Alternatively, genotype as a random slope was used to account for genotypes responding differently depending on treatment (e.g. genotype A grows faster than B under one treatment but not another).

For the resetting to ambient and acute heat stress stages, a series of models were first fitted and compared to test whether acclimation to ambient conditions (t=10 weeks) was reached in all possible treatment combinations coming from t=8. The models included combinations of the following variables: interaction between treatments at t=4 and t=8, and fragment size as possible fixed effects, plus genotype and tank as a random intercept. For the best fit model, a Tukey post hoc test was used to compare growth between different combinations of treatment history. For the acute heat stress exposure at t=14, six statistical models were used to test for the effect of treatment at t=4, t=8 and t=14 over fragment growth at t=14 (i.e. heat stress vs. ambient in relation to treatment history). The most complex model included a three-way interaction among treatments at t=4, t=8 and t=14 (fixed effects), fragment size (as a fixed effect) and genotypes and tank as random intercepts. Subsequent models were a subset of this model. The difference between growth of fragments exposed vs not exposed to heat stress was used as a proxy for the potential for enhanced thermal tolerance.

Additionally, the estimated random intercept of genotype was extracted to evaluate the overall performance of each genotype at t=14.

4.3.5.2 Maximum quantum yield (Fv/Fm)

A similar statistical approach to that of linear growth was used to estimate changes in maximum quantum yield (Fv/Fm) for the same experimental time points. However, because multiple observations of Fv/Fm were taken from each fragment at different positions, position was also included as random intercept. The response variable was: $\left(\frac{Fv}{Fm}\right)_{t+1} = \log_{10}\left(\frac{Yield_{t+1}}{Yield_t}\right)$

4.3.5.3 Symbiont associations

Symbiodiniaceae and bacterial diversity analyses were performed using the relative abundance of the ITS2 type profile and 16S rRNA gene ASV data obtained from either SymPortal or QIIME2/Phyloseq. The effects of treatment (t=4 and t=8), tank and genotype on community composition were tested with a permutational multivariate analysis of variance (PERMANOVA) using Bray-Curtis similarity distance with the function *adonis* from the R package 'vegan' (Oksanen et al., 2013). Treatment-specificity of the bacterial community was assessed by calculating the compositional similarities of all 189 samples with the Bray-Curtis similarity distance and visualising the data with a non-metric multidimensional scaling (NMDS) plot using the phyloseq package.

For the bacterial communities, variation in alpha diversity was evaluated through species richness (number of ASVs) and species diversity (Chao1 and Shannon index). Each measure of alpha diversity was analysed using a linear mixed effect model with treatment as a fixed effect and tank as random intercept. Chao1 estimates were \log_{10} transformed to meet the normality assumption. Differences in beta diversity were analysed using PERMANOVA with 999 permutations. Pairwise comparisons were performed using the function *pairwise.perm.manova* (with 999 permutations and BH method) from the package *RVAideMemoire* (Hervé and Hervé, 2019). Differences in beta diversity were visualised using an NMDS fit with Bray-Curtis distances. Bacterial indicator taxa analysis (i.e., indicative of a specific treatment) was performed using a multi-level pattern analysis with 999 permutations with the function *IndVal-multipatt* from the package *indicspecies* (De Cáceres, 2013, De Cáceres and Legendre, 2009). Indicator analysis was carried out at two separate levels including family and genus with $\alpha = 0.05$.

To compare differences in the relative abundance of bacterial families among treatments, a linear model with treatment as a fixed effect was fitted to the ten most abundant families in the rarefied dataset using the Bayesian package 'brms' (Bürkner, 2017). A zero-inflated beta distribution was used for all families. To quantify differences in the predicted relative abundance of each family among treatments, the 95% credible interval of the posterior distribution of the difference between relative abundances of each pair of treatments was calculated. When the 95% credible interval overlapped with zero, it was assumed that the relative abundances were not different. To identify differences in relative abundances of particular families differentially abundant among treatment combinations (i.e., in a non-rarefied dataset), a differential expression analysis based on a negative binomial distribution was performed using the function DESeq (Wald test) from the package DESeq2 (Love et al., 2014). Log2FoldChange values were used to compare significant differences among treatment combinations, to identify not only the order of magnitude in relative abundances between treatments but also which treatment favoured the abundance of each particular taxa.

To investigate associations between pairs of bacterial families or Symbiodiniaceae types, a Spearman rank correlation test was computed for each pair of bacterial family and Symbiodiniaceae type profiles that were present in at least ten samples.

4.4 Results

4.4.1 Growth

4.4.1.1 Growth before and after transplantation (plasticity)

Temperature and $p\text{CO}_2$ treatment significantly affected the growth of corals after 4 weeks of incubation ($t = 4$ weeks) (Table C.S1, C.S2). For a given fragment size, growth was significantly higher for fragments in the HIGH treatment relative to fragments in AMBIENT and MID treatments, which were not significantly different from each other (Fig. 4.2a; Table C.S3). Growth significantly decreased with increasing fragment size (Table C.S2). Despite random effect variance being low, genotype was included in the best-fit model.

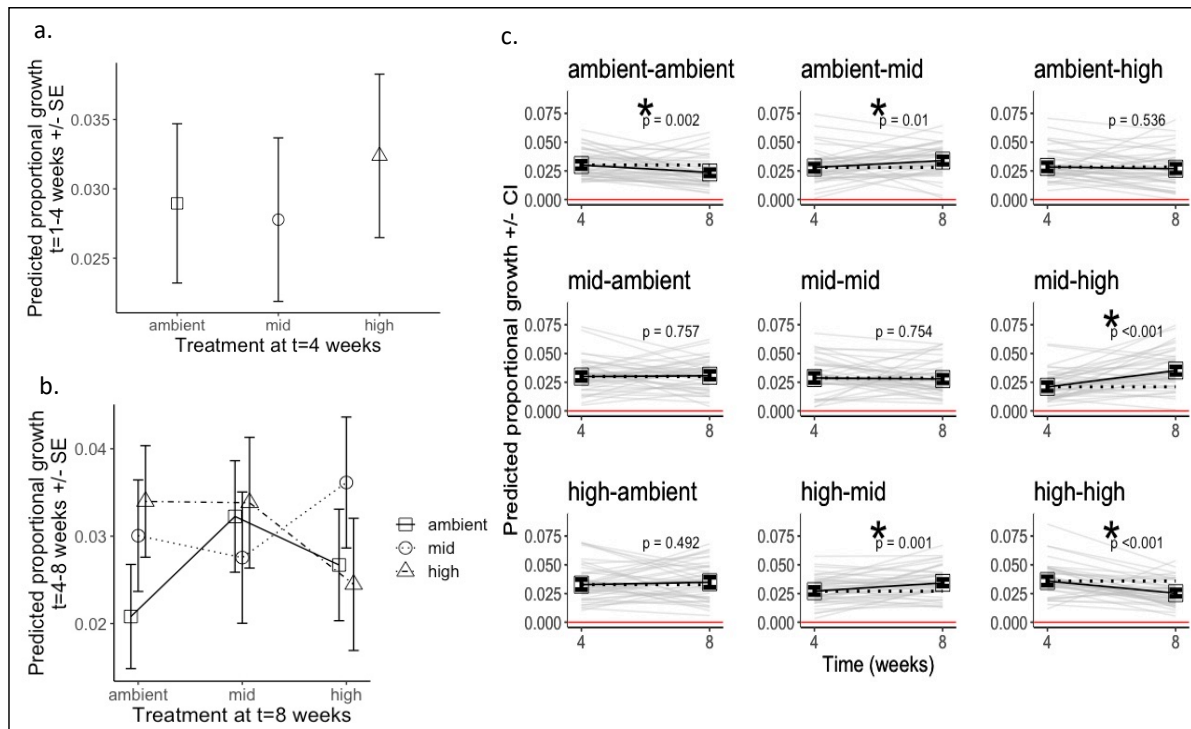


Figure 4. 2 Panel a: Proportional growth from t=0 to t=4 weeks by the best-fit model depending on treatment at t=4. Number of observations: total=378, number of genotypes=21. Panel b: Proportional growth by the best-fit model at t=8 weeks for the different treatments over 4 to 8 weeks. Symbols represent origin treatment whereas x-axis distribution represents the destination treatments. Number of observations: total=378, number of genotypes=21. Panel c: Proportional growth between origin treatment at t=4 weeks in relation to growth at the destination treatment at t=8. The solid black lines represent the fitted model and its predictions, whereas the dotted line is representative of no proportional change between time points. Grey lines represent variation for individual genotypes within each group. Red lines used to observe potential negative growth. Asterisk indicate significant differences in growth rate between timepoints.

After transplantation, growth was affected not only by the destination treatment (t = 4-8 weeks) but also by the treatment experienced at t=1-4 weeks. Following model selection (Table C.S4), the best-fit model revealed that the interaction of treatment at t=4 and t=8 was significant, meaning that growth of coral fragments after reciprocal transplantation among treatments was influenced by the previous treatment mid conditions (Table C.S5). In addition, growth at t=8 significantly decreased with fragment size at t=4. When comparing growth rate under each of the destination treatments, there were no significant differences for the majority of fragments coming from different origin treatments

(Fig. 4.2b; Table C.S6), suggesting that the different treatment levels were not generating an effect on growth of sufficient magnitude to allow the detection of plasticity. Although genotype showed an overall low variance, some genotypes contributed more than others to the growth rate (i.e., ranging from -0.01 to 0.02 relative to the ~ 0.03 found in mean growth), regardless of the treatment combination (Fig. C.S1).

Individual models (i.e., based on the best-fit model), confirmed the absence of clear patterns of plasticity triggered by the different treatment intensities and combinations. (Fig. 4.2c; Table C.S7). In other words, despite the fact that growth rate at t=8 weeks was either similar or greater than growth at t=4 weeks, the treatment with the highest intensity (HIGH) was not necessarily triggering the appearance of new and better performing phenotypes, suggesting that this was a consequence of a disturbance effect due to transplantation, not evidence for beneficial acclimation. Interestingly, fragments without transplantation had a significantly lower growth rate at t=8 weeks relative to t=4 weeks, with the exception of fragments under mid treatment in both incubation periods, suggesting that a 4-week exposure to high can increase growth in adult coral fragments, but extended exposure 8 weeks causes a decline in growth. No negative growth was recorded, which confirms that exposure to any treatment combination did not cause tissue mortality. Hence, growth rate was either sustained or enhanced when adult corals experienced a change in treatment conditions, although such plastic responses do not qualify as beneficial acclimation considering the absence of a clear effect of treatment. Finally, growth rates were also lowered over time in some cases of non-transplanted treatment combinations (e.g., HIGH-HIGH), which seems to be a cumulative effect of high temperature on growth.

4.4.1.2 Growth during heat stress exposure (31 °C)

After a two-week acclimation period at ambient conditions, growth rate was similar among fragments, despite having different treatment histories. From a set of linear models (Table C.S8), the best-fit model included the interaction of treatment at t= 4 and t=8 weeks and showed that those previous treatments did not significantly influence growth over t=8-10 weeks (Fig. C.S2, Table C.S9). Independent of the treatments, growth significantly decreased with increasing fragment size. Tukey post hoc tests estimates did not show significant differences in growth at t=10 weeks across all possible treatment history comparisons (Table C.S10). Hence, the two-week acclimation period successfully reset growth rate under ambient conditions prior to heat stress exposure and therefore confirmed reversible plasticity in growth rate.

During the heat stress exposure, the best-fit model revealed that overall growth rate of corals was significantly affected by high temperature (i.e., reduced under heat stress relative to ambient); this model included the interaction of treatment at $t = 4$, $t = 8$ and $t = 14$ weeks (Table C.S11, C.S12). However, despite some treatment histories displaying significant effects on growth rate at $t=14$ weeks, Tukey post hoc test confirmed that only in one particular treatment combination (i.e., high-ambient-ambient vs high-ambient-heat stress) was there a significant difference in growth rate (Fig. 4.3; Table C.S13). Size continued to influence growth, as lower growth rates were observed from larger fragments. Although genotype showed an overall low variance, some genotypes contributed more than others to the growth rate (i.e., ranging from -0.03 to 0.03 relative to the ~ 0.05 found in mean growth), regardless of the treatment combination (Fig. C.S3). Interestingly, the contribution of individual genotypes to growth rate was similar across experimental stages, with relatively small variation observed within each of the positive or negative side from the intercept (Fig. C.S1 and Fig. C.S3). Thus, coral fragments were capable of maintaining similar growth rates under heat stress relative to ambient conditions, unless they had experienced HIGH treatment conditions in the first experimental stage and no other conditions other than ambient following transplantation. Nevertheless, the lack of consistent patterns suggests that there is not a clear treatment signal on growth, even under intensified treatment conditions, which limits further interpretation of potential for stress-hardening responses triggered by treatment history.

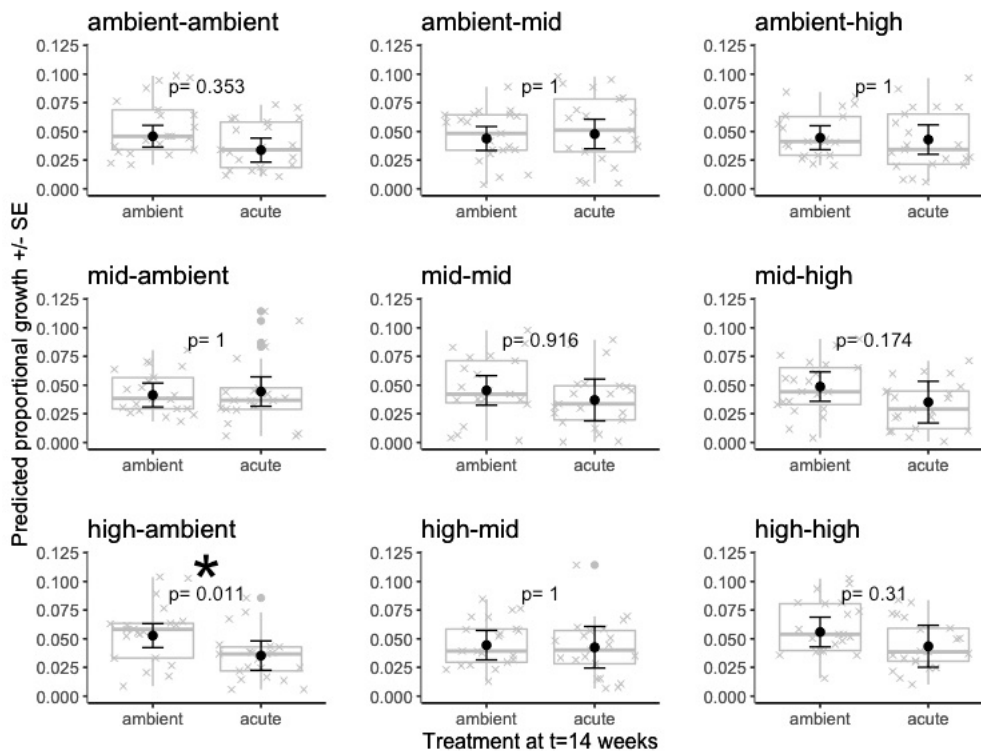


Figure 4. 3 Proportional growth from t=10 to t=14 weeks for heat stress and ambient treatment, considering each treatment history over weeks 0 to 8. Box plots show the distribution of the raw data, grey crosses show the raw data and black points with error bars show the fitted model predictions with the associated standard errors. The asterisk indicates a statistically significant difference.

4.4.2 Photochemical efficiency (Fv/Fm)

4.4.2.1 Fv/Fm before and after transplantation (plasticity)

Following model selection (Table C.S14), the best-fit model showed that prior to transplantation, treatment had a significant effect on the mean Fv/Fm after 4 weeks of incubation (t=4 weeks) (Table C.S15). For a given fragment size, Fv/Fm was significantly higher for fragments under ambient treatment relative to fragments in mid and high (Fig. 4.4a; Table C.S15). Tukey post hoc tests confirmed differences in Fv/Fm among treatments (Table C.S16). There was also a significant effect of Fv/Fm at t=0 on the Fv/Fm found at t=4, suggesting that higher yields are expected if higher yields were previously observed. Additionally, Fv/Fm significantly increased with increasing fragment size. Despite random effect variance being low, genotype was included in the best-fit model.

After transplantation, Fv/Fm was affected not only by the destination treatment (t=4-8 weeks) but also by the treatment experienced over the period t=1-4 weeks. Following model selection (Table C.S17), the best-fit model revealed that the interaction of treatment at t=4 and t=8 was significant, meaning that Fv/Fm of coral fragments after reciprocal transplantation among treatments was influenced by the previous treatment conditions (Table C.S18). In addition, size at t=8 weeks had a significant effect on the Fv/Fm observed, suggesting that a higher yield can be expected from larger fragment size. When comparing Fv/Fm under each of the destination treatments, there were significant differences among fragments coming from a variety of origin treatments (Fig. 4.4b; Table C.S19). Results revealed that increasingly severe treatment conditions had a negative effect on Fv/Fm (i.e., increased decline in slope); a pattern previously observed prior to transplantation. It was also evident that there was a carryover effect from HIGH treatment, represented by higher Fv/Fm values recorded in fragments that experienced HIGH prior to transplantation (t=1-4 weeks) across all possible treatment combinations that followed reciprocal transplantation (t=4-8 weeks). However, under HIGH treatment post transplantation, and despite the significant reduction in Fv/Fm across all treatment combinations, fragments that previously experienced HIGH treatment performed better than fragments that previously experienced MID or AMBIENT. Most importantly, the Fv/Fm values observed for HIGH-HIGH combination, were similar to the expected values for AMB-AMB, suggesting that prior exposure to HIGH treatment enabled the coral fragments to maintain healthy Fv/Fm values despite higher intensity treatment conditions. Although genotype showed an overall low variance, some genotypes contributed more than others to Fv/Fm (i.e., ranging from -0.03 to 0.03 relative to the ~0.55 found in mean Fv/Fm), regardless of the treatment combination (Fig. C.S4). Thus, these findings suggest that not all transplanted lines exhibited plasticity in Fv/Fm but a more in-depth comparison across treatment histories uncovered particular patterns of beneficial acclimation via phenotypic plasticity.

Indeed, by using individual models (i.e., based on the best-fit model), plasticity and beneficial acclimation in Fv/Fm in response to treatment conditions were verified via two major lines of evidence (Fig. 4.4c; Table C.S20). First, the decline of Fv/Fm was significantly influenced by increasing intensity of treatment conditions following transplantation, considering that fragments that were under AMBIENT during the first 4-week period (i.e., ambient-high > ambient-mid > ambient-ambient) exhibited a significant decline in Fv/Fm. Second, the effect of higher intensity treatments (HIGH) on the Fv/Fm decline at t= 8 weeks was dampened if fragments had been preconditioned to a 4-week exposure to similar treatment conditions (i.e., slope of decline: ambient-high > mid-high > high-high). These lines of evidence confirmed beneficial acclimation via phenotypic plasticity, and also that the

response was reversible considering the improvement observed in Fv/Fm values for HIGH-AMB treatment history and the positive slope generated post transplantation. Hence, treatment history had a significant effect on Fv/Fm values and allowed the detection of plasticity in adult coral fragments. Additionally, preconditioning fragments to intensified treatment conditions allowed the detection of phenotypes capable to sustain better Fv/Fm rates under elevated treatment conditions, which is clear evidence for beneficial acclimation via phenotypic plasticity.

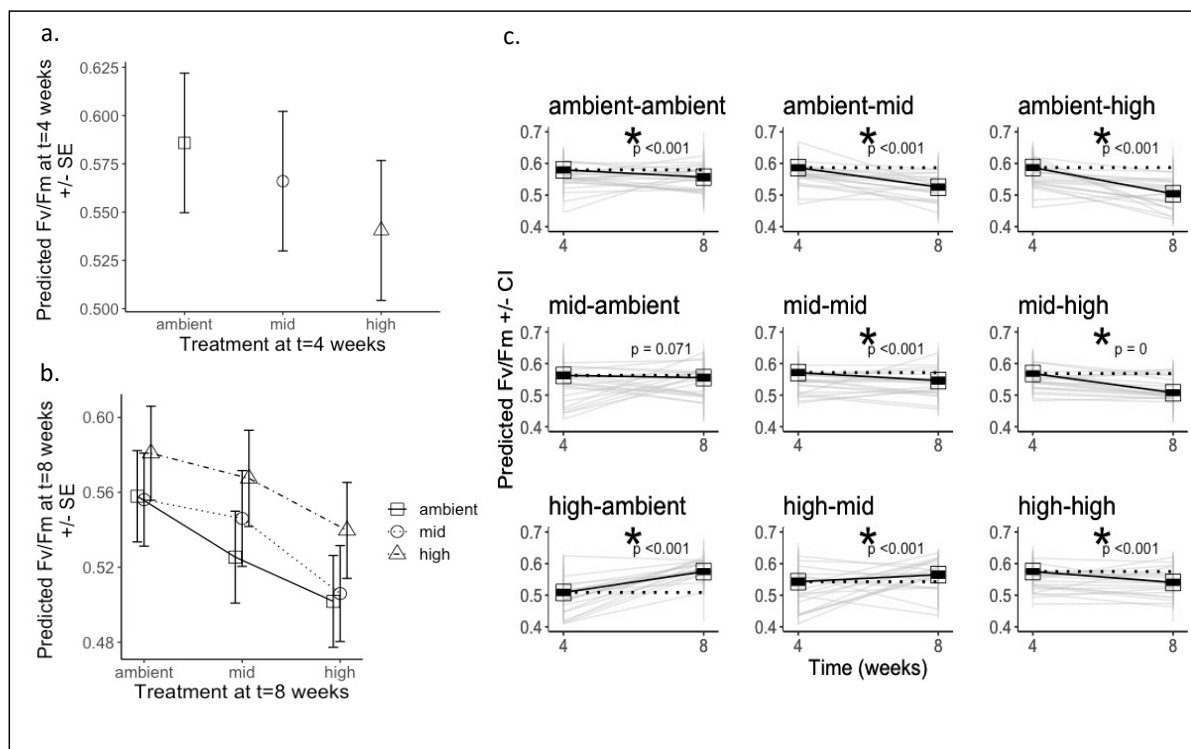


Figure 4.4 Panel a: Predicted Fv/Fm at t=4 weeks by the best-fit model depending on treatment at t=4. Number of observations: total=378, number of genotypes=21. Panel b: Predicted mean Fv/Fm by the best-fit model at t=8 weeks for the different treatments. Symbols represent origin treatment whereas x-axis distribution represent destination treatments. Panel c: Predicted mean Fv/Fm between origin treatment at t=4 weeks in relation to linear extension at destination treatment at t=8 weeks. Grey lines represent variation for individual genotypes within each group.

4.4.2.2 Fv/Fm during heat stress exposure (31 °C)

Based on a test of statistical models (Table C.S21), the best-fit model included the addition of treatment at t=4 and t=8 weeks and showed that treatment history significantly influenced Fv/Fm at t=10 weeks (Table C.S22). Size also had a significant effect on yield, with Fv/Fm higher in larger fragments. The mean Fv/Fm at t=10 weeks (i.e., after the two-week preacclimation period at ambient conditions) ranged from 0.52 to 0.57, consistent with previous observations at ambient conditions (Fig. C.S5). The majority of treatment combinations did not show significant differences among them, although two particular combinations 1) AMBIENT-HIGH and 2) HIGH-HIGH were significantly different from the rest, but not from each other (Table C.S23). Hence, the two-week acclimation period successfully reset Fv/Fm to expected values for ambient conditions for fragments coming from any treatment history, therefore suggesting reversible plasticity in Fv/Fm.

During the heat stress exposure, photosynthetic efficiency was lower in fragments under the heat stress treatment relative to the ambient control. From a set of statistical models (Table C.S24), the best-fit model included the interaction of treatment at t=4, t=8 and t=14 weeks. The best-fit model revealed that Fv/Fm was significantly lower in the heat stress treatment compared to corals under ambient conditions (Table C.S25) for all treatment histories. However, past treatment history influenced the magnitude of the effect. There was a 25% reduction in Fv/Fm in fragments with an ambient-ambient history (i.e., ambient controls) when exposed to heat stress. In contrast the decline in Fv/Fm was 10-20% for ambient-high, high-high, high-mid, and mid-ambient. An even smaller reduction in Fv/Fm <8% was recorded for mid-mid, mid-high, high-ambient and ambient-mid treatments. The results indicate that past exposure to MID and HIGH treatments has a beneficial effect on thermal tolerance of coral fragments (i.e., a hardening response). Size continued to influence Fv/Fm, displaying a positive correlation. Although genotype showed low variance overall, some genotypes contributed more to the variation in Fv/Fm than others (i.e., ranging from -0.04 to 0.04 relative to the ~0.5 found in mean Fv/Fm), regardless of the treatment combination (Fig. C.S6). Interestingly, the contribution of individual genotypes to Fv/Fm values was similar across experimental stages, with relatively small variation observed within each of the positive or negative side of the intercept (Fig. C.S4 and Fig. C.S6). Tukey post hoc test confirmed that the difference in Fv/Fm between heat stress and ambient was significant for all treatment histories (Fig. 4.5; Table S26). Finally, visual signs of tissue paling were observed in some fragments, but was not associated to particular genotypes, and mostly evident in AMB-AMB-heat stress (i.e., colour scores from coral health chart not included in this study). Thus, while photosynthetic efficiency was affected by the heat stress, the magnitude of reduction in Fv/Fm varied among treatment histories.

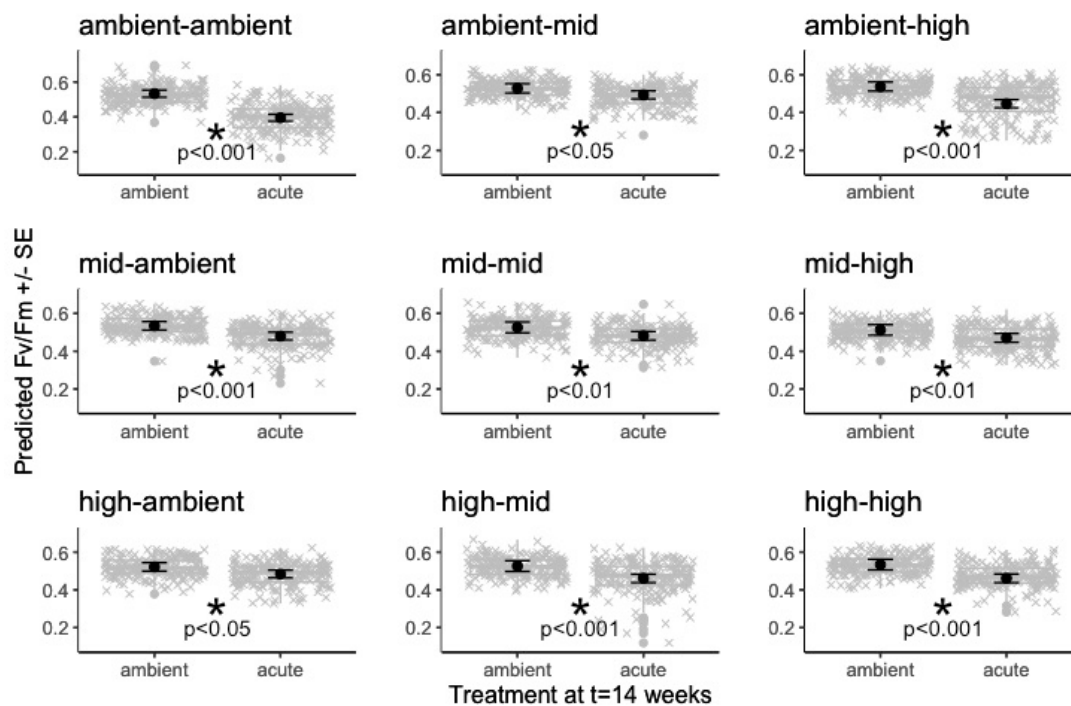


Figure 4. 5 Predicted Fv/Fm at t=14 weeks for heat stress and ambient treatments, considering each treatment history over the period 1-8 weeks. Box plots show the distribution of the raw data, grey crosses show the raw data and black points with error bars show the fitted model predictions with the associated standard errors. Percentage of decline among treatments and time points are described in the main text

4.4.3 Correlation between growth and Fv/Fm at different experimental stages

A strong positive correlation was evident in the growth rate of genotypes four weeks after transplantation (t = 8 weeks) relative to the growth rates during the heat stress phase (Fig. 4.6a). Similarly, a moderate positive correlation was found in the Fv/Fm of genotypes four weeks after transplantation relative to the Fv/Fm observed during the heat stress (Fig. 4.6b). These results show that genotypes performing better than expected at t=4 weeks were likely to also perform better than expected at t=8 weeks (i.e., during heat stress of 31°C). However, the relative performance in growth was not related to relative performance of Fv/Fm at any of the time points (Fig. 4.6c, 4.6d).

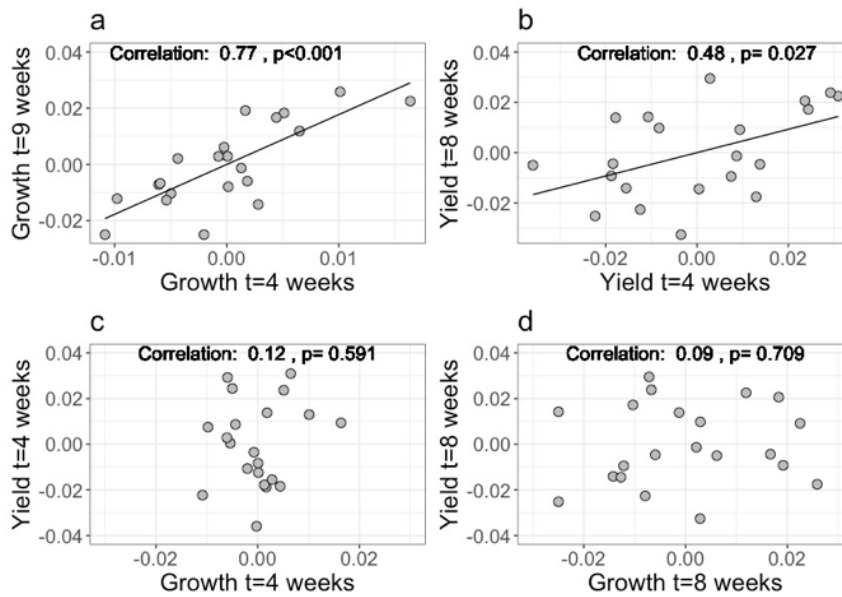


Figure 4. 6 Correlation between the random effects estimates of genotype from the best-fit models estimating yield and growth at t=4 weeks and t=8 weeks. Panel a: Estimates showing growth at t=8 weeks relative to growth at t=8 weeks. Trendy line represents a positive correlation. Panel b: Estimates showing Fv/Fm at t=4 weeks relative to Fv/Fm at t=8 weeks. Panel c: Estimates showing growth at t=4 weeks relative to Fv/Fm at t=4 weeks. Panel d: Estimates showing growth at t=8 weeks relative to Fv/Fm at t=8 weeks. Correlation values based on the Spearman Rank correlation coefficient analysis. Significant correlations among pairs are shown inside the matrix.

4.4.4 Symbiotic associations

4.4.4.1 Symbiodiniaceae communities 4 weeks after transplantation (plasticity stage; t=8 weeks)

A total of 8,769,849 raw reads were obtained for the 189 samples across all treatments, ranging from 15,007 to 81,414 per sample. An average number of 46,157 pair-end reads were obtained per sample after sequencing and downstream filtering steps reduced this to 28,606 reads. A total of 350 reads were found in the blank sample, however, no ITS2 profiles were predicted by SymPortal.

The Symbiodiniaceae composition, 4 weeks after transplantation (t=8 weeks), was significantly affected by genotype, which explained ~51% of the variation ($R^2=0.508$, Table C.S27; Fig. 4.7). Treatment at t=4 and treatment at t=8 weeks had no significant effect on the community composition, and explained less than 1% of the variation (Table C.S27); the remaining ~48% of variance being

unexplained. Type profiles C3:C3dq (associated species: none) and C3.k:C3a (associated species: none) were the most common profiles among the fragments (Fig. C.S7).

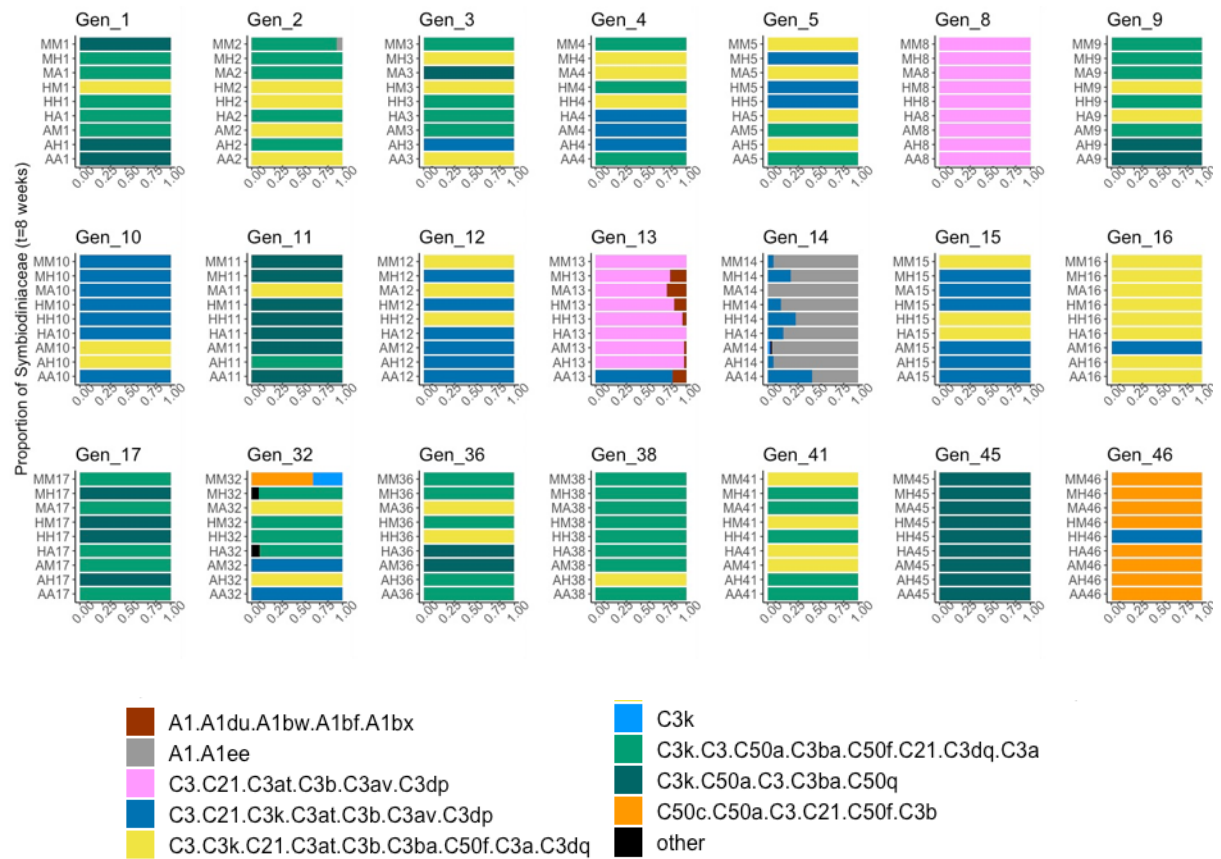


Figure 4. 7 Relative abundance of Symbiodiniaceae type profiles. Each block corresponds to fragments of the same genotype, belonging to different treatment histories. Each bar corresponds to a different fragment, each one labelled by two letters and a number: the first letter corresponds to treatment at t=4 weeks (A for ‘AMBIENT’, M for ‘MID’, and H for ‘HIGH’), the second letter to treatment at t=8 weeks, and the number is the genotype. Different colours show different Symbiodiniaceae type profiles.

4.4.4.2 Bacterial communities 4 weeks after transplantation (plasticity stage; t=8 weeks)

A total of 3,272,962 bacterial sequences were retrieved from the *A. loripes* fragments (n=189) four weeks after transplantation across all treatment histories, corresponding to 1,308 unique ASVs. The number of reads per sample ranged from 37,374 to 119,684. On average, 79,128 pair-end reads were obtained per sample after sequencing with downstream filtering steps reducing this to 54,363 reads. The maximum number of ASVs per sample was 46,491 (i.e., encompassing both unique and

shared ASVs in a non-rarefied dataset). Rarefaction analysis showed curve asymptotes at ~3,000 reads (Fig. C.S8), thus the dataset was rarefied to even depth of 3,000, with only one sample being excluded from the analysis (i.e., HM42). The remaining samples encompassed a total of 1,308 taxa retained following rarefaction. A total of 280 merged non-chimeric reads were recovered from the blank sample (i.e., DNA extraction control) and clustered into two ASVs, however these ASVs did not have any bacterial taxonomic affiliation and were not present in any of the 189 coral recruit samples (i.e., dataset analysed simultaneously with chapter 2).

After rarefying the data set, alpha diversity was significantly different for particular treatment combinations when considering origin and destination at t=4 and t=8 weeks, respectively (Table C.S28, Fig. C.S9). Species richness was also significantly different among particular treatment combinations (Table C.S29- C.S30). Interestingly, species richness was significantly higher for treatments histories that did not include transplantation (e.g., MID-MID or HIGH-HIGH), with a general trend suggesting higher diversity indices for the HIGH-HIGH treatment history. Moreover, the number of unique and shared ASVs (i.e., rarefied data set) varied according to treatment history as observed in three main groups clustered according to destination treatment (Fig. C.S10, Table C.S31), with an increased number of ASVs observed when higher levels of stress were experienced in either the origin or destination treatment (i.e., HIGH, relative to MID and AMBIENT). For example, of the 456 total ASVs when destination treatment was AMBIENT, the HIGH-AMB treatment history had 133 unique ASVs, followed by MID-AMBIENT (121) and AMBIENT-AMBIENT (107), suggesting that elevated temperature and $p\text{CO}_2$ can increase diversity of bacterial communities and that such patterns can be retained even after transplantation (i.e., as observed in the diversity indices). For all three grouped destination treatments, the number of shared ASVs across each combination ranged from 18 to 26, although when clustering all possible combinations, there were seven shared bacterial taxa, including three from the genus *Ruegeria* plus one undescribed Rhodobacteraceae ASV. The three remaining taxa were affiliated with the genera *Endozoicomonas* (n=2) and *Sphingomonas* (n=1) (Table C.S31).

In contrast, beta diversity varied depending on treatment history and coral genotype. For example, Bray-Curtis dissimilarity matrices showed that the interaction of treatment at t=4 and t=8 weeks had a significant effect on bacterial community composition in coral fragments at t=8 weeks ($p < 0.01$, $R^2 = 0.02$, Table C.S32- C.S33), although it explained only 2% of variation. When treated independently, treatment at t=4 and t=8 weeks had a significant effect on the composition, although both only explained 1% of the variation ($p < 0.01$, $R^2 = 0.01$). Interestingly, genotype had a significant

effect and explained 14% of variation in community composition ($p < 0.01$, $R^2 = 0.14$, Table C.S32). In addition, aquarium also had a significant effect on the bacterial communities, although it explained only 1% of the variation ($p > 0.01$, $R^2 = 0.01$, Table C.S32). The remaining 77% variance remained unexplained. Hence, a weak segregation of distances was observed and pairwise PERMANOVA confirmed significant differences among treatments pairs at t=8 weeks (ambient:mid < 0.03 ; ambient:high < 0.003 ; mid:high < 0.05 (Fig. C.S11).

The indicator species analysis did not reveal high fidelity associations of particular taxa to each treatment. Indeed, a total of 18 taxa were identified (i.e. ASV level) (Table C.S34, $\alpha = 0.05$, p -value < 0.05), with the majority associated to the family Rhodobacteraceae. However, fidelity values ranged from 10-57%, and consequently, none of these ASVs were considered as an indicator for any specific treatment history considering that their relative abundances across groups were not sufficiently different. From all treatment histories, most indicator ASVs were detected in the HIGH-HIGH treatment combination (eight out of 18), including the genera *Ruegeria*, *Turicibacter*, *Actibacterium*, *Filomicrobium*, and *Tateyamaria*. At the family level (Table C.S35), a total of seven indicator taxa were identified (Kiloniellaceae, Pirellulaceae, Arcobacteraceae, Pseudonocardiaceae, Saprospiraceae, Hyphomicrobiales and another uncultured alphaproteobacteria), which continued to show low fidelity values ranging from 10-47% and hence were not considered indicative of particular treatment history effects. Thus, small differences in relative abundances of bacterial taxa across treatment histories did not allow a clear categorisation of indicators with high fidelity values.

Based on the rarefied dataset, relative abundances of the top 10 most abundant bacterial families did not vary among treatments histories and all possible comparisons (Table C.S36- C.S37). Rhodobacteraceae and Endozoicomonadaceae were consistently the most abundant bacterial families across treatment histories (Fig. 4.8), with the exception of HIGH-HIGH where Endozoicomonas seemed much reduced but not necessarily detected in the analysis. Similarly, the analysis at the genus level (i.e., top 10 most abundant genera) did not show significant differences in relative abundance of bacterial taxa following comparisons among treatment histories (Fig. C.S12, Table C.S38- C.S39), although Endozoicomonas continued to display much lower abundance and much scattered presence across samples under HIGH-HIGH.

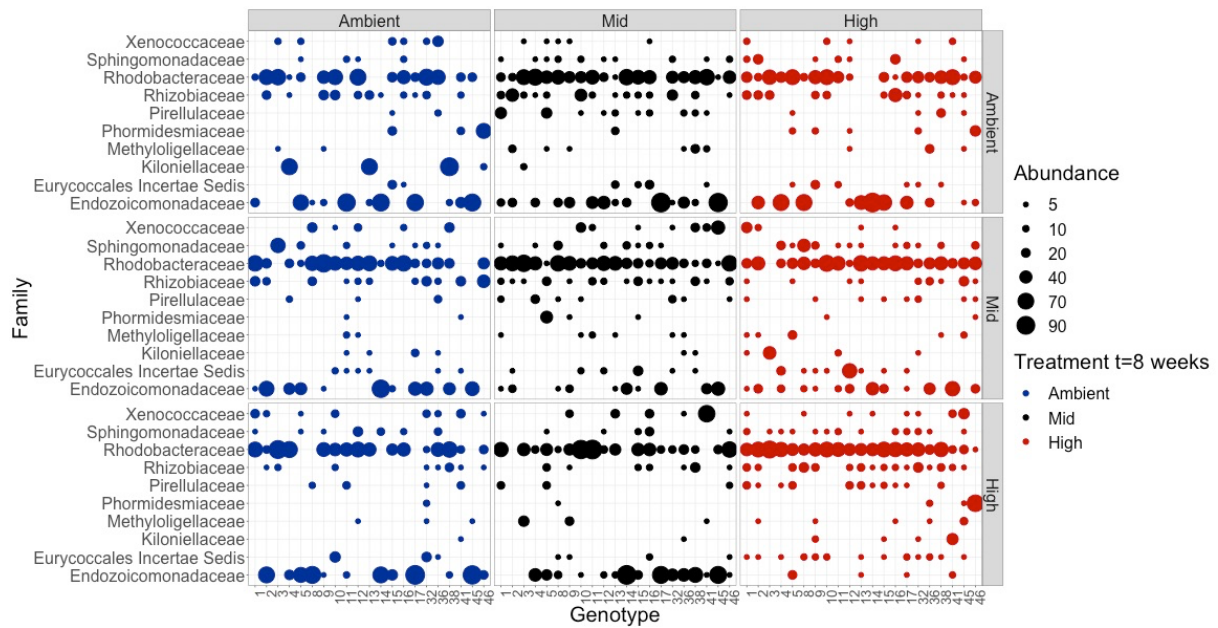


Figure 4. 8 Relative abundance of the top 10 bacterial families (y-axis) among individual genotypes of coral fragments (x-axis) at t=8 weeks, across each of the nine treatment histories (n= 117 total families).

Analysis of the non-rarefied dataset revealed that particular taxa can be differentially abundant depending on the treatment history comparison (Tables C.S40, Fig. C.S13). Indeed, I detected that incubation under more extreme conditions at any time during the experiment (e.g., HIGH or MID relative to AMBIENT) not only increased the number of taxa showing significant differences among treatment histories but also influenced the magnitude of change (i.e., log2fold change values). For example, relative abundance of Rhodobacteraceae was up to 23-times higher in HIGH-AMB corals relative to AMB-AMB from origin treatment HIGH or AMB that had AMB as destination, or to 7-times higher HIGH-HIGH relative to AMB-AMB. Overall, the majority of differentially represented microbial taxa were more abundant in corals that underwent transplantation between different treatment conditions, and more likely to display higher relative abundances in if MID or HIGH treatments were experienced.

4.4.4.3 Correlation of relative abundances across symbiont members

The relative abundance of Symbiodiniaceae and bacterial taxa did not exhibit any clear correlation at t=8 weeks (Fig. 4.9). However, a weak positive correlation was found between two symbiont members: *S. microadriaticum* and the bacterial family Endozoicomonadaceae. Similarly, Spearman Rank correlation coefficients revealed weak correlations in relative abundances between

pairs of bacterial families (top 10 most abundant), with the exception being the strong negative correlation between Endozoicomonadaceae and Rhodobacteraceae.

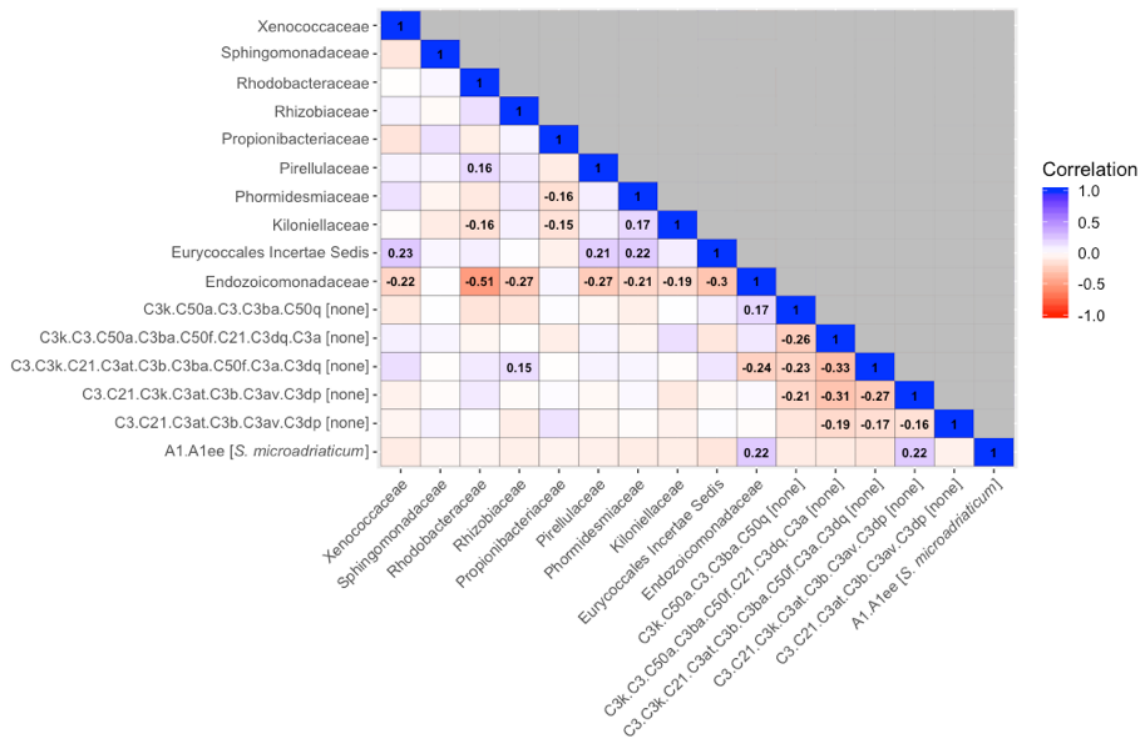


Figure 4. 9 Correlation in relative abundance among Symbiodiniaceae types and bacterial families for adult coral fragments 4 weeks after transplantation (t=8 weeks). Correlation values based on the Spearman Rank correlation coefficient analysis. Significant correlations among pairs are shown inside the matrix.

4.5 Discussion

Phenotypic responses of adult coral fragments to a combination of elevated temperature and pCO_2 were assessed under controlled laboratory conditions. Beneficial acclimation via phenotypic plasticity was observed for Fv/Fm but not consistently for growth, whereas symbiont community structure appeared to be influenced primarily by host genotype rather than treatment conditions. Further, exposure of fragments to heat stress revealed evidence for a hardening response in Fv/Fm, but not growth.

4.5.1 Growth

4.5.1.1 Plasticity stage

Plasticity stage - Analysis of growth rates across coral fragments demonstrated that growth can be maintained under some simulated climate change scenarios. However, there was no clear evidence that maintenance of growth was due to beneficial plasticity. Instead, the environmental treatments appeared to have little effect on growth, and variation in growth rates among treatment was not consistent with expectation of beneficial acclimation. It is possible that the observed changes across treatment histories that followed transplantation were a disturbance effect, where growth is either maintained, diminish or enhanced when there is a change in treatment conditions. Indeed, changing environmental conditions has been linked to faster growth in other reciprocal transplant experiments. For instance, foreign corals were found to grow faster than native corals at their home sites, although host genotype was a strong driver of variation (Drury et al., 2017). Moreover, a cumulative negative effect of high temperature on growth was detected in fragments incubated for both periods under the higher intensity treatment (high-high), which reduces the likelihood of beneficial plasticity in other treatment histories despite the maintenance or even the increase in growth rates observed in fragments transplanted from current-day ambient conditions to climate change conditions predicted for the end of this century. While other common garden nursery experiments have shown that one-third of growth variance in corals can be attributed to host genotype (Morikawa and Palumbi, 2019), in *A. loripes* I found that genotype did not have a statistically significant effect on growth. It is also important to acknowledge that genetic variation in a phenotypic proxy for fitness like growth rates, may not necessarily reflect differences on fitness over time (Edmunds, 2017), although in this particular study case, *Acropora* species were not evaluated and much of the variation remained unexplained. Although previous work has already shown that preconditioning corals to a pulse of moderate thermal stress can increase their upper thermal tolerance limits (Bellantuono et al., 2012, Middlebrook et al., 2008), my work added another level of complexity by including reciprocal transplantation with longer duration periods. This allowed us to confirm that although a rapid switch in environmental conditions can act as a promoter of growth, longer incubation periods to controlled climate change conditions can have negative effects on the growth rate of the coral host. Additionally, the results show that the relative maintenance or increase in growth rate that followed transplantation for particular treatment histories was not due to plasticity and therefore beneficial acclimation was not occurring.

4.5.1.2 Heat tolerance stage

Heat tolerance stage - Interestingly, my results revealed that growth rates were not always reduced under heat stress relative to ambient conditions. Therefore, corroborating the maintenance or increase in growth rate during the plasticity stage (i.e., transplantation to higher intensity treatments) was not due to plasticity, but instead that growth rate is tolerant to these conditions in *A. loripes*. However, it is important to consider that reductions in growth rate can be triggered after and not during heat stress events (Gold and Palumbi, 2018, Lizcano-Sandoval et al., 2019). My results also showed that declines in growth rate under heat stress only occurred for particular treatment combinations (Amb-Amb and High-Amb), and was lower when fragments previously experienced conditions of higher temperature and lower pH. When evaluating the interaction between environmental history and physical parameters on coral health, Wall and colleagues concluded that corals with a history of greater $p\text{CO}_2$ variability had higher constitutive antioxidative and immune activity (i.e., catalase, superoxide dismutase, prophenoloxidase) and Fv/Fm, although there was no clear interaction for temperature (Wall et al., 2018). Consequently, it is possible that the coral fragments in my study enhanced their antioxidant activity after experiencing changes in treatment conditions, and managed to reduce additional stress that would have resulted in bleaching. I argue that genotype played an important role in such responses, and although it was not a significant factor, some coral genotypes performed better than others. In fact, the strong positive correlation observed between growth rate after transplantation and during the heat stress phase favours the hypothesis that genotype plays an important role in sustaining growth rate despite changes in environmental conditions. It is important, however, to consider that the rate of growth may act synergistically with other traits (e.g., photosynthetic efficiency), and may also be dependent on association with particular members of the coral holobiont. Notably, larger fragments displayed lower growth rates relative to smaller fragments, which could be explained by competition of space in the tanks or by an increased ramification of branches that limited the detection of new areas via image-based methods.

4.5.2 Maximum photochemical efficiency (Fv/Fm)

4.5.2.1 Plasticity stage

Plasticity stage - In contrast with growth data, a consistent reduction in the maximum PSII photochemical efficiency (Fv/Fm) of coral fragments was evident with the increasing intensity of temperature and $p\text{CO}_2$. Similar results have been reported for other coral species (Hoadley et al., 2015) and marine taxa like seagrass (Repolho et al., 2017), although the observed reduction in Fv/Fm has previously been attributed to seawater warming rather than acidification conditions. The fact that Fv/Fm declined similarly in the second stage of the experiment, when only temperature and not $p\text{CO}_2$

was elevated, is consistent with the notion that higher temperature is likely to be the stronger driver of the effect of treatment condition on Fv/Fm. Importantly, the negative effect of future climate change condition on Fv/Fm was dampened from 4-8 weeks if fragments had prior exposure to higher intensity treatment conditions, which is clear evidence of beneficial acclimation. This result is consistent with previous work showing that some coral and fish species can, at least to some extent, acclimate to a warming and acidifying ocean via developmental and/or transgenerational acclimation (Donelson et al., 2012, Putnam and Gates, 2015). Moreover, there was a positive carry-over effect of the HIGH treatment on Fv/Fm when transplanted to AMBIENT conditions, and Fv/Fm was maintained at control levels in the HIGH-HIGH treatment. The effect of prior treatment on Fv/Fm was less evident in the MID treatment compared with HIGH, suggesting that a threshold of higher temperature and pCO₂ may need to be reached for plasticity in Fv/Fm to be induced. Indeed, it was evident that during this post transplantation period, the reduction in Fv/Fm of fragments under HIGH treatment was diminished if they have previously experienced HIGH, and accentuated if prior treatment conditions were less intense (i.e., AMB > HIGH). Although the full extent of the mechanisms underpinning the beneficial acclimation response remain unclear, they might include physiological processes triggered by the coral host and/or its symbionts, particularly the photosynthetic microalgae (Symbiodiniaceae).

Prior exposure may have played a role in the relative enhancement of Fv/Fm by triggering protective mechanisms to reduce the detrimental effect of increased temperature and CO₂. Indeed, beneficial acclimation in Fv/Fm in adult coral fragments, combined with the lack of variation in the community structure of Symbiodiniaceae, suggest that prior exposure to elevated conditions can induce an acclimatory response on the Photosystem II. It is possible that this response was underpinned by a range of different mechanisms within the photosystem function and repair, cellular growth and division, and acquired heat tolerance processes (Robison and Warner, 2006, Iglesias-Prieto et al., 1992, Rowan, 2004, Wang et al., 2012). The mechanisms can include modifying the lipid composition of the plastic thylakoid membrane to increase thermal stability (e.g., warmer summer months and acclimation periods) (Tchernov et al., 2004, Díaz-Almeyda et al., 2010, Hill et al., 2009), and also the ability to repair the D1 protein, a protein component of the PSII (Warner et al., 1999). Furthermore, the acclimatory response can also be a function of genotypic effects of the Symbiodiniaceae or due to host genotypic effects on Symbiodiniaceae communities. For example, genotype-specific Symbiodiniaceae communities that are capable of diminishing temperature-related stress generated by treatment conditions (e.g., enhanced thermal tolerance by *Cladocopium* or better performance under high-light intensities by *Symbiodinium microadriaticum*) (Boulotte et al., 2016, Middlebrook et al., 2010, Barshis et al., 2010, Reynolds et al., 2008), whereas stable associations

between coral-Symbiodiniaceae (Tonk et al., 2013) and/or the microbiome (Ziegler et al., 2017) have also been evident on enhanced performance of corals under stress. Moreover, the observed rebound of Fv/Fm values to expected levels when transplanted back to ambient conditions confirmed that plasticity in Fv/Fm is reversible in the absence of elevated temperature and $p\text{CO}_2$. Hence, treatment conditions negatively influenced the Fv/Fm response of coral fragments, however the different treatment combinations confirmed that such effect can be buffered due to preconditioning, which confirmed beneficial acclimation and its reversibility. Importantly, Fv/Fm values were higher in larger fragments, despite the standardised use of similar areas when measuring Fv/Fm across fragments. It is possible that larger issue areas benefit the overall response of Fv/Fm to stressors due to the increased number of Symbiodiniaceae cells simultaneously responding to reduce the detrimental effect of elevated temperature and $p\text{CO}_2$.

4.5.2.2 Heat tolerance stage

Heat tolerance stage - At the end of the heat stress experiment it was clear that high temperature differentially affected Fv/Fm depending on the treatment history of the coral. Currently, it is acknowledged that environmental history is an important factor influencing the response of corals to physiological stress (Brown et al., 2000a, Brown et al., 2002b, Ainsworth et al., 2016) and the capacity of corals to acclimatise and/or adapt to climate change (Dixon et al., 2015, Palumbi et al., 2014, Torda et al., 2017). As expected, Fv/Fm was consistently lower under heat stress for all treatment histories, likely owing to temperature-mediated damage to the photosynthetic machinery (Lesser, 1997, Jones et al., 1998, Warner et al., 1999). However, I also detected evidence of increased thermal tolerance as a result of prior exposure to elevated temperature and $p\text{CO}_2$ conditions (i.e. a thermal hardening response). The decline in Fv/Fm was greatest in fragments that had no prior experience of elevated temperature and $p\text{CO}_2$ (i.e. MID and HIGH treatments), proceeded by a recent exposure to HIGH treatment following AMB exposure (AMB-HIGH). All other treatments exhibited a smaller decline in Fv/Fm when exposed to high temperature for 4 weeks. This shows that exposure to MID or HIGH treatment during the first 4 weeks of the experiment (i.e., prior to transplantation) had a beneficial effect on reducing the detrimental effect of high temperature on Fv/Fm. These findings suggest that exposure to different levels of stress promotes enhanced thermal tolerance, a process of photoacclimation that could be linked to various properties of Symbiodiniaceae photomachinery and rates of electron transport (Warner et al., 2010). It is important to recognise that all fragments from the different treatment histories experienced ambient conditions prior to heat stress, suggesting that the role of prior exposure was maintained as a memory despite the resetting period.

4.5.3 Host genotypic effects on growth and Fv/Fm

My results showed that the contribution of genotype to Fv/Fm was lower than its contribution to growth rate. Although changes in Fv/Fm as a response to stressful conditions would be primarily linked to acclimation of the Symbiodiniaceae communities, it was interesting to find that the overall contribution of the coral host genotype remained similar between the plasticity and heat stress stages. Indeed, a positive correlation in Fv/Fm occurred between experimental stages where the effect of genotype was analysed separately, suggesting that strong performing genotypes are likely to maintain their strong performance during heat stress. It is possible that this effect is driven by genotype-specific Symbiodiniaceae communities capable of diminishing temperature-related stress generated by treatment conditions (Boulotte et al., 2016, Middlebrook et al., 2010, Barshis et al., 2010), or due to stable associations between coral-Symbiodiniaceae (Tonk et al., 2013) and/or the microbiome (Ziegler et al., 2017).

4.5.4 Symbiodiniaceae and bacterial community composition structure

Coral genotype was the single most influential factor shaping and explaining Symbiodiniaceae (50%) and bacterial (15%) community structure. Treatment history may not have had a significant effect on the Symbiodiniaceae communities due to the strong specificity that can occur between species of coral and Symbiodiniaceae (Tonk et al., 2013, Mieog et al., 2009, Rouze et al., 2019) and which was also observed here. Additionally, it is possible that levels of warming and acidification and/or exposure times were not sufficient to trigger shifting and/or shuffling of symbiont strains. Similarly, bacterial communities at the family and genus levels (i.e., top 10 most abundant) showed minimal variation with treatment history. However, a more detailed analysis of relative abundances, including both abundant and rare taxa at the ASV level, showed some taxa were significantly more abundant under particular treatment histories, yet it was difficult to interpret these patterns in the context of the experimental design or host response. For example, for some comparisons the relative abundance of particular taxa was higher for histories that did not experience transplantation but included higher levels of stress (e.g., HIGH relative to AMB), whereas other taxa had higher relative abundance in transplanted treatment histories. Lack of a consistent response amongst community members may reflect the “Anna Karenina” principle as increased α -diversity and β -dispersion have been observed in the microbiome of heat-stressed individuals characterised as model organisms (e.g., *Aiptasia*) (Ahmed et al., 2019), as well as in corals (Pootakham et al., 2019, Ziegler et al., 2017). Alternatively, it could be attributed to the maintenance of ‘core’ microbial associations despite

external stressors, as previous studies have hypothesised that more stable microbiomes can be expected in organisms experiencing temperature and $p\text{CO}_2$ stress, including corals (Yachi and Loreau, 1999, Ziegler et al., 2016). Although it has been proposed that corals with a stable microbiome are more physiologically resilient to dual stresses of ocean warming and acidification conditions (Grottoli et al., 2018), it remains unclear how the lack of variation observed in this study correlates to the particular traits (growth and F_v/F_m). Finally, while genotype seems to drive most of the community dynamics, a lot of the variation remained unexplained.

Previous studies have highlighted the importance of the interplay between the coral and its associated microbiome when assessing the coral holobiont's nutrition and/or stress tolerance (Matthews et al., 2020). In my study, there was no clear correlation between Symbiodiniaceae and the bacterial community at the end of the reversible acclimation period, although a weak positive correlation was found between two symbiont members: *S. microadriaticum* and the bacterial family Endozoicomonadaceae. This is interesting considering that Endozoicomonas species are commonly assumed to provide an important role in coral holobiont functioning due to their widespread prevalence, high abundance and apparent metabolic versatility (Neave et al., 2017, Ding et al., 2016). Studies of Symbiodiniaceae-bacteria co-dynamics have shown significant correlations of multiple bacterial taxa mostly with *Durisdinium trenchii* and *D. glynni* and some *Cladocopium* spp. (Quigley et al., 2020), whereas others have found that only limited Symbiodiniaceae-bacteria co-occurrences remain consistent over time due to seasonality (Epstein et al., 2019).

4.5.5 Conclusions

Here I have used a reciprocal transplant experiment into elevated temperature and $p\text{CO}_2$ conditions followed by a more severe heat stress event to evaluate patterns of beneficial acclimation in adult coral fragments under ocean warming and acidification conditions, and determine how those patterns could be retained as a memory to influence responses to heat stress. I describe an important colony effect and a relative stability of Symbiodiniaceae contributing to the reduced effect of thermal stress in some phenotypes following exposure to high temperature. I propose that future studies exploring the plasticity of adult corals to further climate change expand my approach by examining the molecular mechanisms (e.g., gene expression plasticity, DNA methylation) underpinning the response I observed. This is particularly important as strong but divergent transcriptomic responses can be expected (Davies et al., 2016) and epigenetic mechanisms may be involved in host gene expression in response to environmental stress (Torda et al., 2017) and in regulating host-symbionts relationships (Negri and Jablonka, 2016). Furthermore, in response to the unprecedented loss of corals around the

globe, coral restoration strategies are being actively explored (Bostrom-Einarsson et al., 2020). In this context, my research suggests that exposing coral fragments to a dynamic but controlled environment might be a way to diversify phenotypes and enhance thermal tolerance, thus increasing the probability of success in restoration strategies using clonal propagation of parental colonies.

Chapter 5 – General Discussion

Climate change is challenging the physiological tolerance limits of corals, yet many questions remain about how coral populations and communities will respond to predicted future ocean warming and acidification (Hughes et al., 2017a). The current rate of environmental change may be too fast for genetic adaptation to keep pace (Merila and Hendry, 2014). However, phenotypic plasticity may facilitate rapid phenotypic adjustment (Bowler, 2005, Pigliucci et al., 2006) and could act as an alternate pathway for corals to persist under predicted climate change conditions (Torda et al., 2017), particularly in relation to acclimation and hardening responses observed under other environmental stressors (Foo and Byrne, 2016, Chevin et al., 2013, Putnam et al., 2017). While acclimation and hardening can occur in a range of organisms including corals, it remains unclear if they are sufficient to counteract current rate of ocean warming and acidification. In fact, it is still unclear how different life stages of corals will respond to the combined effects of elevated temperature and reduced pH, and if plastic responses will be beneficial.

The research presented in this thesis investigated the potential for beneficial acclimation and stress-hardening in both early and adult life stages of coral exposed to future climate change scenarios, and to assess the role of microbial symbiont communities in acclimation responses. I found consistent evidence for thermal hardening in larvae, which displayed enhanced tolerance to extreme temperature (35.5°C) after 10-days of preconditioning under elevated climate conditions (high temperature and $p\text{CO}_2$), although it is important to consider the potential for genetic selection to have occurred on the batch cultures. Further, there was clear evidence of beneficial acclimation in maximum photochemical efficiency (Fv/Fm) in adult coral fragments, and subtle evidence for a similar effect in coral recruits. Treatment conditions had minimal effect on Symbiodiniaceae or bacterial community structure in adult fragments, suggesting that acclimation of Fv/Fm in the coral holobiont was due to photoacclimation of the existing symbionts rather than shuffling or swapping of the symbiont community. Furthermore, thermal hardening was evident in both coral recruit and adult life stages exposed to heat stress after a “relaxation” period under ambient conditions. These findings show that a memory of past exposure to elevated temperature and $p\text{CO}_2$ can enhance performance during an acute heat stress event. Unexpectedly, treatment conditions did not have a consistent effect on coral growth rates at any life stage. Moreover, although this assessment was not an objective of this thesis, I discovered that colony is a major driver of the microbiome variation in adult corals, whereas in recruits the majority of the variation remained unexplained. Ideally, future studies should track individual crosses of colonies to be able to track genetic and maternal effects on their offspring. Together with an expansion on the evaluation of types of symbionts and their beneficial functions

across different experimental time points, this will allow a better understanding of the role of different members of the coral holobiont to counteract the effects of rapid climate change conditions. These results highlight the potential for phenotypic plasticity to buffer some of the negative effects of climate change on corals, including in demographically important early life history stages. My results suggest that phenotypic plasticity in the host coral and associated symbionts could help corals persist under future warming and acidification conditions. It is important to consider that other effects such as mortality may be encountered over longer time frames than those considered in this study.

My research highlights the potential importance of plastic responses triggered by exposure of corals to climate change conditions, suggesting that prior exposure to elevated temperature and $p\text{CO}_2$, even over short periods, can increase tolerance of corals to acute and chronic stress, without necessarily reducing the survivorship over time. In this context, the enhanced thermal tolerance observed in aposymbiotic larvae under acute heat stress indicates that benefits can arise in the coral host following exposure to more challenging rearing conditions without relying on Symbiodiniaceae. Indeed, in nature larvae that are caught up in the surface waters or other locally hot water pools (e.g., reef flats), or that are swept off the reef could be exposed to high temperature and high light conditions (van Oppen et al., 2018, Baird et al.), which may have lasting effects on their resilience. Consequently, a similar approach could be optimised and applied for coral reef restoration efforts. For example, research groups aiming to collect coral spawn and transport it to other locations, could include an exposure of larvae to elevated conditions prior to deployment to increase the subsequent temperature tolerance.

The mechanisms underpinning beneficial acclimation and thermal hardening may differ between coral life stages and the traits investigated. The absence of Symbiodiniaceae in the larvae suggests that the enhanced survivorship under thermal stress was a response from the coral host (Heyward and Negri, 2010, Hayward et al., 2001). Potential mechanisms include the regulation of gene expression underpinning the coral heat stress response, involving a wide array of cellular processes such as the induction of molecular chaperones (e.g., Heat shock proteins, Hsps) and antioxidant enzymes, but also Ca^{2+} homeostasis disruption, cytoskeletal reorganization, and altered cell signalling and transcriptional regulation (DeSalvo et al., 2008, Downs et al., 2002, Downs et al., 2000, DeSalvo et al., 2010, Meyer et al., 2011b). Furthermore, levels of gene expression can be affected by epigenetic processes, including the stable modification of chromosomal regions by DNA methylation, interaction of small non-coding RNA products with gene promoters or enzymatic modification of histones. Indeed,

DNA methylation has been hypothesized as a potential adaptive mechanism in response to changes in environmental conditions by influencing the phenotypic plasticity of the organism (Angers et al., 2010, Roberts and Gavery, 2012, Verhoeven et al., 2016, Putnam et al., 2016), although its role into the acclimation responses of corals and potential variation among life stages remains unclear (Torda et al., 2017, Suzuki and Bird, 2008, Dixon et al., 2014, Dixon et al., 2016). To better understand the mechanisms underpinning acclimatory responses, further studies should expand the temporal molecular sampling of larvae during the rearing and heat stress stages to better define the time when treatment conditions activate the molecular response underpinning thermal tolerance. Moreover, analysis of epigenetic markers in recently settled recruits, could reveal whether the enhanced thermal tolerance is likely to stay throughout coral development.

By contrast, beneficial acclimation in Fv/Fm in coral recruits and adult fragments, combined with the lack of variation in the community structure of Symbiodiniaceae, suggest that prior exposure to elevated conditions can induce an acclimatory response within the photosystem II of their algal symbionts. Such a successful acclimatory response could be underpinned by differential photosystem function and repair, cellular growth and division, and acquired heat tolerance (Robison and Warner, 2006, Iglesias-Prieto et al., 1992, Rowan, 2004, Wang et al., 2012). Mechanisms involved in the response could include modifying the lipid composition of the plastic thylakoid membrane to increase thermal stability (e.g., warmer summer months and acclimation periods) (Tchernov et al., 2004, Díaz-Almeyda et al., 2010, Hill et al., 2009), and also the ability to repair the D1 protein, a protein component of the PSII (Warner et al., 1999). Furthermore, the acclimatory response could be a function of genotypic effects of the Symbiodiniaceae or due to host genotypic effects on Symbiodiniaceae communities. In fact, symbiont community diversity metrics may function as indicators of resilience when assessing host performance (Howe-Kerr et al., 2020, Quigley et al., 2018). For example, particular Symbiodiniaceae are capable of diminishing temperature-related stress generated by treatment conditions (e.g., enhanced thermal tolerance by *Cladocopium* or better performance under high-light intensities by *Symbiodinium microadriaticum*) (Boulotte et al., 2016, Middlebrook et al., 2010, Barshis et al., 2010, Reynolds et al., 2008), although stable associations between coral-Symbiodiniaceae (Tonk et al., 2013) and/or the microbiome (Ziegler et al., 2017) have also been shown to enhance the performance of corals under stress.

My research found a stronger signal of beneficial acclimation in the response of Fv/Fm in adult fragments than in coral juveniles. However, it is still unclear how responses change over time and thus

how much time is needed to induce an acclimatory response. Interestingly, the prior exposure time used in adult fragments (4 weeks) was half of the time used in coral recruits (8 weeks), yet the response recorded in recruits was much more subtle. One explanation for this difference could be the expected winnowing of the coral recruit-Symbiodiniaceae associations in developing recruits vs the more established Symbiodiniaceae community in adult fragments (Berkelmans and van Oppen, 2006, Robison and Warner, 2006, Baker, 2001, Quigley et al., 2020). Additional molecular mechanisms (e.g., DNA methylation) could influence the modulation of protective antioxidant pathways helping the PSII endure thermal stress (Robison and Warner, 2006, Iglesias-Prieto et al., 1992, Rowan, 2004, Wang et al., 2012), which could also be a function of the previous exposure of adult corals to environmental fluctuations on the reef throughout their lifetime until collection occurred. A four-week exposure period appears to be sufficient for the induction of beneficial acclimation in Fv/Fm, and also to reset its values to the expected ambient levels as observed during the resetting period prior to heat stress (2 weeks). Indeed, rapid acclimation to higher temperatures has been observed after 1-2 weeks acclimation to warm conditions (Bay and Palumbi, 2015), whereas the opposite has been observed following 6-month exposure (Schoepf et al., 2019), suggesting limitation to the acclimatory response. However, the intensity of the response is likely to be influenced by a number of factors, including symbiont associations and molecular responses occurring at different coral life stages. A primary uncertainty is how long the beneficial acclimation is maintained which should be addressed by future research testing recovery rates after chronic heat stress exposure. Similarly, it would be valuable to repeat a heat stress exposure on survivors, aiming to evaluate if the response remains similar or if longer incubation periods, and age, modulates the manifestation and intensity of acclimation signs.

These research findings can improve the efficacy of reef restoration approaches as acclimation of coral fragments under more dynamic environments prior to final site deployment may be beneficial for inducing more resilient phenotypes when using both sexual reproduction and clonal propagation (Bostrom-Einarsson et al., 2020, Randall et al., 2020). For example, a passive exposure approach may be to use coral gardening approaches that employ *in situ* nurseries (e.g., reef lagoons) prior to deployment of fragments on damaged reefs. The usually higher temperature and CO₂ expected in reef lagoons (Jokiel, 2016), may act as the trigger that corals need for activating acclimatory responses via phenotypic plasticity. Conversely, young corals may be exposed to more extreme environments during the aquaculture process as part of their early development. The exposure of corals to a more dynamic and challenging environment prior to reef deployment, could not only promote acclimatory responses in the coral host but also the acquisition of a diversified microbiome. Hence, complementing current

strategies on direct restoration interventions and potentially providing corals with a more robust stress memory to better respond to rapid environmental change.

Reducing greenhouse gas emissions undoubtedly remains the best option to stabilise the climate (IPCC, 2019) and protect coral reefs but despite immediate action reef waters will continue to warm in the foreseeable future. Therefore, direct interventions may increasingly be required to help corals cope with both chronic and acute environmental change. These interventions may buffer populations under stress and help in their adaptation but will require extensive research and development before their feasibility, risks and benefits can be fully understood (van Oppen et al., 2017, McDonald et al., 2019). The approaches currently examined encompass various alternatives of selective breeding (i.e., crossbreeding of selected corals based on desirable traits, potentially including translocation of colonies among locations), manipulation of the coral microbiome (i.e., targeted inoculation of coral with natural or lab-evolved more tolerant microbes – including bacteria and Symbiodiniaceae), and also preconditioning of corals to desired environmental conditions (Anthony et al., 2020, National Academies of Sciences and Medicine, 2019).

Strategies to enhance the tolerance of corals based on their phenotypic plasticity should be merged with research to optimise aquaculture processes for asexually produced clones (i.e., clonal propagation of adult coral fragments) and sexually produced offspring (i.e., coral larvae and early juvenile stages) for out planting on the reef (Bostrom-Einarsson et al., 2020). While promising results are emerging from the laboratory or small-scale field experiments, the feasibility of up-scaling challenge future implementation and impact. Based on the results presented in this thesis, incorporating knowledge gained from studies based on the mechanisms underpinning acclimation and hardening responses, could become a complementary pathway to enhance the tolerance of different life stages of coral to help them endure climate change conditions predicted for this century. Hence, this strategy could potentially reduce the costs and timeframes of current reef restoration strategies as well as better informing future reef predictions by considering both genetic and plasticity mechanisms.

This thesis has generated important insights into the effects of future climate scenarios on the performance of different coral life stages, and their ability to withstand thermal stress events which can be used to better inform predictions of future reef states. Furthermore, this thesis shows that

acclimation of corals to more extreme environments may be beneficial for inducing more temperature resilient phenotypes which is directly relevant to proposed reef restoration and adaptation approaches. In this context, future experiments and research may expand these findings by reproducing the thesis experimental design in the field, particularly in highly variable environments. Importantly, further research should also consider the potential for selection on genotypes that can occur during the development of early life stages. Hence, this thesis has advanced our understanding of the potential strategies that could assist coral populations respond to rapid climate change and inform intervention efforts to accelerate these processes.

References

- ABREGO, D., ULSTRUP, K. E., WILLIS, B. L. & VAN OPPEN, M. J. H. 2008. Species-specific interactions between algal endosymbionts and coral hosts define their bleaching response to heat and light stress. *Proceedings of the Royal Society B-Biological Sciences*, 275, 2273-2282.
- ABREGO, D., WILLIS, B. L. & VAN OPPEN, M. J. 2012. Impact of light and temperature on the uptake of algal symbionts by coral juveniles. *PLoS One*, 7, e50311.
- ACINAS, S. G., SARMA-RUPAVTARM, R., KLEPAC-CERAJ, V. & POLZ, M. F. 2005. PCR-induced sequence artifacts and bias: insights from comparison of two 16S rRNA clone libraries constructed from the same sample. *Appl Environ Microbiol*, 71, 8966-9.
- ADJEROUD, M., KAYAL, M., IBORRA-CANTONNET, C., VERCELLONI, J., BOSSERELLE, P., LIAO, V., CHANCERELLE, Y., CLAUDET, J. & PENIN, L. 2018. Recovery of coral assemblages despite acute and recurrent disturbances on a South Central Pacific reef. *Sci Rep*, 8, 9680.
- AHMED, H. I., HERRERA, M., LIEW, Y. J. & ARANDA, M. 2019. Long-Term Temperature Stress in the Coral Model *Aiptasia* Supports the "Anna Karenina Principle" for Bacterial Microbiomes. *Front Microbiol*, 10, 975.
- AINSWORTH, T. D., HERON, S. F., ORTIZ, J. C., MUMBY, P. J., GRECH, A., OGAWA, D., EAKIN, C. M. & LEGGAT, W. 2016. Climate change disables coral bleaching protection on the Great Barrier Reef. *Science*, 352, 338-42.
- ALBRIGHT, R. & MASON, B. 2013. Projected near-future levels of temperature and pCO₂ reduce coral fertilization success. *PLoS One*, 8, e56468.
- ALVAREZ-FILIP, L., DULVY, N. K., GILL, J. A., COTE, I. M. & WATKINSON, A. R. 2009. Flattening of Caribbean coral reefs: region-wide declines in architectural complexity. *Proc Biol Sci*, 276, 3019-25.
- ANDERSON, K. D. 2016. *Temporal and spatial variation in the growth of branching corals*.
- ANGERS, B., CASTONGUAY, E. & MASSICOTTE, R. 2010. Environmentally induced phenotypes and DNA methylation: how to deal with unpredictable conditions until the next generation and after. *Mol Ecol*, 19, 1283-95.
- ANGILLETTA, M. J. 2009. *Thermal Adaptation: A Theoretical and Empirical Synthesis*, Oxford, Oxford University Press, UK.
- ANTHONY, K. R., KLINE, D. I., DIAZ-PULIDO, G., DOVE, S. & HOEGH-GULDBERG, O. 2008. Ocean acidification causes bleaching and productivity loss in coral reef builders. *Proc Natl Acad Sci U S A*, 105, 17442-6.
- ANTHONY, K. R. N., HELMSTEDT, K. J., BAY, L. K., FIDELMAN, P., HUSSEY, K. E., LUNDGREN, P., MEAD, D., MCLEOD, I. M., MUMBY, P. J., NEWLANDS, M., SCHAFFELKE, B., WILSON, K. A. & HARDISTY, P. E. 2020. Interventions to help coral reefs under global change-A complex decision challenge. *PLoS One*, 15, e0236399.
- APPRILL, A., MARLOW, H. Q., MARTINDALE, M. Q. & RAPPE, M. S. 2009. The onset of microbial associations in the coral *Pocillopora meandrina*. *ISME J*, 3, 685-99.
- APPRILL, A., MARLOW, H. Q., MARTINDALE, M. Q. & RAPPE, M. S. 2012. Specificity of associations between bacteria and the coral *Pocillopora meandrina* during early development. *Appl Environ Microbiol*, 78, 7467-75.
- BABCOCK, R. & MUNDY, C. 1996. Coral recruitment: Consequences of settlement choice for early growth and survivorship in two scleractinians. *Journal of Experimental Marine Biology and Ecology*, 206, 179-201.
- BABCOCK, R. C. 1991. Comparative Demography of Three Species of Scleractinian Corals Using Age- and Size-Dependent Classifications. *Ecological Monographs*, 61, 225-244.
- BAIRD, A. H., BHAGOOLI, R., RALPH, P. J. & TAKAHASHI, S. 2009. Coral bleaching: the role of the host. *Trends Ecol Evol*, 24, 16-20.
- BAIRD, A. H., GILMOUR, J. P., KAMIKI, T. M., NONAKA, M., PRATCHETT, M. S., YAMAMOTO, H. H. & YAMASAKI, H. Temperature tolerance of symbiotic and non-symbiotic coral larvae. 2006.

- 10th International Coral Reef Symposium U6 - ctx_ver=Z39.88-2004&ctx_enc=info%3Aofi%2Fenc%3AUTF-8&rft_id=info%3Aid%2Fsummon.serialssolutions.com&rft_val_fmt=info%3Aofi%2Ffmt%3Akev%3Amtx%3Abook&rft.genre=proceeding&rft.title=Temperature+tolerance+of+symbiotic+and+non-symbiotic+coral+larvae&rft.au=Baird%2C+Andrew+H&rft.au=Gilmour%2C+James+P&rft.au=Kamiki%2C+Takayuki+M&rft.au=Nonaka%2C+Masanori&rft.date=2006&rft.pub=10th+International+Coral+Reef+Symposium&rft.externalDBID=7374617475733D707562&rft.externalDocID=oai_researchonline_jcu_edu_au_4340¶mdict=en-US U7 - Conference Proceeding.
- BAKER, A. C. 2001. Ecosystems: reef corals bleach to survive change. *Nature*, 411, 765.
- BAKER, A. C. 2003. Flexibility and specificity in coral-algal symbiosis: Diversity, ecology, and biogeography of Symbiodinium. *Annual Review of Ecology Evolution and Systematics*, 34, 661-689.
- BAKER, A. C., STARGER, C. J., MCCLANAHAN, T. R. & GLYNN, P. W. 2004. Coral reefs: corals' adaptive response to climate change. *Nature*, 430, 741.
- BARLOW, J., FRANCA, F., GARDNER, T. A., HICKS, C. C., LENNOX, G. D., BERENQUER, E., CASTELLO, L., ECONOMO, E. P., FERREIRA, J., GUENARD, B., GONTIJO LEAL, C., ISAAC, V., LEES, A. C., PARR, C. L., WILSON, S. K., YOUNG, P. J. & GRAHAM, N. A. J. 2018. The future of hyperdiverse tropical ecosystems. *Nature*, 559, 517-526.
- BARSHIS, D. J., BIRKELAND, C., TOONEN, R. J., GATES, R. D. & STILLMAN, J. H. 2018. High-frequency temperature variability mirrors fixed differences in thermal limits of the massive coral *Porites lobata*. *J Exp Biol*, 221.
- BARSHIS, D. J., LADNER, J. T., OLIVER, T. A., SENECA, F. O., TRAYLOR-KNOWLES, N. & PALUMBI, S. R. 2013. Genomic basis for coral resilience to climate change. *Proc Natl Acad Sci U S A*, 110, 1387-92.
- BARSHIS, D. J., STILLMAN, J. H., GATES, R. D., TOONEN, R. J., SMITH, L. W. & BIRKELAND, C. 2010. Protein expression and genetic structure of the coral *Porites lobata* in an environmentally extreme Samoan back reef: does host genotype limit phenotypic plasticity? *Mol Ecol*, 19, 1705-20.
- BAY, L. K., DOYLE, J., LOGAN, M. & BERKELMANS, R. 2016. Recovery from bleaching is mediated by threshold densities of background thermo-tolerant symbiont types in a reef-building coral. *Royal Society Open Science*, 3, 160322.
- BAY, R. A. & PALUMBI, S. R. 2015. Rapid Acclimation Ability Mediated by Transcriptome Changes in Reef-Building Corals. *Genome Biol Evol*, 7, 1602-12.
- BELLANTUONO, A. J., GRANADOS-CIFUENTES, C., MILLER, D. J., HOEGH-GULDBERG, O. & RODRIGUEZ-LANETTY, M. 2012. Coral thermal tolerance: tuning gene expression to resist thermal stress. *PLoS One*, 7, e50685.
- BERKELMANS, R. & VAN OPPEN, M. J. 2006. The role of zooxanthellae in the thermal tolerance of corals: a 'nugget of hope' for coral reefs in an era of climate change. *Proc Biol Sci*, 273, 2305-12.
- BERNASCONI, R., STAT, M., KOENDERS, A., PAPANINI, A., BUNCE, M. & HUGGETT, M. J. 2019. Establishment of Coral-Bacteria Symbioses Reveal Changes in the Core Bacterial Community With Host Ontogeny. *Front Microbiol*, 10, 1529.
- BLACKALL, L. L., WILSON, B. & VAN OPPEN, M. J. 2015. Coral-the world's most diverse symbiotic ecosystem. *Mol Ecol*, 24, 5330-47.
- BONDURIANSKY, R., CREAN, A. J. & DAY, T. 2012. The implications of nongenetic inheritance for evolution in changing environments. *Evol Appl*, 5, 192-201.
- BONGAERTS, P., RIGINOS, C., HAY, K. B., VAN OPPEN, M. J., HOEGH-GULDBERG, O. & DOVE, S. 2011. Adaptive divergence in a scleractinian coral: physiological adaptation of *Seriatopora hystrix* to shallow and deep reef habitats. *BMC Evol Biol*, 11, 303.

- BONK, F., POPP, D., HARMS, H. & CENTLER, F. 2018. PCR-based quantification of taxa-specific abundances in microbial communities: Quantifying and avoiding common pitfalls. *J Microbiol Methods*, 153, 139-147.
- BONTHOND, G., MERSELIS, D. G., DOUGAN, K. E., GRAFF, T., TODD, W., FOURQUIREAN, J. W. & RODRIGUEZ-LANETTY, M. 2018. Inter-domain microbial diversity within the coral holobiont *Siderastrea siderea* from two depth habitats. *PeerJ*, 6, e4323.
- BOSTROM-EINARSSON, L., BABCOCK, R. C., BAYRAKTAROV, E., CECCARELLI, D., COOK, N., FERSE, S. C. A., HANCOCK, B., HARRISON, P., HEIN, M., SHAVER, E., SMITH, A., SUGGETT, D., STEWART-SINCLAIR, P. J., VARDI, T. & MCLEOD, I. M. 2020. Coral restoration - A systematic review of current methods, successes, failures and future directions. *PLoS One*, 15, e0226631.
- BOULOTTE, N. M., DALTON, S. J., CARROLL, A. G., HARRISON, P. L., PUTNAM, H. M., PEPLOW, L. M. & VAN OPPEN, M. J. 2016. Exploring the Symbiodinium rare biosphere provides evidence for symbiont switching in reef-building corals. *ISME J*, 10, 2693-2701.
- BOURNE, D., IIDA, Y., UTHICKE, S. & SMITH-KEUNE, C. 2008. Changes in coral-associated microbial communities during a bleaching event. *ISME J*, 2, 350-63.
- BOURNE, D. G., GARREN, M., WORK, T. M., ROSENBERG, E., SMITH, G. W. & HARVELL, C. D. 2009. Microbial disease and the coral holobiont. *Trends Microbiol*, 17, 554-62.
- BOURNE, D. G., MORROW, K. M. & WEBSTER, N. S. 2016. Insights into the Coral Microbiome: Underpinning the Health and Resilience of Reef Ecosystems. *Annu Rev Microbiol*, 70, 317-40.
- BOWLER, K. 2005. Acclimation, heat shock and hardening. *Journal of Thermal Biology*, 30, 125-130.
- BROOKS, J. P. 2016. Challenges for case-control studies with microbiome data. *Ann Epidemiol*, 26, 336-341 e1.
- BROWN, B. E., DOWNS, C. A., DUNNE, R. P. & GIBB, S. W. 2002a. Exploring the basis of thermotolerance in the reef coral *Goniastrea aspera*. *Marine Ecology Progress Series*, 242, 119-129.
- BROWN, B. E., DUNNE, R., GOODSON, M. & DOUGLAS, A. 2002b. Experience shapes the susceptibility of a reef coral to bleaching. *Coral Reefs*, 21, 119-126.
- BROWN, B. E. & DUNNE, R. P. 2008. Solar radiation modulates bleaching and damage protection in a shallow water coral. *Marine Ecology Progress Series*, 362, 99-107.
- BROWN, B. E., DUNNE, R. P., GOODSON, M. S. & DOUGLAS, A. E. 2000a. Marine ecology - Bleaching patterns in reef corals. *Nature*, 404, 142-143.
- BROWN, B. E., DUNNE, R. P., WARNER, M. E., AMBARSARI, I., FITT, W. K., GIBB, S. W. & CUMMINGS, D. G. 2000b. Damage and recovery of Photosystem II during a manipulative field experiment on solar bleaching in the coral *Goniastrea aspera*. *Marine Ecology Progress Series*, 117-124.
- BÜRKNER, P. 2017. brms: An R package for Bayesian multilevel models using Stan. *Journal of Statistical Software*, 80, 1-28.
- BURTON, E. A. & WALTER, L. M. 1987. Relative precipitation rates of aragonite and Mg calcite from seawater: Temperature or carbonate ion control? *Geology*, 15, 111.
- CAI, W., BORLACE, S., LENGAINNE, M., VAN RENSCH, P., COLLINS, M., VECCHI, G., TIMMERMANN, A., SANTOSO, A., MCPHADEN, M. J., WU, L., ENGLAND, M. H., WANG, G., GUILYARDI, E. & JIN, F. 2014. Increasing frequency of extreme El Niño events due to greenhouse warming. *Nature Climate Change*, 4, 111-116.
- CALLAHAN, B. J., MCMURDIE, P. J., ROSEN, M. J., HAN, A. W., JOHNSON, A. J. & HOLMES, S. P. 2016. DADA2: High-resolution sample inference from illumina amplicon data. *Nat Methods*, 13, 581-3.
- CAMACHO, C., COULOURIS, G., AVAGYAN, V., MA, N., PAPADOPOULOS, J., BEALER, K. & MADDEN, T. L. 2009. BLAST+: architecture and applications. *BMC Bioinformatics*, 10, 421.
- CAPORASO, J. G., KUCZYNSKI, J., STOMBAUGH, J., BITTINGER, K., BUSHMAN, F. D., COSTELLO, E. K., FIERER, N., PENA, A. G., GOODRICH, J. K., GORDON, J. I., HUTTLEY, G. A., KELLEY, S. T., KNIGHTS, D., KOENIG, J. E., LEY, R. E., LOZUPONE, C. A., MCDONALD, D., MUEGGE, B. D., PIRRUNG, M., REEDER, J., SEVINSKY, J. R., TURNBAUGH, P. J., WALTERS, W. A., WIDMANN, J.,

- YATSUNENKO, T., ZANEVELD, J. & KNIGHT, R. 2010. QIIME allows analysis of high-throughput community sequencing data. *Nat Methods*, 7, 335-6.
- CAPORASO, J. G., LAUBER, C. L., WALTERS, W. A., BERG-LYONS, D., HUNTLEY, J., FIERER, N., OWENS, S. M., BETLEY, J., FRASER, L., BAUER, M., GORMLEY, N., GILBERT, J. A., SMITH, G. & KNIGHT, R. 2012. Ultra-high-throughput microbial community analysis on the Illumina HiSeq and MiSeq platforms. *ISME J*, 6, 1621-4.
- CARLOS, C., TORRES, T. T. & OTTOBONI, L. M. 2013. Bacterial communities and species-specific associations with the mucus of Brazilian coral species. *Sci Rep*, 3, 1624.
- CAROSELLI, E., GIZZI, F., PRADA, F., MARCHINI, C., AIRI, V., KAANDORP, J., FALINI, G., DUBINSKY, Z. & GOFFREDO, S. 2018. Low and variable pH decreases recruitment efficiency in populations of a temperate coral naturally present at a CO₂ vent. *Limnology and Oceanography*, 64, 1059-1069.
- CASTILLO, K. D. & HELMUTH, B. S. T. 2005. Influence of thermal history on the response of *Montastraea annularis* to short-term temperature exposure. *Marine Biology*, 148, 261-270.
- CHAN, N. C. & CONNOLLY, S. R. 2013. Sensitivity of coral calcification to ocean acidification: a meta-analysis. *Glob Chang Biol*, 19, 282-90.
- CHAN, W. Y., PELOW, L. M., MENENDEZ, P., HOFFMANN, A. A. & VAN OPPEN, M. J. H. 2019. The roles of age, parentage and environment on bacterial and algal endosymbiont communities in *Acropora* corals. *Mol Ecol*, 28, 3830-3843.
- CHEN, P. Y., CHEN, C. C., CHU, L. & MCCARL, B. 2015. Evaluating the economic damage of climate change on global coral reefs. *Global Environmental Change-Human and Policy Dimensions*, 30, 12-20.
- CHEVIN, L. M., COLLINS, S. & LEFEVRE, F. 2013. Phenotypic plasticity and evolutionary demographic responses to climate change: taking theory out to the field. *Functional Ecology*, 27, 966-979.
- CHUA, C. M., LEGGAT, W., MOYA, A. & BAIRD, A. H. 2013a. Near-future reductions in pH will have no consistent ecological effects on the early life-history stages of reef corals. *Marine Ecology Progress Series*, 486, 143-151.
- CHUA, C. M., LEGGAT, W., MOYA, A. & BAIRD, A. H. 2013b. Temperature affects the early life history stages of corals more than near future ocean acidification. *Marine Ecology Progress Series*, 475, 85-92.
- CLARKE, G. M. & MCKENZIE, J. A. 1987. Developmental stability of insecticide resistant phenotypes in blowfly; a result of canalizing natural selection. *Nature*, 325, 345-346.
- COLLINS, M., R. KNUITTI, J. ARBLASTER, J.-L. DUFRESNE, T. FICHEFET, P. FRIEDLINGSTEIN, X. GAO, W.J. GUTOWSKI, T. JOHNS, G. KRINNER, M. SHONGWE, C. TEBALDI, A.J. WEAVER AND M. WEHNE 2013. *Long-term climate change: Projections, commitments and irreversibility*, Cambridge University Press, Cambridge, United Kingdom and New York, NY, USA, Stocker, T.F., D. Qin, G.-K. Plattner, M. Tignor, S.K. Allen, J. Boschung, A. Nauels, Y. Xia, V. Bex and P.M. Midgale.
- CONLAN, J. A., HUMPHREY, C. A., SEVERATI, A. & FRANCIS, D. S. 2017. Influence of different feeding regimes on the survival, growth, and biochemical composition of *Acropora* coral recruits. *PLoS One*, 12, e0188568.
- COSTEA, P. I., ZELLER, G., SUNAGAWA, S., PELLETIER, E., ALBERTI, A., LEVENEZ, F., TRAMONTANO, M., DRIESSEN, M., HERCOG, R., JUNG, F. E., KULTIMA, J. R., HAYWARD, M. R., COELHO, L. P., ALLEN-VERCOE, E., BERTRAND, L., BLAUT, M., BROWN, J. R. M., CARTON, T., COOLS-PORTIER, S., DAIGNEAULT, M., DERRIEN, M., DRUESNE, A., DE VOS, W. M., FINLAY, B. B., FLINT, H. J., GUARNER, F., HATTORI, M., HEILIG, H., LUNA, R. A., VAN HYLCKAMA Vlieg, J., JUNICK, J., KLYMIUK, I., LANGELLA, P., LE CHATELIER, E., MAI, V., MANICHANH, C., MARTIN, J. C., MERY, C., MORITA, H., O'TOOLE, P. W., ORVAIN, C., PATIL, K. R., PENDERS, J., PERSSON, S., PONS, N., POPOVA, M., SALONEN, A., SAULNIER, D., SCOTT, K. P., SINGH, B., SLEZAK, K., VEIGA, P., VERSALOVIC, J., ZHAO, L., ZOETENDAL, E. G., EHRLICH, S. D., DORE, J. & BORK, P. 2017.

- Towards standards for human fecal sample processing in metagenomic studies. *Nat Biotechnol*, 35, 1069-1076.
- CRUZ, D. W. D. & HARRISON, P. L. 2017. Enhanced larval supply and recruitment can replenish reef corals on degraded reefs. *Sci Rep*, 7, 13985.
- DAVIES, S. W., MARCHETTI, A., RIES, J. B. & CASTILLO, K. D. 2016. Thermal and pCO₂ Stress Elicit Divergent Transcriptomic Responses in a Resilient Coral. *Frontiers in Marine Science*, 3.
- DAVIES, S. W., MATZ, M. V. & VIZE, P. D. 2013. Ecological complexity of coral recruitment processes: effects of invertebrate herbivores on coral recruitment and growth depends upon substratum properties and coral species. *PLoS One*, 8, e72830.
- DAVIES, S. W., WHAM, D. C., KANKE, M. R. & MATZ, M. V. 2019. Contrasting population genetic structure in *Acropora* coral hosts and their algal symbionts across multiple spatial scales. *bioRxiv*, 575183.
- DE CÁCERES, M. 2013. How to use the indicpecies package (ver. 1.7. 1). *R Proj*, 29.
- DE CÁCERES, M. & LEGENDRE, P. 2009. Associations between species and groups of sites: indices and statistical inference. *Ecology*, 90, 3566-3574.
- DE VALCK, J. & ROLFE, J. 2019. Comparing biodiversity valuation approaches for the sustainable management of the Great Barrier Reef, Australia. *Ecosystem Services*, 35, 23-31.
- DE'ATH, G., FABRICIUS, K. E., SWEATMAN, H. & PUOTINEN, M. 2012. The 27-year decline of coral cover on the Great Barrier Reef and its causes. *Proc Natl Acad Sci U S A*, 109, 17995-9.
- DESALVO, M. K., SUNAGAWA, S., VOOLSTRA, C. R. & MEDINA, M. 2010. Transcriptomic responses to heat stress and bleaching in the elkhorn coral *Acropora palmata*. *Marine Ecology Progress Series*, 402, 97-113.
- DESALVO, M. K., VOOLSTRA, C. R., SUNAGAWA, S., SCHWARZ, J. A., STILLMAN, J. H., COFFROTH, M. A., SZMANT, A. M. & MEDINA, M. 2008. Differential gene expression during thermal stress and bleaching in the Caribbean coral *Montastraea faveolata*. *Mol Ecol*, 17, 3952-71.
- DÍAZ-ALMEYDA, E., THOMÉ, P. E., EL HAFIDI, M. & IGLESIAS-PRIETO, R. 2010. Differential stability of photosynthetic membranes and fatty acid composition at elevated temperature in *Symbiodinium*. *Coral Reefs*, 30, 217-225.
- DIMOND, J. L. & ROBERTS, S. B. 2016. Germline DNA methylation in reef corals: patterns and potential roles in response to environmental change. *Mol Ecol*, 25, 1895-904.
- DING, J. Y., SHIU, J. H., CHEN, W. M., CHIANG, Y. R. & TANG, S. L. 2016. Genomic Insight into the Host-Endosymbiont Relationship of *Endozoicomonas montiporae* CL-33(T) with its Coral Host. *Front Microbiol*, 7, 251.
- DIXON, G. B., BAY, L. K. & MATZ, M. V. 2014. Bimodal signatures of germline methylation are linked with gene expression plasticity in the coral *Acropora millepora*. *BMC Genomics*, 15, 1109.
- DIXON, G. B., BAY, L. K. & MATZ, M. V. 2016. Genic DNA methylation drives codon bias in stony corals. *Molecular Biology and Evolution*, msw100.
- DIXON, G. B., DAVIES, S. W., AGLYAMOVA, G. A., MEYER, E., BAY, L. K. & MATZ, M. V. 2015. Genomic determinants of coral heat tolerance across latitudes. *Science*, 348, 1460-2.
- DONELSON, J. M. & MUNDAY, P. L. 2015. Transgenerational plasticity mitigates the impact of global warming to offspring sex ratios. *Glob Chang Biol*, 21, 2954-62.
- DONELSON, J. M., MUNDAY, P. L., MCCORMICK, M. I. & PITCHER, C. R. 2012. Rapid transgenerational acclimation of a tropical reef fish to climate change. *Nature Climate Change*, 2, 30-32.
- DONEY, S. C., FABRY, V. J., FEELY, R. A. & KLEYPAS, J. A. 2009. Ocean acidification: the other CO₂ problem. *Ann Rev Mar Sci*, 1, 169-92.
- DONNER, S. D., RICKBEIL, G. J. M. & HERON, S. F. 2017. A new, high-resolution global mass coral bleaching database. *PLoS One*, 12, e0175490.
- DORAN, H., BLIESE, P., BATES, D. & DOWLING, M. 2007. Estimating the multilevel Rasch model: with the lme4 package. *Journal of Statistical Software*, 20, 74.
- DOROPOULOS, C., WARD, S., MARSHALL, A., DIAZ-PULIDO, G. & MUMBY, P. J. 2012a. Interactions among chronic and acute impacts on coral recruits: the importance of size-escape thresholds. *Ecology*, 93, 2131-2138.

- DOROPOULOS, C., WARD, S., MARSHALL, A., DIAZ-PULIDO, G. & MUMBY, P. J. 2012b. Interactions among chronic and acute impacts on coral recruits: the importance of size-escape thresholds. *Ecology*, 93, 2131-8.
- DOVE, S., ORTIZ, J. C., ENRIQUEZ, S., FINE, M., FISHER, P., IGLESIAS-PRieto, R., THORNHILL, D. & HOEGH-GULDBERG, O. 2006. Response of holosymbiont pigments from the scleractinian coral *Montipora monasteriata* to short-term heat stress.
- DOVE, S. G., KLINE, D. I., PANTOS, O., ANGLY, F. E., TYSON, G. W. & HOEGH-GULDBERG, O. 2013. Future reef decalcification under a business-as-usual CO₂ emission scenario. *Proc Natl Acad Sci U S A*, 110, 15342-7.
- DOWNS, C. A., FAUTH, J. E., HALAS, J. C., DUSTAN, P., BEMISS, J. & WOODLEY, C. M. 2002. Oxidative stress and seasonal coral bleaching. *Free Radic Biol Med*, 33, 533-43.
- DOWNS, C. A., MUELLER, E., PHILLIPS, S., FAUTH, J. E. & WOODLEY, C. M. 2000. A molecular biomarker system for assessing the health of coral (*Montastraea faveolata*) during heat stress. *Mar Biotechnol (NY)*, 2, 533-44.
- DRURY, C., MANZELLO, D. & LIRMAN, D. 2017. Genotype and local environment dynamically influence growth, disturbance response and survivorship in the threatened coral, *Acropora cervicornis*. *PLoS One*, 12, e0174000.
- EAKIN, C. M., MORGAN, J. A., HERON, S. F., SMITH, T. B., LIU, G., ALVAREZ-FILIP, L., BACA, B., BARTELS, E., BASTIDAS, C., BOUCHON, C., BRANDT, M., BRUCKNER, A. W., BUNKLEY-WILLIAMS, L., CAMERON, A., CAUSEY, B. D., CHIAPPONE, M., CHRISTENSEN, T. R., CRABBE, M. J., DAY, O., DE LA GUARDIA, E., DIAZ-PULIDO, G., DIRESTA, D., GIL-AGUDELO, D. L., GILLIAM, D. S., GINSBURG, R. N., GORE, S., GUZMAN, H. M., HENDEE, J. C., HERNANDEZ-DELGADO, E. A., HUSAIN, E., JEFFREY, C. F., JONES, R. J., JORDAN-DAHLGREN, E., KAUFMAN, L. S., KLINE, D. I., KRAMER, P. A., LANG, J. C., LIRMAN, D., MALLELA, J., MANFRINO, C., MARECHAL, J. P., MARKS, K., MIHALY, J., MILLER, W. J., MUELLER, E. M., MULLER, E. M., OROZCO TORO, C. A., OXFORD, H. A., PONCE-TAYLOR, D., QUINN, N., RITCHIE, K. B., RODRIGUEZ, S., RAMIREZ, A. R., ROMANO, S., SAMHOURI, J. F., SANCHEZ, J. A., SCHMAHL, G. P., SHANK, B. V., SKIRVING, W. J., STEINER, S. C., VILLAMIZAR, E., WALSH, S. M., WALTER, C., WEIL, E., WILLIAMS, E. H., ROBERSON, K. W. & YUSUF, Y. 2010. Caribbean corals in crisis: record thermal stress, bleaching, and mortality in 2005. *PLoS One*, 5, e13969.
- EDMUNDS, P. J. 2005. The effect of sub-lethal increases in temperature on the growth and population trajectories of three scleractinian corals on the southern Great Barrier Reef. *Oecologia*, 146, 350-64.
- EDMUNDS, P. J. 2007. Evidence for a decadal-scale decline in the growth rates of juvenile scleractinian corals. *Marine Ecology Progress Series*, 341, 1-13.
- EDMUNDS, P. J. & ELAHI, R. 2007. The Demographics of a 15-Year Decline in Cover of the Caribbean Reef Coral *Montastraea Annularis*. *Ecological Monographs*, 77, 3-18.
- EDMUNDS, P. J., GATES, R. D. & GLEASON, D. F. 2001. The biology of larvae from the reef coral *Porites astreoides*, and their response to temperature disturbances. *Marine Biology*, 139, 981-989.
- EDMUNDS, P. J. 2014. Is acclimation beneficial to scleractinian corals, *Porites* spp.? *Marine Biology*, 161, 1531-1542.
- EDMUNDS, P. J. 2017. Intraspecific variation in growth rate is a poor predictor of fitness for reef corals. *Ecology*, 98, 2191-2200.
- EPSTEIN, H. E., SMITH, H. A., CANTIN, N. E., MOCELLIN, V. J. L., TORDA, G. & VAN OPPEN, M. J. H. 2019. Temporal Variation in the Microbiome of *Acropora* Coral Species Does Not Reflect Seasonality. *Front Microbiol*, 10, 1775.
- EREN, A. M., MORRISON, H. G., LESCAULT, P. J., REVEILLAUD, J., VINEIS, J. H. & SOGIN, M. L. 2015. Minimum entropy decomposition: unsupervised oligotyping for sensitive partitioning of high-throughput marker gene sequences. *ISME J*, 9, 968-79.
- ERFTEMEIJER, P. L., RIEGL, B., HOEKSEMA, B. W. & TODD, P. A. 2012. Environmental impacts of dredging and other sediment disturbances on corals: a review. *Mar Pollut Bull*, 64, 1737-65.

- FABRICIUS, K. E., LANGDON, C., UTHICKE, S., HUMPHREY, C., NOONAN, S., DE'ATH, G., OKAZAKI, R., MUEHLEHNER, N., GLAS, M. S. & LOUGH, J. M. 2011. Losers and winners in coral reefs acclimatized to elevated carbon dioxide concentrations. *Nature Climate Change*, 1, 165-169.
- FERRIER-PAGES, C., GATTUSO, J. P., DALLOT, S. & JAUBERT, J. 2000. Effect of nutrient enrichment on growth and photosynthesis of the zooxanthellate coral *Stylophora pistillata*. *Coral Reefs*, 19, 103-113.
- FITT, W. K., BROWN, B. E., WARNER, M. E. & DUNNE, R. 2001. Coral bleaching: interpretation of thermal tolerance limits and thermal thresholds in tropical corals. *Coral Reefs*, 20, 51-65.
- FOO, S. A. & BYRNE, M. 2016. Acclimatization and Adaptive Capacity of Marine Species in a Changing Ocean. *Adv Mar Biol*, 74, 69-116.
- FORSMAN, Z. H., PAGE, C. A., TOONEN, R. J. & VAUGHAN, D. 2015. Growing coral larger and faster: micro-colony-fusion as a strategy for accelerating coral cover. *PeerJ*, 3, e1313.
- FOURNIER, D. A., SKAUG, H. J., ANCHETA, J., IANELLI, J., MAGNUSSON, A., MAUNDER, M. N., NIELSEN, A. & SIBERT, J. 2012. AD Model Builder: using automatic differentiation for statistical inference of highly parameterized complex nonlinear models. *Optimization Methods and Software*, 27, 233-249.
- FOX, R. J., DONELSON, J. M., SCHUNTER, C., RAVASI, T. & GAITAN-ESPITIA, J. D. 2019. Beyond buying time: the role of plasticity in phenotypic adaptation to rapid environmental change. *Philos Trans R Soc Lond B Biol Sci*, 374, 20180174.
- FULLER, Z. L., MOCELLIN, V. J. L., MORRIS, L. A., CANTIN, N., SHEPHERD, J., SARRE, L., PENG, J., LIAO, Y., PICKRELL, J., ANDOLFATTO, P., MATZ, M., BAY, L. K. & PRZEWORSKI, M. 2020. CORAL GENOMICS: Population genetics of the coral *Acropora millepora*: Toward genomic prediction of bleaching. *Science (American Association for the Advancement of Science)*, 369, 268.
- GARDNER, S. G., CAMP, E. F., SMITH, D. J., KAHLKE, T., OSMAN, E. O., GENDRON, G., HUME, B. C. C., POGOREUTZ, C., VOOLSTRA, C. R. & SUGGETT, D. J. 2019. Coral microbiome diversity reflects mass coral bleaching susceptibility during the 2016 El Niño heat wave. *Ecology and Evolution*, 9, 938-956.
- GARDNER, T. A., COTE, I. M., GILL, J. A., GRANT, A. & WATKINSON, A. R. 2003. Long-term region-wide declines in Caribbean corals. *Science*, 301, 958-60.
- GATES, R. D. & EDMUNDS, P. J. 1999. The Physiological Mechanisms of Acclimatization in Tropical Reef Corals. *American Zoologist*, 39, 30-43.
- GIBSON, G. & WAGNER, G. 2000. Canalization in evolutionary genetics: a stabilizing theory? *Bioessays*, 22, 372-80.
- GIERZ, S., AINSWORTH, T. D. & LEGGAT, W. 2020. Diverse symbiont bleaching responses are evident from 2-degree heating week bleaching conditions as thermal stress intensifies in coral. *Marine and Freshwater Research*.
- GILMOUR, J. P., SMITH, L. D., HEYWARD, A. J., BAIRD, A. H. & PRATCHETT, M. S. 2013. Recovery of an isolated coral reef system following severe disturbance. *Science*, 340, 69-71.
- GOLD, Z. & PALUMBI, S. R. 2018. Long-term growth rates and effects of bleaching in *Acropora hyacinthus*. *Coral Reefs*, 37, 267-277.
- GROTTOLI, A. G., DALCIN MARTINS, P., WILKINS, M. J., JOHNSTON, M. D., WARNER, M. E., CAI, W. J., MELMAN, T. F., HOADLEY, K. D., PETTAY, D. T., LEVAS, S. & SCHOEPF, V. 2018. Coral physiology and microbiome dynamics under combined warming and ocean acidification. *PLoS One*, 13, e0191156.
- GUEST, J. R., BAIRD, A. H., MAYNARD, J. A., MUTTAQIN, E., EDWARDS, A. J., CAMPBELL, S. J., YEWDALL, K., AFFENDI, Y. A. & CHOU, L. M. 2012. Contrasting patterns of coral bleaching susceptibility in 2010 suggest an adaptive response to thermal stress. *PLoS One*, 7, e33353.
- HARRISON, P. L., BABCOCK, R. C., BULL, G. D., OLIVER, J. K., WALLACE, C. C. & WILLIS, B. L. 1984. Mass spawning in tropical reef corals. *Science*, 223, 1186-9.
- HAYWARD, D. C., CATMULL, J., REECE-HOYES, J. S., BERGHAMMER, H., DODD, H., HANN, S. J., MILLER, D. J. & BALL, E. E. 2001. Gene structure and larval expression of *cnox-2Am* from the coral *Acropora millepora*. *Dev Genes Evol*, 211, 10-9.

- HERNANDEZ-AGREDA, A., LEGGAT, W., BONGAERTS, P. & AINSWORTH, T. D. 2016. The Microbial Signature Provides Insight into the Mechanistic Basis of Coral Success across Reef Habitats. *MBio*, 7, e00560-16.
- HERON, S. F., MAYNARD, J. A., VAN HOOIDONK, R. & EAKIN, C. M. 2016. Warming Trends and Bleaching Stress of the World's Coral Reefs 1985-2012. *Sci Rep*, 6, 38402.
- HERVÉ, M. & HERVÉ, M. M. 2019. Package 'RVAideMemoire'.
- HEYWARD, A. J. & NEGRI, A. P. 2010. Plasticity of larval pre-competency in response to temperature: observations on multiple broadcast spawning coral species. *Coral Reefs*, 29, 631-636.
- HILL, R., ULSTRUP, K. E. & RALPH, P. J. 2009. Temperature Induced Changes in Thylakoid Membrane Thermostability of Cultured, Freshly Isolated, and Expelled Zooxanthellae from Scleractinian Corals. *Bulletin of Marine Science*, 85, 223-244.
- HOADLEY, K. D., PETTAY, D. T., GROTTOLI, A. G., CAI, W. J., MELMAN, T. F., SCHOEPF, V., HU, X., LI, Q., XU, H., WANG, Y., MATSUI, Y., BAUMANN, J. H. & WARNER, M. E. 2015. Physiological response to elevated temperature and pCO₂ varies across four Pacific coral species: Understanding the unique host+symbiont response. *Sci Rep*, 5, 18371.
- HOEGH-GULDBERG, O. 2012. The adaptation of coral reefs to climate change: Is the Red Queen being outpaced? *Scientia Marina*, 76, 403-408.
- HOEGH-GULDBERG, O., JACOB, D., TAYLOR, M., GUILLEN BOLANOS, T., BINDI, M., BROWN, S., CAMILLONI, I. A., DIEDHIOU, A., DJALANTE, R., EBI, K., ENGELBRECHT, F., GUIOT, J., HIJIOKA, Y., MEHROTRA, S., HOPE, C. W., PAYNE, A. J., PORTNER, H. O., SENEVIRATNE, S. I., THOMAS, A., WARREN, R. & ZHOU, G. 2019. The human imperative of stabilizing global climate change at 1.5 degrees C. *Science*, 365, 1263.
- HOEGH-GULDBERG, O., MUMBY, P. J., HOOTEN, A. J., STENECK, R. S., GREENFIELD, P., GOMEZ, E., HARVELL, C. D., SALE, P. F., EDWARDS, A. J., CALDEIRA, K., KNOWLTON, N., EAKIN, C. M., IGLESIAS-PRIETO, R., MUTHIGA, N., BRADBURY, R. H., DUBI, A. & HATZIOLOS, M. E. 2007. Coral reefs under rapid climate change and ocean acidification. *Science*, 318, 1737-42.
- HOFFMANN, A. A., SØRENSEN, J. G. & LOESCHCKE, V. 2003. Adaptation of Drosophila to temperature extremes: bringing together quantitative and molecular approaches. Elsevier Ltd.
- HOOGENBOOM, M. O., FRANK, G. E., CHASE, T. J., JURRIANS, S., ÁLVAREZ-NORIEGA, M., PETERSON, K., CRITCHELL, K., BERRY, K. L. E., NICOLET, K. J., RAMSBY, B. & PALEY, A. S. 2017. Environmental Drivers of Variation in Bleaching Severity of Acropora Species during an Extreme Thermal Anomaly. *Frontiers in Marine Science*, 4.
- HOWE-KERR, L. I., BACHELOT, B., WRIGHT, R. M., KENKEL, C. D., BAY, L. K. & CORREA, A. M. S. 2020. Symbiont community diversity is more variable in corals that respond poorly to stress. *Glob Chang Biol*, 26, 2220-2234.
- HOWELLS, E. J., BELTRAN, V. H., LARSEN, N. W., BAY, L. K., WILLIS, B. L. & VAN OPPEN, M. J. H. 2012. Coral thermal tolerance shaped by local adaptation of photosymbionts. *Nature Climate Change*, 2, 116-120.
- HOWELLS, E. J., BERKELMANS, R., VAN OPPEN, M. J., WILLIS, B. L. & BAY, L. K. 2013. Historical thermal regimes define limits to coral acclimatization. *Ecology*, 94, 1078-88.
- HUGHES, T. P., ANDERSON, K. D., CONNOLLY, S. R., HERON, S. F., KERRY, J. T., LOUGH, J. M., BAIRD, A. H., BAUM, J. K., BERUMEN, M. L., BRIDGE, T. C., CLAAR, D. C., EAKIN, C. M., GILMOUR, J. P., GRAHAM, N. A. J., HARRISON, H., HOBBS, J.-P. A., HOEY, A. S., HOOGENBOOM, M., LOWE, R. J., MCCULLOCH, M. T., PANDOLFI, J. M., PRATCHETT, M., SCHOEPF, V., TORDA, G. & WILSON, S. K. 2018a. Spatial and temporal patterns of mass bleaching of corals in the Anthropocene. *Science (New York, N.Y.)*, 359, 80-83.
- HUGHES, T. P., BAIRD, A. H., BELLWOOD, D. R., CARD, M., CONNOLLY, S. R., FOLKE, C., GROSBERG, R., HOEGH-GULDBERG, O., JACKSON, J. B., KLEYPAS, J., LOUGH, J. M., MARSHALL, P., NYSTROM, M., PALUMBI, S. R., PANDOLFI, J. M., ROSEN, B. & ROUGHGARDEN, J. 2003. Climate change, human impacts, and the resilience of coral reefs. *Science*, 301, 929-33.

- HUGHES, T. P., BARNES, M. L., BELLWOOD, D. R., CINNER, J. E., CUMMING, G. S., JACKSON, J. B. C., KLEYPAS, J., VAN DE LEEMPUT, I. A., LOUGH, J. M., MORRISON, T. H., PALUMBI, S. R., VAN NES, E. H. & SCHEFFER, M. 2017a. Coral reefs in the Anthropocene. *Nature*, 546, 82-90.
- HUGHES, T. P., KERRY, J. T., ALVAREZ-NORIEGA, M., ALVAREZ-ROMERO, J. G., ANDERSON, K. D., BAIRD, A. H., BABCOCK, R. C., BEGER, M., BELLWOOD, D. R., BERKELMANS, R., BRIDGE, T. C., BUTLER, I. R., BYRNE, M., CANTIN, N. E., COMEAU, S., CONNOLLY, S. R., CUMMING, G. S., DALTON, S. J., DIAZ-PULIDO, G., EAKIN, C. M., FIGUEIRA, W. F., GILMOUR, J. P., HARRISON, H. B., HERON, S. F., HOEY, A. S., HOBBS, J. A., HOOGENBOOM, M. O., KENNEDY, E. V., KUO, C. Y., LOUGH, J. M., LOWE, R. J., LIU, G., MCCULLOCH, M. T., MALCOLM, H. A., MCWILLIAM, M. J., PANDOLFI, J. M., PEARS, R. J., PRATCHETT, M. S., SCHOEPF, V., SIMPSON, T., SKIRVING, W. J., SOMMER, B., TORDA, G., WACHENFELD, D. R., WILLIS, B. L. & WILSON, S. K. 2017b. Global warming and recurrent mass bleaching of corals. *Nature*, 543, 373-377.
- HUGHES, T. P., KERRY, J. T., BAIRD, A. H., CONNOLLY, S. R., DIETZEL, A., EAKIN, C. M., HERON, S. F., HOEY, A. S., HOOGENBOOM, M. O., LIU, G., MCWILLIAM, M. J., PEARS, R. J., PRATCHETT, M. S., SKIRVING, W. J., STELLA, J. S. & TORDA, G. 2018b. Global warming transforms coral reef assemblages. *Nature*, 556, 492-496.
- HUGHES, T. P., KERRY, J. T., CONNOLLY, S. R., BAIRD, A. H., EAKIN, C. M., HERON, S. F., HOEY, A. S., HOOGENBOOM, M. O., JACOBSON, M., LIU, G., PRATCHETT, M. S., SKIRVING, W. & TORDA, G. 2018c. Ecological memory modifies the cumulative impact of recurrent climate extremes. *Nature Climate Change*, 9, 40-43.
- HUMANES, A., NOONAN, S. H., WILLIS, B. L., FABRICIUS, K. E. & NEGRI, A. P. 2016. Cumulative Effects of Nutrient Enrichment and Elevated Temperature Compromise the Early Life History Stages of the Coral *Acropora tenuis*. *PLoS One*, 11, e0161616.
- HUME, B. C., VOOLSTRA, C. R., ARIF, C., D'ANGELO, C., BURT, J. A., EYAL, G., LOYA, Y. & WIEDENMANN, J. 2016. Ancestral genetic diversity associated with the rapid spread of stress-tolerant coral symbionts in response to Holocene climate change. *Proc Natl Acad Sci U S A*, 113, 4416-21.
- HUME, B. C. C., SMITH, E. G., ZIEGLER, M., WARRINGTON, H. J. M., BURT, J. A., LAJEUNESSE, T. C., WIEDENMANN, J. & VOOLSTRA, C. R. 2019. SymPortal: A novel analytical framework and platform for coral algal symbiont next-generation sequencing ITS2 profiling. *Mol Ecol Resour*, 19, 1063-1080.
- IGLESIAS-PRIETO, R., MATTA, J. L., ROBINS, W. A. & TRENCH, R. K. 1992. Photosynthetic response to elevated temperature in the symbiotic dinoflagellate *Symbiodinium microadriaticum* in culture. *Proc Natl Acad Sci U S A*, 89, 10302-5.
- IPCC. 2018. *Global Warming of 1.5 °C* [Online]. Available: <https://www.ipcc.ch/sr15/> [Accessed].
- IPCC. 2019. *Special Report on the Ocean and Cryosphere in a Changing Climate (SROCC)* [Online]. Available: www.ipcc.ch/report/srocc [Accessed].
- JOHNSTON, I. A. & WILSON, R. S. 2006. Temperature-induced developmental plasticity in ectotherms. *Comparative Developmental Physiology*, Oxford University Press, New York, 124-138.
- JOKIEL, P. L. 2016. Predicting the impact of ocean acidification on coral reefs: evaluating the assumptions involved. *ICES Journal of Marine Science*, 73, 550-557.
- JONES, A. M., BERKELMANS, R., VAN OPPEN, M. J., MIEOG, J. C. & SINCLAIR, W. 2008. A community change in the algal endosymbionts of a scleractinian coral following a natural bleaching event: field evidence of acclimatization. *Proc Biol Sci*, 275, 1359-65.
- JONES, R. J. 2008. Coral bleaching, bleaching-induced mortality, and the adaptive significance of the bleaching response. *Marine Biology*, 154, 65-80.
- JONES, R. J. & HOEGH-GULDBERG, O. 2001. Diurnal changes in the photochemical efficiency of the symbiotic dinoflagellates (Dinophyceae) of corals: photoprotection, photoinactivation and the relationship to coral bleaching. *Plant, Cell & Environment*, 24, 89-99.
- JONES, R. J., HOEGH-GULDBERG, O., LARKUM, A. W. D. & SCHREIBER, U. 1998. Temperature-induced bleaching of corals begins with impairment of the CO₂ fixation mechanism in zooxanthellae. *Plant, Cell and Environment*, 21, 1219-1230.

- KARIM, W., NAKAEMA, S. & HIDAKA, M. 2015. Temperature Effects on the Growth Rates and Photosynthetic Activities of Symbiodinium Cells. *Journal of Marine Science and Engineering*, 3, 368-381.
- KENKEL, C. D. & BAY, L. K. 2016. The role of vertical symbiont transmission in altering cooperation and fitness of coral-Symbiodinium symbioses. *bioRxiv*.
- KENKEL, C. D. & MATZ, M. V. 2016. Gene expression plasticity as a mechanism of coral adaptation to a variable environment. *Nature Ecology & Evolution*, 1, 0014.
- KENKEL, C. D., MOYA, A., STRAHL, J., HUMPHREY, C. & BAY, L. K. 2018. Functional genomic analysis of corals from natural CO₂-seeps reveals core molecular responses involved in acclimatization to ocean acidification. *Glob Chang Biol*, 24, 158-171.
- KESHAVMURTHY, S., FONTANA, S., MEZAKI, T., GONZALEZ LDEL, C. & CHEN, C. A. 2014. Doors are closing on early development in corals facing climate change. *Sci Rep*, 4, 5633.
- KIMES, N. E., VAN NOSTRAND, J. D., WEIL, E., ZHOU, J. & MORRIS, P. J. 2010. Microbial functional structure of *Montastraea faveolata*, an important Caribbean reef-building coral, differs between healthy and yellow-band diseased colonies. *Environ Microbiol*, 12, 541-56.
- KLEYPAS, J. A., BUDDEMEIER, R. W., ARCHER, D., GATTUSO, J. P., LANGDON, C. & OPDYKE, B. N. 1999. Geochemical consequences of increased atmospheric carbon dioxide on coral reefs. *Science*, 284, 118-20.
- KRAUSE, G. H. & WEIS, E. 1991. Chlorophyll Fluorescence and Photosynthesis: The Basics. *Annual Review of Plant Physiology and Plant Molecular Biology*, 42, 313-349.
- LAJEUNESSE, T. C., PARKINSON, J. E., GABRIELSON, P. W., JEONG, H. J., REIMER, J. D., VOOLSTRA, C. R. & SANTOS, S. R. 2018. Systematic Revision of Symbiodiniaceae Highlights the Antiquity and Diversity of Coral Endosymbionts. *Curr Biol*, 28, 2570-2580 e6.
- LAWSON, C. A., POSSELL, M., SEYMOUR, J. R., RAINA, J. B. & SUGGETT, D. J. 2019. Coral endosymbionts (Symbiodiniaceae) emit species-specific volatiles that shift when exposed to thermal stress. *Sci Rep*, 9, 17395.
- LEMA, K. A., BOURNE, D. G. & WILLIS, B. L. 2014. Onset and establishment of diazotrophs and other bacterial associates in the early life history stages of the coral *Acropora millepora*. *Mol Ecol*, 23, 4682-95.
- LESSER, M. P. 1997. Oxidative stress causes coral bleaching during exposure to elevated temperatures. *Coral Reefs*, 16, 187-192.
- LEVIN, R. A., BELTRAN, V. H., HILL, R., KJELLEBERG, S., MCDUGALD, D., STEINBERG, P. D. & VAN OPPEN, M. J. 2016. Sex, Scavengers, and Chaperones: Transcriptome Secrets of Divergent Symbiodinium Thermal Tolerances. *Mol Biol Evol*, 33, 2201-15.
- LIEW, Y. J., HOWELLS, E. J., WANG, X., MICHELL, C. T., BURT, J. A., IDAGHDOUR, Y. & ARANDA, M. 2020. Intergenerational epigenetic inheritance in reef-building corals. *Nature Climate Change*, 10, 254-259.
- LIEW, Y. J., ZOCCOLA, D., LI, Y., TAMBUTTE, E., VENN, A. A., MICHELL, C. T., CUI, G., DEUTEKOM, E. S., KAANDORP, J. A., VOOLSTRA, C. R., FORET, S., ALLEMAND, D., TAMBUTTE, S. & ARANDA, M. 2018. Epigenome-associated phenotypic acclimatization to ocean acidification in a reef-building coral. *Sci Adv*, 4, eaar8028.
- LIRMAN, D. & SCHOPMEYER, S. 2016. Ecological solutions to reef degradation: optimizing coral reef restoration in the Caribbean and Western Atlantic. *PeerJ*, 4, e2597.
- LITTLE, A. G., KUNISUE, T., KANNAN, K. & SEEBACHER, F. 2013. Thyroid hormone actions are temperature-specific and regulate thermal acclimation in zebrafish (*Danio rerio*). *BMC Biol*, 11, 26.
- LITTMAN, R. A., WILLIS, B. L. & BOURNE, D. G. 2009a. Bacterial communities of juvenile corals infected with different Symbiodinium (dinoflagellate) clades. *Marine Ecology Progress Series*, 389, 45-59.
- LITTMAN, R. A., WILLIS, B. L., PFEFFER, C. & BOURNE, D. G. 2009b. Diversities of coral-associated bacteria differ with location, but not species, for three acroporid corals on the Great Barrier Reef. *FEMS Microbiol Ecol*, 68, 152-63.

- LIZCANO-SANDOVAL, L. D., MARULANDA-GÓMEZ, Á., LÓPEZ-VICTORIA, M. & RODRIGUEZ-RAMIREZ, A. 2019. Climate Change and Atlantic Multidecadal Oscillation as Drivers of Recent Declines in Coral Growth Rates in the Southwestern Caribbean. *Frontiers in Marine Science*, 6.
- LOUGH, J. M., ANDERSON, K. D. & HUGHES, T. P. 2018. Increasing thermal stress for tropical coral reefs: 1871-2017. *Sci Rep*, 8, 6079.
- LOVE, M., ANDERS, S. & HUBER, W. 2014. Differential analysis of count data—the DESeq2 package. *Genome Biol*, 15, 10.1186.
- MCCLANAHAN, T. R., ATEWEBERHAN, M., MUHANDO, C. A., MAINA, J. & MOHAMMED, M. S. 2007. Effects of Climate and Seawater Temperature Variation on Coral Bleaching and Mortality. *Ecological Monographs*, 77, 503-525.
- MATSUDA, S. B., HUFFMYER, A. S., LENZ, E. A., DAVIDSON, J. M., HANCOCK, J. R., PRZYBYLOWSKI, A., INNIS, T., GATES, R. D. & BAROTT, K. L. 2020. Coral Bleaching Susceptibility Is Predictive of Subsequent Mortality Within but Not Between Coral Species. *Frontiers in Ecology and Evolution*, 8.
- MATTHEWS, J. L., RAINA, J. B., KAHLKE, T., SEYMOUR, J. R., VAN OPPEN, M. J. H. & SUGGETT, D. J. 2020. Symbiodiniaceae-bacteria interactions: rethinking metabolite exchange in reef-building corals as multi-partner metabolic networks. *Environ Microbiol*.
- MATZ, M. V., TREML, E. A., AGLYAMOVA, G. V. & BAY, L. K. 2018. Potential and limits for rapid genetic adaptation to warming in a Great Barrier Reef coral. *PLoS Genet*, 14, e1007220.
- MAXWELL, K. & JOHNSON, G. N. 2000. Chlorophyll fluorescence—a practical guide. *Journal of Experimental Botany*, 51, 659-668.
- MAYFIELD, A. B., CHAN, P. H., PUTNAM, H. M., CHEN, C. S. & FAN, T. Y. 2012. The effects of a variable temperature regime on the physiology of the reef-building coral *Seriatopora hystrix*: results from a laboratory-based reciprocal transplant. *J Exp Biol*, 215, 4183-95.
- MAYFIELD, A. B., WANG, Y. B., CHEN, C. S., LIN, C. Y. & CHEN, S. H. 2014. Compartment-specific transcriptomics in a reef-building coral exposed to elevated temperatures. *Mol Ecol*, 23, 5816-30.
- MAYNARD, J. A., BAIRD, A. H. & PRATCHETT, M. S. 2008. Revisiting the Cassandra syndrome; the changing climate of coral reef research.
- MCDONALD, J., MCGEE, J., BRENT, K. & BURNS, W. 2019. Governing geoengineering research for the Great Barrier Reef. *Climate Policy*, 19, 801-811.
- MCGOWAN, H. & THEOBALD, A. 2017. ENSO Weather and Coral Bleaching on the Great Barrier Reef, Australia. *Geophysical Research Letters*, 44, 10,601-10,607.
- MCMURDIE, P. J. & HOLMES, S. 2013. phyloseq: an R package for reproducible interactive analysis and graphics of microbiome census data. *PLoS One*, 8, e61217.
- MEISSNER, K. J., LIPPMANN, T. & SEN GUPTA, A. 2012. Large-scale stress factors affecting coral reefs: open ocean sea surface temperature and surface seawater aragonite saturation over the next 400 years. *Coral Reefs*, 31, 309-319.
- MERILA, J. & HENDRY, A. P. 2014. Climate change, adaptation, and phenotypic plasticity: the problem and the evidence. *Evol Appl*, 7, 1-14.
- MEYER, E., AGLYAMOVA, G. V. & MATZ, M. V. 2011a. Profiling gene expression responses of coral larvae (*Acropora millepora*) to elevated temperature and settlement inducers using a novel RNA-Seq procedure. *Mol Ecol*, 20, 3599-616.
- MEYER, E., AGLYAMOVA, G. V. & MATZ, M. V. 2011b. Profiling gene expression responses of coral larvae (*Acropora millepora*) to elevated temperature and settlement inducers using a novel RNA-Seq procedure. *Molecular Ecology*, 20, 3599-3616.
- MIDDLEBROOK, R., ANTHONY, K. R., HOEGH-GULDBERG, O. & DOVE, S. 2010. Heating rate and symbiont productivity are key factors determining thermal stress in the reef-building coral *Acropora formosa*. *J Exp Biol*, 213, 1026-34.
- MIDDLEBROOK, R., HOEGH-GULDBERG, O. & LEGGAT, W. 2008. The effect of thermal history on the susceptibility of reef-building corals to thermal stress. *J Exp Biol*, 211, 1050-6.

- MIEOG, J. C., OLSEN, J. L., BERKELMANS, R., BLEULER-MARTINEZ, S. A., WILLIS, B. L. & VAN OPPEN, M. J. 2009. The roles and interactions of symbiont, host and environment in defining coral fitness. *PLoS One*, 4, e6364.
- MORGAN, J. L., DARLING, A. E. & EISEN, J. A. 2010. Metagenomic sequencing of an in vitro-simulated microbial community. *PLoS One*, 5, e10209.
- MORIKAWA, M. K. & PALUMBI, S. R. 2019. Using naturally occurring climate resilient corals to construct bleaching-resistant nurseries. *Proc Natl Acad Sci U S A*, 116, 10586-10591.
- MORROW, K. M., BOURNE, D. G., HUMPHREY, C., BOTTE, E. S., LAFFY, P., ZANEVELD, J., UTHICKE, S., FABRICIUS, K. E. & WEBSTER, N. S. 2015. Natural volcanic CO₂ seeps reveal future trajectories for host-microbial associations in corals and sponges. *ISME J*, 9, 894-908.
- MUMBY, P. J. 1999. Bleaching and hurricane disturbances to populations of coral recruits in Belize. *Marine Ecology Progress Series*, 190, 27-35.
- MUNDAY, P. L., WARNER, R. R., MONRO, K., PANDOLFI, J. M. & MARSHALL, D. J. 2013. Predicting evolutionary responses to climate change in the sea. *Ecol Lett*, 16, 1488-500.
- MUSCATINE, L. 1990. The role of symbiotic algae in carbon and energy flux in reef corals. *Ecosystems of the world*, 25, 75-87.
- NATIONAL ACADEMIES OF SCIENCES, E. & MEDICINE 2019. *A Research Review of Interventions to Increase the Persistence and Resilience of Coral Reefs*, National Academies Press.
- NEAVE, M. J., MICHELL, C. T., APPRILL, A. & VOOLSTRA, C. R. 2017. Endozoicomonas genomes reveal functional adaptation and plasticity in bacterial strains symbiotically associated with diverse marine hosts. *Sci Rep*, 7, 40579.
- NEGRI, A. P., MARSHALL, P. A. & HEYWARD, A. J. 2007. Differing effects of thermal stress on coral fertilization and early embryogenesis in four Indo Pacific species. *Coral Reefs*, 26, 759-763.
- NEGRI, I. & JABLONKA, E. 2016. Editorial: Epigenetics as a Deep Intimate Dialogue between Host and Symbionts. *Front Genet*, 7, 7.
- NOZAWA, Y. & HARRISON, P. L. 2007. Effects of elevated temperature on larval settlement and post-settlement survival in scleractinian corals, *Acropora solitaryensis* and *Favites chinensis*. *Marine Biology*, 152, 1181-1185.
- NOZAWA, Y. & HARRISON, P. L. 2008. Temporal patterns of larval settlement and survivorship of two broadcast-spawning acroporid corals. *Marine Biology*, 155, 347-351.
- OKSANEN, J., BLANCHET, F. G., KINDT, R., LEGENDRE, P., MINCHIN, P. R., O'HARA, R., SIMPSON, G. L., SOLYMOS, P., STEVENS, M. H. & WAGNER, H. 2013. Package 'vegan'. *Community ecology package, version*, 2, 1-295.
- OLIVER, E. C. J., BURROWS, M. T., DONAT, M. G., SEN GUPTA, A., ALEXANDER, L. V., PERKINS-KIRKPATRICK, S. E., BENTHUYSEN, J. A., HOBDDAY, A. J., HOLBROOK, N. L. J., MOORE, P. J., THOMSEN, M. S., WERNBERG, T. & SMALE, D. A. 2019. Projected Marine Heatwaves in the 21st Century and the Potential for Ecological Impact. *Frontiers in Marine Science*, 6.
- OLIVER, T. A. & PALUMBI, S. R. 2009. Distributions of stress-resistant coral symbionts match environmental patterns at local but not regional scales. *Marine ecology progress series*, 378, 93-103.
- OLIVER, T. A. & PALUMBI, S. R. 2011. Many corals host thermally resistant symbionts in high-temperature habitat. *Coral Reefs*, 30, 241-250.
- ORTIZ, J. C., WOLFF, N. H., ANTHONY, K. R. N., DEVLIN, M., LEWIS, S. & MUMBY, P. J. 2018. Impaired recovery of the Great Barrier Reef under cumulative stress. *Sci Adv*, 4, eaar6127.
- OSBORNE, K., DOLMAN, A. M., BURGESS, S. C. & JOHNS, K. A. 2011. Disturbance and the Dynamics of Coral Cover on the Great Barrier Reef (1995-2009). *Plos One*, 6.
- PACKARD, G. C., PACKARD, M. J. & MCDANIEL, L. L. 2001. Seasonal change in the capacity for supercooling by neonatal painted turtles. *J Exp Biol*, 204, 1667-72.
- PALUMBI, S. R., BARSHIS, D. J., TRAYLOR-KNOWLES, N. & BAY, R. A. 2014. Mechanisms of reef coral resistance to future climate change. *Science*, 344, 895-8.

- PALUMBI, S. R., VOLLMER, S., ROMANO, S., OLIVER, T. A. & LADNER, J. 2011. The role of genes in understanding the evolutionary ecology of reef building corals. *Evolutionary Ecology*, 26, 317-335.
- PARKASH, R., SINGH, D. & LAMBHOD, C. 2014. Divergent strategies for adaptations to stress resistance in two tropical *Drosophila* species: effects of developmental acclimation in *D. bipunctata* and the invasive species *D. malerkotliana*. *J Exp Biol*, 217, 924-34.
- PEARSE, V. & MUSCATINE, L. 1971. Role of Symbiotic Algae (Zooxanthellae) in Coral Calcification. *Biological Bulletin*, 141, 350-363.
- PEIXOTO, R. S., ROSADO, P. M., LEITE, D. C., ROSADO, A. S. & BOURNE, D. G. 2017. Beneficial Microorganisms for Corals (BMC): Proposed Mechanisms for Coral Health and Resilience. *Front Microbiol*, 8, 341.
- PERRY, C. T. & MORGAN, K. M. 2017. Bleaching drives collapse in reef carbonate budgets and reef growth potential on southern Maldives reefs. *Sci Rep*, 7, 40581.
- PERRY, C. T., MURPHY, G. N., KENCH, P. S., SMITHERS, S. G., EDINGER, E. N., STENECK, R. S. & MUMBY, P. J. 2013. Caribbean-wide decline in carbonate production threatens coral reef growth. *Nat Commun*, 4, 1402.
- PETTAY, D. T., WHAM, D. C., SMITH, R. T., IGLESIAS-PRIETO, R. & LAJEUNESSE, T. C. 2015. Microbial invasion of the Caribbean by an Indo-Pacific coral zooxanthella. *Proc Natl Acad Sci U S A*, 112, 7513-8.
- PIERSMA, T. & DRENT, J. 2003. Phenotypic flexibility and the evolution of organismal design. *Trends in Ecology & Evolution*, 18, 228-233.
- PIGLIUCCI, M., MURREN, C. J. & SCHLICHTING, C. D. 2006. Phenotypic plasticity and evolution by genetic assimilation. *J Exp Biol*, 209, 2362-7.
- PINEDA, J., RIEBENSAHM, D. & MEDEIROS-BERGEN, D. 2002. *Semibalanus balanoides* in winter and spring: larval concentration, settlement, and substrate occupancy. *Marine Biology*, 140, 789-800.
- POLATO, N. R., ALTMAN, N. S. & BAUMS, I. B. 2013. Variation in the transcriptional response of threatened coral larvae to elevated temperatures. *Mol Ecol*, 22, 1366-82.
- POOTAKHAM, W., MHUANTONG, W., YOOCHA, T., PUTCHIM, L., JOMCHAI, N., SONTHIROD, C., NAKTANG, C., KONGKACHANA, W. & TANGPHATSORNRUANG, S. 2019. Heat-induced shift in coral microbiome reveals several members of the Rhodobacteraceae family as indicator species for thermal stress in *Porites lutea*. *Microbiologyopen*, 8, e935.
- PRATCHETT, M. S., ANDERSON, K. D., HOOGENBOOM, M. O., WIDMAN, E., BAIRD, A. H., PANDOLFI, J. M., EDMUNDS, P. J. & LOUGH, J. M. 2015. Spatial, Temporal and Taxonomic Variation in Coral Growth-Implications for the Structure and Function of Coral Reef Ecosystems. *Oceanography and Marine Biology: An Annual Review*, Vol 53, 53, 215-295.
- PRATCHETT, M. S., CABALLES, C. F., NEWMAN, S. J., WILSON, S. K., MESSMER, V. & PRATCHETT, D. J. 2020. Bleaching susceptibility of aquarium corals collected across northern Australia. *Coral Reefs*, 39, 663-673.
- PRZESLAWSKI, R., BYRNE, M. & MELLIN, C. 2015. A review and meta-analysis of the effects of multiple abiotic stressors on marine embryos and larvae. *Glob Chang Biol*, 21, 2122-40.
- PUTNAM, H. M., BAROTT, K. L., AINSWORTH, T. D. & GATES, R. D. 2017. The Vulnerability and Resilience of Reef-Building Corals. *Curr Biol*, 27, R528-R540.
- PUTNAM, H. M., DAVIDSON, J. M. & GATES, R. D. 2016. Ocean acidification influences host DNA methylation and phenotypic plasticity in environmentally susceptible corals. *Evol Appl*, 9, 1165-1178.
- PUTNAM, H. M. & EDMUNDS, P. J. 2011. The physiological response of reef corals to diel fluctuations in seawater temperature. *Journal of Experimental Marine Biology and Ecology*, 396, 216-223.
- PUTNAM, H. M. & GATES, R. D. 2015. Preconditioning in the reef-building coral *Pocillopora damicornis* and the potential for trans-generational acclimatization in coral larvae under future climate change conditions. *J Exp Biol*, 218, 2365-72.

- QUAST, C., PRUESSE, E., YILMAZ, P., GERKEN, J., SCHWEER, T., YARZA, P., PEPLIES, J. & GLOCKNER, F. O. 2013. The SILVA ribosomal RNA gene database project: improved data processing and web-based tools. *Nucleic Acids Res*, 41, D590-6.
- QUIGLEY, K. M., ALVAREZ ROA, C., TORDA, G., BOURNE, D. G. & WILLIS, B. L. 2020. Co-dynamics of Symbiodiniaceae and bacterial populations during the first year of symbiosis with *Acropora tenuis* juveniles. *Microbiologyopen*, 9, e959.
- QUIGLEY, K. M., BAY, L. K. & VAN OPPEN, M. J. H. 2019. The active spread of adaptive variation for reef resilience. *Ecol Evol*, 9, 11122-11135.
- QUIGLEY, K. M., BAY, L. K. & WILLIS, B. L. 2018. Leveraging new knowledge of Symbiodinium community regulation in corals for conservation and reef restoration. *Marine Ecology Progress Series*, 600, 245-253.
- QUIGLEY, K. M., WILLIS, B. L. & BAY, L. K. 2016. Maternal effects and Symbiodinium community composition drive differential patterns in juvenile survival in the coral *Acropora tenuis*. *R Soc Open Sci*, 3, 160471.
- RAINA, J. B., TAPIOLAS, D., WILLIS, B. L. & BOURNE, D. G. 2009. Coral-associated bacteria and their role in the biogeochemical cycling of sulfur. *Appl Environ Microbiol*, 75, 3492-501.
- RANDALL, C. J., NEGRI, A. P., QUIGLEY, K. M., FOSTER, T., RICARDO, G. F., WEBSTER, N. S., BAY, L. K., HARRISON, P. L., BABCOCK, R. C. & HEYWARD, A. J. 2020. Sexual production of corals for reef restoration in the Anthropocene. *Marine Ecology Progress Series*, 635, 203-232.
- RANDALL, C. J. & SZMANT, A. M. 2009a. Elevated temperature affects development, survivorship, and settlement of the elkhorn coral, *Acropora palmata* (Lamarck 1816). *Biol Bull*, 217, 269-82.
- RANDALL, C. J. & SZMANT, A. M. 2009b. Elevated temperature reduces survivorship and settlement of the larvae of the Caribbean scleractinian coral, *Favia fragum* (Esper). *Coral Reefs*, 28, 537-545.
- RASBAND, W. S. 2012. *ImageJ In: HEALTH*, U. S. N. I. O. (ed.). Bethesda, Maryland, USA.
- REPOLHO, T., DUARTE, B., DIONÍSIO, G., PAULA, J. R., LOPES, A. R., ROSA, I. C., GRILO, T. F., CAÇADOR, I., CALADO, R. & ROSA, R. 2017. Seagrass ecophysiological performance under ocean warming and acidification. *Scientific reports*, 7, 41443.
- REYNOLDS, J. M., BRUNS, B. U., FITT, W. K. & SCHMIDT, G. W. 2008. Enhanced photoprotection pathways in symbiotic dinoflagellates of shallow-water corals and other cnidarians. *Proc Natl Acad Sci U S A*, 105, 13674-8.
- RICHMOND, R. H., TISTHAMMER, K. H. & SPIES, N. P. 2018. The Effects of Anthropogenic Stressors on Reproduction and Recruitment of Corals and Reef Organisms. *Frontiers in Marine Science*, 5.
- RITCHIE, K. B. 2006. Regulation of microbial populations by coral surface mucus and mucus-associated bacteria. *Marine Ecology Progress Series*, 322, 1-14.
- ROBBINS, S. J., SINGLETON, C. M., CHAN, C. X., MESSER, L. F., GEERS, A. U., YING, H., BAKER, A., BELL, S. C., MORROW, K. M., RAGAN, M. A., MILLER, D. J., FORET, S., REFUGE, C., VOOLSTRA, C. R., TYSON, G. W. & BOURNE, D. G. 2019. A genomic view of the reef-building coral *Porites lutea* and its microbial symbionts. *Nat Microbiol*, 4, 2090-2100.
- ROBERTS, S. B. & GAVERY, M. R. 2012. Is there a relationship between DNA methylation and phenotypic plasticity in invertebrates? *Frontiers in physiology*, 2, 116.
- ROBINSON, M. & SHINE, T. 2018. Achieving a climate justice pathway to 1.5 °C. *Nature Climate Change*, 8, 564-569.
- ROBISON, J. D. & WARNER, M. E. 2006. Differential impacts of photoacclimation and thermal stress on the photobiology of four different phylotypes of Symbiodinium (Pyrrophyta). *Journal of phycology*, 42, 568-579.
- RODRIGUEZ-LANETTY, M., HARI, S. & HOEGH-GULDBERG, O. 2009. Early molecular responses of coral larvae to hyperthermal stress. *Mol Ecol*, 18, 5101-14.
- ROHWER, F. & KELLEY, S. 2004. Culture-Independent Analyses of Coral-Associated Microbes. In: ROSENBERG, E. & LOYA, Y. (eds.) *Coral Health and Disease*. Berlin, Heidelberg: Springer Berlin Heidelberg.

- ROHWER, F., SEGURITAN, V., AZAM, F. & KNOWLTON, N. 2002. Diversity and distribution of coral-associated bacteria. *Marine Ecology Progress Series*, 243, 1-10.
- ROSADO, P. M., LEITE, D. C. A., DUARTE, G. A. S., CHALOUB, R. M., JOSPIN, G., NUNES DA ROCHA, U., J, P. S., DINI-ANDREOTE, F., EISEN, J. A., BOURNE, D. G. & PEIXOTO, R. S. 2019. Marine probiotics: increasing coral resistance to bleaching through microbiome manipulation. *ISME J*, 13, 921-936.
- ROSENBERG, E., KOREN, O., RESHEF, L., EFRONY, R. & ZILBER-ROSENBERG, I. 2007. The role of microorganisms in coral health, disease and evolution. *Nat Rev Microbiol*, 5, 355-62.
- RÖTHIG, T., OCHSENKÜHN, M. A., ROIK, A., VAN DER MERWE, R. & VOOLSTRA, C. R. 2016. Long-term salinity tolerance is accompanied by major restructuring of the coral bacterial microbiome. *Molecular Ecology*, 25, 1308-1323.
- ROUZE, H., LECELLIER, G., POCHON, X., TORDA, G. & BERTEAUX-LECELLIER, V. 2019. Unique quantitative Symbiodiniaceae signature of coral colonies revealed through spatio-temporal survey in Moorea. *Sci Rep*, 9, 7921.
- ROWAN, R. 2004. Coral bleaching: thermal adaptation in reef coral symbionts. *Nature*, 430, 742.
- SALIH, A., LARKUM, A., COX, G., KUHL, M. & HOEGH-GULDBERG, O. 2000. Fluorescent pigments in corals are photoprotective. *Nature*, 408, 850-3.
- SCHLOSS, P. D., WESTCOTT, S. L., RYABIN, T., HALL, J. R., HARTMANN, M., HOLLISTER, E. B., LESNIEWSKI, R. A., OAKLEY, B. B., PARKS, D. H., ROBINSON, C. J., SAHL, J. W., STRES, B., THALLINGER, G. G., VAN HORN, D. J. & WEBER, C. F. 2009. Introducing mothur: open-source, platform-independent, community-supported software for describing and comparing microbial communities. *Appl Environ Microbiol*, 75, 7537-41.
- SCHOEPP, V., CARRION, S. A., PFEIFER, S. M., NAUGLE, M., DUGAL, L., BRUYN, J. & MCCULLOCH, M. T. 2019. Stress-resistant corals may not acclimatize to ocean warming but maintain heat tolerance under cooler temperatures. *Nat Commun*, 10, 4031.
- SCHOEPP, V., STAT, M., FALTER, J. L. & MCCULLOCH, M. T. 2015a. Limits to the thermal tolerance of corals adapted to a highly fluctuating, naturally extreme temperature environment. *Sci Rep*, 5, 17639.
- SCHOEPP, V., STAT, M., FALTER, J. L. & MCCULLOCH, M. T. 2015b. Limits to the thermal tolerance of corals adapted to a highly fluctuating, naturally extreme temperature environment. *Sci Rep*, 5, 17639.
- SCHÖTTNER, S., HOFFMANN, F., CÁRDENAS, P., RAPP, H. T., BOETIUS, A. & RAMETTE, A. 2013. Relationships between host phylogeny, host type and bacterial community diversity in cold-water coral reef sponges. *PloS one* U6 - ctx_ver=Z39.88-2004&ctx_enc=info%3Aofi%2Fenc%3AUTF-8&rft_id=info%3Aasid%2Fsummon.serialsolutions.com&rft_val_fmt=info%3Aofi%2Ffmt%3Akev%3Amtx%3Ajournal&rft.genre=article&rft.atitle=Relationships+between+host+phylogeny%2C+host+type+and+bacterial+community+diversity+in+cold-water+coral+reef+sponges&rft.jtitle=PloS+one&rft.au=Sch%C3%B6ttner%2C+Sandra&rft.au=Hoffmann%2C+Friederike&rft.au=C%C3%A1rdenas%2C+Paco&rft.au=Rapp%2C+Hans+Tore&rft.date=2013&rft.eissn=1932-6203&rft.volume=8&rft.issue=2&rft.spage=e55505&rft_id=info%3Apmid%2F23393586&rft.externalDocID=23393586¶mdict=en-US U7 - Journal Article, 8, e55505.
- SCOTT, G. R. & JOHNSTON, I. A. 2012. Temperature during embryonic development has persistent effects on thermal acclimation capacity in zebrafish. *Proc Natl Acad Sci U S A*, 109, 14247-52.
- SHARP, K. H., DISTEL, D. & PAUL, V. J. 2012. Diversity and dynamics of bacterial communities in early life stages of the Caribbean coral *Porites astreoides*. *ISME J*, 6, 790-801.
- SHARP, K. H., SNEED, J. M., RITCHIE, K. B., MCDANIEL, L. & PAUL, V. J. 2015. Induction of Larval Settlement in the Reef Coral *Porites astreoides* by a Cultivated Marine Roseobacter Strain. *Biol Bull*, 228, 98-107.

- SILVERSTEIN, R. N., CUNNING, R. & BAKER, A. C. 2015. Change in algal symbiont communities after bleaching, not prior heat exposure, increases heat tolerance of reef corals. *Global change biology*, 21, 236-249.
- SINCLAIR, B. J. & ROBERTS, S. P. 2005. Acclimation, shock and hardening in the cold. *Journal of Thermal Biology*, 30, 557-562.
- SINHA, R., ABU-ALI, G., VOGTMANN, E., FODOR, A. A., REN, B., AMIR, A., SCHWAGER, E., CRABTREE, J., MA, S., MICROBIOME QUALITY CONTROL PROJECT, C., ABNET, C. C., KNIGHT, R., WHITE, O. & HUTTENHOWER, C. 2017. Assessment of variation in microbial community amplicon sequencing by the Microbiome Quality Control (MBQC) project consortium. *Nat Biotechnol*, 35, 1077-1086.
- SIPOS, R., SZEKELY, A. J., PALATINSZKY, M., REVESZ, S., MARIALIGETI, K. & NIKOLAUSZ, M. 2007. Effect of primer mismatch, annealing temperature and PCR cycle number on 16S rRNA gene-targeting bacterial community analysis. *FEMS Microbiol Ecol*, 60, 341-50.
- SMITH, E. G., VAUGHAN, G. O., KETCHUM, R. N., MCPARLAND, D. & BURT, J. A. 2017. Symbiont community stability through severe coral bleaching in a thermally extreme lagoon. *Sci Rep*, 7, 2428.
- STANLEY, G. D. 2003. The evolution of modern corals and their early history. *Earth-Science Reviews*, 60, 195-225.
- STAT, M., BIRD, C. E., POCHON, X., CHASQUI, L., CHAUKA, L. J., CONCEPCION, G. T., LOGAN, D., TAKABAYASHI, M., TOONEN, R. J. & GATES, R. D. 2011. Variation in Symbiodinium ITS2 sequence assemblages among coral colonies. *PLoS One*, 6, e15854.
- SUZUKI, G., OKADA, W., YASUTAKE, Y., KAI, S., FUJIKURA, Y., TANITA, I., YAMASHITA, H., HAYASHIBARA, T., ANDO, W., NOGAMI, K. & FUDO, M. 2018. Interspecific differences in the post-settlement survival of *Acropora* corals under a common garden experiment. *Fisheries Science*, 84, 849-856.
- SUZUKI, M. M. & BIRD, A. 2008. DNA methylation landscapes: provocative insights from epigenomics. *Nat Rev Genet*, 9, 465-76.
- SWEET, M. J., BROWN, B. E., DUNNE, R. P., SINGLETON, I. & BULLING, M. 2017. Evidence for rapid, tide-related shifts in the microbiome of the coral *Coelastrea aspera*. *Coral Reefs*, 36, 815-828.
- TCHERNOV, D., GORBUNOV, M. Y., DE VARGAS, C., NARAYAN YADAV, S., MILLIGAN, A. J., HAGGBLOM, M. & FALKOWSKI, P. G. 2004. Membrane lipids of symbiotic algae are diagnostic of sensitivity to thermal bleaching in corals. *Proc Natl Acad Sci U S A*, 101, 13531-5.
- TEAM, R. C. 2013. R: A language and environment for statistical computing.
- TEWKSBURY, J. J., HUEY, R. B. & DEUTSCH, C. A. 2008. Ecology. Putting the heat on tropical animals. *Science*, 320, 1296-7.
- THERNEAU, T. M. & LUMLEY, T. 2014. Package 'survival'. *Survival analysis Published on CRAN*.
- THOMPSON, J. R., RIVERA, H. E., CLOSEK, C. J. & MEDINA, M. 2014. Microbes in the coral holobiont: partners through evolution, development, and ecological interactions. *Front Cell Infect Microbiol*, 4, 176.
- THOMSON, A. M., CALVIN, K. V., SMITH, S. J., KYLE, G. P., VOLKE, A., PATEL, P., DELGADO-ARIAS, S., BOND-LAMBERTY, B., WISE, M. A., CLARKE, L. E. & EDMONDS, J. A. 2011. RCP4.5: a pathway for stabilization of radiative forcing by 2100. *Climatic Change*, 109, 77-94.
- THORNHILL, D. J., HOWELLS, E. J., WHAM, D. C., STEURY, T. D. & SANTOS, S. R. 2017. Population genetics of reef coral endosymbionts (Symbiodinium, Dinophyceae). *Mol Ecol*, 26, 2640-2659.
- TONK, L., SAMPAYO, E. M., WEEKS, S., MAGNO-CANTO, M. & HOEGH-GULDBERG, O. 2013. Host-specific interactions with environmental factors shape the distribution of symbiodinium across the Great Barrier Reef. *PLoS One*, 8, e68533.
- TORDA, G., DONELSON, J. M., ARANDA, M., BARSHIS, D. J., BAY, L. K., BERUMEN, M. L., BOURNE, D. G., CANTIN, N., FORET, S. & MATZ, M. V. 2017. Rapid adaptive responses to climate change in corals. *Nature Climate Change*, 7, 627-636.

- TRAN, C. & HADFIELD, M. G. 2011. Larvae of *Pocillopora damicornis* (Anthozoa) settle and metamorphose in response to surface-biofilm bacteria. *Marine Ecology Progress Series*, 433, 85-96.
- TRAPON, M. L. 2013. *Variation in early post-settlement growth and mortality of scleractinian corals*.
- TRAPON, M. L., PRATCHETT, M. S., HOEY, A. S. & BAIRD, A. H. 2013. Influence of fish grazing and sedimentation on the early post-settlement survival of the tabular coral *Acropora cytherea*. *Coral Reefs*, 32, 1051-1059.
- ULSTRUP, K. E., HILL, R., VAN OPPEN, M. J. H., LARKUM, A. W. D. & RALPH, P. J. 2008. Seasonal variation in the photo-physiology of homogeneous and heterogeneous Symbiodinium consortia in two scleractinian corals. *Marine Ecology Progress Series*, 361, 139-150.
- UTHICKE, S., PATEL, F., KARELITZ, S., LUTER, H. M., WEBSTER, N. S. & LAMARE, M. 2020. Key biological responses over two generations of the sea urchin *Echinometra* sp. A under future ocean conditions. *Marine Ecology Progress Series*, 637, 87-101.
- VAN DE WATER, J. A., MELKONIAN, R., VOOLSTRA, C. R., JUNCA, H., BERAUD, E., ALLEMAND, D. & FERRIER-PAGES, C. 2017. Comparative Assessment of Mediterranean Gorgonian-Associated Microbial Communities Reveals Conserved Core and Locally Variant Bacteria. *Microb Ecol*, 73, 466-478.
- VAN HOOIDONK, R., MAYNARD, J., TAMELANDER, J., GOVE, J., AHMADIA, G., RAYMUNDO, L., WILLIAMS, G., HERON, S. F. & PLANES, S. 2016. Local-scale projections of coral reef futures and implications of the Paris Agreement. *Sci Rep*, 6, 39666.
- VAN HOOIDONK, R., MAYNARD, J. A., MANZELLO, D. & PLANES, S. 2014. Opposite latitudinal gradients in projected ocean acidification and bleaching impacts on coral reefs. *Glob Chang Biol*, 20, 103-12.
- VAN HOOIDONK, R., MAYNARD, J. A. & PLANES, S. 2013. Temporary refugia for coral reefs in a warming world. *Nature Climate Change*, 3, 508-511.
- VAN OPPEN, M. J. H. & BLACKALL, L. L. 2019. Coral microbiome dynamics, functions and design in a changing world. *Nat Rev Microbiol*, 17, 557-567.
- VAN OPPEN, M. J. H., BONGAERTS, P., FRADE, P., PELOW, L. M., BOYD, S. E., NIM, H. T. & BAY, L. K. 2018. Adaptation to reef habitats through selection on the coral animal and its associated microbiome. *Mol Ecol*, 27, 2956-2971.
- VAN OPPEN, M. J. H., GATES, R. D., BLACKALL, L. L., CANTIN, N., CHAKRAVARTI, L. J., CHAN, W. Y., CORMICK, C., CREAN, A., DAMJANOVIC, K., EPSTEIN, H., HARRISON, P. L., JONES, T. A., MILLER, M., PEARS, R. J., PELOW, L. M., RAFTOS, D. A., SCHAFFELKE, B., STEWART, K., TORDA, G., WACHENFELD, D., WEEKS, A. R. & PUTNAM, H. M. 2017. Shifting paradigms in restoration of the world's coral reefs. *Glob Chang Biol*, 23, 3437-3448.
- VAN OPPEN, M. J. H. & LOUGH, J. M. 2009. *Coral bleaching: patterns, processes, causes, and consequences*, New York;Berlin;, Springer.
- VANWONTERGHEM, I. & WEBSTER, N. S. 2020. Coral Reef Microorganisms in a Changing Climate. *iScience*, 23, 100972.
- VERHOEVEN, K. J. F., VONHOLDT, B. M. & SORK, V. L. 2016. Epigenetics in ecology and evolution: what we know and what we need to know INTRODUCTION. *Molecular Ecology*, 25, 1631-1638.
- VIA, S. & LANDE, R. 1985. Genotype-environment interaction and the evolution of phenotypic plasticity. *Evolution*, 505-522.
- VIYAKARN, V., LALITPATTARAKIT, W., CHINFAK, N., JANDANG, S., KUANUI, P., KHOKIATTIWONG, S. & CHAVANICH, S. 2015. Effect of lower pH on settlement and development of coral, *Pocillopora damicornis* (Linnaeus, 1758). *Ocean Science Journal*, 50, 475-480.
- WADDINGTON, C. H. 2014. *The strategy of the genes*, Routledge.
- WALL, C. B., RICCI, C. A., FOULDS, G. E., MYDLARZ, L. D., GATES, R. D. & PUTNAM, H. M. 2018. The effects of environmental history and thermal stress on coral physiology and immunity. *Marine Biology*, 165, 1-15.

- WANG, J.-T., MENG, P.-J., CHEN, Y.-Y. & CHEN, C. A. 2012. Determination of the Thermal Tolerance of Symbiodinium Using the Activation Energy for Inhibiting Photosystem II Activity. *Zoological studies*, 51.
- WARNER, M. E., FITT, W. K. & SCHMIDT, G. W. 1999. Damage to photosystem II in symbiotic dinoflagellates: a determinant of coral bleaching. *Proc Natl Acad Sci U S A*, 96, 8007-12.
- WARNER, M. E., LESSER, M. P. & RALPH, P. J. 2010. Chlorophyll Fluorescence in Reef Building Corals. *Chlorophyll a Fluorescence in Aquatic Sciences: Methods and Applications*. Dordrecht: Springer Netherlands.
- WEBSTER, N. S., NEGRI, A. P., BOTTE, E. S., LAFFY, P. W., FLORES, F., NOONAN, S., SCHMIDT, C. & UTHICKE, S. 2016. Host-associated coral reef microbes respond to the cumulative pressures of ocean warming and ocean acidification. *Sci Rep*, 6, 19324.
- WEBSTER, N. S. & REUSCH, T. B. H. 2017. Microbial contributions to the persistence of coral reefs. *ISME J*.
- WEBSTER, N. S., SMITH, L. D., HEYWARD, A. J., WATTS, J. E., WEBB, R. I., BLACKALL, L. L. & NEGRI, A. P. 2004. Metamorphosis of a scleractinian coral in response to microbial biofilms. *Appl Environ Microbiol*, 70, 1213-21.
- WEBSTER, N. S., NEGRI, A. P., FLORES, F., HUMPHREY, C., SOO, R., BOTTE, E. S., VOGEL, N. & UTHICKE, S. 2013. Near-future ocean acidification causes differences in microbial associations within diverse coral reef taxa. *Environ Microbiol Rep*, 5, 243-51.
- WILLIAMS, A. D., BROWN, B. E., PUTCHIM, L. & SWEET, M. J. 2015. Age-Related Shifts in Bacterial Diversity in a Reef Coral. *PLoS One*, 10, e0144902.
- WILLIS, B. L., BABCOCK, R. C., HARRISON, P. L. & WALLACE, C. C. 1997. Experimental hybridization and breeding incompatibilities within the mating systems of mass spawning reef corals. *Coral Reefs*, 16, S53-S65.
- WILSON, J. & HARRISON, P. 2005. Post-settlement mortality and growth of newly settled reef corals in a subtropical environment. *Coral Reefs*, 24, 418-421.
- WILSON, R. S. & FRANKLIN, C. E. 2002. Testing the beneficial acclimation hypothesis. *Trends in Ecology & Evolution*, 17, 66-70.
- WILSON, S. K., ROBINSON, J. P. W., CHONG-SENG, K., ROBINSON, J. & GRAHAM, N. A. J. 2019. Boom and bust of keystone structure on coral reefs. *Coral Reefs*, 38, 625-635.
- YACHI, S. & LOREAU, M. 1999. Biodiversity and ecosystem productivity in a fluctuating environment: the insurance hypothesis. *Proc Natl Acad Sci U S A*, 96, 1463-8.
- YORIFUJI, M., HARI, S., NAKAMURA, R. & FUDO, M. 2017. Shift of symbiont communities in *Acropora tenuis* juveniles under heat stress. *PeerJ*, 5, e4055.
- YOUNG, C. N., SCHOPMEYER, S. A. & LIRMAN, D. 2012. A Review of Reef Restoration and Coral Propagation Using the Threatened Genus *Acropora* in the Caribbean and Western Atlantic. *Bulletin of Marine Science*, 88, 1075-1098.
- YUAN, X., YUAN, T., HUANG, H., JIANG, L., ZHOU, W. & LIU, S. 2018. Elevated CO₂ delays the early development of scleractinian coral *Acropora gemmifera*. *Sci Rep*, 8, 2787.
- ZANEVELD, J. R., MCMINDS, R. & VEGA THURBER, R. 2017. Stress and stability: applying the Anna Karenina principle to animal microbiomes. *Nat Microbiol*, 2, 17121.
- ZIEGLER, M., GRUPSTRA, C. G. B., BARRETO, M. M., EATON, M., BAOMAR, J., ZUBIER, K., AL-SOFYANI, A., TURKI, A. J., ORMOND, R. & VOOLSTRA, C. R. 2019. Coral bacterial community structure responds to environmental change in a host-specific manner. *Nature Communications*, 10, 3092-11.
- ZIEGLER, M., ROIK, A., PORTER, A., ZUBIER, K., MUDARRIS, M. S., ORMOND, R. & VOOLSTRA, C. R. 2016. Coral microbial community dynamics in response to anthropogenic impacts near a major city in the central Red Sea. *Mar Pollut Bull*, 105, 629-40.
- ZIEGLER, M., SENECA, F. O., YUM, L. K., PALUMBI, S. R. & VOOLSTRA, C. R. 2017. Bacterial community dynamics are linked to patterns of coral heat tolerance. *Nat Commun*, 8, 14213.

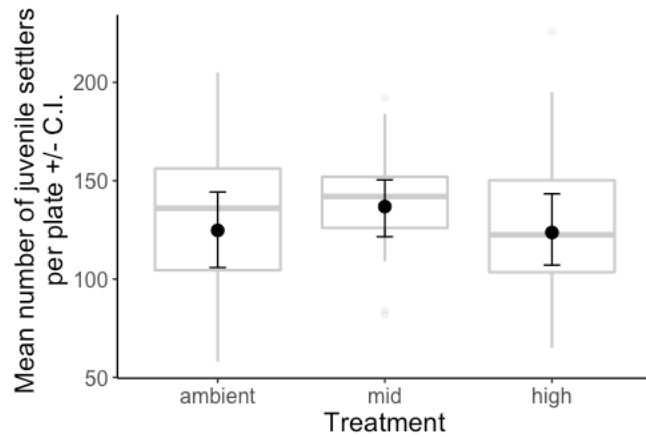
Appendix A – Chapter 2

A.1 Recruits: settlement success

Table A.S 1 Coefficients of the generalised linear mixed effect model predicting the number of recruits settling among treatments.

	Estimate	Std. Error	t-value	p-value
Intercept (ambient)	0. 73941	0.16286	4.54	<0.001
Treatment-Mid	0.01924	0.22921	0.08	0.93
Treatment-High	-0.00151	0.23040	-0.01	0.99

Figure A.S 1 Settlement success of corals from the three treatments per plate. Black circles show the fitted model and the error bars show the 95% confidence intervals. The grey boxplots show the distribution of the raw data.



A.2 Recruits: growth

Table A.S 2 List of statistical models used to predict basal growth of coral recruits relative to the exposure to treatment, size (diameter) and time. The shaded area indicates the best-fit model.

Model	Fixed effect	Random effect	AICc	Akaike weights
1	Diameter*treatment + time*treatment	Individual nested in plate (intercept), tank (intercept)	-4179.56	0.010
2	Diameter + time*treatment	Individual nested in plate (intercept), tank (intercept)	-4183.48	0.077
3	Diameter*treatment + time	Individual nested in plate (intercept), tank (intercept)	-4182.42	0.045
4	Diameter + treatment + time	Individual nested in plate (intercept), tank (intercept)	-4186.10	0.296
5	Diameter + treatment + time	tank (intercept)	-4089.32	<0.001
6	Diameter + treatment + time	Individual nested in plate (intercept)	-4187.40	0.568

Table A.S 3 Coefficient estimates for the best-fit linear model to estimate recruit basal growth relation to treatment, diameter and time.

	Estimate	Std. Error	Z value	Pr(> z)
(Intercept) (ambient at time1)	0.07466	0.00487	15.32	<0.001
diameter	-0.00887	0.00442	-2.01	0.045
treatment (high)	-0.00682	0.00371	-1.84	0.066
treatment (mid)	-0.00770	0.00363	-2.12	0.034
time2	-0.00408	0.00158	-2.58	0.010

Table A.S 4 Tukey Posthoc Test estimates of pairwise comparisons among treatments.

	Estimate	Std. Error	z value	Pr(> z)
--	----------	------------	---------	----------

high - control == 0	-0.0068163	0.0037129	-1.836	0.1483
mid - control == 0	-0.0077033	0.0036317	-2.121	0.0797
mid - high == 0	-0.0008869	0.0052582	-0.169	0.9835

A.3 Symbiotic associations

A.3.1 Symbiodiniaceae communities at t=6 weeks

Table A.S 5 PERMANOVA test results (partial R² and p-values) for the effect of treatment on Symbiodiniaceae relative composition using Bray-Curtis similarity distance. Number of permutations=999.

	df	SumsOfSqs	MeanSqs	F.Model	R ²	Pr(>F)	
treatment	2	3.0329	1.51645	9.3811	0.24983	0.01	***
tank	6	1.8329	0.30549	1.8898	0.15098	0.08	
residuals	45	7.2742	0.16165		0.59919		
total	53	12.1400			1.0000		

Table A.S 6 Proportion of Symbiodiniaceae types present in individuals from a general approach and also for each treatment at t = 6 weeks.

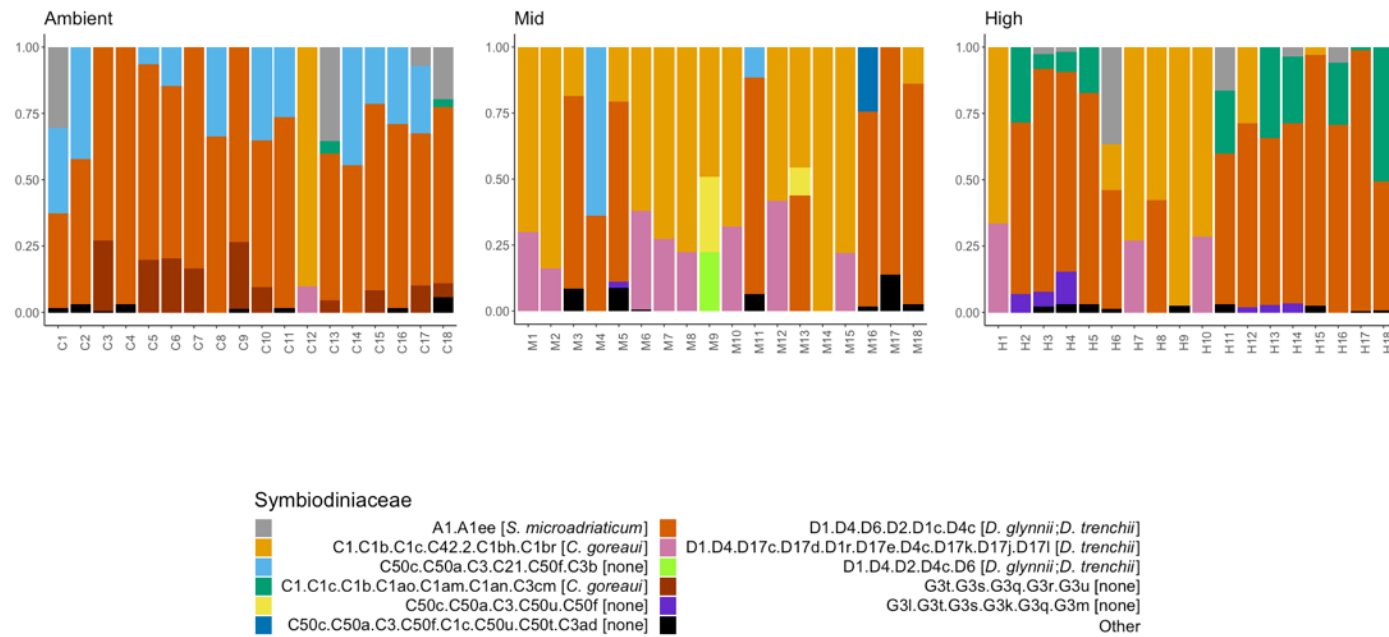
Symbiodiniaceae type profile	Associated species	Proportion		
		Ambient	Mid	High
A1.A1ee	<i>S. microadriaticum</i>	0.05	0.00	0.04
C1.C1b.C1c.C42.2.C1bh.C1br	<i>C. goreau</i>	0.05	0.45	0.23
C1.C1c.C1b.C1ao.C1am.C1an.C3cm	<i>C. goreau</i>	0.00	0.00	0.12
C50c.C50a.C3.C21.C50f.C3b	None	0.17	0.04	0.00

C3.C3b	.00	.00	.00	.00	.00	.00	.00	.00	.00	.00	.00	.00	.00	.00	.00	.00	.00	.00
C3.C40	.00	.00	.00	.00	.00	.00	.00	.00	.00	.00	.00	.00	.00	.00	.00	.00	.00	.00
C50c	.00	.00	.00	.00	.00	.00	.00	.00	.00	.00	.00	.00	.00	.00	.00	.00	.00	.02
C50c.C50a.C3.C21.C50f.C3b	.32	.42	.00	.00	.06	.15	.00	.34	.00	.35	.26	.00	.00	.45	.21	.29	.25	.00
C50c.C50a.C3.C50f.C1c.C50u.C50t.C3ad	.00	.00	.00	.00	.00	.00	.00	.00	.00	.00	.00	.00	.00	.00	.00	.00	.00	.00
C50c.C50a.C3.C50u.C50f	.00	.00	.00	.00	.00	.00	.00	.00	.00	.00	.00	.00	.00	.00	.00	.00	.00	.00
D1.D4.D17c.D17d.D17e.D4c.D17k.D17j.D17l	.00	.00	.00	.00	.00	.00	.00	.00	.00	.00	.00	.10	.00	.00	.00	.00	.00	.00
D1.D4.D2.D4c.D6	.00	.00	.00	.00	.00	.00	.00	.00	.00	.00	.00	.00	.00	.00	.00	.00	.00	.00
D1.D4.D6.D2.D1c.D4c	.36	.55	.73	.97	.74	.65	.84	.66	.74	.55	.72	.00	.55	.55	.70	.69	.58	.66
F3.1	.00	.00	.00	.00	.00	.00	.00	.00	.00	.00	.00	.00	.00	.00	.00	.00	.00	.00
F3e	.00	.00	.00	.00	.00	.00	.00	.00	.00	.00	.00	.00	.00	.00	.00	.00	.00	.03
G3l.G3k.G3m	.00	.00	.00	.00	.00	.00	.00	.00	.00	.00	.00	.00	.00	.00	.00	.00	.00	.00
G3l.G3t.G3s.G3k.G3q.G3m	.00	.00	.00	.00	.00	.00	.00	.00	.00	.00	.00	.00	.00	.00	.00	.00	.00	.00
G3l.G3v	.00	.00	.00	.00	.00	.00	.00	.00	.00	.00	.00	.00	.00	.00	.00	.00	.00	.00
G3t	.00	.00	.00	.00	.00	.00	.00	.00	.00	.00	.00	.00	.00	.00	.00	.00	.00	.00
G3t.G3s.G3q.G3r	.02	.03	.00	.03	.00	.00	.00	.00	.00	.00	.02	.00	.00	.00	.00	.02	.00	.00
G3t.G3s.G3q.G3r.G3u	.00	.00	.27	.00	.20	.20	.16	.00	.25	.10	.00	.00	.04	.00	.08	.00	.10	.05

G3t	.00	.00	.00	.00	.00	.00	.00	.00	.00	.01	.00	.00	.00	.00	.00	.00	.00	.00
G3t.G3s.G3q.G3r	.00	.00	.00	.00	.00	.00	.00	.00	.00	.00	.00	.03	.00	.00	.00	.00	.00	.00
G3t.G3s.G3q.G3r.G3u	.00	.00	.00	.00	.00	.00	.00	.00	.00	.00	.00	.00	.00	.00	.00	.00	.00	.00

The higher relative abundance and overall presence in the majority of recruits corresponded to type D (including D1.D4.D6.D2.D1c.D4c; associated species: *D. glynnii*) which was present in 14 of the 18 recruits sampled. Similarly, 8 out of 18 recruits, harboured type C (C1.C1b.C1c.C42.2.C1bh.C1br; associated species: *C. goreau*), and three of these eight recruits had a similar combination of type profiles as the one found in some recruits in mid treatment, which included type D (D1.D4.D17c.D17d.D1r.D17e.D4c.D17k.D17j.D17l; associated species: *D. trenchii*). Interestingly, type A (A1.A1ee, associated species: *S. microadriaticum*) was present in 6 recruits, and it is a type that also appeared in recruits from control condition but not in mid treatment. Moreover, a new group of type C also appeared clustering C1.C1c.C1b.C1ao.C1am.C1an.C3cm (associated species: *C. goreau*). Additional types were found with very low relative abundance (other background symbionts < 5% relative abundance: A1, C15, C3, G3t). Overall, it seems that types and their abundance found on recruits under high treatment were a combination of patterns that were found on recruits under control and mid treatment, but with a potential transition from type C50 (orange) in control to C1 (dark blue) in high treatment when comparing between treatments. Such similarities and differences on types among treatments could potentially explain the patterns found on the basal extension and survival rates among treatments.

Figure A.S 2 Composition of Symbiodiniaceae communities in the 6-week old recruit *A. loripes* at the individual level in each of three treatments. Colours represent specific type profiles, where other background symbionts represent <10% relative abundance. Number of replicates: 18 recruits individually sampled per treatment (6 individuals per each of three tanks, with a total of 54 recruits across treatments).



A.3.2 Bacterial communities at t=6 weeks

Figure A.S 3 Rarefaction curve corresponding to the relation of observed ASVs relative to sequencing depth (number of reads per sample).

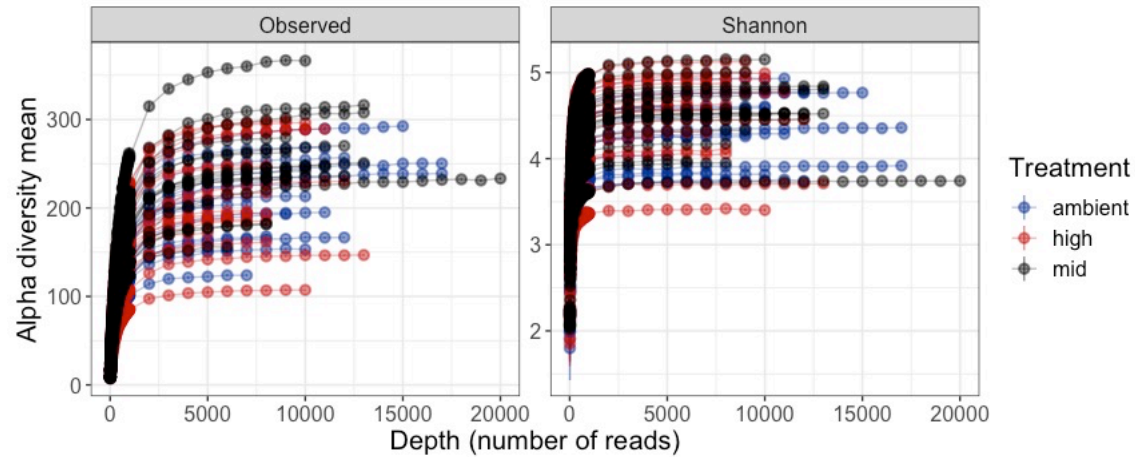
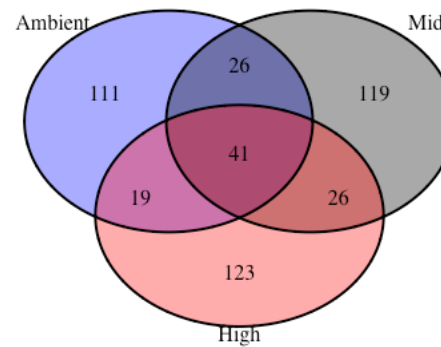


Figure A.S 4 Venn diagram corresponding to number of ASVs on 6-week old recruit corals among treatments. Overlapping shades represent shared number of ASVs between treatments. Total number of ASVs: 10986.



Alpha diversity:

Table A.S 10 Coefficient estimates of the observed ASVs in 6-week old recruit corals among treatments.

	Estimate	Std. Error	Z value	Pr(> z)
M - A == 0	0.16897	0.10230	1.652	0.224
H - A == 0	0.02595	0.10248	0.253	0.965
H - M == 0	-0.14302	0.10228	-1.398	0.342

Table A.S 11 Coefficient estimates for Shannon diversity index in 6-week old recruit corals among treatments.

	Estimate	Std. Error	Z value	Pr(> z)
M - A == 0	0.01951	0.01825	1.070	0.533
H - A == 0	0.01778	0.01825	0.975	0.593
H - M == 0	-0.00173	0.01825	-0.095	0.995

Table A.S 12 Coefficient estimates of the observed ASVs in 6-week old recruit corals among treatments.

	Estimate	Std. Error	Z value	Pr(> z)
M - A == 0	0.07494	0.05069	1.478	0.301
H - A == 0	0.00705	0.05069	0.139	0.989

H - M == 0	-0.06789	0.05069	-1.339	0.373
------------	----------	---------	--------	-------

Figure A.S 5 Alpha diversity of microbial communities in 6-week old recruit corals among treatments. Plots represent species richness (ASV counts=left) and species diversity index (Shannon=middle and Chao1=right).

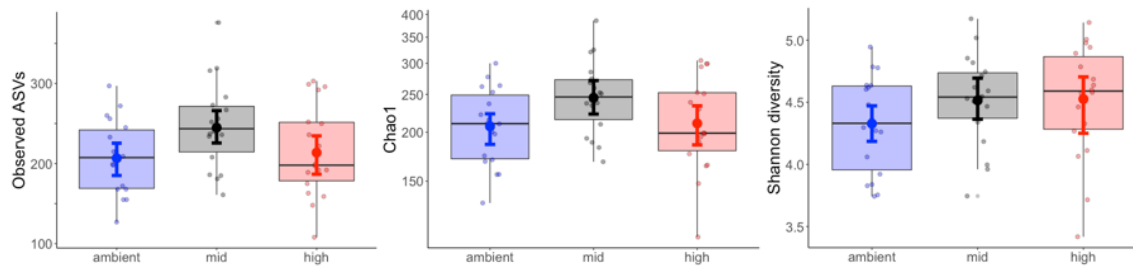


Table A.S 13 PERMANOVA test results (partial R2 and p-values) for the effect of treatment on the relative composition of bacterial communities using Bray-Curtis similarity distance. Number of permutations=999

	Df	SumOfSqs	R2	F	p-value	
Treatment	2	1.313	0.055	1.508	0.001	***
Tank	1	0.513	0.021	1.184	0.108	
Residual	50	21.693	0.922			
Total	53	23.521	1.000			

Table A.S 14 Permutation test for homogeneity of multivariate dispersions. Number of permutations=999

Df	Sum Sq	Mean Sq	F	N. perm	p-value
----	--------	---------	---	---------	---------

Groups	2	0.001	0.000	0.526	999	0.610
Residuals	51	0.051	0.001			

Table A.S 15 Indicator taxa for 6-week old coral recruits under different treatments. Indval analysis done at the species level (ASV) and included alpha parameters of 0.05.

Treatment	ASV	(specificity)	(fidelity)	tat	_value	ingdom	ylum	P	CI	O	Famil	Genu	Specie
Ambient	b3b7a3da523a01897f03ce8073c8101d	.846	.222	.434	.050	acteria	yanobacteria	C	Ox	P	Phormidismiaceae	Phormidium MBIC10003	uncultured bacterium
Mid	6eec16e3f06ef7b4c97fa5709bc2ce73	.786	.500	.627	.002	acteria	yanobacteria	C	Ox	N	Phormidismiaceae	Trichodesmium IMS101	uncultured bacterium
Mid	25d6e17e4bb698698a71b63bc4587903	.889	.278	.497	.033	acteria	yanobacteria	C	Ox	N	Nostocales Incertae Sedis	Roseofilum AO1-A	uncultured cyanobacterium
High	771ab3f96746d2ce5b1016f31fbc6375	.706	.333	.049	.048	acteria	yanobacteria	C	Ox	P	Phormidismiaceae	Acrophormium PCC-7375	ambiguous_taxa
High	758721da7294b3d3c834d38ff3d3fa79	.000	.222	.471	.024	acteria	yanobacteria	C	Ox	P	Nodosilineaceae	Halonema TFE P1	uncultured cyanobacterium

Table A.S 16 Indicator taxa for 6-week old coral recruits under different treatments. Indval analysis done at the genus level and included alpha parameters of 0.05.

Treatment	ASV	A (specificity)	B (fidelity)	st	p_value	Kingdom	Phylum	Class	Order	Family	Genus	Species
-----------	-----	-----------------	--------------	----	---------	---------	--------	-------	-------	--------	-------	---------

Ambient	f53625710a03f89025d95c493c3f2db2	0.7778	0.3889	0.55	0.011	D_0__Bacteria	D_1__Proteobacteria	D_2__Alphaproteobacteria	D_3__Sphingomonadales	D_4__Sphingomonadales	D_5__Erythro bacter	NA
Mid	25d6e17e4bb698698a71b63bc4587903	0.889	0.278	0.497	0.034	D_0__Bacteria	D_1__Cyanobacteria	D_2__Oxyphotobacteria	D_3__Nostocales	D_4__Nostocales Incertae Sedis	D_5__Roseofilum AO1-A	D_6__uncultured cyanobacterium
Mid	6eec16e3f06ef7b4c97fa5709bc2ce73	0.609	0.556	0.582	0.020	D_0__Bacteria	D_1__Cyanobacteria	D_2__Oxyphotobacteria	D_3__Nostocales	D_4__Phormidiaceae	D_5__Trichodesmium IMS101	D_6__uncultured bacterium
Mid	21c1b2fca3b5797a7d2dd513333ccbe9	0.579	0.500	0.538	0.047	D_0__Bacteria	D_1__Planctomycetes	D_2__Phycisphaerae	D_3__Phycisphaerales	D_4__Phycisphaeraeae	D_5__SM1A02	D_6__uncultured organism
High	49d0c602c71ffc2258b09be24936b16f	0.765	0.389	0.545	0.020	D_0__Bacteria	D_1__Proteobacteria	D_2__Alphaproteobacteria	D_3__uncultured	D_4__uncultured alpha proteobacterium	D_5__	D_6__

Table A.S 17 Indicator taxa for 6-week old coral recruits under different treatments. Indval analysis done at the family level and included alpha parameters of 0.05.

Treatment	ASV	A (specificity)	B (fidelity)	stat	p_value	Kingdom	Phylum	Class	Order	Family	Genus	Species
Mid	25d6e17e4bb698698a71b63bc4587903	0.727	0.500	0.603	0.007	D_0__Bacteria	D_1__Cyanobacteria	D_2__Oxyphotobacteria	D_3__Nostocales	D_4__Nostocales Incertae Sedis	D_5__Roseofilum AO1-A	D_6__uncultured cyanobacterium
Mid	6eec16e3f06ef7b4c97fa5709bc2ce73	0.609	0.556	0.582	0.020	D_0__Bacteria	D_1__Cyanobacteria	D_2__Oxyphotobacteria	D_3__Nostocales	D_4__Phormidiaceae	D_5__Trichodesmium IMS101	D_6__uncultured bacterium
High	49d0c602c71ffc2258b09be24936b16f	0.765	0.389	0.545	0.019	D_0__Bacteria	D_1__Proteobacteria	D_2__Alphaproteobacteria	D_3__uncultured	D_4__uncultured alpha proteobacterium	D_5__	D_6__

Table A.S 18 Individual models among bacterial families used to estimate difference in relative abundances from the top ten most abundant following a zero-inflated beta-regression.

Zero-inflated beta regression (logit link)

Rhizobiaceae

term	estimate	std.error	conf.low	conf.high
b_Intercept	-2.473	0.188	-2.865	-2.113
b_zi_Intercept	-1.004	0.540	-2.107	0.006
b_treat_2H	0.449	0.234	-0.009	0.919
b_treat_2M	-0.082	0.272	-0.631	0.464
b_zi_treat_2H	0.008	0.788	-1.506	1.549
b_zi_treat_2M	0.537	0.745	-0.911	2.054
phi	28.963	7.031	16.708	44.542

Phycisphaeraceae

term	estimate	std.error	conf.low	conf.high
b_Intercept	-2.445	0.213	-2.897	-2.044
b_zi_Intercept	1.030	0.553	-0.019	2.119
b_treat_2H	-0.098	0.295	-0.688	0.462
b_treat_2M	-0.183	0.259	-0.660	0.360
b_zi_treat_2H	-0.316	0.777	-1.808	1.148
b_zi_treat_2M	-1.518	0.758	-2.967	-0.053

phi	65.910	20.399	31.446	110.027
-----	--------	--------	--------	---------

Xenococcaceae

term	estimate	std.error	conf.low	conf.high
b_Intercept	-2.530	0.209	-2.942	-2.140
b_zi_Intercept	-0.229	0.483	-1.175	0.751
b_treat_2H	0.262	0.318	-0.359	0.893
b_treat_2M	0.266	0.293	-0.308	0.813
b_zi_treat_2H	0.958	0.716	-0.411	2.434
b_zi_treat_2M	0.443	0.668	-0.934	1.777
phi	30.478	9.664	15.141	52.275

Rhodopirillaceae

term	estimate	std.error	conf.low	conf.high
b_Intercept	-2.215	0.178	-2.551	-1.866
b_zi_Intercept	-0.015	0.496	-0.971	0.923
b_treat_2H	-0.474	0.343	-1.161	0.183
b_treat_2M	-0.029	0.263	-0.542	0.450
b_zi_treat_2H	1.318	0.783	-0.151	2.872

b_zi_treat_2M	0.466	0.704	-0.932	1.836
phi	45.399	14.854	20.428	78.270

Phormidesmiaceae

term	estimate	std.error	conf.low	conf.high
b_Intercept	-1.772	0.147	-2.059	-1.484
b_zi_Intercept	-2.141	0.756	-3.779	-0.834
b_treat_2H	-0.349	0.235	-0.803	0.106
b_treat_2M	-0.337	0.224	-0.781	0.109
b_zi_treat_2H	0.883	0.963	-0.935	2.835
b_zi_treat_2M	0.005	1.081	-2.150	2.170
phi	18.557	3.881	11.474	26.837

Nostocaceae

term	estimate	std.error	conf.low	conf.high
b_Intercept	-2.293	0.251	-2.812	-1.830
b_zi_Intercept	0.460	0.503	-0.504	1.472
b_treat_2H	0.408	0.299	-0.164	1.014
b_treat_2M	0.142	0.364	-0.615	0.867
b_zi_treat_2H	-0.707	0.699	-2.166	0.735
b_zi_treat_2M	0.262	0.730	-1.112	1.746
phi	25.035	7.968	12.400	43.263

Kiloniellaceae

term	estimate	std.error	conf.low	conf.high
------	----------	-----------	----------	-----------

b_Intercept	-2.260	0.197	-2.651	-1.864
b_zi_Intercept	-0.446	0.501	-1.488	0.571
b_treat_2H	0.113	0.264	-0.423	0.616
b_treat_2M	-0.016	0.280	-0.590	0.515
b_zi_treat_2H	-0.028	0.720	-1.469	1.372
b_zi_treat_2M	0.225	0.677	-1.088	1.586
phi	23.370	6.196	12.677	36.706

Unknown Family

term	estimate	std.error	conf.low	conf.high
b_Intercept	-1.725	0.206	-2.159	-1.330
b_zi_Intercept	0.024	0.456	-0.862	0.924
b_treat_2H	-0.552	0.303	-1.143	0.043
b_treat_2M	-0.577	0.302	-1.199	0.029
b_zi_treat_2H	-0.499	0.680	-1.901	0.825
b_zi_treat_2M	-0.264	0.655	-1.551	0.989
phi	21.629	5.959	11.603	35.302

uncultured

term	estimate	std.error	conf.low	conf.high
b_Intercept	-2.401	0.227	-2.861	-1.967
b_zi_Intercept	-0.248	0.490	-1.257	0.695
b_treat_2H	0.163	0.365	-0.629	0.838
b_treat_2M	-0.019	0.327	-0.666	0.622
b_zi_treat_2H	1.264	0.742	-0.151	2.729

b_zi_treat_2M	0.720	0.726	-0.698	2.124
phi	26.216	8.350	12.491	44.246

Beta regression (logit link)

Rhodobacteraceae

term	estimate	std.error	conf.low	conf.high
b_Intercept	-1.273	0.173	-1.617	-0.934
b_treat_2H	0.254	0.232	-0.229	0.712
b_treat_2M	0.091	0.231	-0.377	0.535
phi	10.246	1.980	6.706	14.454

Table A.S 19 Results from the posterior distribution of difference as the outcome for each model and bacterial family

Family	Contrast	Posterior distribution of difference			
		Mean	Upper 95% C.I.	Lower 95% C.I.	
Kiloniellaceae	A-H	0.001	0.193	-0.209	No difference
Kiloniellaceae	A-M	-0.001	0.200	-0.189	No difference
Kiloniellaceae	M-H	0.014	0.229	-0.195	No difference
Nostocaceae	A-H	0.003	0.180	-0.176	No difference
Nostocaceae	A-M	0.000	0.185	-0.189	No difference
Nostocaceae	M-H	0.040	0.257	-0.175	No difference
Phormidesmiaceae	A-H	0.003	0.246	-0.251	No difference
Phormidesmiaceae	A-M	0.001	0.260	-0.258	No difference
Phormidesmiaceae	M-H	-0.011	0.221	-0.224	No difference
Phycisphaeraceae	A-H	0.003	0.125	-0.121	No difference
Phycisphaeraceae	A-M	-0.001	0.116	-0.123	No difference
Phycisphaeraceae	M-H	-0.016	0.111	-0.128	No difference
Rhizobiaceae	A-H	0.001	0.166	-0.158	No difference
Rhizobiaceae	A-M	0.000	0.160	-0.166	No difference
Rhizobiaceae	M-H	0.041	0.224	-0.131	No difference
Rhodobacteraceae	A-H	0.000	0.345	-0.363	No difference
Rhodobacteraceae	A-M	-0.003	0.337	-0.341	No difference
Rhodobacteraceae	M-H	0.029	0.414	-0.339	No difference
Rhodopirillaceae	A-H	-0.001	0.165	-0.169	No difference
Rhodopirillaceae	A-M	-0.003	0.162	-0.168	No difference
Rhodopirillaceae	M-H	-0.024	0.097	-0.173	No difference

uncultured	A-H	-0.004	0.169	-0.180	No difference
uncultured	A-M	0.003	0.176	-0.176	No difference
uncultured	M-H	-0.007	0.171	-0.186	No difference
Unknown Family	A-H	-0.003	0.269	-0.268	No difference
Unknown Family	A-M	-0.002	0.254	-0.279	No difference
Unknown Family	M-H	0.003	0.204	-0.195	No difference
Xenococcaceae	A-H	0.000	0.152	-0.156	No difference
Xenococcaceae	A-M	-0.001	0.152	-0.152	No difference
Xenococcaceae	M-H	-0.012	0.177	-0.190	No difference

Figure A.S 7 Relative abundances of the top 10 bacterial genera (y-axis) among 6-week old coral recruits across each of three treatments (ambient, mid, high) (x-axis).

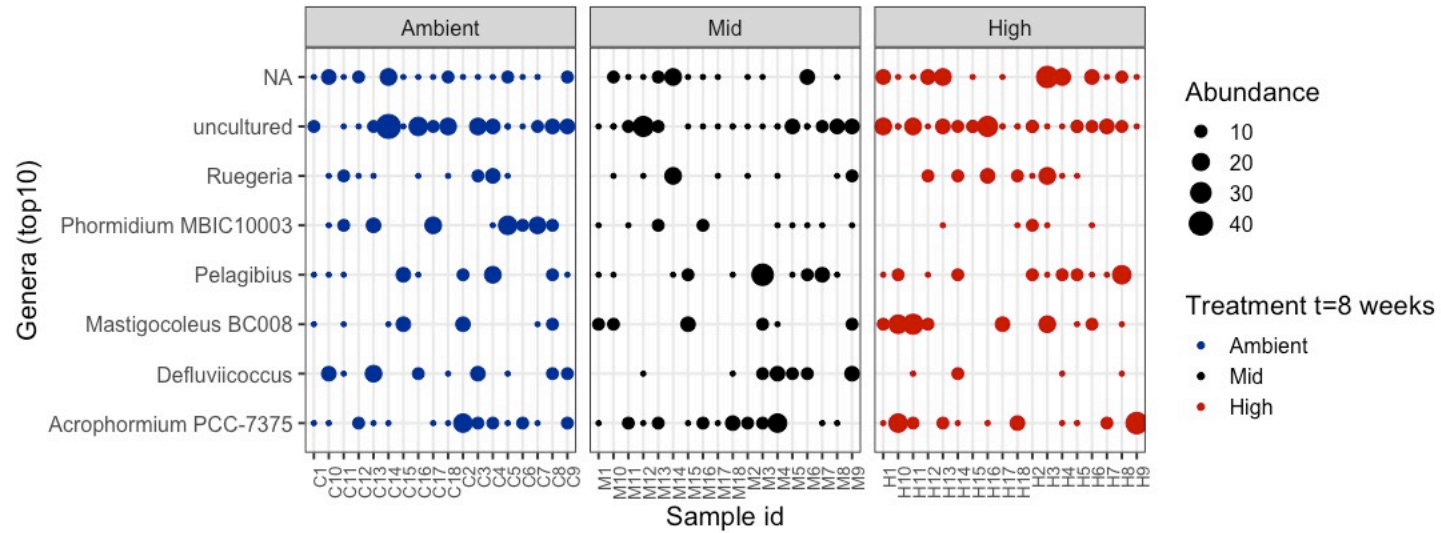


Table A.S 20 Individual models among bacterial genera used to estimate difference in relative abundances from the top ten most abundant following a zero-inflated beta-regression.

term	estimate	std.error	conf.low	conf.high	Genus
b_Intercept	-2.2087641	0.13060516	-2.4910694	-1.9707478	uncultured
b_treat_1H	-0.1149283	0.17243089	-0.4624741	0.22814791	uncultured
b_treat_1M	-0.2618951	0.18039325	-0.6103655	0.11447545	uncultured
phi	27.7219732	4.28941926	20.0097621	36.567504	uncultured
zi	0.47584291	0.04066607	0.39441753	0.55257973	uncultured

b_Intercept	-2.2207871	0.16966513	-2.5767502	-1.8867224	Defluviicoccus
b_treat_1H	-0.4781632	0.35178837	-1.2105086	0.19041707	Defluviicoccus
b_treat_1M	-0.0297125	0.25655357	-0.5417105	0.45985269	Defluviicoccus
phi	45.0895259	14.3973555	21.8206149	77.4883485	Defluviicoccus
zi	0.62341516	0.06517854	0.48690442	0.74502252	Defluviicoccus
b_Intercept	-2.4393291	0.17159623	-2.7716677	-2.0948842	(NA) Family Rhodobacteraceae
b_treat_1H	0.33202014	0.23771891	-0.1308025	0.80829136	(NA) Family Rhodobacteraceae
b_treat_1M	-0.0135383	0.24454647	-0.4867441	0.47245058	(NA) Family Rhodobacteraceae
phi	28.5926966	6.52044737	17.2359777	41.8261038	(NA) Family Rhodobacteraceae
b_Intercept	-2.3946089	0.17367216	-2.7338739	-2.0641526	Acrophormium PCC-7375
b_treat_1H	0.24706572	0.24729125	-0.2552424	0.73124672	Acrophormium PCC-7375
b_treat_1M	0.10520154	0.2323917	-0.3545237	0.55436246	Acrophormium PCC-7375
phi	26.4398615	6.38677517	15.2814952	39.9227401	Acrophormium PCC-7375
zi	0.3023523	0.0594243	0.19488505	0.43119514	Acrophormium PCC-7375
b_Intercept	-2.554252	0.19732184	-2.9596262	-2.1647009	Ruegeria
b_treat_1H	0.27159652	0.27275566	-0.2577963	0.82234072	Ruegeria
b_treat_1M	-0.0249089	0.27729521	-0.5871282	0.53384233	Ruegeria
phi	43.8735953	13.1043404	22.5622245	72.0518977	Ruegeria
zi	0.53305808	0.06857085	0.40228429	0.67050508	Ruegeria
b_Intercept	-2.3633924	0.25967038	-2.9103894	-1.8684779	Mastigocoleus BC008
b_treat_1H	0.46103861	0.31272223	-0.1307592	1.0977651	Mastigocoleus BC008
b_treat_1M	0.19389488	0.3693873	-0.5544651	0.91626647	Mastigocoleus BC008
phi	27.834656	9.00123357	13.4504285	48.1542757	Mastigocoleus BC008
zi	0.58838387	0.06611895	0.45718707	0.71224723	Mastigocoleus BC008
b_Intercept	-1.9942908	0.15848603	-2.3100436	-1.6839518	Phormidium MBIC10003
b_treat_1H	-0.70226	0.3230689	-1.3520415	-0.1019215	Phormidium MBIC10003

b_treat_1M	-0.6839979	0.25352225	-1.1831356	-0.1810893	Phormidium MBIC10003
phi	45.5827059	14.5253949	21.8020566	78.3542343	Phormidium MBIC10003
zi	0.57096928	0.0656638	0.43983205	0.69626486	Phormidium MBIC10003
b_Intercept	-2.3377584	0.22009911	-2.7848804	-1.9254685	Pelagibius
b_treat_1H	0.03180608	0.29278081	-0.5517577	0.5800625	Pelagibius
b_treat_1M	0.02652744	0.29308023	-0.5425428	0.62480235	Pelagibius
phi	26.2327473	7.13131778	14.475612	41.6982004	Pelagibius
zi	0.44564848	0.06620686	0.31579344	0.58220239	Pelagibius

Table A.S 21 Results from the posterior distribution of difference as the outcome for each model and bacterial family

Genus	Contrast	max	min	mean	
uncultured	A-M	0.1697927	-0.2054919	-0.012042	No difference
uncultured	A-H	0.16483746	-0.1860837	-0.0080117	No difference
uncultured	M-H	0.1588759	-0.1561329	0.00357178	No difference
Defluviicoccus	A-M	0.15655741	-0.1602827	2.82E-05	No difference
Defluviicoccus	A-H	0.1184096	-0.1614726	-0.0115847	No difference
Defluviicoccus	M-H	0.11939915	-0.1687856	-0.0118043	No difference
(NA) Family Rhodobacteraceae	A-M	0.15443424	-0.1633776	-0.0039514	No difference
(NA) Family Rhodobacteraceae	A-H	0.18715105	-0.1296386	0.02803701	No difference
(NA) Family Rhodobacteraceae	M-H	0.19300996	-0.1333987	0.02835042	No difference
Acrophormium PCC-7375	A-M	0.19170105	-0.1652087	0.00694261	No difference
Acrophormium PCC-7375	A-H	0.20040232	-0.1727703	0.01443275	No difference
Acrophormium PCC-7375	M-H	0.20622864	-0.1972812	0.00791484	No difference
Ruegeria	A-M	0.12856236	-0.1307155	0.00076644	No difference
Ruegeria	A-H	0.16509217	-0.1275449	0.01099811	No difference

Ruegeria	M-H	0.16213049	-0.1368424	0.00816362	No difference
Mastigocoleus BC008	A-M	0.19459633	-0.1822403	0.00340007	No difference
Mastigocoleus BC008	A-H	0.24994057	-0.1679752	0.01926523	No difference
Mastigocoleus BC008	M-H	0.23784407	-0.1945877	0.01325385	No difference
Phormidium MBIC10003	A-M	0.11953114	-0.2001059	-0.0253083	No difference
Phormidium MBIC10003	A-H	0.12133438	-0.1998642	-0.0238416	No difference
Phormidium MBIC10003	M-H	0.12362247	-0.1225092	-0.0010041	No difference
Pelagibius	A-M	0.17853632	-0.1883231	-0.0020965	No difference
Pelagibius	A-H	0.18661005	-0.1794939	0.00123899	No difference
Pelagibius	M-H	0.18247251	-0.1871695	-0.0016016	No difference

DeSeq2 Analysis of non-rarefied dataset (Bacteria)

Analysis of the non-rarefied dataset revealed that the presence and abundance of bacterial families and genera varied among treatments (Tables A.S20- A.S22). For example, when comparing mid and ambient treatments (Fig. A.S9a, Table A.S20), the family Rhodobacteraceae was abundant in both treatments, but had higher relative abundance in samples from the mid treatment. Similarly, both genera in the family Phormidesmiaceae were more abundant in the mid treatment than under ambient conditions. When comparing samples from the high and ambient treatments, the majority of families were significantly more abundant in high than in ambient (Fig. A.S9b, Table A.S21). Rhodobacteraceae were abundant in both treatments but due to differentially abundant genera, with Phormidesmiaceae being more abundant in samples from the high treatment.

A greater number of bacterial families were found to have significantly different abundances between the mid and high treatments (Fig. A.S9c, Table A.S22). With the exception of Xenococcaceae and Nodosilineaceae, the majority of bacterial families had a higher abundance in the high treatment compared

to the mid treatment. Similar to other treatment comparisons, Rhodobacteraceae was the most diverse family represented by several genera, although all of them were more abundant in high. Thus, the analysis of the relative abundances using a non-rarefied dataset of bacterial communities revealed how bacterial families can be differentially abundant depending on treatment, and also that the magnitude within members of the same family can be different at the genus level.

Figure A.S 8 DESeq2 estimates of differentially abundant bacterial families in 6-week old coral recruits, comparing mid:ambient (panel a), high:ambient (panel b) and mid:high (panel c). For each panel, values and magnitude of log2FoldChange favour abundance of a family in the first treatment (negative) or in the second treatment (positive); separated by dotted blue line. Colours represent genus from each particular family.

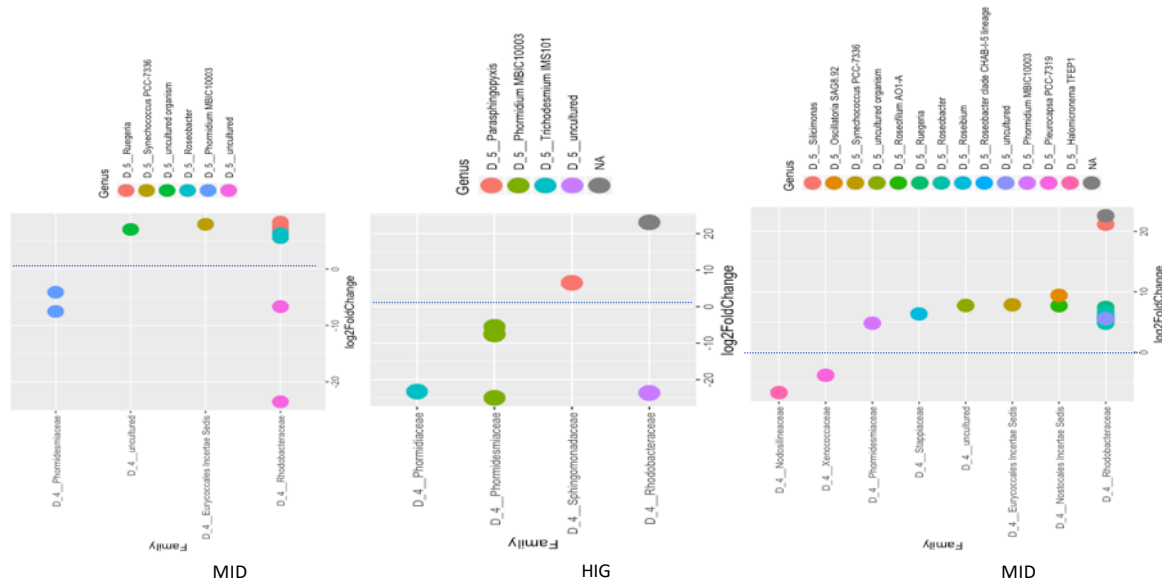


Table A.S 22 Estimates of differentially abundant bacteria (non-rarefied dataset) between mid and ambient treatments. Only significantly different taxa displayed. Log2FoldChange (x) values compare abundances found in mid as reference treatment compared to abundances found in ambient. Its value represents magnitude of difference (2^x), whereas its sign represents direction: negative favours reference treatment mid and positive favours ambient.

	base Mean	log2Fo ldChange	lfcSE	stat	pvalue	padj	Kingdom	Phylum	Class	Order	Family	Genus	Species
a428e4b832c28d6e3158913467a41c74	14.1 1812 38	7.0227 7279	2.02 9960 29	3.45 9561 66	0.00 0541 06	0.01 8335 77	D_0_ _Bact eria	D_1__Ch loroflexi	D_2__Anae rolineae	D_3__Ard enticaten ales	D_4__uncultu red	D_5__uncult ured organism	D_6__
bff54a89c93a675e92427e5c87cd94b4	21.1 9769 55	7.9337 6426	2.16 4990 36	3.66 4572 55	0.00 0247 75	0.01 2594 06	D_0_ _Bact eria	D_1__Cy anobacte ria	D_2__Oxyp hotobacteri a	D_3__Eur yococales	D_4__Eurycoc cales Incertae Sedis	D_5__Synech ococcus PCC- 7336	D_6__uncultured bacterium
f46439a03402e4acdc145c21993fc569	17.6 6666 04	- 4.1092 163	1.30 8505 32	3.14 0389 5	0.00 1687 23	0.04 6782 39	D_0_ _Bact eria	D_1__Cy anobacte ria	D_2__Oxyp hotobacteri a	D_3__Pho rmidesmi ales	D_4__Phormi desmiaceae	D_5__Phormi dium MBIC10003	D_6__uncultured bacterium
4757954099b61da7bb805149c2c871ce	17.9 2778 18	- 7.5217 847	2.16 2559 06	- 3.47 8187	0.00 0504 82	0.01 8335 77	D_0_ _Bact eria	D_1__Cy anobacte ria	D_2__Oxyp hotobacteri a	D_3__Pho rmidesmi ales	D_4__Phormi desmiaceae	D_5__Phormi dium MBIC10003	D_6__uncultured bacterium
8841fca1a05232be8450c8f460dca05	10.6 4960 97	6.9410 6308	1.95 1433 93	3.55 6903 97	0.00 0375 25	0.01 6350 23	D_0_ _Bact eria	D_1__Pr oteobact eria	D_2__Alph aproteobac teria	D_3__Rh odobacter ales	D_4__Rhodob acteraceae	D_5__Rueger ia	Ambiguous_taxa
b2353d08f7956a594b453a69bb9545b0	27.8 8272 89	8.3294 7947	1.38 1637 66	6.02 8700 34	1.65 E-09	2.52 E-07	D_0_ _Bact eria	D_1__Pr oteobact eria	D_2__Alph aproteobac teria	D_3__Rh odobacter ales	D_4__Rhodob acteraceae	D_5__Rueger ia	Ambiguous_taxa
da6716ea2e55536112ca1ad676ea568c	11.0 1365 68	- 6.6550 484	2.01 4748 99	- 3.30 3165	0.00 0956	0.02 9158 03	D_0_ _Bact eria	D_1__Pr oteobact eria	D_2__Alph aproteobac teria	D_3__Rh odobacter ales	D_4__Rhodob acteraceae	D_5__uncult ured	NA
9bc18f2b3516626e3071b519c4e43de6	12.0 3436 11	- 23.541 864	2.65 5696 22	8.86 4667 7	7.67 E-19	2.34 E-16	D_0_ _Bact eria	D_1__Pr oteobact eria	D_2__Alph aproteobac teria	D_3__Rh odobacter ales	D_4__Rhodob acteraceae	D_5__uncult ured	D_6__uncultured alpha proteobacterium

7093b740c64465d776e3ea0137de5424	15.5 9536 86	7.4913 6004	1.48 8796 4	5.03 1823 05	4.86 E-07	4.94 E-05	D_0_ _Bact eria	D_1__Pr oteobact eria	D_2__Alph aproteobac teria	D_3__Rh odobacter ales	D_4__Rhodob acteraceae	D_5__Rueger ia	NA
c242722c38216dc4e39f2dc0d84c95aa	11.9 4227 72	6.2921 4854	1.27 7060 96	4.92 7054 19	8.35 E-07	6.37 E-05	D_0_ _Bact eria	D_1__Pr oteobact eria	D_2__Alph aproteobac teria	D_3__Rh odobacter ales	D_4__Rhodob acteraceae	D_5__Roseob acter	NA
40d711e110b3dfe95b6d4009f93239d2	30.8 3893 52	5.5718 3492	1.15 5009 35	4.82 4060 46	1.41 E-06	8.58 E-05	D_0_ _Bact eria	D_1__Pr oteobact eria	D_2__Alph aproteobac teria	D_3__Rh odobacter ales	D_4__Rhodob acteraceae	D_5__Roseob acter	NA

Table A.S 23 Estimates of differentially abundant bacteria (non-rarefied dataset) between high and ambient treatments. Only significantly different taxa displayed. Log2FoldChange (x) values compare abundances found in high as reference treatment compared to abundances found in ambient. Its value represents magnitude of difference (2^x), whereas its sign represents direction: negative favours reference treatment high and positive favours ambient.

	base Mean	log2Fo ldChan ge	lfcSE	stat	pval ue	padj	Kingd om	Phylum	Class	Order	Family	Genus	Species
12f2c42b1bce548bab1b110036af1cb5	9.33 1387 17	- 23.271 711	2.92 6232 75	- 7.95 2788 9	1.82 E-15	1.15 E-13	D_0_ _Bacter ia	D_1__Cy anobacte ria	D_2__Oxyp hotobacteri a	D_3__Nost ocales	D_4__Phor midiaceae	D_5__Tricho desmium IMS101	D_6__uncultured bacterium
249b0a49e3694231fa2e17d19fa3ebb8	90.1 9099 21	- 5.5354 582	1.32 9174 79	- 4.16 4582 6	3.12 E-05	0.00 1310 08	D_0_ _Bacter ia	D_1__Cy anobacte ria	D_2__Oxyp hotobacteri a	D_3__Phor midesmial es	D_4__Phor midesmiace ae	D_5__Phormi dium MBIC10003	D_6__uncultured bacterium
b3b7a3da523a01897f03ce8073c8101d	33.0 2944 04	- 24.979 975	2.92 5462 87	- 8.53 8811	1.36 E-17	1.14 E-15	D_0_ _Bacter ia	D_1__Cy anobacte ria	D_2__Oxyp hotobacteri a	D_3__Phor midesmial es	D_4__Phor midesmiace ae	D_5__Phormi dium MBIC10003	D_6__uncultured bacterium
f46439a03402e4acdc145c21993fc569	17.3 2479 25	- 7.5374 967	1.32 6167 12	- 5.68 3670 3	1.32 E-08	6.64 E-07	D_0_ _Bacter ia	D_1__Cy anobacte ria	D_2__Oxyp hotobacteri a	D_3__Phor midesmial es	D_4__Phor midesmiace ae	D_5__Phormi dium MBIC10003	D_6__uncultured bacterium

4757954099b61da7bb805149c2c871ce	17.8 3866 03	- 7.5789 314	2.18 0701 93	- 3.47 5455	0.00 0509 99	0.01 8359 55	D_0__Bacteria	D_1__Cyanobacteria	D_2__Oxyphotobacteria	D_3__Phor midesmiales	D_4__Phor midesmiaceae	D_5__Phormidium MBIC10003	D_6__uncultured bacterium
9bc18f2b3516626e3071b519c4e43de6	12.4 1276 24	- 23.653 351	2.68 7121 19	8.80 2487 6	1.34 E-18	3.37 E-16	D_0__Bacteria	D_1__Proteobacteria	D_2__Alphaproteobacteria	D_3__Rhodobacterales	D_4__Rhodobacteraceae	D_5__uncultured	D_6__uncultured alpha proteobacterium
07cbe0c6eb1e9f6bdc20bbb5f630a1b5	14.2 2043 45	23.088 7642	2.69 8592 59	8.55 5854 02	1.17 E-17	1.14 E-15	D_0__Bacteria	D_1__Proteobacteria	D_2__Alphaproteobacteria	D_3__Rhodobacterales	D_4__Rhodobacteraceae	NA	NA
9dca105210d57265c2465fd5b3e87dce	8.23 4578 92	6.5046 4324	1.97 8074 09	3.28 8371 89	0.00 1007 69	0.03 1742 12	D_0__Bacteria	D_1__Proteobacteria	D_2__Alphaproteobacteria	D_3__Sphingomonadales	D_4__Sphingomonadaceae	D_5__Parasphingopyxis	D_6__uncultured bacterium

Table A.S 24 Estimates of differentially abundant bacteria (non-rarefied dataset) between mid and high treatments. Only significantly different taxa displayed. Log2FoldChange (x) values compare abundances found in mid as reference treatment compared to abundances found in high. Its value represents magnitude of difference (2^x), whereas its sign represents direction: negative favours reference treatment mid and positive favours high.

	base Mean	log2Fo ldChange	lfcSE	stat	pvalue	padj	Kingdom	Phylum	Class	Order	Family	Genus	Species
bff54a89c93a675e92427e5c87cd94b4	20.7 2533 17	7.8618 8946	2.16 3014 61	3.63 4690 87	0.00 0278 31	0.00 9240 03	D_0__Bacteria	D_1__Cyanobacteria	D_2__Oxyphotobacteria	D_3__Eurycoccales	D_4__Eurycoccales Incertae Sedis	D_5__Synechococcus PCC-7336	D_6__uncultured bacterium
fb14348fda73f4a2a3bb0121066d5afc	24.3 1920 61	- 3.8009 647	1.22 7063 9	3.09 7609 4	0.00 1950 88	0.04 0480 83	D_0__Bacteria	D_1__Cyanobacteria	D_2__Oxyphotobacteria	D_3__Nostocales	D_4__Xenococcaceae	D_5__Pleurocapsa PCC-7319	NA
249b0a49e3694231fa2e17d19fa3ebb8	55.1 3331 49	4.8177 2769	1.51 1261 85	3.18 7884 13	0.00 1433 18	0.03 2805 17	D_0__Bacteria	D_1__Cyanobacteria	D_2__Oxyphotobacteria	D_3__Phormidiales	D_4__Phormidiales	D_5__Phormidium MBIC10003	D_6__uncultured bacterium

25d6e17e4bb69 8698a71b63bc4 587903	45.7 5374 24	7.7158 6289	1.57 3973 74	4.90 2154 79	9.48 E-07	6.29 E-05	D_0_ _Bact eria	D_1__Cy anobact eria	D_2__Oxy photobact eria	D_3__No stocales	D_4__Nostoc ales Incertae Sedis	D_5__Roseofilum AO1-A	D_6__unculture d cyanobacterium
163fbcc0e43cbb 461052525d416 5fc6f	60.7 4453 2	9.4132 2995	1.61 4324 78	5.83 1063 3	5.51 E-09	6.09 E-07	D_0_ _Bact eria	D_1__Cy anobact eria	D_2__Oxy photobact eria	D_3__No stocales	D_4__Nostoc ales Incertae Sedis	D_5__Oscillatoria SAG8.92	D_6__unculture d Oscillatoria sp.
0328eab0cbcec2 4bac862f03d34a 1c25	5.53 3241 02	5.9566 8503	1.93 5773 88	3.07 7159 53	0.00 2089 83	0.04 0813 23	D_0_ _Bact eria	D_1__Pr oteobact eria	D_2__Alph aproteoba acteria	D_3__Rh odobacte rales	D_4__Rhodob acteraceae	D_5__Roseobact er clade CHAB-I-5 lineage	NA
abba7ccc04f75b 3621f805d7551 aa882	7.28 3288 14	6.3532 9587	2.11 0997 59	3.00 9617 78	0.00 2615 77	0.04 5707 08	D_0_ _Bact eria	D_1__Pr oteobact eria	D_2__Alph aproteoba acteria	D_3__Rhi zobiales	D_4__Stappia ceae	D_5__Roseibium	Ambiguous_taxa
3634f35743b1cc f52a4b86ba4ddf a215	3.32 8796 21	5.0529 1756	1.67 8544 01	3.01 0297 93	0.00 2609 92	0.04 5707 08	D_0_ _Bact eria	D_1__Pr oteobact eria	D_2__Alph aproteoba acteria	D_3__Rh odobacte rales	D_4__Rhodob acteraceae	D_5__uncultured	D_6__unculture d alpha proteobacterium
2d091d4d9af44f 88c91386d590b 1f010	13.3 5156 55	21.187 3988	2.64 6299 64	8.00 6424 69	1.18 E-15	1.96 E-13	D_0_ _Bact eria	D_1__Pr oteobact eria	D_2__Alph aproteoba acteria	D_3__Rh odobacte rales	D_4__Rhodob acteraceae	D_5__Silicimonas	D_6__unculture d bacterium
74ebf22ad382d 244752f652937 d2821a	9.76 5640 52	22.587 9847	2.62 4309 98	8.60 7209 08	7.49 E-18	2.49 E-15	D_0_ _Bact eria	D_1__Pr oteobact eria	D_2__Alph aproteoba acteria	D_3__Rh odobacte rales	D_4__Rhodob acteraceae	NA	NA
d4b8fd70133c6 8f72e85d30147 4685de	163. 6124 1	5.3511 5952	1.26 1067 05	4.24 3358 45	2.20 E-05	0.00 0953 82	D_0_ _Bact eria	D_1__Pr oteobact eria	D_2__Alph aproteoba acteria	D_3__Rh odobacte rales	D_4__Rhodob acteraceae	D_5__uncultured	D_6__unculture d alpha proteobacterium
7093b740c6446 5d776e3ea0137 de5424	15.4 1796 48	7.4354 1035	1.48 9858 47	4.99 0682 35	6.02 E-07	4.99 E-05	D_0_ _Bact eria	D_1__Pr oteobact eria	D_2__Alph aproteoba acteria	D_3__Rh odobacte rales	D_4__Rhodob acteraceae	D_5__Ruegeria	NA
c242722c38216 d4ae39f2dc0d84 c95aa	11.8 0414 44	5.6820 0014	1.31 6847 29	4.31 4851 22	1.60 E-05	0.00 0883 73	D_0_ _Bact eria	D_1__Pr oteobact eria	D_2__Alph aproteoba acteria	D_3__Rh odobacte rales	D_4__Rhodob acteraceae	D_5__Roseobact er	NA
40d711e110b3d fe95b6d4009f93 239d2	30.2 3608 93	4.7992 8696	1.13 3580 6	4.23 3741 27	2.30 E-05	0.00 0953 82	D_0_ _Bact eria	D_1__Pr oteobact eria	D_2__Alph aproteoba acteria	D_3__Rh odobacte rales	D_4__Rhodob acteraceae	D_5__Roseobact er	NA
5411aa5545987 ab86d2a951b86 938168	6.92 6975 33	6.2816 0367	1.78 7007 99	3.51 5151 41	0.00 0439 5	0.01 2159 59	D_0_ _Bact eria	D_1__Pr oteobact eria	D_2__Alph aproteoba acteria	D_3__Rh odobacte rales	D_4__Rhodob acteraceae	D_5__Roseobact er	NA

5d274c4209cbd 92728e136f4d6 a4eb30	9.90 3092 27	6.7968 2246	1.80 5939 95	3.76 3592 73	0.00 0167 49	0.00 6178 5	D_0_ _Bact eria	D_1__Pr oteobact eria	D_2__Alph aproteoba acteria	D_3__Rh odobacte rales	D_4__Rhodob acteraceae	D_5__Roseobact er	NA
63c82afa242d9b ebab04b757c9c 7cf4f	4.22 5362 1	5.5689 23	1.75 2250 97	3.17 8153 75	0.00 1482 16	0.03 2805 17	D_0_ _Bact eria	D_1__Pr oteobact eria	D_2__Alph aproteoba acteria	D_3__Rh odobacte rales	D_4__Rhodob acteraceae	D_5__uncultured	NA
110462cb19a30 7f6ecea87c867b ae0fb	19.0 5202 15	7.7402 9422	2.16 3086 14	3.57 8356 9	0.00 0345 76	0.01 0435 7	D_0_ _Bact eria	D_1__Pr oteobact eria	D_2__Alph aproteoba acteria	D_3__Tha lassobacu lales	D_4__uncultu red	D_5__uncultured organism	D_6__
758721da7294b 3d3c834d38ff3d 3fa79	9.67 0989 83	- 6.6704 959	1.97 4396 11	3.37 8499 3	0.00 0728 83	0.01 8613 1	D_0_ _Bact eria	D_1__Cy anobact eria	D_2__Oxy photobact eria	D_3__Ph ormidesm iales	D_4__Nodosil ineaceae	D_5__Halomicro nema TFEP1	D_6__unculture d cyanobacterium

Appendix B – Chapter 3

B.1 Coral recruits: settlement success

Table B.S 1 List of statistical models used to predict variation in settlement success across treatments at t=0 weeks. The shaded area indicates the best-fit model.

Model	Fixed effect	Random effect	AICc	Akaike weights
1	Treatment (t=0 weeks)	Tank (intercept)	-15.398	0.269
2	Treatment (t=0 weeks)	NA	-17.398	0.731

Table B.S 2 Coefficients of the generalised linear mixed effect model predicting the number of recruits settling among treatments.

	Estimate	Std. Error	t-value	p-value
Intercept (AMBIENT)	5.9328	0.0491	120.86	<0.001
Treatment-MID	0.0490	0.0694	0.71	0.48
Treatment-HIGH	0.3620	0.0694	5.21	<0.001

Table B.S 3 Tukey Posthoc Test estimates of pairwise comparisons among treatments for settlement.

	Estimate	Std. Error	z value	Pr(> z)
AMBIENT - MID	0.952	0.0690	-0.676	0.7791
AMBIENT - HIGH	0.696	0.0505	-4.993	<0.001
MID - HIGH	0.731	0.0530	-4.317	<0.001

B.2 Coral recruits: survival

Table B.S 4 List of statistical models used to predict survival of coral recruits relative to the exposure to treatment at t=8 weeks. The shaded area indicates the best-fit model.

Model	Fixed effect	Random effect	AICc	Akaike weights
1	Treatment (8 weeks)	Tank (intercept)	14214.36	>0.99
2	Treatment (8 weeks)	NA	14549.76	<0.01

Table B.S 5 Coefficients of the generalised linear mixed effect model predicting the survival rate of number of recruits among treatments at t=8 weeks. Number of observations: total=10689, tank=36.

	Estimate	Std. Error	t-value	p-value
Intercept (AMBIENT)	0.4100	0.1257	3.26	<0.001
Treatment-MID	-0.4470	0.1773	-2.52	0.0117
Treatment-HIGH	-0.0792	0.1760	-0.45	0.6529

Random effect variance(s):

Tank → Variance 0.171, StdDev 0.4136

Table B.S 6 Tukey Posthoc Test estimates of pairwise comparisons among treatments for survival at t=8 weeks; confidence level used: 0.95

	Estimate	Std. Error	z value	Pr(> z)
AMBIENT - MID	0.1058	0.0442	2.397	0.0436 (<0.05)
AMBIENT - HIGH	0.0180	0.0438	0.410	0.9116
MID - HIGH	-0.0879	0.0438	-2.007	0.1105

Table B.S 7 List of statistical models used to predict survival of coral recruits relative to the exposure to treatment at t=16 weeks. The shaded area indicates the best-fit model.

Model	Fixed effect	Random effect	AICc	Akaike weights
1	Treatment (8 weeks) * treatment (16 weeks)	Tank (intercept)	12601.36	>0.99
2	Treatment (8 weeks) * Treatment (16 weeks)	NA	13074.98	<0.01

Table B.S 8 Coefficients of the generalised linear mixed effect model predicting the survival rate of number of recruits among treatments at t=16 weeks.

Number of observations: total=10689, tank=36.

	Estimate	Std. Error	z value	Pr(> z)
(Intercept) Treatment-AMB (8 weeks)	-0.386	0.277	-1.40	0.1630
Treatment-MID (8 weeks)	-0.934	0.393	-2.38	0.0173
Treatment-HIGH (8 weeks)	-0.265	0.390	-0.68	0.4974
Treatment-MID (16 weeks)	-1.159	0.397	-2.92	<0.001
Treatment-HIGH (16 weeks)	-0.374	0.392	-0.95	0.3410
treat_1Mid:treat_2Mid	1.140	0.560	2.03	0.0419
treat_1High:treat_2Mid	1.450	0.555	2.61	0.0090
treat_1Mid:treat_2High	0.591	0.556	1.06	0.2879
treat_1High:treat_2High	0.173	0.552	0.31	0.7546

Random effect variance(s):

Tank → Variance 0.2879, StdDev 0.5366

Table B.S 9 Tukey Posthoc Test estimates of pairwise comparisons among treatments for survival at t=16 weeks; confidence level used: 0.95

contrast	estimate	SE	df	z.ratio	p.value
Ambient-Ambient – Mid-Ambient	0.194644	0.0897	Inf	2.170	0.4258
Ambient-Ambient – High-Ambient	0.055016	0.0895	Inf	0.615	0.9995
Ambient-Ambient – Ambient-Mid	0.221503	0.0900	Inf	2.460	0.2518
Ambient-Ambient – Mid-Mid	0.195627	0.0899	Inf	2.175	0.4220
Ambient-Ambient – High-Mid	-0.005233	0.0894	Inf	-0.059	1.0000
Ambient-Ambient – Ambient-High	0.069301	0.0897	Inf	0.772	0.9976
Ambient-Ambient – Mid-High	0.154483	0.0899	Inf	1.718	0.7356
Ambient-Ambient – High-High	0.090804	0.0894	Inf	1.015	0.9846
Mid-Ambient – High-Ambient	-0.139627	0.0893	Inf	-1.564	0.8244
Mid-Ambient – Ambient-Mid	0.026859	0.0898	Inf	0.299	1.0000
Mid-Ambient – Mid-Mid	0.000983	0.0897	Inf	0.011	1.0000
Mid-Ambient – High-Mid	-0.199876	0.0892	Inf	-2.241	0.3787
Mid-Ambient – Ambient-High	-0.125343	0.0895	Inf	-1.400	0.8983
Mid-Ambient – Mid-High	-0.040160	0.0897	Inf	-0.448	1.0000
Mid-Ambient – High-High	-0.103840	0.0892	Inf	-1.164	0.9640
High-Ambient – Ambient-Mid	0.166486	0.0896	Inf	1.858	0.6429
High-Ambient – Mid-Mid	0.140610	0.0895	Inf	1.571	0.8207
High-Ambient – High-Mid	-0.060249	0.0889	Inf	-0.677	0.9991
High-Ambient – Ambient-High	0.014284	0.0893	Inf	0.160	1.0000
High-Ambient – Mid-High	0.099467	0.0895	Inf	1.112	0.9727
High-Ambient – High-High	0.035787	0.0890	Inf	0.402	1.0000
Ambient-Mid – Mid-Mid	-0.025876	0.0901	Inf	-0.287	1.0000
Ambient-Mid – High-Mid	-0.226735	0.0895	Inf	2.533	0.2160
Ambient-Mid – Ambient-High	-0.152202	0.0899	Inf	-1.694	0.7507
Ambient-Mid – Mid-High	-0.067019	0.0900	Inf	-0.744	0.9981
Ambient-Mid – High-High	-0.130699	0.0896	Inf	-1.459	0.8744
Mid-Mid – High-Mid	-0.200859	0.0894	Inf	-2.247	0.3751
Mid-Mid – Ambient-High	-0.126326	0.0898	Inf	-1.408	0.8954
Mid-Mid – Mid-High	-0.041143	0.0899	Inf	-0.457	1.0000

Mid-Mid – High-High	-0.104823	0.0895	Inf	-1.172	0.9625
High-Mid – Ambient-High	0.074533	0.0892	Inf	0.836	0.9958
High-Mid – Mid-High	0.159716	0.0894	Inf	1.787	0.6911
High-Mid – High-High	0.096036	0.0889	Inf	1.080	0.9771
Ambient-High – Mid-High	0.085183	0.0897	Inf	0.949	0.9900
Ambient-High – High-High	0.021503	0.0893	Inf	0.241	1.0000
Mid-High – High-High	-0.063680	0.0895	Inf	-0.712	0.9986

Table B.S 10 List of statistical models used to predict survival of coral recruits relative to the exposure to treatment at t=18 weeks. The shaded area indicates the best-fit model.

Model	Fixed effect	Random effect	AICc	Akaike weights
1	Treatment (8 weeks) * treatment (16 weeks)	Tank (intercept)	12083.76	>0.99
2	Treatment (8 weeks) * Treatment (16 weeks)	NA	12144.88	<0.01

Table B.S 11 Coefficients of the generalised linear mixed effect model predicting the survival rate of number of recruits among treatments at t=18 weeks.

Number of observations: total=10689, tank=36.

	Estimate	Std. Error	z value	Pr(> z)
(Intercept) Treatment-AMB (8,16 weeks)	-0.7060	0.1081	-6.53	<0.001
Treatment-MID (8 weeks)	-0.9547	0.1052	-9.07	<0.001
Treatment-HIGH (8 weeks)	-0.2293	0.0906	-2.53	0.0114
Treatment-MID (16 weeks)	-1.0327	0.1667	-6.20	<0.001
Treatment-HIGH (16 weeks)	-0.0456	0.1503	-0.30	0.7617
treat_1Mid:treat_2Mid	1.1979	0.1662	7.21	<0.001
treat_1High:treat_2Mid	1.3735	0.1420	9.67	<0.001
treat_1Mid:treat_2High	0.4140	0.1463	2.83	0.0047
treat_1High:treat_2High	0.1002	0.1246	0.80	0.4214

Random effect variance(s):

Tank → Variance 0.20542, StdDev 0.52328

Table B.S 12 Tukey Posthoc Test estimates of pairwise comparisons among treatments for survival at t=18 weeks; confidence level used: 0.95

contrast	estimate	SE	df	z.ratio	p.value
Ambient-Ambient – Mid-Ambient	0.1722	0.0190	Inf	9.042	<.0001
Ambient-Ambient – High-Ambient	0.0482	0.0181	Inf	2.657	0.1634
Ambient-Ambient – Ambient-Mid	0.1832	0.0379	Inf	4.829	<.0001
Ambient-Ambient – Mid-Mid	0.1493	0.0377	Inf	3.964	0.0024
Ambient-Ambient – High-Mid	-0.0224	0.0364	Inf	-0.613	0.9995
Ambient-Ambient – Ambient-High	0.0123	0.0372	Inf	0.330	1.0000
Ambient-Ambient – Mid-High	0.1174	0.0376	Inf	3.122	0.0470
Ambient-Ambient – High-High	0.0395	0.0366	Inf	1.078	0.9774
Mid-Ambient – High-Ambient	-0.1241	0.0170	Inf	-7.290	<.0001
Mid-Ambient – Ambient-Mid	0.0110	0.0374	Inf	0.293	1.0000
Mid-Ambient – Mid-Mid	-0.0230	0.0372	Inf	-0.618	0.9995
Mid-Ambient – High-Mid	-0.1946	0.0359	Inf	-5.417	<.0001
Mid-Ambient – Ambient-High	-0.1600	0.0367	Inf	-4.361	0.0004
Mid-Ambient – Mid-High	-0.0548	0.0371	Inf	-1.478	0.8660
Mid-Ambient – High-High	-0.1328	0.0361	Inf	-3.681	0.0072
High-Ambient – Ambient-Mid	0.1351	0.0369	Inf	3.655	0.0079
High-Ambient – Mid-Mid	0.1011	0.0367	Inf	2.758	0.1281
High-Ambient – High-Mid	-0.0705	0.0354	Inf	-1.991	0.5495
High-Ambient – Ambient-High	-0.0359	0.0362	Inf	-0.992	0.9867
High-Ambient – Mid-High	0.0693	0.0366	Inf	1.892	0.6194
High-Ambient – High-High	-0.0087	0.0356	Inf	-0.245	1.0000
Ambient-Mid – Mid-Mid	-0.0339	0.0207	Inf	-1.640	0.7826
Ambient-Mid – High-Mid	-0.2056	0.0184	Inf	-11.177	<.0001

Ambient-Mid – Ambient-High	-0.1710	0.0375	Inf	-4.559	0.0002
Ambient-Mid – Mid-High	-0.0658	0.0379	Inf	-1.736	0.7240
Ambient-Mid – High-High	-0.1438	0.0369	Inf	-3.896	0.0031
Mid-Mid – High-Mid	-0.1716	0.0178	Inf	-9.632	<.0001
Mid-Mid – Ambient-High	-0.1370	0.0372	Inf	-3.681	0.0072
Mid-Mid – Mid-High	-0.0319	0.0376	Inf	-0.847	0.9954
Mid-Mid – High-High	-0.1098	0.0366	Inf	-2.999	0.0674
High-Mid – Ambient-High	0.0346	0.0360	Inf	0.962	0.9891
High-Mid – Mid-High	0.1398	0.0364	Inf	3.839	0.0039
High-Mid – High-High	0.0618	0.0354	Inf	1.748	0.7165
Ambient-High – Mid-High	0.1052	0.0192	Inf	5.473	<.0001
Ambient-High – High-High	0.0272	0.0171	Inf	1.586	0.8126
Mid-High – High-High	-0.0779	0.0179	Inf	-4.344	0.0005

Table B.S 13 List of statistical models used to predict survival of coral recruits relative to the exposure to treatment at t=23 weeks. The shaded area indicates the best-fit model.

Model	Fixed effect	Random effect	AICc	Akaike weights
1	Treatment (8 weeks) * treatment (16 weeks) * treatment (23 weeks)	Tank (intercept)	10030.98	0.974
2	Treatment (8 weeks) * Treatment (16 weeks) * treatment (23 weeks)	NA	10038.20	0.026

Table B.S 14 Coefficients of the generalised linear mixed effect model predicting the survival rate of number of recruits among treatments at t=23 weeks.

Number of observations: total=10689, tank=24.

	Estimate	Std. Error	z value	Pr(> z)
(Intercept) Treatment-AMB (8,16,23 weeks)	-1.2261	0.1278	-9.59	<0.01

Treatment-MID (8 weeks)	-0.8927	0.1714	-5.21	<0.01
Treatment-HIGH (8 weeks)	-0.3229	0.1449	-2.23	0.02585
Treatment-MID (16 weeks)	-0.8032	0.2120	-3.79	0.00015
Treatment-HIGH (16 weeks)	0.2028	0.1725	1.18	0.23967
treat_4Acute	-0.3916	0.1915	-2.05	0.04085
treat_1Mid:treat_2Mid	1.1853	0.2637	4.50	<0.01
treat_1High:treat_2Mid	1.5655	0.2252	6.95	<0.01
treat_1Mid:treat_2High	0.4254	0.2278	1.87	0.06190
treat_1High:treat_2High	0.0655	0.1927	0.34	0.73380
treat_1Mid:treat_4Acute	0.5422	0.2473	2.19	0.02831
treat_1High:treat_4Acute	-0.0217	0.2221	-0.10	0.92227
treat_2Mid:treat_4Acute	0.3844	0.3034	1.27	0.20508
treat_2High:treat_4Acute	0.1169	0.2558	0.46	0.64761
treat_1Mid:treat_2Mid:treat_4Acute	-0.7327	0.3796	-1.93	0.05362
treat_1High:treat_2Mid:treat_4Acute	-0.5702	0.3298	-1.73	0.08389
treat_1Mid:treat_2High:treat_4Acute	-0.4440	0.3325	-1.34	0.18169
treat_1High:treat_2High:treat_4Acute	0.2813	0.2910	0.97	0.33372

Random effect variance(s):

Tank → Variance 0.01794, StdDev 0.1339

Table B.S 15 Tukey Posthoc Test estimates of pairwise comparisons among treatments for survival at t=23 weeks; confidence level used: 0.95

Contrast (history)	estimate	SE	df	z.ratio	p.value
Ambient,Ambient,Ambient Mid,Ambient,Ambient	- 0.1205	0.0236	Inf	5.1167	0.0000
Ambient,Ambient,Ambient High,Ambient,Ambient	- 0.0515	0.0224	Inf	2.3047	0.6801
Ambient,Ambient,Ambient Ambient,Mid,Ambient	- 0.1107	0.0315	Inf	3.5107	0.0466

Ambient,Ambient,Ambient - Mid,Mid,Ambient	0.0765	0.0304	Inf	2.5138	0.5195
Ambient,Ambient,Ambient High,Mid,Ambient	-0.0855	0.0284	Inf	-3.0141	0.1931
Ambient,Ambient,Ambient Ambient,High,Ambient	-0.0366	0.0297	Inf	-1.2317	0.9991
Ambient,Ambient,Ambient Mid,High,Ambient	0.0442	0.0305	Inf	1.4499	0.9937
Ambient,Ambient,Ambient High,High,Ambient	0.0103	0.0284	Inf	0.3613	1.0000
Ambient,Ambient,Ambient Ambient,Ambient,Acute	0.0191	0.0308	Inf	0.6207	1.0000
Ambient,Ambient,Ambient Mid,Ambient,Acute	0.0617	0.0297	Inf	2.0797	0.8284
Ambient,Ambient,Ambient High,Ambient,Acute	0.0615	0.0288	Inf	2.1362	0.7951
Ambient,Ambient,Ambient Ambient,Mid,Acute	0.0689	0.0310	Inf	2.2196	0.7408
Ambient,Ambient,Ambient - Mid,Mid,Acute	0.0586	0.0311	Inf	1.8856	0.9176
Ambient,Ambient,Ambient - High,Mid,Acute	-0.0157	0.0284	Inf	-0.5544	1.0000
Ambient,Ambient,Ambient Ambient,High,Acute	-0.0298	0.0300	Inf	-0.9949	0.9999
Ambient,Ambient,Ambient - Mid,High,Acute	0.0263	0.0308	Inf	0.8536	1.0000
Ambient,Ambient,Ambient - High,High,Acute	-0.0304	0.0289	Inf	-1.0525	0.9999
Mid,Ambient,Ambient High,Ambient,Ambient	-0.0690	0.0212	Inf	-3.2483	0.1038
Mid,Ambient,Ambient - Ambient,Mid,Ambient	-0.0098	0.0307	Inf	-0.3205	1.0000
Mid,Ambient,Ambient - Mid,Mid,Ambient	-0.0440	0.0296	Inf	-1.4835	0.9918
Mid,Ambient,Ambient - High,Mid,Ambient	-0.2060	0.0275	Inf	-7.4940	0.0000
Mid,Ambient,Ambient Ambient,High,Ambient	-0.1571	0.0289	Inf	-5.4379	0.0000
Mid,Ambient,Ambient - Mid,High,Ambient	-0.0763	0.0297	Inf	-2.5697	0.4764

Mid,Ambient,Ambient - High,High,Ambient	-0.1102	0.0276	Inf	-4.0010	0.0079
Mid,Ambient,Ambient Ambient,Ambient,Acute	-0.1014	0.0300	Inf	-3.3738	0.0717
Mid,Ambient,Ambient - Mid,Ambient,Acute	-0.0588	0.0288	Inf	-2.0374	0.8512
Mid,Ambient,Ambient - High,Ambient,Acute	-0.0590	0.0279	Inf	-2.1158	0.8074
Mid,Ambient,Ambient - Ambient,Mid,Acute	-0.0516	0.0302	Inf	-1.7054	0.9660
Mid,Ambient,Ambient - Mid,Mid,Acute	-0.0619	0.0303	Inf	-2.0455	0.8470
Mid,Ambient,Ambient - High,Mid,Acute	-0.1362	0.0275	Inf	-4.9514	0.0001
Mid,Ambient,Ambient - Ambient,High,Acute	-0.1503	0.0291	Inf	-5.1586	0.0000
Mid,Ambient,Ambient - Mid,High,Acute	-0.0942	0.0300	Inf	-3.1459	0.1378
Mid,Ambient,Ambient - High,High,Acute	-0.1509	0.0281	Inf	-5.3793	0.0000
High,Ambient,Ambient Ambient,Mid,Ambient	0.0591	0.0298	Inf	1.9859	0.8765
High,Ambient,Ambient - Mid,Mid,Ambient	0.0250	0.0286	Inf	0.8733	1.0000
High,Ambient,Ambient - High,Mid,Ambient	-0.1370	0.0264	Inf	-5.1884	0.0000
High,Ambient,Ambient Ambient,High,Ambient	-0.0882	0.0279	Inf	-3.1629	0.1316
High,Ambient,Ambient - Mid,High,Ambient	-0.0073	0.0287	Inf	-0.2548	1.0000
High,Ambient,Ambient - High,High,Ambient	-0.0413	0.0265	Inf	-1.5584	0.9861
High,Ambient,Ambient Ambient,Ambient,Acute	-0.0324	0.0291	Inf	-1.1145	0.9998
High,Ambient,Ambient - Mid,Ambient,Acute	0.0102	0.0278	Inf	0.3666	1.0000
High,Ambient,Ambient - High,Ambient,Acute	0.0099	0.0268	Inf	0.3698	1.0000
High,Ambient,Ambient - Ambient,Mid,Acute	0.0174	0.0293	Inf	0.5938	1.0000
High,Ambient,Ambient - Mid,Mid,Acute	0.0071	0.0293	Inf	0.2407	1.0000
High,Ambient,Ambient - High,Mid,Acute	-0.0673	0.0264	Inf	-2.5444	0.4958
High,Ambient,Ambient - Ambient,High,Acute	-0.0814	0.0281	Inf	-2.8924	0.2566
High,Ambient,Ambient - Mid,High,Acute	-0.0253	0.0290	Inf	-0.8724	1.0000

High,Ambient,Ambient - High,High,Acute	-0.0820	0.0270	Inf	-3.0354	0.1832
Ambient,Mid,Ambient - Mid,Mid,Ambient	-0.0341	0.0257	Inf	-1.3256	0.9978
Ambient,Mid,Ambient - High,Mid,Ambient	-0.1962	0.0232	Inf	-8.4384	0.0000
Ambient,Mid,Ambient - Ambient,High,Ambient	-0.1473	0.0307	Inf	-4.7944	0.0002
Ambient,Mid,Ambient - Mid,High,Ambient	-0.0664	0.0315	Inf	-2.1114	0.8100
Ambient,Mid,Ambient - High,High,Ambient	-0.1004	0.0295	Inf	-3.4077	0.0646
Ambient,Mid,Ambient - Ambient,Ambient,Acute	-0.0915	0.0318	Inf	-2.8776	0.2651
Ambient,Mid,Ambient - Mid,Ambient,Acute	-0.0489	0.0307	Inf	-1.5950	0.9824
Ambient,Mid,Ambient - High,Ambient,Acute	-0.0492	0.0298	Inf	-1.6514	0.9751
Ambient,Mid,Ambient - Ambient,Mid,Acute	-0.0417	0.0320	Inf	-1.3045	0.9982
Ambient,Mid,Ambient - Mid,Mid,Acute	-0.0521	0.0320	Inf	-1.6264	0.9786
Ambient,Mid,Ambient - High,Mid,Acute	-0.1264	0.0294	Inf	-4.2955	0.0023
Ambient,Mid,Ambient - Ambient,High,Acute	-0.1405	0.0309	Inf	-4.5388	0.0008
Ambient,Mid,Ambient - Mid,High,Acute	-0.0844	0.0317	Inf	-2.6606	0.4084
Ambient,Mid,Ambient - High,High,Acute	-0.1411	0.0299	Inf	-4.7134	0.0003
Mid,Mid,Ambient - High,Mid,Ambient	-0.1621	0.0218	Inf	-7.4373	0.0000
Mid,Mid,Ambient - Ambient,High,Ambient	-0.1132	0.0296	Inf	-3.8206	0.0158
Mid,Mid,Ambient - Mid,High,Ambient	-0.0323	0.0304	Inf	-1.0635	0.9999
Mid,Mid,Ambient - High,High,Ambient	-0.0663	0.0283	Inf	-2.3409	0.6531
Mid,Mid,Ambient - Ambient,Ambient,Acute	-0.0574	0.0307	Inf	-1.8671	0.9240
Mid,Mid,Ambient - Mid,Ambient,Acute	-0.0148	0.0296	Inf	-0.5008	1.0000
Mid,Mid,Ambient - High,Ambient,Acute	-0.0151	0.0287	Inf	-0.5263	1.0000
Mid,Mid,Ambient - Ambient,Mid,Acute	-0.0076	0.0309	Inf	-0.2465	1.0000
Mid,Mid,Ambient - Mid,Mid,Acute	-0.0180	0.0310	Inf	-0.5799	1.0000
Mid,Mid,Ambient - High,Mid,Acute	-0.0923	0.0283	Inf	-3.2637	0.0994
Mid,Mid,Ambient - Ambient,High,Acute	-0.1064	0.0299	Inf	-3.5621	0.0393

Mid, Mid, Ambient - Mid, High, Acute	-0.0503	0.0307	Inf	-1.6402	0.9767
Mid, Mid, Ambient - High, High, Acute	-0.1070	0.0288	Inf	-3.7139	0.0233
High, Mid, Ambient - Ambient, High, Ambient	0.0489	0.0275	Inf	1.7793	0.9498
High, Mid, Ambient - Mid, High, Ambient	0.1297	0.0283	Inf	4.5831	0.0006
High, Mid, Ambient - High, High, Ambient	0.0958	0.0261	Inf	3.6753	0.0267
High, Mid, Ambient - Ambient, Ambient, Acute	0.1047	0.0287	Inf	3.6490	0.0292
High, Mid, Ambient - Mid, Ambient, Acute	0.1472	0.0274	Inf	5.3690	0.0000
High, Mid, Ambient - High, Ambient, Acute	0.1470	0.0264	Inf	5.5599	0.0000
High, Mid, Ambient - Ambient, Mid, Acute	0.1544	0.0289	Inf	5.3440	0.0000
High, Mid, Ambient - Mid, Mid, Acute	0.1441	0.0289	Inf	4.9827	0.0001
High, Mid, Ambient - High, Mid, Acute	0.0698	0.0260	Inf	2.6809	0.3938
High, Mid, Ambient - Ambient, High, Acute	0.0557	0.0277	Inf	2.0079	0.8660
High, Mid, Ambient - Mid, High, Acute	0.1118	0.0286	Inf	3.9091	0.0113
High, Mid, Ambient - High, High, Acute	0.0551	0.0266	Inf	2.0703	0.8336
Ambient, High, Ambient - Mid, High, Ambient	0.0808	0.0236	Inf	3.4230	0.0616
Ambient, High, Ambient - High, High, Ambient	0.0469	0.0209	Inf	2.2467	0.7220
Ambient, High, Ambient - Ambient, Ambient, Acute	0.0558	0.0300	Inf	1.8571	0.9273
Ambient, High, Ambient - Mid, Ambient, Acute	0.0984	0.0288	Inf	3.4113	0.0639
Ambient, High, Ambient - High, Ambient, Acute	0.0981	0.0279	Inf	3.5166	0.0457
Ambient, High, Ambient - Ambient, Mid, Acute	0.1055	0.0302	Inf	3.4904	0.0497
Ambient, High, Ambient - Mid, Mid, Acute	0.0952	0.0303	Inf	3.1466	0.1375
Ambient, High, Ambient - High, Mid, Acute	0.0209	0.0275	Inf	0.7591	1.0000
Ambient, High, Ambient - Ambient, High, Acute	0.0068	0.0291	Inf	0.2335	1.0000
Ambient, High, Ambient - Mid, High, Acute	0.0629	0.0299	Inf	2.0999	0.8168
Ambient, High, Ambient - High, High, Acute	0.0062	0.0280	Inf	0.2203	1.0000
Mid, High, Ambient - High, High, Ambient	-0.0340	0.0219	Inf	-1.5489	0.9870

Mid,High,Ambient - Ambient,Ambient,Acute	-0.0251	0.0308	Inf	-0.8144	1.0000
Mid,High,Ambient - Mid,Ambient,Acute	0.0175	0.0296	Inf	0.5911	1.0000
Mid,High,Ambient - High,Ambient,Acute	0.0172	0.0287	Inf	0.6005	1.0000
Mid,High,Ambient - Ambient,Mid,Acute	0.0247	0.0310	Inf	0.7968	1.0000
Mid,High,Ambient - Mid,Mid,Acute	0.0144	0.0310	Inf	0.4632	1.0000
Mid,High,Ambient - High,Mid,Acute	-0.0600	0.0283	Inf	-2.1165	0.8070
Mid,High,Ambient - Ambient,High,Acute	-0.0740	0.0299	Inf	-2.4754	0.5494
Mid,High,Ambient - Mid,High,Acute	-0.0180	0.0307	Inf	-0.5850	1.0000
Mid,High,Ambient - High,High,Acute	-0.0747	0.0289	Inf	-2.5871	0.4632
High,High,Ambient - Ambient,Ambient,Acute	0.0089	0.0287	Inf	0.3089	1.0000
High,High,Ambient - Mid,Ambient,Acute	0.0515	0.0275	Inf	1.8723	0.9222
High,High,Ambient - High,Ambient,Acute	0.0512	0.0265	Inf	1.9319	0.8999
High,High,Ambient - Ambient,Mid,Acute	0.0586	0.0290	Inf	2.0254	0.8573
High,High,Ambient - Mid,Mid,Acute	0.0483	0.0290	Inf	1.6674	0.9726
High,High,Ambient - High,Mid,Acute	-0.0260	0.0261	Inf	-0.9971	0.9999
High,High,Ambient - Ambient,High,Acute	-0.0401	0.0278	Inf	-1.4423	0.9940
High,High,Ambient - Mid,High,Acute	0.0160	0.0287	Inf	0.5581	1.0000
High,High,Ambient - High,High,Acute	-0.0407	0.0267	Inf	-1.5270	0.9888
Ambient,Ambient,Acute - Mid,Ambient,Acute	0.0426	0.0240	Inf	1.7775	0.9502
Ambient,Ambient,Acute - High,Ambient,Acute	0.0423	0.0228	Inf	1.8526	0.9288
Ambient,Ambient,Acute - Ambient,Mid,Acute	0.0498	0.0313	Inf	1.5883	0.9831
Ambient,Ambient,Acute - Mid,Mid,Acute	0.0394	0.0314	Inf	1.2579	0.9988
Ambient,Ambient,Acute - High,Mid,Acute	-0.0349	0.0287	Inf	-1.2154	0.9992
Ambient,Ambient,Acute - Ambient,High,Acute	-0.0490	0.0303	Inf	-1.6179	0.9797
Ambient,Ambient,Acute - Mid,High,Acute	0.0071	0.0311	Inf	0.2290	1.0000
Ambient,Ambient,Acute - High,High,Acute	-0.0496	0.0292	Inf	-1.6966	0.9676
Mid,Ambient,Acute - High,Ambient,Acute	-0.0003	0.0212	Inf	-0.0128	1.0000

Mid,Ambient,Acute - Ambient,Mid,Acute	0.0072	0.0302	Inf	0.2379	1.0000
Mid,Ambient,Acute - Mid,Mid,Acute	-0.0031	0.0302	Inf	-0.1042	1.0000
Mid,Ambient,Acute - High,Mid,Acute	-0.0775	0.0275	Inf	-2.8224	0.2985
Mid,Ambient,Acute - Ambient,High,Acute	-0.0916	0.0291	Inf	-3.1485	0.1368
Mid,Ambient,Acute - Mid,High,Acute	-0.0355	0.0299	Inf	-1.1865	0.9994
Mid,Ambient,Acute - High,High,Acute	-0.0922	0.0280	Inf	-3.2924	0.0914
High,Ambient,Acute - Ambient,Mid,Acute	0.0075	0.0293	Inf	0.2545	1.0000
High,Ambient,Acute - Mid,Mid,Acute	-0.0029	0.0293	Inf	-0.0981	1.0000
High,Ambient,Acute - High,Mid,Acute	-0.0772	0.0265	Inf	-2.9177	0.2424
High,Ambient,Acute - Ambient,High,Acute	-0.0913	0.0281	Inf	-3.2431	0.1054
High,Ambient,Acute - Mid,High,Acute	-0.0352	0.0290	Inf	-1.2143	0.9993
High,Ambient,Acute - High,High,Acute	-0.0919	0.0270	Inf	-3.4005	0.0661
Ambient,Mid,Acute - Mid,Mid,Acute	-0.0103	0.0259	Inf	-0.3987	1.0000
Ambient,Mid,Acute - High,Mid,Acute	-0.0847	0.0226	Inf	-3.7386	0.0213
Ambient,Mid,Acute - Ambient,High,Acute	-0.0987	0.0305	Inf	-3.2403	0.1062
Ambient,Mid,Acute - Mid,High,Acute	-0.0427	0.0313	Inf	-1.3649	0.9968
Ambient,Mid,Acute - High,High,Acute	-0.0994	0.0294	Inf	-3.3749	0.0715
Mid,Mid,Acute - High,Mid,Acute	-0.0743	0.0227	Inf	-3.2795	0.0949
Mid,Mid,Acute - Ambient,High,Acute	-0.0884	0.0305	Inf	-2.8993	0.2527
Mid,Mid,Acute - Mid,High,Acute	-0.0323	0.0313	Inf	-1.0337	0.9999
Mid,Mid,Acute - High,High,Acute	-0.0890	0.0295	Inf	-3.0218	0.1895
High,Mid,Acute - Ambient,High,Acute	-0.0141	0.0278	Inf	-0.5070	1.0000
High,Mid,Acute - Mid,High,Acute	0.0420	0.0286	Inf	1.4677	0.9927
High,Mid,Acute - High,High,Acute	-0.0147	0.0266	Inf	-0.5521	1.0000
Ambient,High,Acute - Mid,High,Acute	0.0561	0.0242	Inf	2.3133	0.6737
Ambient,High,Acute - High,High,Acute	-0.0006	0.0219	Inf	-0.0285	1.0000
Mid,High,Acute - High,High,Acute	-0.0567	0.0229	Inf	-2.4813	0.5448

B.3 Coral recruits: growth

Table B.S 16 List of statistical models used to predict basal growth rate of coral recruits relative to the exposure to treatment at t=8 weeks. The shaded area indicates the best-fit model.

Model	Fixed effect	Random effect	AICc	Akaike weights
1	Treatment (8 weeks) + log(size) (0 weeks)	Tray nested in tank (intercept)	-758.542	0.269
2	Treatment (8 weeks) + log(size) (0 weeks)	Tank (intercept)	-760.542	0.731
3	Treatment (8 weeks) + log(size) (0 weeks)	NA	-732.530	<0.01

Table B.S 17 Coefficients of the generalised linear mixed effect model predicting the basal growth rate of recruits among treatments at t=8 weeks. Number of observations: total=360, tank=36.

	Estimate	Std. Error	t-value	p-value
Intercept (AMBIENT)	0.16125	0.01461	11.04	<0.001
Treatment-MID	0.00566	0.01822	0.31	0.756
Treatment-HIGH	0.03003	0.01828	1.64	0.101
Log(size) (0 weeks)	-0.12551	0.05046	-2.49	0.013

Random effect variance(s):

Tank → Variance 0.00138, StdDev 0.03714

Table B.S 18 Tukey Posthoc Test estimates of pairwise comparisons among treatments for basal growth rate at t=8 weeks; confidence level used: 0.95

Contrast	Estimate	Std. Error	df	t. ratio	Pr(> z)
AMBIENT - MID	-0.00563	0.0191	33.0	-0.296	0.9530
AMBIENT - HIGH	-0.03010	0.0191	33.4	-1.575	0.2703
MID - HIGH	-0.02447	0.0192	34.0	-1.275	0.4190

Table B.S 19 List of statistical models used to predict basal growth rate of coral recruits relative to the exposure to treatment at t=16 weeks. The shaded area indicates the best-fit model.

Model	Fixed effect	Random effect	AICc	Akaike weights
1	Treatment (8 weeks) * treatment (16 weeks) + log(size) (8 weeks)	Tank (intercept)	-549.392	>0.99
2	Treatment (8 weeks) * treatment (16 weeks) + log(size) (8 weeks)	NA	-478.584	<0.01

Table B.S 20 Coefficients of the generalised linear mixed effect model predicting the basal growth rate of recruits among treatments at t=16 weeks. Number of observations: total=360, tank=36.

	Estimate	Std. Error	z value	Pr(> z)
(Intercept) AMBIENT (8,16 weeks)	0.1527	0.0390	3.91	<0.001
Treatment2-MID (16 weeks)	0.0380	0.0528	0.72	0.472
Treatment2-HIGH (16 weeks)	0.0513	0.0528	0.97	0.331
Treatment1-MID (8 weeks)	0.0203	0.0527	0.38	0.701
Treatment1-HIGH (8 weeks)	0.0887	0.0529	1.68	0.094
log(size_1) (8 weeks)	0.1559	0.0288	5.41	<0.001
treat_2Mid:treat_1Mid	0.0248	0.0746	0.33	0.739
treat_2High:treat_1Mid	0.0156	0.0746	0.21	0.834

treat_2Mid:treat_1High	-0.0717	0.0746	-0.96	0.336
treat_2High:treat_1High	-0.0654	0.0747	-0.88	0.381

Random effect variance(s):

Tank → Variance 0.004558, StdDev 0.006751

Table B.S 21 Tukey Posthoc Test estimates of pairwise comparisons among treatments for basal growth rate at t=16 weeks; confidence level used: 0.95

contrast	estimate	SE	df	t.ratio	p.value
Ambient,Ambient - Mid,Ambient	-0.020	0.061	26.918	-0.333	1.000
Ambient,Ambient - High,Ambient	-0.089	0.061	27.208	-1.454	0.866
Ambient,Ambient - Ambient,Mid	-0.038	0.061	27.017	-0.624	0.999
Ambient,Ambient - Mid,Mid	-0.083	0.061	27.137	-1.363	0.902
Ambient,Ambient - High,Mid	-0.055	0.061	27.394	-0.902	0.991
Ambient,Ambient - Ambient,High	-0.051	0.061	27.040	-0.843	0.994
Ambient,Ambient - Mid,High	-0.087	0.061	26.940	-1.432	0.875
Ambient,Ambient - High,High	-0.075	0.061	27.073	-1.225	0.944
Mid,Ambient - High,Ambient	-0.069	0.061	27.144	-1.123	0.965
Mid,Ambient - Ambient,Mid	-0.018	0.061	26.980	-0.291	1.000
Mid,Ambient - Mid,Mid	-0.063	0.061	27.081	-1.031	0.979
Mid,Ambient - High,Mid	-0.035	0.061	27.310	-0.571	1.000
Mid,Ambient - Ambient,High	-0.031	0.061	26.999	-0.511	1.000
Mid,Ambient - Mid,High	-0.067	0.061	26.924	-1.099	0.969
Mid,Ambient - High,High	-0.054	0.061	27.027	-0.892	0.992
High,Ambient - Ambient,Mid	0.051	0.061	26.962	0.833	0.995
High,Ambient - Mid,Mid	0.006	0.061	26.918	0.092	1.000

High,Ambient - High,Mid	0.034	0.061	26.936	0.552	1.000
High,Ambient - Ambient,High	0.037	0.061	26.949	0.614	0.999
High,Ambient - Mid,High	0.002	0.061	27.058	0.026	1.000
High,Ambient - High,High	0.014	0.061	26.934	0.232	1.000
Ambient,Mid - Mid,Mid	-0.045	0.061	26.936	-0.741	0.998
Ambient,Mid - High,Mid	-0.017	0.061	27.051	-0.281	1.000
Ambient,Mid - Ambient,High	-0.013	0.061	26.915	-0.220	1.000
Ambient,Mid - Mid,High	-0.049	0.061	26.939	-0.807	0.996
Ambient,Mid - High,High	-0.037	0.061	26.920	-0.602	0.999
Mid,Mid - High,Mid	0.028	0.061	26.962	0.460	1.000
Mid,Mid - Ambient,High	0.032	0.061	26.927	0.522	1.000
Mid,Mid - Mid,High	-0.004	0.061	27.010	-0.066	1.000
Mid,Mid - High,High	0.009	0.061	26.919	0.140	1.000
High,Mid - Ambient,High	0.004	0.061	27.027	0.062	1.000
High,Mid - Mid,High	-0.032	0.061	27.194	-0.525	1.000
High,Mid - High,High	-0.020	0.061	26.999	-0.320	1.000
Ambient,High - Mid,High	-0.036	0.061	26.951	-0.588	1.000
Ambient,High - High,High	-0.023	0.061	26.916	-0.382	1.000
Mid,High - High,High	0.013	0.061	26.969	0.206	1.000

Table B.S 22 List of statistical models used to predict basal growth rate of coral recruits relative to the exposure to treatment at t=18 weeks. The shaded area indicates the best-fit model.

Model	Fixed effect	Random effect	AICc	Akaike weights
1	Treatment (8 weeks) * treatment (16 weeks) + log(size) (16 weeks)	Tray nested in tank (intercept)	-1252.056	>0.99

2	Treatment (8 weeks) * treatment (16 weeks) + log(size) (16 weeks)	Tank (intercept)	-1211.246	<0.01
3	Treatment (8 weeks) * treatment (16 weeks) + log(size) (16 weeks)	NA	-1207.410	<0.01

Table B.S 23 Coefficients of the generalised linear mixed effect model predicting the basal growth rate of recruits among treatments at t=18 weeks. Number of observations: total=358, tank=24, tray=62.

	Estimate	Std. Error	z value	Pr(> z)
(Intercept) AMBIENT (8,16 weeks)	0.121052	0.011882	10.19	<0.001
Treatment2-MID (16 weeks)	0.008476	0.014641	0.58	0.56
Treatment2-HIGH (16 weeks)	0.015590	0.014573	1.07	0.28
Treatment1-MID (8 weeks)	0.012113	0.014543	0.83	0.40
Treatment1-HIGH (8 weeks)	0.015099	0.014697	1.03	0.30
log(size_2) (16 weeks)	-0.025930	0.005899	-4.40	<0.001
treat_2Mid:treat_1Mid	-0.000182	0.019829	-0.01	0.99
treat_2High:treat_1Mid	-0.004009	0.017735	-0.23	0.82
treat_2Mid:treat_1High	0.025088	0.018689	1.34	0.18
treat_2High:treat_1High	0.008429	0.020597	0.41	0.68

Random effect variance(s):

Tank → Variance 1.123e-07, StdDev 0.0003352

Tray:tank → Variance 0.0006421, StdDev 0.2534

Table B.S 24 Tukey Posthoc Test estimates of pairwise comparisons among treatments for basal growth rate at t=18 weeks; confidence level used: 0.95

contrast	estimate	SE	df	t.ratio	p.value
----------	----------	----	----	---------	---------

Ambient,Ambient - Mid,Ambient	-0.012	0.015	42.738	-0.793	0.997
Ambient,Ambient - High,Ambient	-0.015	0.016	44.572	-0.984	0.985
Ambient,Ambient - Ambient,Mid	-0.008	0.016	69.648	-0.539	1.000
Ambient,Ambient - Mid,Mid	-0.021	0.016	69.348	-1.329	0.919
Ambient,Ambient - High,Mid	-0.049	0.015	72.209	-3.243	0.044
Ambient,Ambient - Ambient,High	-0.015	0.015	64.778	-0.992	0.985
Ambient,Ambient - Mid,High	-0.024	0.015	64.601	-1.560	0.822
Ambient,Ambient - High,High	-0.039	0.016	58.388	-2.445	0.280
Mid,Ambient - High,Ambient	-0.003	0.012	160.131	-0.248	1.000
Mid,Ambient - Ambient,Mid	0.004	0.015	76.052	0.260	1.000
Mid,Ambient - Mid,Mid	-0.008	0.015	75.373	-0.564	1.000
Mid,Ambient - High,Mid	-0.037	0.014	74.942	-2.541	0.230
Mid,Ambient - Ambient,High	-0.003	0.015	70.591	-0.209	1.000
Mid,Ambient - Mid,High	-0.012	0.015	70.352	-0.797	0.997
Mid,Ambient - High,High	-0.027	0.015	66.761	-1.749	0.714
High,Ambient - Ambient,Mid	0.007	0.015	75.233	0.468	1.000
High,Ambient - Mid,Mid	-0.005	0.015	73.719	-0.358	1.000
High,Ambient - High,Mid	-0.034	0.014	72.757	-2.341	0.332
High,Ambient - Ambient,High	0.000	0.015	70.338	0.000	1.000
High,Ambient - Mid,High	-0.009	0.015	70.571	-0.587	1.000
High,Ambient - High,High	-0.024	0.015	65.638	-1.556	0.824
Ambient,Mid - Mid,Mid	-0.012	0.014	89.688	-0.860	0.994
Ambient,Mid - High,Mid	-0.041	0.012	175.735	-3.346	0.027
Ambient,Mid - Ambient,High	-0.007	0.015	72.676	-0.471	1.000
Ambient,Mid - Mid,High	-0.016	0.015	72.813	-1.058	0.978
Ambient,Mid - High,High	-0.031	0.015	68.560	-2.005	0.546
Mid,Mid - High,Mid	-0.028	0.012	169.296	-2.343	0.323

Mid, Mid - Ambient, High	0.005	0.015	71.576	0.358	1.000
Mid, Mid - Mid, High	-0.003	0.015	71.776	-0.231	1.000
Mid, Mid - High, High	-0.019	0.015	67.275	-1.215	0.950
High, Mid - Ambient, High	0.034	0.014	70.622	2.346	0.330
High, Mid - Mid, High	0.025	0.014	70.989	1.736	0.722
High, Mid - High, High	0.010	0.015	69.593	0.646	0.999
Ambient, High - Mid, High	-0.009	0.010	296.778	-0.841	0.996
Ambient, High - High, High	-0.024	0.015	42.273	-1.560	0.820
Mid, High - High, High	-0.015	0.015	42.265	-0.992	0.985

Figure B.S 1 Mean basal growth for the history combinations of treatments at t=3 (18 weeks) after all fragments were moved to ambient conditions for a two-week period. Symbols represent origin treatment (at t=8 weeks) whereas x-axis distribution represent destination treatments (at t=16 weeks). Number of observations: total=358, tank=24, tray=62.

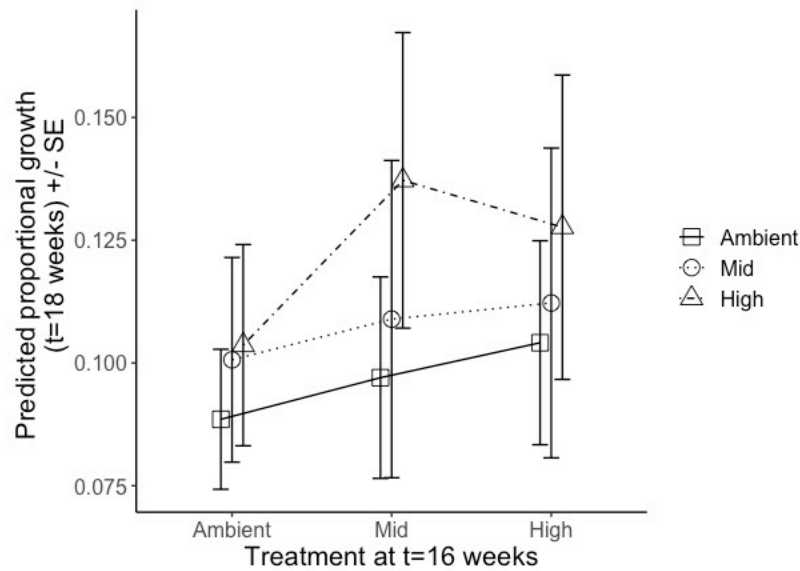


Table B.S 25 List of statistical models used to predict basal growth rate of coral recruits relative to the exposure to treatment at t=23 weeks. The shaded area indicates the best-fit model.

Model	Fixed effect	Random effect	AICc	Akaike weights
1	Treatment (8 weeks) * treatment (16 weeks) * treatment (23 weeks) + log(size) (18 weeks)	Tray nested in tank (intercept)	-1286.741	0.222

2	Treatment (8 weeks) * treatment (16 weeks) * treatment (23 weeks) + log(size) (18 weeks)	Tank (intercept)	-1288.579	0.557
3	Treatment (8 weeks) * treatment (16 weeks) * treatment (23 weeks) + log(size) (18 weeks)	NA	-1286.727	0.221

Table B.S 26 Coefficients of the generalised linear mixed effect model predicting the basal growth rate of recruits among treatments at t=23 weeks. Number of observations: total=347, tank=24.

	Estimate	Std. Error	z value	Pr(> z)
(Intercept) AMBIENT (8,16, 23 weeks)	0.101217	0.010506	9.63	<0.001
treat_4Acute	0.027097	0.012811	2.12	0.03442
treat_2Mid	0.010660	0.013738	0.78	0.43777
treat_2High	0.024973	0.012911	1.93	0.05308
treat_1Mid	0.015710	0.011359	1.38	0.16664
treat_1High	0.027512	0.011553	2.38	0.01725
log(size_3)	-0.017694	0.004941	-3.58	<0.001
treat_4Acute:treat_2Mid	-0.027213	0.018570	-1.47	0.14280
treat_4Acute:treat_2High	-0.025412	0.018070	-1.41	0.15963
treat_4Acute:treat_1Mid	-0.022310	0.016042	-1.39	0.16431
treat_4Acute:treat_1High	-0.021549	0.015889	-1.36	0.17503
treat_2Mid:treat_1Mid	-0.024526	0.016516	-1.48	0.13755
treat_2High:treat_1Mid	0.005866	0.015935	0.37	0.71278
treat_2Mid:treat_1High	-0.000516	0.016595	-0.03	0.97518
treat_2High:treat_1High	-0.031740	0.015995	-1.98	0.04721
treat_4Acute:treat_2Mid:treat_1Mid	0.043875	0.022931	1.91	0.05570
treat_4Acute:treat_2High:treat_1Mid	0.010766	0.022591	0.48	0.63367
treat_4Acute:treat_2Mid:treat_1High	0.041215	0.022832	1.81	0.07105
treat_4Acute:treat_2High:treat_1High	0.020853	0.022449	0.93	0.35295

Random effect variance(s):

Tank → Variance 6.38e-05, StdDev 0.007987

Table B.S 27 Tukey Posthoc Test estimates of pairwise comparisons among treatments for basal growth rate at t=23 weeks; confidence level used: 0.95

contrast	estimate	SE	df	t.ratio	p.value
Ambient,Ambient,Ambient - Mid,Ambient,Ambient	-0.015	0.012	312.063	-1.334	0.997
Ambient,Ambient,Ambient - High,Ambient,Ambient	-0.027	0.012	313.163	-2.317	0.671
Ambient,Ambient,Ambient - Ambient,Mid,Ambient	-0.010	0.015	73.239	-0.704	1.000
Ambient,Ambient,Ambient - Mid,Mid,Ambient	-0.002	0.014	64.727	-0.120	1.000
Ambient,Ambient,Ambient - High,Mid,Ambient	-0.038	0.014	65.637	-2.666	0.424
Ambient,Ambient,Ambient - Ambient,High,Ambient	-0.025	0.014	64.939	-1.758	0.946
Ambient,Ambient,Ambient - Mid,High,Ambient	-0.046	0.014	62.328	-3.347	0.107
Ambient,Ambient,Ambient - High,High,Ambient	-0.021	0.014	63.879	-1.474	0.990
Ambient,Ambient,Ambient - Ambient,Ambient,Acute	-0.027	0.014	63.519	-1.935	0.887
Ambient,Ambient,Ambient - Mid,Ambient,Acute	-0.020	0.014	63.158	-1.459	0.991
Ambient,Ambient,Ambient - High,Ambient,Acute	-0.033	0.014	64.784	-2.348	0.647
Ambient,Ambient,Ambient - Ambient,Mid,Acute	-0.010	0.014	64.714	-0.734	1.000
Ambient,Ambient,Ambient - Mid,Mid,Acute	-0.023	0.014	63.696	-1.658	0.968
Ambient,Ambient,Ambient - High,Mid,Acute	-0.057	0.014	65.129	-4.064	0.014
Ambient,Ambient,Ambient - Ambient,High,Acute	-0.026	0.014	67.467	-1.845	0.921
Ambient,Ambient,Ambient - Mid,High,Acute	-0.037	0.014	63.628	-2.620	0.455
Ambient,Ambient,Ambient - High,High,Acute	-0.022	0.014	64.326	-1.542	0.984
Mid,Ambient,Ambient - High,Ambient,Ambient	-0.012	0.011	310.572	-1.052	1.000
Mid,Ambient,Ambient - Ambient,Mid,Ambient	0.005	0.014	67.460	0.343	1.000
Mid,Ambient,Ambient - Mid,Mid,Ambient	0.014	0.014	58.291	1.016	1.000
Mid,Ambient,Ambient - High,Mid,Ambient	-0.022	0.014	58.829	-1.621	0.973

Mid,Ambient,Ambient - Ambient,High,Ambient	-0.009	0.014	59.313	-0.673	1.000
Mid,Ambient,Ambient - Mid,High,Ambient	-0.031	0.013	57.172	-2.290	0.687
Mid,Ambient,Ambient - High,High,Ambient	-0.005	0.014	57.831	-0.377	1.000
Mid,Ambient,Ambient - Ambient,Ambient,Acute	-0.011	0.014	58.939	-0.843	1.000
Mid,Ambient,Ambient - Mid,Ambient,Acute	-0.005	0.014	59.024	-0.353	1.000
Mid,Ambient,Ambient - High,Ambient,Acute	-0.017	0.014	58.324	-1.286	0.998
Mid,Ambient,Ambient - Ambient,Mid,Acute	0.005	0.014	59.223	0.381	1.000
Mid,Ambient,Ambient - Mid,Mid,Acute	-0.008	0.014	57.738	-0.566	1.000
Mid,Ambient,Ambient - High,Mid,Acute	-0.042	0.014	58.524	-3.063	0.206
Mid,Ambient,Ambient - Ambient,High,Acute	-0.011	0.014	61.558	-0.777	1.000
Mid,Ambient,Ambient - Mid,High,Acute	-0.021	0.014	57.705	-1.557	0.982
Mid,Ambient,Ambient - High,High,Acute	-0.006	0.014	58.067	-0.450	1.000
High,Ambient,Ambient - Ambient,Mid,Ambient	0.017	0.014	66.865	1.168	0.999
High,Ambient,Ambient - Mid,Mid,Ambient	0.026	0.013	57.076	1.904	0.898
High,Ambient,Ambient - High,Mid,Ambient	-0.010	0.013	57.194	-0.755	1.000
High,Ambient,Ambient - Ambient,High,Ambient	0.003	0.014	59.060	0.199	1.000
High,Ambient,Ambient - Mid,High,Ambient	-0.019	0.013	57.419	-1.407	0.993
High,Ambient,Ambient - High,High,Ambient	0.007	0.013	57.056	0.503	1.000
High,Ambient,Ambient - Ambient,Ambient,Acute	0.000	0.014	59.893	0.030	1.000
High,Ambient,Ambient - Mid,Ambient,Acute	0.007	0.014	60.498	0.516	1.000
High,Ambient,Ambient - High,Ambient,Acute	-0.006	0.013	57.081	-0.413	1.000
High,Ambient,Ambient - Ambient,Mid,Acute	0.017	0.014	59.119	1.254	0.998
High,Ambient,Ambient - Mid,Mid,Acute	0.004	0.013	57.067	0.314	1.000
High,Ambient,Ambient - High,Mid,Acute	-0.030	0.013	57.118	-2.205	0.742
High,Ambient,Ambient - Ambient,High,Acute	0.001	0.014	61.004	0.084	1.000
High,Ambient,Ambient - Mid,High,Acute	-0.009	0.013	57.072	-0.680	1.000
High,Ambient,Ambient - High,High,Acute	0.006	0.013	57.054	0.429	1.000

Ambient, Mid, Ambient - Mid, Mid, Ambient	0.009	0.012	324.321	0.713	1.000
Ambient, Mid, Ambient - High, Mid, Ambient	-0.027	0.012	324.231	-2.187	0.761
Ambient, Mid, Ambient - Ambient, High, Ambient	-0.014	0.015	68.742	-0.971	1.000
Ambient, Mid, Ambient - Mid, High, Ambient	-0.036	0.014	67.036	-2.479	0.553
Ambient, Mid, Ambient - High, High, Ambient	-0.010	0.014	66.847	-0.698	1.000
Ambient, Mid, Ambient - Ambient, Ambient, Acute	-0.016	0.015	69.376	-1.125	1.000
Ambient, Mid, Ambient - Mid, Ambient, Acute	-0.010	0.015	69.853	-0.667	1.000
Ambient, Mid, Ambient - High, Ambient, Acute	-0.022	0.014	66.950	-1.553	0.983
Ambient, Mid, Ambient - Ambient, Mid, Acute	0.000	0.015	68.790	0.014	1.000
Ambient, Mid, Ambient - Mid, Mid, Acute	-0.013	0.014	66.841	-0.875	1.000
Ambient, Mid, Ambient - High, Mid, Acute	-0.047	0.014	67.013	-3.225	0.140
Ambient, Mid, Ambient - Ambient, High, Acute	-0.016	0.015	70.699	-1.068	1.000
Ambient, Mid, Ambient - Mid, High, Acute	-0.026	0.014	66.840	-1.803	0.934
Ambient, Mid, Ambient - High, High, Acute	-0.011	0.014	66.885	-0.768	1.000
Mid, Mid, Ambient - High, Mid, Ambient	-0.036	0.011	310.064	-3.195	0.127
Mid, Mid, Ambient - Ambient, High, Ambient	-0.023	0.014	59.196	-1.685	0.962
Mid, Mid, Ambient - Mid, High, Ambient	-0.045	0.014	57.637	-3.303	0.121
Mid, Mid, Ambient - High, High, Ambient	-0.019	0.013	57.104	-1.401	0.994
Mid, Mid, Ambient - Ambient, Ambient, Acute	-0.025	0.014	60.231	-1.845	0.920
Mid, Mid, Ambient - Mid, Ambient, Acute	-0.019	0.014	60.923	-1.351	0.996
Mid, Mid, Ambient - High, Ambient, Acute	-0.031	0.013	57.051	-2.317	0.668
Mid, Mid, Ambient - Ambient, Mid, Acute	-0.009	0.014	59.280	-0.631	1.000
Mid, Mid, Ambient - Mid, Mid, Acute	-0.021	0.013	57.132	-1.590	0.977
Mid, Mid, Ambient - High, Mid, Acute	-0.055	0.013	57.061	-4.110	0.013
Mid, Mid, Ambient - Ambient, High, Acute	-0.024	0.014	61.091	-1.780	0.940
Mid, Mid, Ambient - Mid, High, Acute	-0.035	0.013	57.144	-2.583	0.482
Mid, Mid, Ambient - High, High, Acute	-0.020	0.013	57.062	-1.476	0.989

High, Mid, Ambient - Ambient, High, Ambient	0.013	0.014	59.467	0.945	1.000
High, Mid, Ambient - Mid, High, Ambient	-0.009	0.014	58.021	-0.651	1.000
High, Mid, Ambient - High, High, Ambient	0.017	0.013	57.253	1.257	0.998
High, Mid, Ambient - Ambient, Ambient, Acute	0.011	0.014	60.781	0.771	1.000
High, Mid, Ambient - Mid, Ambient, Acute	0.017	0.014	61.594	1.251	0.998
High, Mid, Ambient - High, Ambient, Acute	0.005	0.013	57.093	0.342	1.000
High, Mid, Ambient - Ambient, Mid, Acute	0.027	0.014	59.586	1.996	0.859
High, Mid, Ambient - Mid, Mid, Acute	0.014	0.013	57.305	1.067	1.000
High, Mid, Ambient - High, Mid, Acute	-0.020	0.013	57.065	-1.450	0.991
High, Mid, Ambient - Ambient, High, Acute	0.011	0.014	61.294	0.823	1.000
High, Mid, Ambient - Mid, High, Acute	0.001	0.013	57.326	0.075	1.000
High, Mid, Ambient - High, High, Acute	0.016	0.013	57.156	1.183	0.999
Ambient, High, Ambient - Mid, High, Ambient	-0.022	0.011	310.425	-1.909	0.906
Ambient, High, Ambient - High, High, Ambient	0.004	0.011	310.509	0.357	1.000
Ambient, High, Ambient - Ambient, Ambient, Acute	-0.002	0.014	61.241	-0.167	1.000
Ambient, High, Ambient - Mid, Ambient, Acute	0.004	0.014	61.661	0.317	1.000
Ambient, High, Ambient - High, Ambient, Acute	-0.008	0.014	59.211	-0.607	1.000
Ambient, High, Ambient - Ambient, Mid, Acute	0.014	0.014	60.848	1.046	1.000
Ambient, High, Ambient - Mid, Mid, Acute	0.002	0.014	58.989	0.112	1.000
Ambient, High, Ambient - High, Mid, Acute	-0.032	0.014	59.307	-2.379	0.625
Ambient, High, Ambient - Ambient, High, Acute	-0.002	0.014	62.907	-0.112	1.000
Ambient, High, Ambient - Mid, High, Acute	-0.012	0.014	58.980	-0.873	1.000
Ambient, High, Ambient - High, High, Acute	0.003	0.014	59.100	0.225	1.000
Mid, High, Ambient - High, High, Ambient	0.026	0.011	310.206	2.293	0.688
Mid, High, Ambient - Ambient, Ambient, Acute	0.019	0.014	59.074	1.426	0.993
Mid, High, Ambient - Mid, Ambient, Acute	0.026	0.014	59.348	1.912	0.895
Mid, High, Ambient - High, Ambient, Acute	0.013	0.014	57.660	0.993	1.000

Mid,High,Ambient - Ambient,Mid,Acute	0.036	0.014	58.973	2.651	0.436
Mid,High,Ambient - Mid,Mid,Acute	0.023	0.013	57.283	1.721	0.954
Mid,High,Ambient - High,Mid,Acute	-0.011	0.014	57.800	-0.793	1.000
Mid,High,Ambient - Ambient,High,Acute	0.020	0.014	61.143	1.464	0.990
Mid,High,Ambient - Mid,High,Acute	0.010	0.013	57.263	0.728	1.000
Mid,High,Ambient - High,High,Acute	0.025	0.014	57.487	1.834	0.923
High,High,Ambient - Ambient,Ambient,Acute	-0.006	0.014	59.758	-0.466	1.000
High,High,Ambient - Mid,Ambient,Acute	0.000	0.014	60.325	0.022	1.000
High,High,Ambient - High,Ambient,Acute	-0.012	0.013	57.111	-0.915	1.000
High,High,Ambient - Ambient,Mid,Acute	0.010	0.014	59.064	0.756	1.000
High,High,Ambient - Mid,Mid,Acute	-0.003	0.013	57.054	-0.189	1.000
High,High,Ambient - High,Mid,Acute	-0.036	0.013	57.160	-2.707	0.399
High,High,Ambient - Ambient,High,Acute	-0.006	0.014	60.982	-0.408	1.000
High,High,Ambient - Mid,High,Acute	-0.016	0.013	57.057	-1.183	0.999
High,High,Ambient - High,High,Acute	-0.001	0.013	57.067	-0.074	1.000
Ambient,Ambient,Acute - Mid,Ambient,Acute	0.007	0.012	311.271	0.579	1.000
Ambient,Ambient,Acute - High,Ambient,Acute	-0.006	0.011	310.849	-0.521	1.000
Ambient,Ambient,Acute - Ambient,Mid,Acute	0.017	0.014	61.150	1.212	0.999
Ambient,Ambient,Acute - Mid,Mid,Acute	0.004	0.014	59.663	0.280	1.000
Ambient,Ambient,Acute - High,Mid,Acute	-0.030	0.014	60.469	-2.198	0.747
Ambient,Ambient,Acute - Ambient,High,Acute	0.001	0.014	63.506	0.054	1.000
Ambient,Ambient,Acute - Mid,High,Acute	-0.010	0.014	59.628	-0.702	1.000
Ambient,Ambient,Acute - High,High,Acute	0.005	0.014	60.001	0.392	1.000
Mid,Ambient,Acute - High,Ambient,Acute	-0.013	0.012	311.913	-1.095	1.000
Mid,Ambient,Acute - Ambient,Mid,Acute	0.010	0.014	61.522	0.724	1.000
Mid,Ambient,Acute - Mid,Mid,Acute	-0.003	0.014	60.200	-0.208	1.000
Mid,Ambient,Acute - High,Mid,Acute	-0.037	0.014	61.216	-2.672	0.421

Mid,Ambient,Acute - Ambient,High,Acute	-0.006	0.014	64.010	-0.424	1.000
Mid,Ambient,Acute - Mid,High,Acute	-0.016	0.014	60.154	-1.187	0.999
Mid,Ambient,Acute - High,High,Acute	-0.001	0.014	60.636	-0.095	1.000
High,Ambient,Acute - Ambient,Mid,Acute	0.023	0.014	59.298	1.661	0.967
High,Ambient,Acute - Mid,Mid,Acute	0.010	0.013	57.140	0.726	1.000
High,Ambient,Acute - High,Mid,Acute	-0.024	0.013	57.058	-1.793	0.936
High,Ambient,Acute - Ambient,High,Acute	0.007	0.014	61.101	0.489	1.000
High,Ambient,Acute - Mid,High,Acute	-0.004	0.013	57.153	-0.268	1.000
High,Ambient,Acute - High,High,Acute	0.011	0.013	57.066	0.841	1.000
Ambient,Mid,Acute - Mid,Mid,Acute	-0.013	0.011	310.405	-1.129	1.000
Ambient,Mid,Acute - High,Mid,Acute	-0.047	0.011	310.524	-4.104	0.006
Ambient,Mid,Acute - Ambient,High,Acute	-0.016	0.014	62.937	-1.146	0.999
Ambient,Mid,Acute - Mid,High,Acute	-0.026	0.014	59.017	-1.928	0.889
Ambient,Mid,Acute - High,High,Acute	-0.011	0.014	59.168	-0.829	1.000
Mid,Mid,Acute - High,Mid,Acute	-0.034	0.011	310.123	-3.024	0.195
Mid,Mid,Acute - Ambient,High,Acute	-0.003	0.014	60.972	-0.223	1.000
Mid,Mid,Acute - Mid,High,Acute	-0.013	0.013	57.052	-0.994	1.000
Mid,Mid,Acute - High,High,Acute	0.002	0.013	57.083	0.115	1.000
High,Mid,Acute - Ambient,High,Acute	0.031	0.014	61.171	2.243	0.718
High,Mid,Acute - Mid,High,Acute	0.021	0.013	57.215	1.524	0.985
High,Mid,Acute - High,High,Acute	0.035	0.013	57.093	2.634	0.447
Ambient,High,Acute - Mid,High,Acute	-0.010	0.012	311.808	-0.895	1.000
Ambient,High,Acute - High,High,Acute	0.005	0.012	311.853	0.400	1.000
Mid,High,Acute - High,High,Acute	0.015	0.011	310.059	1.333	0.997

B.4 Coral recruits: photochemical efficiency (Fv/Fm)

Table B.S 28 List of statistical models used to predict Fv/Fm of coral recruits relative to the exposure to treatment at t=8 weeks. The shaded area indicates the best-fit model.

Model	Fixed effect	Random effect	AICc	Akaike weights
1	Treatment (8 weeks) + yield (0 weeks)	Tray nested in tank (intercept)	-959.176	0.269
2	Treatment (8 weeks) + yield (0 weeks)	Tank (intercept)	-961.176	0.731
3	Treatment (8 weeks) + yield (0 weeks)	NA	-940.294	<0.01

Table B.S 29 Coefficients of the generalised linear mixed effect model predicting Fv/Fm of recruits among treatments at t=8 weeks. Number of observations: total=288, tank=36.

	Estimate	Std. Error	z value	Pr(> z)
Intercept (AMBIENT)	0.14177	0.0303	13.78	<0.001
Treatment-MID	0.0177	0.0103	1.71	0.08657
Treatment-HIGH	-0.0183	0.0103	-1.77	0.07669
yield (0 weeks)	0.2354	0.0642	3.67	<0.001

Random effect variance(s):

Tank → Variance 0.0004176, StdDev 0.02044

Table B.S 30 Tukey Posthoc Test estimates of pairwise comparisons among treatments for Fv/Fm at t=8 weeks; confidence level used: 0.95

Contrast	Estimate	Std. Error	df	t. ratio	Pr(> z)
AMBIENT - MID	-0.0177	0.0108	33.1	-1.641	0.2432
AMBIENT - HIGH	0.0182	0.0108	33.0	1.691	0.2237
MID - HIGH	0.0359	0.0108	32.9	3.337	0.0058

Table B.S 31 List of statistical models used to predict Fv/Fm of coral recruits relative to the exposure to treatment at t=16 weeks. The shaded area indicates the best-fit model.

Model	Fixed effect	Random effect	AICc	Akaike weights
1	Treatment (8 weeks) * treatment (16 weeks) + yield (8 weeks)	Tray nested in tank (intercept)	-1035.530	0.232
2	Treatment (8 weeks) * treatment (16 weeks) + yield (8 weeks)	Tank (intercept)	-1037.530	0.631
2	Treatment (8 weeks) * treatment (16 weeks) + yield (8 weeks)	NA	-1034.476	0.137

Table B.S 32 Coefficients of the generalised linear mixed effect model predicting Fv/Fm of recruits among treatments at t=16 weeks. Number of observations: total=288, tank=36.

	Estimate	Std. Error	z value	Pr(> z)
(Intercept) AMBIENT (8,16 weeks)	0.37872	0.02780	13.62	<0.001
Treatment2-MID (16 weeks)	-0.01593	0.01212	-1.31	0.189
Treatment2-HIGH (16 weeks)	-0.01695	0.01218	-1.39	0.164
Treatment1-MID (8 weeks)	0.01409	0.01211	1.16	0.245
Treatment1-HIGH (8 weeks)	0.00645	0.01214	0.53	0.595
yield_1 (8 weeks)	0.28541	0.05095	5.60	<0.001

treat_2Mid:treat_1Mid	0.01935	0.01719	1.13	0.260
treat_2High:treat_1Mid	0.02646	0.01717	1.54	0.123
treat_2Mid:treat_1High	0.03323	0.01714	1.94	0.053
treat_2High:treat_1High	-0.01677	0.01716	-0.98	0.329

Random effect variance(s):

Tank → Variance 0.0001218, StdDev 0.01104

Table B.S 33 Tukey Posthoc Test estimates of pairwise comparisons among treatments for Fv/Fm at t=16 weeks; confidence level used: 0.95

contrast	estimate	SE	df	t.ratio	p.value
Ambient,Ambient - Mid,Ambient	-0.014	0.014	26.806	-1.003	0.982
Ambient,Ambient - High,Ambient	-0.006	0.014	26.995	-0.450	1.000
Ambient,Ambient - Ambient,Mid	0.016	0.014	26.820	1.137	0.963
Ambient,Ambient - Mid,Mid	-0.018	0.014	27.096	-1.254	0.936
Ambient,Ambient - High,Mid	-0.024	0.014	26.879	-1.685	0.750
Ambient,Ambient - Ambient,High	0.017	0.014	27.186	1.191	0.952
Ambient,Ambient - Mid,High	-0.024	0.014	28.161	-1.680	0.753
Ambient,Ambient - High,High	0.027	0.014	26.931	1.947	0.590
Mid,Ambient - High,Ambient	0.008	0.014	26.967	0.551	1.000
Mid,Ambient - Ambient,Mid	0.030	0.014	26.813	2.140	0.469
Mid,Ambient - Mid,Mid	-0.004	0.014	27.133	-0.254	1.000
Mid,Ambient - High,Mid	-0.010	0.014	26.862	-0.682	0.999
Mid,Ambient - Ambient,High	0.031	0.014	27.228	2.189	0.440
Mid,Ambient - Mid,High	-0.010	0.014	28.241	-0.690	0.999
Mid,Ambient - High,High	0.041	0.014	26.908	2.949	0.121
High,Ambient - Ambient,Mid	0.022	0.014	26.903	1.586	0.804

High,Ambient - Mid,Mid	-0.011	0.014	27.759	-0.799	0.996
High,Ambient - High,Mid	-0.017	0.014	26.832	-1.235	0.941
High,Ambient - Ambient,High	0.023	0.014	27.919	1.627	0.782
High,Ambient - Mid,High	-0.018	0.014	29.388	-1.220	0.945
High,Ambient - High,High	0.034	0.014	26.812	2.400	0.324
Ambient,Mid - Mid,Mid	-0.034	0.014	27.244	-2.384	0.331
Ambient,Mid - High,Mid	-0.040	0.014	26.827	-2.822	0.155
Ambient,Mid - Ambient,High	0.001	0.014	27.354	0.058	1.000
Ambient,Mid - Mid,High	-0.040	0.014	28.467	-2.792	0.162
Ambient,Mid - High,High	0.011	0.014	26.859	0.812	0.995
Mid,Mid - High,Mid	-0.006	0.014	27.466	-0.425	1.000
Mid,Mid - Ambient,High	0.034	0.014	26.811	2.453	0.298
Mid,Mid - Mid,High	-0.006	0.014	27.192	-0.444	1.000
Mid,Mid - High,High	0.045	0.014	27.606	3.180	0.074
High,Mid - Ambient,High	0.040	0.014	27.599	2.857	0.144
High,Mid - Mid,High	0.000	0.014	28.882	-0.017	1.000
High,Mid - High,High	0.051	0.014	26.812	3.635	0.027
Ambient,High - Mid,High	-0.041	0.014	27.101	-2.890	0.136
Ambient,High - High,High	0.011	0.014	27.753	0.747	0.997
Mid,High - High,High	0.051	0.014	29.129	3.568	0.030

Table B.S 34 List of statistical models used to predict Fv/Fm of coral recruits relative to the exposure to treatment at t=18 weeks. The shaded area indicates the best-fit model.

Model	Fixed effect	Random effect	AICc	Akaike weights
-------	--------------	---------------	------	----------------

1	Treatment (8 weeks) * treatment (16 weeks) + yield (16 weeks)	Tray nested in tank (intercept)	-1085.558	0.849
2	Treatment (8 weeks) * treatment (16 weeks) + yield (16 weeks)	Tank (intercept)	-1081.310	0.102
3	Treatment (8 weeks) * treatment (16 weeks) + yield (16 weeks)	NA	-1079.864	0.049

Table B.S 35 Coefficients of the generalised linear mixed effect model predicting Fv/Fm of recruits among treatments at t=18 weeks. Number of observations: total=288, tank=24, tray=62.

	Estimate	Std. Error	z value	Pr(> z)
(Intercept) AMBIENT (8,16 weeks)	0.35179	0.02880	12.22	<0.001
Treatment2-MID (16 weeks)	0.00205	0.01087	0.19	0.851
Treatment2-HIGH (16 weeks)	0.00790	0.01087	0.73	0.467
Treatment1-MID (8 weeks)	0.02700	0.01090	2.48	0.013
Treatment1-HIGH (8 weeks)	0.02197	0.01084	2.03	0.043
yield_2 (16 weeks)	0.36837	0.05265	7.00	<0.001
treat_2Mid:treat_1Mid	-0.01276	0.01525	-0.84	0.403
treat_2High:treat_1Mid	-0.02456	0.01452	-1.69	0.091
treat_2Mid:treat_1High	-0.00495	0.01478	-0.33	0.738
treat_2High:treat_1High	-0.00939	0.01528	-0.61	0.539

Random effect variance(s):

Tank → Variance 3.672e-06, StdDev 0.001916

Tray:tank → Variance 0.0002057, StdDev 0. 0.01434

Table B.S 36 Tukey Posthoc Test estimates of pairwise comparisons among treatments for Fv/Fm at t=18 weeks; confidence level used: 0.95

contrast	estimate	SE	df	t.ratio	p.value
Ambient,Ambient - Mid,Ambient	-0.028	0.012	42.407	-2.391	0.315
Ambient,Ambient - High,Ambient	-0.021	0.011	42.295	-1.867	0.639
Ambient,Ambient - Ambient,Mid	-0.002	0.012	69.161	-0.180	1.000
Ambient,Ambient - Mid,Mid	-0.016	0.012	69.711	-1.405	0.892
Ambient,Ambient - High,Mid	-0.019	0.012	75.511	-1.613	0.795
Ambient,Ambient - Ambient,High	-0.008	0.012	69.072	-0.719	0.998
Ambient,Ambient - Mid,High	-0.010	0.012	71.779	-0.870	0.994
Ambient,Ambient - High,High	-0.021	0.012	62.178	-1.742	0.719
Mid,Ambient - High,Ambient	0.006	0.011	92.587	0.578	1.000
Mid,Ambient - Ambient,Mid	0.026	0.012	78.425	2.195	0.419
Mid,Ambient - Mid,Mid	0.011	0.011	76.632	0.979	0.987
Mid,Ambient - High,Mid	0.009	0.011	82.139	0.796	0.997
Mid,Ambient - Ambient,High	0.019	0.012	77.507	1.671	0.762
Mid,Ambient - Mid,High	0.017	0.011	77.940	1.521	0.842
Mid,Ambient - High,High	0.007	0.012	71.435	0.594	1.000
High,Ambient - Ambient,Mid	0.019	0.011	77.513	1.685	0.754
High,Ambient - Mid,Mid	0.005	0.012	77.324	0.442	1.000
High,Ambient - High,Mid	0.003	0.011	82.741	0.254	1.000
High,Ambient - Ambient,High	0.013	0.011	77.031	1.149	0.964
High,Ambient - Mid,High	0.011	0.012	79.116	0.976	0.987
High,Ambient - High,High	0.001	0.012	70.619	0.079	1.000
Ambient,Mid - Mid,Mid	-0.014	0.012	61.815	-1.237	0.945
Ambient,Mid - High,Mid	-0.016	0.011	112.228	-1.547	0.830
Ambient,Mid - Ambient,High	-0.006	0.011	77.148	-0.544	1.000

Ambient, Mid - Mid, High	-0.008	0.012	84.615	-0.687	0.999
Ambient, Mid - High, High	-0.018	0.012	68.605	-1.592	0.806
Mid, Mid - High, Mid	-0.002	0.010	107.057	-0.211	1.000
Mid, Mid - Ambient, High	0.008	0.012	80.070	0.694	0.999
Mid, Mid - Mid, High	0.006	0.011	77.253	0.542	1.000
Mid, Mid - High, High	-0.004	0.012	75.072	-0.349	1.000
High, Mid - Ambient, High	0.010	0.011	84.960	0.896	0.993
High, Mid - Mid, High	0.008	0.011	83.025	0.741	0.998
High, Mid - High, High	-0.002	0.012	80.714	-0.168	1.000
Ambient, High - Mid, High	-0.002	0.010	203.816	-0.186	1.000
Ambient, High - High, High	-0.012	0.012	43.967	-1.062	0.977
Mid, High - High, High	-0.010	0.012	50.556	-0.865	0.994

Figure B.S 2 Fv/Fm for the history combinations of treatments at t=3 (18 weeks) after all fragments were moved to ambient conditions for a two-week period. Symbols represent origin treatment (at t=8 weeks) whereas x-axis distribution represent destination treatments (at t=16 weeks). Number of observations: total=288, tank=24, tray=62.

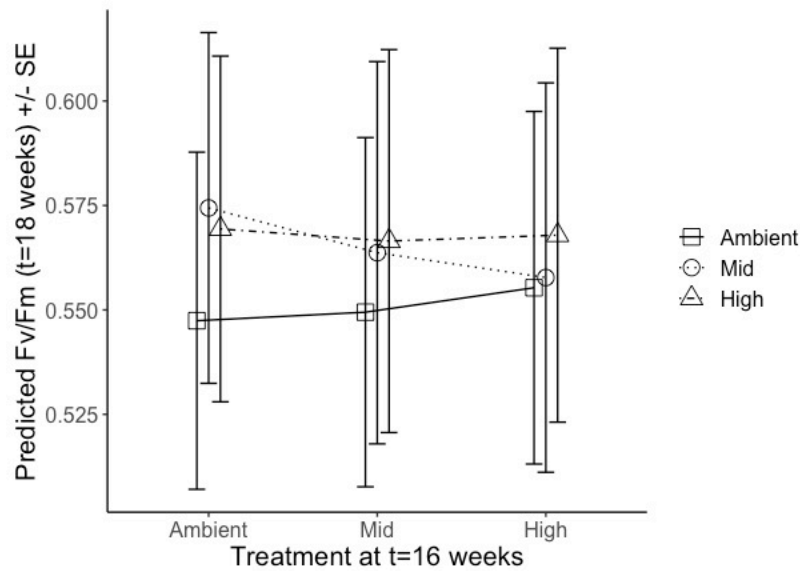


Table B.S 37 List of statistical models used to predict Fv/Fm of coral recruits relative to the exposure to treatment at t=23 weeks. The shaded area indicates the best-fit model.

Model	Fixed effect	Random effect	AICc	Akaike weights
1	Treatment (8 weeks) * treatment (16 weeks) * treatment (23 weeks) + log(size) (18 weeks)	Tray nested in tank (intercept)	-957.5451	0.069

2	Treatment (8 weeks) * treatment (16 weeks) * treatment (23 weeks) + log(size) (18 weeks)	Tank (intercept)	-959.8743	0.221
3	Treatment (8 weeks) * treatment (16 weeks) * treatment (23 weeks) + log(size) (18 weeks)	NA	-962.2059	0.710

Table B.S 38 Coefficients of the generalised linear mixed effect model predicting Fv/Fm of recruits among treatments at t=23 weeks. Number of observations: total=288.

	Estimate	Std. Error	z value	Pr(> z)
(Intercept) AMBIENT (8,16, 23 weeks)	0.44768	0.03834	11.68	<0.001
treat_4Acute	-0.30148	0.01494	-20.18	<0.001
treat_2Mid	-0.02058	0.01494	-1.38	0.1683
treat_2High	-0.00811	0.01496	-0.54	0.5878
treat_1Mid	0.00174	0.01499	0.12	0.9078
treat_1High	-0.00797	0.01497	-0.53	0.5944
yield_3	0.19744	0.06719	2.94	<0.001
treat_4Acute:treat_2Mid	0.14988	0.02117	7.08	<0.001
treat_4Acute:treat_2High	0.19270	0.02122	9.08	<0.001
treat_4Acute:treat_1Mid	0.08734	0.02117	4.13	<0.001
treat_4Acute:treat_1High	0.10167	0.02115	4.81	<0.001
treat_2Mid:treat_1Mid	0.03013	0.02115	1.42	0.1543
treat_2High:treat_1Mid	0.00971	0.02112	0.46	0.6458
treat_2Mid:treat_1High	0.00291	0.02112	0.14	0.8903
treat_2High:treat_1High	0.01372	0.02112	0.65	0.5159
treat_4Acute:treat_2Mid:treat_1Mid	-0.09816	0.02996	-3.28	0.0011
treat_4Acute:treat_2High:treat_1Mid	-0.15175	0.02990	-5.08	<0.001
treat_4Acute:treat_2Mid:treat_1High	-0.09375	0.02989	-3.14	0.0017
treat_4Acute:treat_2High:treat_1High	-0.16113	0.02995	-5.38	<0.001

Residual variance 0.042242, StdErr: 0.0017601

Table B.S 39 Tukey Posthoc Test estimates of pairwise comparisons among treatments for Fv/Fm at t=23 weeks; confidence level used: 0.95

contrast	estimate	SE	df	t.ratio	p.value
Ambient,Ambient,Ambient - Mid,Ambient,Ambient	-0.002	0.016	269.000	-0.112	1.000
Ambient,Ambient,Ambient - High,Ambient,Ambient	0.008	0.015	269.000	0.515	1.000
Ambient,Ambient,Ambient - Ambient,Mid,Ambient	0.021	0.015	269.000	1.332	0.997
Ambient,Ambient,Ambient - Mid,Mid,Ambient	-0.011	0.016	269.000	-0.717	1.000
Ambient,Ambient,Ambient - High,Mid,Ambient	0.026	0.016	269.000	1.651	0.974
Ambient,Ambient,Ambient - Ambient,High,Ambient	0.008	0.015	269.000	0.524	1.000
Ambient,Ambient,Ambient - Mid,High,Ambient	-0.003	0.015	269.000	-0.216	1.000
Ambient,Ambient,Ambient - High,High,Ambient	0.002	0.015	269.000	0.153	1.000
Ambient,Ambient,Ambient - Ambient,Ambient,Acute	0.301	0.015	269.000	19.503	<0.001
Ambient,Ambient,Ambient - Mid,Ambient,Acute	0.212	0.016	269.000	13.590	<0.001
Ambient,Ambient,Ambient - High,Ambient,Acute	0.208	0.016	269.000	13.345	<0.001
Ambient,Ambient,Ambient - Ambient,Mid,Acute	0.172	0.016	269.000	11.096	<0.001
Ambient,Ambient,Ambient - Mid,Mid,Acute	0.151	0.015	269.000	9.780	<0.001
Ambient,Ambient,Ambient - High,Mid,Acute	0.169	0.016	269.000	10.852	<0.001
Ambient,Ambient,Ambient - Ambient,High,Acute	0.117	0.015	269.000	7.553	<0.001
Ambient,Ambient,Ambient - Mid,High,Acute	0.170	0.016	269.000	10.864	<0.001
Ambient,Ambient,Ambient - High,High,Acute	0.171	0.015	269.000	11.025	<0.001
Mid,Ambient,Ambient - High,Ambient,Ambient	0.010	0.015	269.000	0.628	1.000
Mid,Ambient,Ambient - Ambient,Mid,Ambient	0.022	0.015	269.000	1.442	0.994
Mid,Ambient,Ambient - Mid,Mid,Ambient	-0.010	0.016	269.000	-0.614	1.000
Mid,Ambient,Ambient - High,Mid,Ambient	0.027	0.015	269.000	1.771	0.950
Mid,Ambient,Ambient - Ambient,High,Ambient	0.010	0.016	269.000	0.630	1.000

Mid,Ambient,Ambient - Mid,High,Ambient	-0.002	0.015	269.000	-0.103	1.000
Mid,Ambient,Ambient - High,High,Ambient	0.004	0.016	269.000	0.264	1.000
Mid,Ambient,Ambient - Ambient,Ambient,Acute	0.303	0.016	269.000	19.506	<0.001
Mid,Ambient,Ambient - Mid,Ambient,Acute	0.214	0.015	269.000	13.826	<0.001
Mid,Ambient,Ambient - High,Ambient,Acute	0.210	0.015	269.000	13.548	<0.001
Mid,Ambient,Ambient - Ambient,Mid,Acute	0.174	0.016	269.000	11.084	<0.001
Mid,Ambient,Ambient - Mid,Mid,Acute	0.153	0.015	269.000	9.864	<0.001
Mid,Ambient,Ambient - High,Mid,Acute	0.171	0.015	269.000	11.052	<0.001
Mid,Ambient,Ambient - Ambient,High,Acute	0.119	0.015	269.000	7.672	<0.001
Mid,Ambient,Ambient - Mid,High,Acute	0.172	0.015	269.000	11.077	<0.001
Mid,Ambient,Ambient - High,High,Acute	0.172	0.015	269.000	11.145	<0.001
High,Ambient,Ambient - Ambient,Mid,Ambient	0.013	0.015	269.000	0.815	1.000
High,Ambient,Ambient - Mid,Mid,Ambient	-0.019	0.016	269.000	-1.237	0.999
High,Ambient,Ambient - High,Mid,Ambient	0.018	0.015	269.000	1.143	1.000
High,Ambient,Ambient - Ambient,High,Ambient	0.000	0.016	269.000	0.009	1.000
High,Ambient,Ambient - Mid,High,Ambient	-0.011	0.015	269.000	-0.731	1.000
High,Ambient,Ambient - High,High,Ambient	-0.006	0.015	269.000	-0.362	1.000
High,Ambient,Ambient - Ambient,Ambient,Acute	0.294	0.016	269.000	18.905	<0.001
High,Ambient,Ambient - Mid,Ambient,Acute	0.204	0.016	269.000	13.187	<0.001
High,Ambient,Ambient - High,Ambient,Acute	0.200	0.015	269.000	12.913	<0.001
High,Ambient,Ambient - Ambient,Mid,Acute	0.164	0.016	269.000	10.487	<0.001
High,Ambient,Ambient - Mid,Mid,Acute	0.143	0.015	269.000	9.246	<0.001
High,Ambient,Ambient - High,Mid,Acute	0.161	0.015	269.000	10.417	<0.001
High,Ambient,Ambient - Ambient,High,Acute	0.109	0.015	269.000	7.046	<0.001
High,Ambient,Ambient - Mid,High,Acute	0.162	0.016	269.000	10.441	<0.001
High,Ambient,Ambient - High,High,Acute	0.163	0.015	269.000	10.521	<0.001
Ambient,Mid,Ambient - Mid,Mid,Ambient	-0.032	0.016	269.000	-2.035	0.849

Ambient, Mid, Ambient - High, Mid, Ambient	0.005	0.015	269.000	0.326	1.000
Ambient, Mid, Ambient - Ambient, High, Ambient	-0.012	0.016	269.000	-0.804	1.000
Ambient, Mid, Ambient - Mid, High, Ambient	-0.024	0.015	269.000	-1.548	0.986
Ambient, Mid, Ambient - High, High, Ambient	-0.018	0.015	269.000	-1.179	0.999
Ambient, Mid, Ambient - Ambient, Ambient, Acute	0.281	0.015	269.000	18.152	<0.001
Ambient, Mid, Ambient - Mid, Ambient, Acute	0.192	0.016	269.000	12.318	<0.001
Ambient, Mid, Ambient - High, Ambient, Acute	0.187	0.016	269.000	12.059	<0.001
Ambient, Mid, Ambient - Ambient, Mid, Acute	0.152	0.016	269.000	9.741	<0.001
Ambient, Mid, Ambient - Mid, Mid, Acute	0.131	0.015	269.000	8.446	<0.001
Ambient, Mid, Ambient - High, Mid, Acute	0.149	0.016	269.000	9.565	<0.001
Ambient, Mid, Ambient - Ambient, High, Acute	0.096	0.015	269.000	6.230	<0.001
Ambient, Mid, Ambient - Mid, High, Acute	0.149	0.016	269.000	9.584	<0.001
Ambient, Mid, Ambient - High, High, Acute	0.150	0.015	269.000	9.705	<0.001
Mid, Mid, Ambient - High, Mid, Ambient	0.037	0.016	269.000	2.380	0.623
Mid, Mid, Ambient - Ambient, High, Ambient	0.019	0.016	269.000	1.217	0.999
Mid, Mid, Ambient - Mid, High, Ambient	0.008	0.016	269.000	0.508	1.000
Mid, Mid, Ambient - High, High, Ambient	0.014	0.016	269.000	0.868	1.000
Mid, Mid, Ambient - Ambient, Ambient, Acute	0.313	0.016	269.000	19.788	<0.001
Mid, Mid, Ambient - Mid, Ambient, Acute	0.224	0.015	269.000	14.464	<0.001
Mid, Mid, Ambient - High, Ambient, Acute	0.219	0.015	269.000	14.144	<0.001
Mid, Mid, Ambient - Ambient, Mid, Acute	0.183	0.016	269.000	11.428	<0.001
Mid, Mid, Ambient - Mid, Mid, Acute	0.162	0.016	269.000	10.341	<0.001
Mid, Mid, Ambient - High, Mid, Acute	0.181	0.015	269.000	11.672	<0.001
Mid, Mid, Ambient - Ambient, High, Acute	0.128	0.016	269.000	8.217	<0.001
Mid, Mid, Ambient - Mid, High, Acute	0.181	0.015	269.000	11.713	<0.001
Mid, Mid, Ambient - High, High, Acute	0.182	0.016	269.000	11.657	<0.001
High, Mid, Ambient - Ambient, High, Ambient	-0.018	0.016	269.000	-1.119	1.000

High, Mid, Ambient - Mid, High, Ambient	-0.029	0.015	269.000	-1.871	0.920
High, Mid, Ambient - High, High, Ambient	-0.023	0.016	269.000	-1.500	0.990
High, Mid, Ambient - Ambient, Ambient, Acute	0.276	0.016	269.000	17.709	<0.001
High, Mid, Ambient - Mid, Ambient, Acute	0.187	0.015	269.000	12.070	<0.001
High, Mid, Ambient - High, Ambient, Acute	0.182	0.015	269.000	11.784	<0.001
High, Mid, Ambient - Ambient, Mid, Acute	0.147	0.016	269.000	9.311	<0.001
High, Mid, Ambient - Mid, Mid, Acute	0.125	0.016	269.000	8.086	<0.001
High, Mid, Ambient - High, Mid, Acute	0.144	0.015	269.000	9.291	<0.001
High, Mid, Ambient - Ambient, High, Acute	0.091	0.015	269.000	5.897	<0.001
High, Mid, Ambient - Mid, High, Acute	0.144	0.015	269.000	9.319	<0.001
High, Mid, Ambient - High, High, Acute	0.145	0.015	269.000	9.368	<0.001
Ambient, High, Ambient - Mid, High, Ambient	-0.011	0.016	269.000	-0.737	1.000
Ambient, High, Ambient - High, High, Ambient	-0.006	0.015	269.000	-0.371	1.000
Ambient, High, Ambient - Ambient, Ambient, Acute	0.293	0.015	269.000	18.970	<0.001
Ambient, High, Ambient - Mid, Ambient, Acute	0.204	0.016	269.000	12.926	<0.001
Ambient, High, Ambient - High, Ambient, Acute	0.200	0.016	269.000	12.703	<0.001
Ambient, High, Ambient - Ambient, Mid, Acute	0.164	0.015	269.000	10.613	<0.001
Ambient, High, Ambient - Mid, Mid, Acute	0.143	0.015	269.000	9.231	<0.001
Ambient, High, Ambient - High, Mid, Acute	0.161	0.016	269.000	10.224	<0.001
Ambient, High, Ambient - Ambient, High, Acute	0.109	0.016	269.000	6.992	<0.001
Ambient, High, Ambient - Mid, High, Acute	0.162	0.016	269.000	10.230	<0.001
Ambient, High, Ambient - High, High, Acute	0.162	0.016	269.000	10.447	<0.001
Mid, High, Ambient - High, High, Ambient	0.006	0.015	269.000	0.368	1.000
Mid, High, Ambient - Ambient, Ambient, Acute	0.305	0.015	269.000	19.688	<0.001
Mid, High, Ambient - Mid, Ambient, Acute	0.216	0.016	269.000	13.869	<0.001
Mid, High, Ambient - High, Ambient, Acute	0.211	0.016	269.000	13.611	<0.001
Mid, High, Ambient - Ambient, Mid, Acute	0.176	0.016	269.000	11.266	<0.001

Mid,High,Ambient - Mid,Mid,Acute	0.154	0.015	269.000	9.992	<0.001
Mid,High,Ambient - High,Mid,Acute	0.173	0.016	269.000	11.114	<0.001
Mid,High,Ambient - Ambient,High,Acute	0.120	0.015	269.000	7.778	<0.001
Mid,High,Ambient - Mid,High,Acute	0.173	0.016	269.000	11.131	<0.001
Mid,High,Ambient - High,High,Acute	0.174	0.015	269.000	11.254	<0.001
High,High,Ambient - Ambient,Ambient,Acute	0.299	0.015	269.000	19.348	<0.001
High,High,Ambient - Mid,Ambient,Acute	0.210	0.016	269.000	13.449	<0.001
High,High,Ambient - High,Ambient,Acute	0.205	0.016	269.000	13.202	<0.001
High,High,Ambient - Ambient,Mid,Acute	0.170	0.016	269.000	10.938	<0.001
High,High,Ambient - Mid,Mid,Acute	0.149	0.015	269.000	9.627	<0.001
High,High,Ambient - High,Mid,Acute	0.167	0.016	269.000	10.708	<0.001
High,High,Ambient - Ambient,High,Acute	0.115	0.015	269.000	7.403	<0.001
High,High,Ambient - Mid,High,Acute	0.167	0.016	269.000	10.722	<0.001
High,High,Ambient - High,High,Acute	0.168	0.015	269.000	10.876	<0.001
Ambient,Ambient,Acute - Mid,Ambient,Acute	-0.089	0.016	269.000	-5.677	<0.001
Ambient,Ambient,Acute - High,Ambient,Acute	-0.094	0.016	269.000	-5.998	<0.001
Ambient,Ambient,Acute - Ambient,Mid,Acute	-0.129	0.015	269.000	-8.349	<0.001
Ambient,Ambient,Acute - Mid,Mid,Acute	-0.150	0.015	269.000	-9.724	<0.001
Ambient,Ambient,Acute - High,Mid,Acute	-0.132	0.016	269.000	-8.439	<0.001
Ambient,Ambient,Acute - Ambient,High,Acute	-0.185	0.015	269.000	-11.910	<0.001
Ambient,Ambient,Acute - Mid,High,Acute	-0.132	0.016	269.000	-8.386	<0.001
Ambient,Ambient,Acute - High,High,Acute	-0.131	0.015	269.000	-8.446	<0.001
Mid,Ambient,Acute - High,Ambient,Acute	-0.005	0.015	269.000	-0.299	1.000
Mid,Ambient,Acute - Ambient,Mid,Acute	-0.040	0.016	269.000	-2.529	0.510
Mid,Ambient,Acute - Mid,Mid,Acute	-0.061	0.016	269.000	-3.925	0.013
Mid,Ambient,Acute - High,Mid,Acute	-0.043	0.015	269.000	-2.788	0.327
Mid,Ambient,Acute - Ambient,High,Acute	-0.096	0.016	269.000	-6.151	<0.001

Mid,Ambient,Acute - Mid,High,Acute	-0.043	0.015	269.000	-2.754	0.349
Mid,Ambient,Acute - High,High,Acute	-0.042	0.016	269.000	-2.692	0.392
High,Ambient,Acute - Ambient,Mid,Acute	-0.036	0.016	269.000	-2.253	0.716
High,Ambient,Acute - Mid,Mid,Acute	-0.057	0.016	269.000	-3.642	0.034
High,Ambient,Acute - High,Mid,Acute	-0.038	0.015	269.000	-2.488	0.541
High,Ambient,Acute - Ambient,High,Acute	-0.091	0.015	269.000	-5.868	<0.001
High,Ambient,Acute - Mid,High,Acute	-0.038	0.015	269.000	-2.453	0.568
High,Ambient,Acute - High,High,Acute	-0.037	0.015	269.000	-2.400	0.609
Ambient,Mid,Acute - Mid,Mid,Acute	-0.021	0.016	269.000	-1.355	0.997
Ambient,Mid,Acute - High,Mid,Acute	-0.003	0.016	269.000	-0.180	1.000
Ambient,Mid,Acute - Ambient,High,Acute	-0.055	0.016	269.000	-3.542	0.047
Ambient,Mid,Acute - Mid,High,Acute	-0.002	0.016	269.000	-0.146	1.000
Ambient,Mid,Acute - High,High,Acute	-0.002	0.016	269.000	-0.101	1.000
Mid,Mid,Acute - High,Mid,Acute	0.018	0.016	269.000	1.167	0.999
Mid,Mid,Acute - Ambient,High,Acute	-0.034	0.015	269.000	-2.214	0.742
Mid,Mid,Acute - Mid,High,Acute	0.019	0.016	269.000	1.199	0.999
Mid,Mid,Acute - High,High,Acute	0.019	0.015	269.000	1.258	0.999
High,Mid,Acute - Ambient,High,Acute	-0.052	0.016	269.000	-3.381	0.077
High,Mid,Acute - Mid,High,Acute	0.001	0.015	269.000	0.034	1.000
High,Mid,Acute - High,High,Acute	0.001	0.016	269.000	0.082	1.000
Ambient,High,Acute - Mid,High,Acute	0.053	0.016	269.000	3.410	0.070
Ambient,High,Acute - High,High,Acute	0.054	0.015	269.000	3.476	0.058
Mid,High,Acute - High,High,Acute	0.001	0.016	269.000	0.048	1.000

Appendix C – Chapter 4

C.1 Adult fragments: growth

Table C.S 1 List of statistical models used to assess growth among treatments during incubation period t=1 (4 weeks). The shaded area indicates the best-fit model.

Model	Fixed effects	Random effects	AICc	Akaike weights
1	treatment t=1	genotype (slope), tank (intercept)	-2261.29	<0.001
2	treatment t=1	genotype (slope)	-2263.39	<0.001
3	treatment t=1	--	-2139.01	<0.001
4	treatment t=1	genotype (intercept)	-2267.45	<0.001
5	treatment t=1 + size	genotype (intercept)	-2307.69	1.000

Table C.S 2 Coefficient estimates for the best-fit linear model predicting proportional growth rate at t=4 weeks. Asterisks indicate significant effects.

	Estimate	Std. Error	Z value	Pr(> z)	
(Intercept) (A)	0.05483	0.00425	12.91	<0.001	***
treatment 1 (M)	-0.00117	0.00133	-0.88	0.3773	
treatment 1 (H)	0.00343	0.00132	2.59	0.0095	***
log(size at t=0)	-0.01278	0.00191	-6.70	<0.001	***

Random effect variance(s):

Group=Genotype

	Variance	StdDev
(Intercept)	0.000	0.008

Residual variance: 0.010

Table C.S 3 Posthoc test estimates for growth at t=4 weeks for individual comparisons among treatments.

contrast	estimate	SE	df	t.ratio	p.value
ambient-mid	0.00117	0.00133	354	0.879	0.6542
ambient-high	-0.00343	0.00133	354	-2.584	0.0274
mid-high		0.00133	354	-3.465	0.0017

Table C.S 4 List of statistical models used to predict the difference in proportional linear extension between time t=8 and t=4 weeks [i.e., $(\log_{10} \left(\frac{Area_{t=2}}{Area_{t=1}} \right))$] among treatments during incubation period t=8, after transplantation occurred. The shaded area indicates the best-fit model.

Model	Fixed effect	Random effect	AICc	Akaike weights
1	Interaction treatment t=1 * t=2 + size	genotype (intercept)	-2310.26	1.000
2	Addition treatment t=1 + t=2 + size	genotype (intercept)	-2016.09	<0.001
3	Treatment t=2 + size	genotype (intercept)	-2009.21	<0.001

Table C.S 5 Coefficient estimates for the linear model comparing proportional linear extension of fragments under the different treatments at t=8 in relation to the exposure of their previous treatment at t=4. Asterisks indicate significant effects.

	Estimate	Std. Error	Z value	Pr (> z)	
(Intercept) (1 ambient, 2 ambient)	0.058624	0.004340	13.51	<0.001	***
treatment 2(mid)	0.011451	0.002270	5.04	<0.001	***
treatment 2(high)	0.005900	0.002287	2.58	0.0099	***
treatment 1(mid)	0.009251	0.002280	4.06	<0.001	***
treatment 1(high)	0.013170	0.002279	5.78	<0.001	***

log(size t=1)	-0.018078	0.001953	-9.26	<0.001	***
treatment 2(mid): treatment 1(mid)	-0.013959	0.003208	-4.35	<0.001	***
treatment 2(high): treatment 1(mid)	0.000186	0.003209	0.06	0.9538	
treatment 2(mid): treatment 1(high)	-0.011597	0.003208	-3.62	<0.001	***
treatment 2(high): treatment 1(high)	-0.015392	0.003224	-4.77	<0.001	***

Random effect variance(s):

Group=Genotype

	Variance	StdDev
(Intercept)	0.000	0.007

Residual variance: 0.010

Table C.S 6 Post Hoc results of coefficient estimates for the linear model comparing predicted growth of fragments under the different treatments at t=8 in relation to the exposure of their previous treatment at t=4 (treatment combinations). Asterisks indicate significant effects.

contrast	estimate	SE	df	t.ratio	p.value	
amb,amb - mid, amb	-1.14E-02	2.30E-03	348	-4.980	<0.001	*
amb, amb - high, amb	-5.89E-03	2.32E-03	349	-2.547	0.2137	
mid, amb - high, amb	5.55E-03	2.30E-03	348	2.410	0.2816	
amb, mid - high, mid	-6.08E-03	2.30E-03	348	-2.643	0.1727	
amb, mid - mid, mid	2.50E-03	2.30E-03	348	1.092	0.9751	
mid, mid - high, mid	-8.59E-03	2.30E-03	348	-3.735	0.0067	*
amb, high - mid, high	-0.14E-03	2.30E-03	348	-0.063	1.0000	
amb, high - high, high	9.49E-03	2.30E-03	348	4.133	0.0015	*
mid, high - high, high	9.34E-03	2.30E-03	348	4.069	0.0019	*

Figure C.S 1 Residuals of the random intercept of the best-fit model predicting growth after transplantation. Grey line represents what is the expected change on linear extension in relation to the model, with values below this considered worse than the expected and with values above the line considered better than the expected.

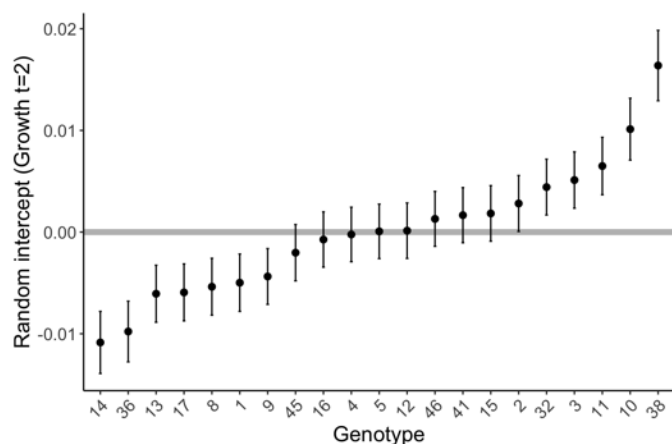


Table C.S 7 Summary statistics of the linear mixed effect models testing for acclimation at t=8, considering all treatment combinations.

ambient-ambient

	Estimate	Std. Error	t value
(Intercept)	0.054174	0.007255	7.467
time2	-0.006537	0.002115	-3.092
log(Size)	-0.012368	0.003754	-3.295

ambient-mid

	Estimate	Std. Error	t value
(Intercept)	0.052734	0.007729	6.823
time2	0.005863	0.002264	2.589
log(Size)	-0.012294	0.003826	-3.213

ambient-high

	Estimate	Std. Error	t value
(Intercept)	0.078266	0.011248	6.958
time2	-0.001575	0.002543	-0.619
log(Size)	-0.023935	0.005483	-4.365

mid-ambient

	Estimate	Std. Error	t value
(Intercept)	0.0536525	0.0095370	5.626
time2	0.0007649	0.0024744	0.309
log(Size)	-0.0115032	0.0046882	-2.454

mid-mid

	Estimate	Std. Error	t value
(Intercept)	0.0706108	0.0092628	7.623
time2	-0.0008699	0.0027772	-0.313
log(Size)	-0.0202064	0.0045361	-4.455

mid-high

	Estimate	Std. Error	t value
(Intercept)	0.063879	0.012285	5.200
time2	0.014142	0.002367	5.975
log(Size)	-0.019985	0.005788	-3.453

high-ambient

	Estimate	Std. Error	t value
(Intercept)	0.065467	0.011981	5.464

time2	0.002095	0.003053	0.686
log(Size)	-0.016007	0.005944	-2.693

high-mid

	Estimate	Std. Error	t value
(Intercept)	0.053118	0.008501	6.248
time2	0.007244	0.002082	3.479
log(Size)	-0.012580	0.004137	-3.041

high-high

	Estimate	Std. Error	t value
(Intercept)	0.061660	0.007626	8.085
time2	-0.010552	0.002370	-4.452
log(Size)	-0.012548	0.003786	-3.314

Table C.S 8 List of statistical models predicting linear growth at t=10 weeks (all fragments under ambient treatment for 2 weeks) relative to the exposure to previous treatments at t=4 and t=8. The shaded area indicates the best-fit model.

Model	Fixed effect	Random effect	AICc	Akaike weights
1	Interaction treatment t=1 * t=2 + size	genotype (intercept)	-2555.24	0.732
2	Interaction treatment t=1 * t=2 + size	genotype (intercept), tank (intercept)	-2553.24	0.268
3	Interaction treatment t=1 * t=2 + size	tank (intercept)	-2469.20	<0.001
4	Interaction treatment t=1 * t=2 + size	NA	-2470.83	<0.001

Table C.S 9 Coefficient estimates for the best-fit linear model predicting the linear growth at t=10 weeks as a function of treatment at t=4 weeks and treatment at t=8 weeks and size at t=8 weeks. Asterisks indicate significant effects. Total observations=378, genotypes=21

	Estimate	Std. Error	z value	Pr(> z)
--	----------	------------	---------	----------

(Intercept) (1amb, 2amb)	0.038163	0.003292	11.59	< 0.001
treat_2M (2mid)	-0.001304	0.001644	-0.79	0.428
treat_2H (2high)	-0.000400	0.001656	-0.24	0.809
treat_1M (1mid)	-0.000250	0.001652	-0.15	0.880
treat_1H (1high)	0.002796	0.001653	1.69	0.091
log(t2) (size, t=8weeks)	-0.011378	0.001462	-7.78	< 0.001
treat_2M:treat_1M	0.003513	0.002322	1.51	0.130
treat_2H:treat_1M	0.001225	0.002321	0.53	0.598
treat_2M:treat_1H	-0.000374	0.002321	-0.16	0.872
treat_2H:treat_1H	-0.000365	0.002337	-0.16	0.876

Random effect variance(s):

Group=Genotype

	Variance	StdDev
(Intercept)	2.347e-05	0.004845

Residual variance: 0.007

Table C.S 10 Tukey Post hoc test estimates of all combinations of treatments confirming no significant differences on growth at t=10 weeks

contrast	estimate	SE	df	t.ratio	p.value
Ambient,Ambient - Mid,Ambient	0.000	0.002	348.596	0.149	1.000
Ambient,Ambient - High,Ambient	-0.003	0.002	348.646	-1.670	0.765
Ambient,Ambient - Ambient,Mid	0.001	0.002	348.223	0.783	0.997
Ambient,Ambient - Mid,Mid	-0.002	0.002	348.615	-1.171	0.962
Ambient,Ambient - High,Mid	-0.001	0.002	348.724	-0.667	0.999
Ambient,Ambient - Ambient,High	0.000	0.002	348.790	0.239	1.000
Ambient,Ambient - Mid,High	-0.001	0.002	349.594	-0.339	1.000
Ambient,Ambient - High,High	-0.002	0.002	348.342	-1.218	0.952

Mid,Ambient - High,Ambient	-0.003	0.002	348.004	-1.834	0.659
Mid,Ambient - Ambient,Mid	0.001	0.002	348.097	0.634	0.999
Mid,Ambient - Mid,Mid	-0.002	0.002	348.003	-1.331	0.922
Mid,Ambient - High,Mid	-0.001	0.002	348.010	-0.823	0.996
Mid,Ambient - Ambient,High	0.000	0.002	348.018	0.091	1.000
Mid,Ambient - Mid,High	-0.001	0.002	348.271	-0.495	1.000
Mid,Ambient - High,High	-0.002	0.002	348.040	-1.373	0.907
High,Ambient - Ambient,Mid	0.004	0.002	348.118	2.465	0.253
High,Ambient - Mid,Mid	0.001	0.002	348.003	0.503	1.000
High,Ambient - High,Mid	0.002	0.002	348.005	1.011	0.985
High,Ambient - Ambient,High	0.003	0.002	348.011	1.925	0.597
High,Ambient - Mid,High	0.002	0.002	348.239	1.333	0.921
High,Ambient - High,High	0.001	0.002	348.054	0.461	1.000
Ambient,Mid - Mid,Mid	-0.003	0.002	348.105	-1.963	0.570
Ambient,Mid - High,Mid	-0.002	0.002	348.154	-1.456	0.875
Ambient,Mid - Ambient,High	-0.001	0.002	348.185	-0.543	1.000
Ambient,Mid - Mid,High	-0.002	0.002	348.672	-1.122	0.971
Ambient,Mid - High,High	-0.003	0.002	348.016	-2.008	0.539
Mid,Mid - High,Mid	0.001	0.002	348.008	0.507	1.000
Mid,Mid - Ambient,High	0.002	0.002	348.015	1.421	0.889
Mid,Mid - Mid,High	0.001	0.002	348.259	0.831	0.996
Mid,Mid - High,High	0.000	0.002	348.045	-0.042	1.000
High,Mid - Ambient,High	0.002	0.002	348.005	0.914	0.992
High,Mid - Mid,High	0.001	0.002	348.194	0.326	1.000
High,Mid - High,High	-0.001	0.002	348.078	-0.549	1.000
Ambient,High - Mid,High	-0.001	0.002	348.162	-0.586	1.000
Ambient,High - High,High	-0.002	0.002	348.101	-1.462	0.872
Mid,High - High,High	-0.001	0.002	348.503	-0.871	0.994

Figure C.S 2 Mean linear growth for the history combinations of treatments at t=10 weeks after all fragments were moved to ambient conditions. Symbols represent origin treatment whereas x-axis distribution represent destination treatments. Number of observations: total=378, number of genotypes=21.

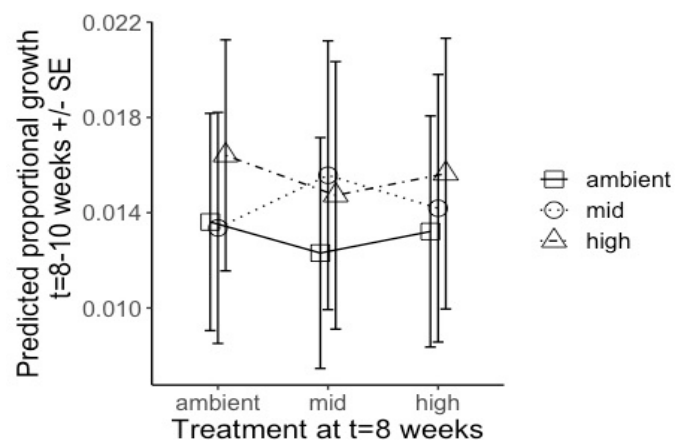


Table C.S 11 List of statistical models predicting linear growth at t=14 (fragments under acute or ambient treatment) relative to the exposure to previous treatments at t=4 and t=8. The shaded area indicates the best-fit model.

Model	Fixed effect	Random effect	AICc	Akaike weights
1	Interaction treatment t=1 * t=2 * t=4 + size	genotype (intercept), tank (intercept)	-2047.88	0.267
2	Interaction treatment t=1 * t=2 * t=4 + size	genotype (intercept)	-2049.98	0.671
3	Interaction treatment t=1 * t=2 * t=4 + size		-1830.83	<0.001
4	Interaction treatment t=1 * t=2 * t=4		-1721.91	<0.001
5	Interaction treatment t=1 * t=2 + interaction t=1 * t=4 + interaction t=2 * t=4 + size	genotype (intercept)	-2042.72	0.169
6	Addition treatment t=1 + t=2 + t=4 + size	genotype (intercept)	-2044.83	0.442

Table C.S 12 Coefficient estimates for the best-fit linear model predicting the linear growth at t=14 as a function of treatment at t=4 and treatment at t=8 and size at t=10 weeks. Asterisks indicate significant effects.

	Estimate	Std. Error	z value	Pr(> z)	
(Intercept) (4Amb, 1A, 2A)	0.120656	0.007151	16.87	<2e-16	***
treatment (4ACUTE)	-0.012136	0.004307	-2.82	0.0048	**
treatment 2 (M)	-0.001965	0.004321	-0.45	0.6492	
treatment 2 (H)	-0.001256	0.004318	-0.29	0.7711	
treatment 1 (M)	-0.004451	0.004322	-1.03	0.3031	
treatment 1 (H)	0.006981	0.004318	1.62	0.1060	
log(size t=3)	-0.034187	0.002862	-11.95	<2e-16	***
treatment 4 (ACU): treatment 2 (M)	0.016013	0.006094	2.63	0.0086	**
treatment 4 (ACU): treatment 2 (H)	0.010426	0.006073	1.72	0.0860	.
treatment 4 (ACU): treatment 1 (M)	0.015130	0.006077	2.49	0.0128	*
treatment 4 (ACU): treatment 1 (H)	-0.005306	0.006073	-0.87	0.3823	
treatment 2 (M): treatment 1 (M)	0.005932	0.006090	0.97	0.3301	
treatment 2 (H): treatment 1 (M)	0.008572	0.006077	1.41	0.1584	
treatment 2 (M): treatment 1 (H)	-0.006403	0.006090	-1.05	0.2931	
treatment 2 (H): treatment 1 (H)	0.004316	0.006097	0.71	0.4791	
treatment 4 (ACU): treatment 2 (M): treatment 1 (M)	-0.027309	0.008604	-3.17	0.0015	**
treatment 4 (Ac): treatment 2 (H): treatment 1 (M)	-0.026964	0.008589	-3.14	0.0017	**
treatment 4 (Ac): treatment 2 (M): treatment 1 (H)	-0.000404	0.008602	-0.05	0.9626	
treatment 4 (Ac): treatment 2 (H): treatment 1 (H)	-0.005391	0.008588	-0.63	0.5302	

Random effect variance(s):

Group=Genotype

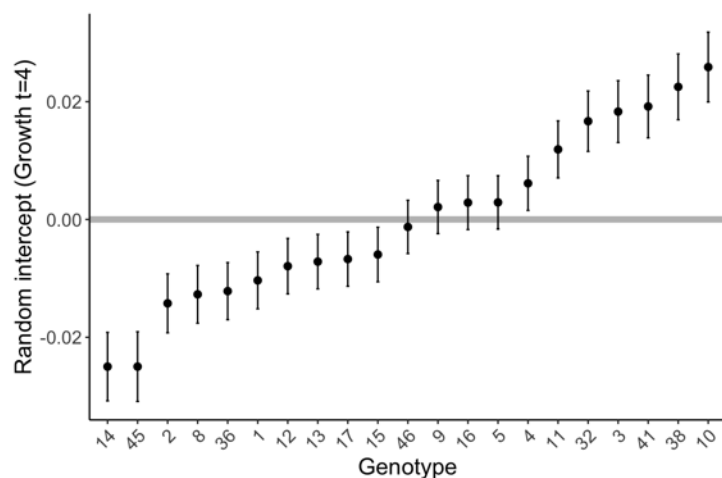
	Variance	StdDev
(Intercept)	0.000	0.015

Residual variance: 0.014

Table C.S 13 Tukey Post hoc test estimates of growth rate at t=14 considering combinations of treatments.

contrast	estimate	SE	df	t.ratio	p.value	
A,A,A - A,A,ACU	0.01214	0.00442	339.09534	2.74606	0.35314	
M,A,A - M,A,ACU	-0.00299	0.00441	339.01220	-0.67922	1.00000	
H,C,A - H,C, ACU	0.01744	0.00441	339.06126	3.95077	0.01135	***
C,M,A - C,M,ACU	-0.00388	0.00441	339.02994	-0.87903	0.99999	
M,M,A - M,M, ACU	0.00830	0.00441	339.01247	1.88326	0.91621	
H,M,A - H,M, ACU	0.00183	0.00441	339.05271	0.41522	1.00000	
A,H,A - C,H, ACU	0.00171	0.00442	339.08466	0.38706	1.00000	
M,H,A - M,H, ACU	0.01354	0.00441	339.02517	3.07134	0.17378	
H,H,A - H,H, ACU	0.01241	0.00441	339.03840	2.81216	0.31037	

Figure C.S 3 Residuals of the random intercept of the best-fit model predicting linear growth during heat stress exposure. Grey line represents what is the expected change on linear extension in relation to the model, with values below this considered worse than the expected and with values above the line considered better than the expected.



C.2Adult fragments: Fv/Fm

Table C.S 14 List of statistical models used to assess maximum quantum yield (Fv/Fm) among treatments during incubation period t=4 weeks. The shaded area indicates the best-fit model.

Model	Fixed effects	Random effects	Df	AICc	Akaike weights
1	treatment t=1 + size + Y.II t=0	genotype (intercept), tank (intercept), position (intercept), position (slope)	11	-6219.86	0.034
2	treatment t=1 + size + Y.II t=0	genotype (intercept), tank (intercept), position (intercept)	9	-6223.88	0.259
3	treatment t=1 + size + Y.II t=0	tank (intercept), position (intercept)	8	-5936.04	<0.001
4	treatment t=1 + size + Y.II t=0	genotype (intercept), position (intercept)	8	-6225.88	0.705

5	treatment t=1 + size + Y.II t=0	genotype (intercept), tank (intercept)	8	-5968.66	<0.001
6	treatment t=1 + size + Y.II t=0	position (intercept)	7	-5918.84	<0.001
7	treatment t=1 + size + Y.II t=0	genotype (intercept)	7	-5970.66	<0.001
8	treatment t=1 + size + Y.II t=0	-	6	-5765.80	<0.001

Table C.S 15 Coefficient estimates for the best-fit linear model predicting Fv/Fm at t=4 as a function of treatment at t=4 weeks, Fv/fm at t=0 and size at t=4 weeks. Asterisks indicate significant effects.

	Estimate	Std. Error	z value	Pr(> z)	
(Intercept) (ambient)	0.42922	0.02604	16.48	< 2e-16	*
Y.II.0 Fv/Fm	0.15000	0.04088	3.67	0.00024	*
log(t1) size	0.03134	0.00345	9.09	< 2e-16	*
treat_1 (high)	-0.04535	0.00224	-20.27	< 2e-16	*
treat_1 (mid)	-0.01981	0.00225	-8.80	< 2e-16	*

Random effect variance(s):

Group=Genotype

	Variance	StdDev
(Intercept)	0.000	0.021

Residual variance: 0.037

Table C.S 16 Tukey Post hoc test estimates of Fv/Fm at t=4 weeks considering comparisons between treatments.

contrast	estimate	SE	df	t.ratio	p.value
A - H	0.0453	0.00224	1669	20.245	<.0001
A - M	0.0198	0.00225	1669	8.784	<.0001
H - M	-0.0255	0.00224	1668	-11.426	<.0001

Table C.S 17 List of statistical models used to predict maximum quantum yield [Fv/Fm] at time t=8 weeks relative to treatment t=4 weeks, i.e., after transplantaion occurred. The shaded area indicates the best-fit model.

Model	Fixed effects	Random effects	Df	AICc	Akaike weights
1	Interaction treatment t=1 * t=2 + size + Y.II t=1	genotype (intercept), tank (intercept), position (intercept), position (slope)	15	-6151.18	0.270
2	Interaction treatment t=1 * t=2 + size + Y.II t=1	genotype (intercept), tank (intercept), position (intercept)	14	-6151.18	0.196
3	Interaction treatment t=1 * t=2 + size + Y.II t=1	tank (intercept), position (intercept)	14	-5842.64	<0.001
4	Interaction treatment t=1 * t=2 + size + Y.II t=1	genotype (intercept), position (intercept)	14	-6153.18	0.533
5	Interaction treatment t=1 * t=2 + size + Y.II t=1	genotype (intercept), tank (intercept),	14	-5924.26	<0.001
6	Interaction treatment t=1 * t=2 + size + Y.II t=1	position (intercept)	13	-5820.90	<0.001
7	Interaction treatment t=1 * t=2 + size + Y.II t=1	genotype (intercept)	13	-5926.26	<0.001
8	Interaction treatment t=1 * t=2 + size + Y.II t=1	-	12	-5726.84	<0.001

Table C.S 18 Coefficient estimates for the best-fit linear model predicting Fv/Fm at t=8 weeks as a function of treatment at t=8 weeks, treatment at t=4 weeks, Fv/Fm at t=4 and size at t=8. Asterisks indicate significant effects.

	Estimate	Std. Error	z value	Pr(> z)	
(Intercept)	0.45050	0.01785	25.23	< 2e-16	***
Y.II.1 (t=4 weeks)	0.11026	0.02756	4.00	6.3e-05	***
treat_1H	0.02299	0.00448	5.13	2.9e-07	***
treat_1M	-0.00181	0.00399	-0.45	0.64965	
treat_2H	-0.05613	0.00397	-14.14	< 2e-16	***
treat_2M	-0.03250	0.00393	-8.27	< 2e-16	***
log(t2)	0.02068	0.00381	5.43	5.5e-08	***

treat_1H:treat_2H	0.01489	0.00586	2.54	0.01110	*
treat_1M:treat_2H	0.00599	0.00555	1.08	0.28098	
treat_1H:treat_2M	0.01907	0.00561	3.40	0.00067	***
treat_1M:treat_2M	0.02245	0.00555	4.05	5.2e-05	***

Random effect variance(s):

Group=Genotype

	Variance	StdDev
(Intercept)	0.000	0.023

Residual variance: 0.038

Group=position

	Variance	StdDev
(Intercept)	0.000	0.023

Residual variance: 0.038

Table C.S 19 Tukey Post hoc test estimates of Fv/Fm at t=8 considering comparisons between treatments at t=4 and treatment at t=8 weeks.

contrast	estimate	SE	df	t.ratio	p.value	
AA – HA amb, amb - high, amb	-0.02294	0.00448	1677	-5.123	<.0001	*
AA – MA amb,amb - mid, amb	0.00183	0.00400	1665	0.457	1.0000	
AA - AH	0.05613	0.00398	1663	14.102	<.0001	*
AA - HH	0.01825	0.00396	1663	4.609	0.0002	
AA - MH	0.05197	0.00403	1666	12.885	<.0001	*
AA - AM	0.03250	0.00394	1662	8.249	<.0001	*
AA - HM	-0.00953	0.00412	1669	-2.312	0.3353	
AA - MM	0.01187	0.00397	1663	2.992	0.0694	

HA – MA high, amb - mid, amb	0.02477	0.00421	1670	5.881	<.0001	*
HA - AH	0.07907	0.00449	1675	17.593	<.0001	*
HA - HH	0.04119	0.00433	1673	9.508	<.0001	*
HA - MH	0.07491	0.00426	1670	17.564	<.0001	*
HA - AM	0.05544	0.00456	1679	12.154	<.0001	*
HA - HM	0.01341	0.00405	1666	3.310	0.0266	
HA - MM	0.03481	0.00432	1673	8.057	<.0001	*
MA - AH	0.05430	0.00400	1664	13.582	<.0001	*
MA - HH	0.01642	0.00395	1662	4.160	0.0011	*
MA - MH	0.05014	0.00396	1662	12.677	<.0001	*
MA - CM	0.03067	0.00403	1666	7.615	<.0001	*
MA - HM	-0.01136	0.00397	1663	-2.858	0.0998	
MA - MM	0.01004	0.00395	1662	2.545	0.2114	
AH - HH amb, high - high, high	-0.03788	0.00396	1663	-9.563	<.0001	*
AH - MH amb, high - mid, high	-0.00416	0.00398	1664	-1.047	0.9812	
AH - AM	-0.02363	0.00398	1664	-5.932	<.0001	*
AH - HM	-0.06566	0.00412	1667	-15.947	<.0001	*
AH - MM	-0.04426	0.00396	1663	-11.178	<.0001	*
HH - MH mid, high - high, high	0.03372	0.00396	1663	8.509	<.0001	*
HH - AM	0.01425	0.00398	1664	3.583	0.0105	
HH - HM	-0.02778	0.00403	1665	-6.896	<.0001	*
HH - MM	-0.00638	0.00394	1662	-1.621	0.7933	
MH - AM	-0.01947	0.00406	1667	-4.795	0.0001	
MH - HM	-0.06150	0.00400	1664	-15.382	<.0001	*
MH - MM	-0.04010	0.00396	1663	-10.138	<.0001	*
AM - HM amb, mid - high, mid	-0.04203	0.00417	1671	-10.067	<.0001	*
AM - MM amb, mid - mid, mid	-0.02063	0.00399	1664	-5.176	<.0001	*
HM - MM mid, mid - high, mid	0.02140	0.00402	1665	5.321	<.0001	*

Figure C.S 4 Residuals of the random intercept of the best-fit model predicting maximum quantum yield (Fv/Fm) after transplantation. Grey line represents what is the expected change on maximum quantum yield (Fv/Fm) in relation to the model, with values below this considered worse than the expected and with values above the line considered better than the expected.

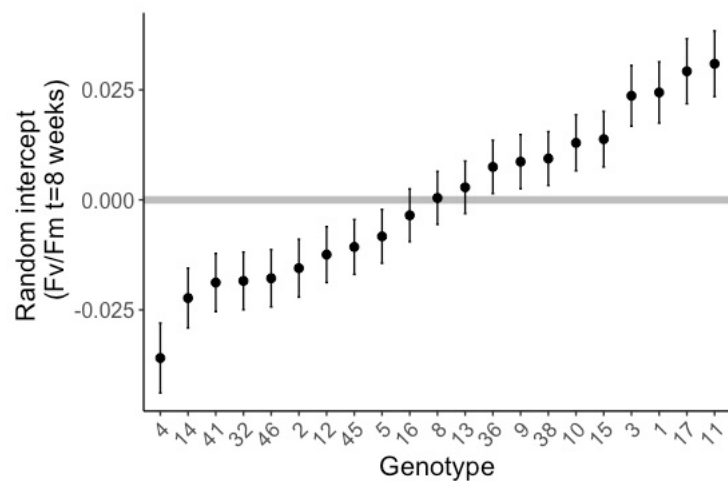


Table C.S 20 Summary statistics of the linear mixed effect models using Fv/Fm testing for acclimation at t=2, considering all treatment combinations.

ambient-ambient

	Estimate	Std. Error	t value
(Intercept)	0.541230	0.030203	17.920
time2	-0.023129	0.003775	-6.126
log(Size)	0.018805	0.014916	1.261

ambient-mid

	Estimate	Std. Error	t value
--	----------	------------	---------

(Intercept)	0.545865	0.029775	18.333
time2	-0.061650	0.003168	-19.462
log(Size)	0.019806	0.014435	1.372

ambient-high

	Estimate	Std. Error	t value
(Intercept)	0.5888567	0.0684762	8.599
time2	-0.0827731	0.0033371	-24.804
log(Size)	-0.0007026	0.0314501	-0.022

mid-ambient

	Estimate	Std. Error	t value
(Intercept)	0.518489	0.039705	13.058
time2	-0.007241	0.004016	-1.803
log(Size)	0.020335	0.018493	1.100

mid-mid

	Estimate	Std. Error	t value
(Intercept)	0.5699778	0.0422909	13.478
time2	-0.0253723	0.0036160	-7.017
log(Size)	0.0006308	0.0199545	0.032

mid-high

	Estimate	Std. Error	t value
(Intercept)	0.578308	0.043030	13.440

time2	-0.060886	0.002941	-20.700
log(Size)	-0.004379	0.019366	-0.226

high-ambient

	Estimate	Std. Error	t value
(Intercept)	0.464059	0.058920	7.876
time2	0.065920	0.003679	17.920
log(Size)	0.020398	0.027565	0.740

high-mid

	Estimate	Std. Error	t value
(Intercept)	0.537410	0.043730	12.289
time2	0.022340	0.004645	4.809
log(Size)	0.002332	0.020252	0.115

high-high

	Estimate	Std. Error	t value
(Intercept)	0.500283	0.039420	12.691
time2	-0.034409	0.003131	-10.989
log(Size)	0.034505	0.018591	1.856

Resetting to ambient conditions t=10 weeks

Table C.S 21 List of statistical models predicting Fv/Fm at t=10 (all fragments under ambient treatment for 2 weeks) relative to the exposure to previous treatments at t=4 and t=8. The shaded area indicates the best-fit model.

Model	Fixed effect	Random effect	AICc	Akaike weights
1	Interaction treatment t=1 * t=2 + size + Fv/Fm t=2	genotype (intercept), tank (intercept), position (intercept)	-6106.16	0.331
2	Addition treatment t=1 + t=2 + size + Fv/Fm t=2	genotype (intercept), tank (intercept), position (intercept)	-5983.62	<0.001
3	Interaction treatment t=1 * t=2 + size + Fv/Fm t=2	genotype (intercept), position (intercept)	-6107.56	0.668
4	Interaction treatment t=1 * t=2 + size + Fv/Fm t=2	tank (intercept), position (intercept)	-5772.44	<0.001
5	Interaction treatment t=1 * t=2 + size + Fv/Fm t=2	genotype (intercept), tank (intercept)	-6026.12	<0.001
6	Interaction treatment t=1 * t=2 + size + Fv/Fm t=2	position (intercept)	-5772.84	<0.001
7	Interaction treatment t=1 * t=2 + size + Fv/Fm t=2	genotype (intercept)	-6027.66	<0.001
8	Interaction treatment t=1 * t=2 + size + Fv/Fm t=2	-	-5761.76	<0.001

Table C.S 22 Coefficient estimates for the best-fit linear model predicting Fv/Fm at t=10 as a function of treatment at t=4 and treatment at t=8 and size at t=8 weeks. Asterisks indicate significant effects.

	Estimate	Std. Error	z value	Pr(> z)	
(Intercept)	0.32811	0.01636	20.06	< 2e-16	***
Y.II.2	0.28206	0.02509	11.24	< 2e-16	***
treat_1H	-0.02044	0.00404	-5.06	4.1e-07	***
treat_1M	-0.01193	0.00401	-2.98	0.0029	**
treat_2H	0.03782	0.00427	8.86	< 2e-16	***
treat_2M	-0.00862	0.00407	-2.12	0.0340	*
log(t3)	0.02420	0.00386	6.26	3.7e-10	***
treat_1H:treat_2H	0.01085	0.00572	1.90	0.0578	.
treat_1M:treat_2H	-0.04053	0.00564	-7.18	6.9e-13	***
treat_1H:treat_2M	0.02576	0.00567	4.55	5.5e-06	***
treat_1M:treat_2M	0.01206	0.00567	2.13	0.0334	*

Random effect variance(s):

Group=Genotype

	Variance	StdDev
(Intercept)	0.000	0.011

Residual variance: 0.038

Group=position

	Variance	StdDev
(Intercept)	0.000	0.010

Residual variance: 0.038

Table C.S 23 Tukey Post hoc test estimates of all combinations of treatments testing significant differences on Fv/Fm at t=10 weeks.

contrast	estimate	SE	df	t.ratio	p.value	
amb,amb - high,amb	0.020	0.004	1663.183	5.048	0.000	*
amb,amb - mid,amb	0.012	0.004	1662.683	2.971	0.074	
amb,amb - amb,high	-0.038	0.004	1673.625	-8.849	0.000	*
amb,amb - high,high	-0.028	0.004	1664.149	-6.982	0.000	*
amb,amb - mid,high	0.015	0.004	1674.145	3.431	0.018	
amb,amb - amb,mid	0.009	0.004	1665.329	2.120	0.460	
amb,amb - high,mid	0.003	0.004	1662.916	0.818	0.996	
amb,amb - mid,mid	0.009	0.004	1663.581	2.108	0.468	
high,amb - mid,amb	-0.008	0.004	1663.093	-2.110	0.467	
high,amb - amb,high	-0.058	0.004	1674.878	-13.362	0.000	*
high,amb - high,high	-0.049	0.004	1665.482	-11.898	0.000	*
high,amb - mid,high	-0.006	0.004	1675.153	-1.322	0.925	

high,amb - amb,mid	-0.012	0.004	1667.910	-2.813	0.112	
high,amb - high,mid	-0.017	0.004	1662.326	-4.277	0.001	*
high,amb - mid,mid	-0.012	0.004	1664.423	-2.941	0.080	
mid,amb - amb,high	-0.050	0.004	1670.774	-11.830	0.000	*
mid,amb - high,high	-0.040	0.004	1662.792	-9.994	0.000	*
mid,amb - mid,high	0.003	0.004	1671.093	0.656	0.999	
mid,amb - amb,mid	-0.003	0.004	1664.418	-0.808	0.997	
mid,amb - high,mid	-0.009	0.004	1662.283	-2.154	0.437	
mid,amb - mid,mid	-0.003	0.004	1662.321	-0.858	0.995	
amb,high - high,high	0.010	0.004	1667.198	2.329	0.325	
amb,high - mid,high	0.052	0.004	1662.111	13.105	0.000	*
amb,high - amb,mid	0.046	0.004	1666.290	11.348	0.000	*
amb,high - high,mid	0.041	0.004	1672.497	9.621	0.000	*
amb,high - mid,mid	0.046	0.004	1668.379	11.181	0.000	*
high,high - mid,high	0.043	0.004	1667.552	10.433	0.000	*
high,high - amb,mid	0.037	0.004	1662.718	9.151	0.000	*
high,high - high,mid	0.032	0.004	1663.852	7.784	0.000	*
high,high - mid,mid	0.037	0.004	1662.128	9.171	0.000	*
mid,high - amb,mid	-0.006	0.004	1666.970	-1.471	0.869	
mid,high - high,mid	-0.011	0.004	1672.730	-2.673	0.158	
mid,high - mid,mid	-0.006	0.004	1668.667	-1.496	0.858	
amb,mid - high,mid	-0.005	0.004	1666.071	-1.290	0.934	
amb,mid - mid,mid	0.000	0.004	1663.341	-0.034	1.000	
high,mid - mid,mid	0.005	0.004	1663.056	1.291	0.934	

Figure C.S 5 Mean Fv/Fm for the history combinations of treatments at t=3 after all fragments were moved to ambient conditions. Symbols represent origin treatment whereas x-axis distribution represent destination treatments. Number of observations: total=378, number of genotypes=21.

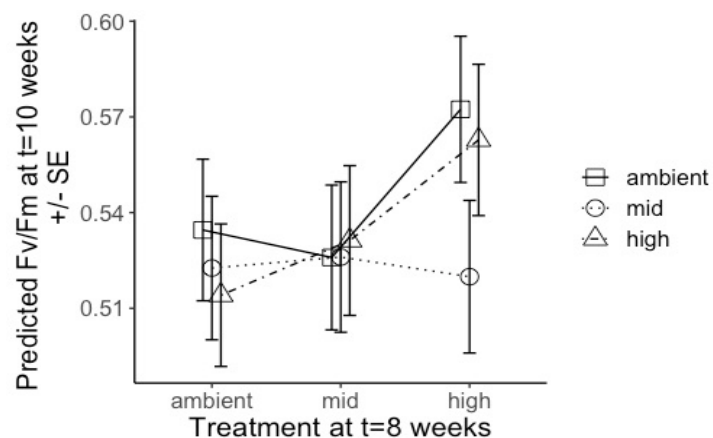


Table C.S 24 List of statistical models predicting Fv/Fm at t=14 (fragments under heat stress or ambient treatment) relative to the exposure to previous treatments at t=4 and t=8 weeks. The shaded area indicates the best-fit model.

Model	Fixed effect	Random effect	AICc	Akaike weights
1	Interaction treatment t=1 * t=2 * t=4 + size + Y.II.3 t=3	genotype (intercept), tank (intercept), position (intercept)	- 10934.10	0.999
2	Interaction treatment t=1 * t=2 * t=4 + size + Y.II.3 t=3	genotype (intercept), position (intercept)	- 10912.84	<0.001
3	Interaction treatment t=1 * t=2 * t=4 + size + Y.II.3 t=3	tank (intercept), position (intercept)	- 10593.22	<0.001
4	Interaction treatment t=1 * t=2 * t=4 + size + Y.II.3 t=3	genotype (intercept), tank (intercept),	- 10824.00	<0.001

Table C.S 25 Coefficient estimates for the best-fit linear model predicting the linear growth at t=14 as a function of treatment at t=4 and treatment at t=8 and size at t=10 weeks. Asterisks indicate significant effects.

	Estimate	Std. Error	z value	Pr(> z)	
(Intercept)	0.12204	0.01448	8.43	< 2e-16	***
Y.II.3	0.40489	0.02066	19.60	< 2e-16	***
treat_1H	0.08898	0.00491	18.13	< 2e-16	***
treat_1M	0.08499	0.00490	17.35	< 2e-16	***
treat_2H	0.05140	0.00743	6.92	4.5e-12	***
treat_2M	0.09814	0.00740	13.25	< 2e-16	***
treat_4Co	0.13808	0.00740	18.66	< 2e-16 *	**
log(t4)	0.02579	0.00366	7.05	1.7e-12	***
treat_1H:treat_2H	-0.07451	0.00693	-10.75	< 2e-16	***
treat_1M:treat_2H	-0.06100	0.00694	-8.78	< 2e-16	***
treat_1H:treat_2M	-0.12149	0.00693	-17.54	< 2e-16	***
treat_1M:treat_2M	-0.09668	0.00691	-14.00	< 2e-16	***
treat_1H:treat_4Co	-0.10056	0.00690	-14.58	< 2e-16	***
treat_1M:treat_4Co	-0.08374	0.00690	-12.13	< 2e-16	***
treat_2H:treat_4Co	-0.04714	0.01047	-4.50	6.7e-06	***
treat_2M:treat_4Co	-0.10330	0.01047	-9.87	< 2e-16	***
treat_1H:treat_2H:treat_4Co	0.08231	0.00975	8.44	< 2e-16	***
treat_1M:treat_2H:treat_4Co	0.03467	0.00975	3.55	0.00038	***
treat_1H:treat_2M:treat_4Co	0.13097	0.00979	13.38	< 2e-16	***
treat_1M:treat_2M:treat_4Co	0.09341	0.00978	9.55	< 2e-16	***

Random effect variance(s):

Group=position

	Variance	StdDev

(Intercept)	0.000	0.010
-------------	-------	-------

Random effect variance(s):

Group=Genotype

	Variance	StdDev
(Intercept)	0.000	0.019

Random effect variance(s):

Group=tank

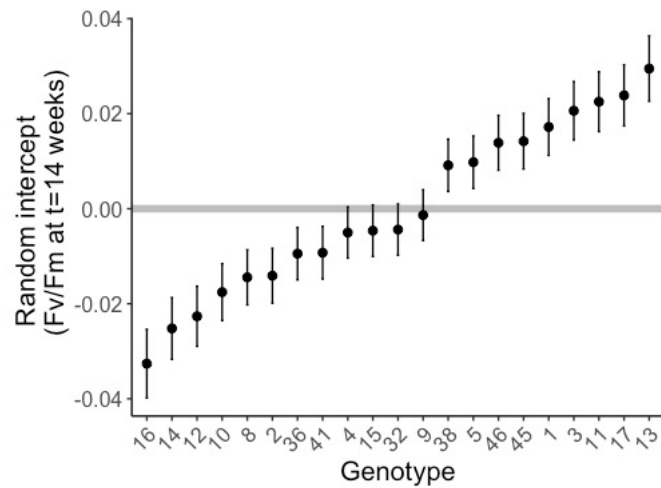
	Variance	StdDev
(Intercept)	0.000	0.005

Residual variance: 0.047

Table C.S 26 Tukey Post hoc test estimates of growth rate at t=14 weeks considering combinations of treatments.

contrast	estimate	SE	df	z.ratio	p.value	
C,C,Ac - C,C,Co	-0.138	0.010	Inf	-14.321	0.000	*
H,C,Ac - H,C,Co	-0.037	0.010	Inf	-3.891	0.012	*
M,C,Ac - M,C,Co	-0.054	0.010	Inf	-5.636	0.000	*
C,H,Ac - C,H,Co	-0.091	0.010	Inf	-9.408	0.000	*
H,H,Ac - H,H,Co	-0.073	0.010	Inf	-7.520	0.000	*
M,H,Ac - M,H,Co	-0.042	0.010	Inf	-4.346	0.002	*
C,M,Ac - C,M,Co	-0.035	0.010	Inf	-3.605	0.034	*
H,M,Ac - H,M,Co	-0.065	0.010	Inf	-6.756	0.000	*
M,M,Ac - M,M,Co	-0.044	0.010	Inf	-4.608	0.001	*

Figure C.S 6 Residuals of the random intercept of the best-fit model predicting maximum quantum yield [Fv/Fm] during the thermal stress exposure at t=14 weeks. Grey line represents what is the expected change on Fv/Fm in relation to the model, with values below this considered worse than the expected and with values above the line considered better than the expected.



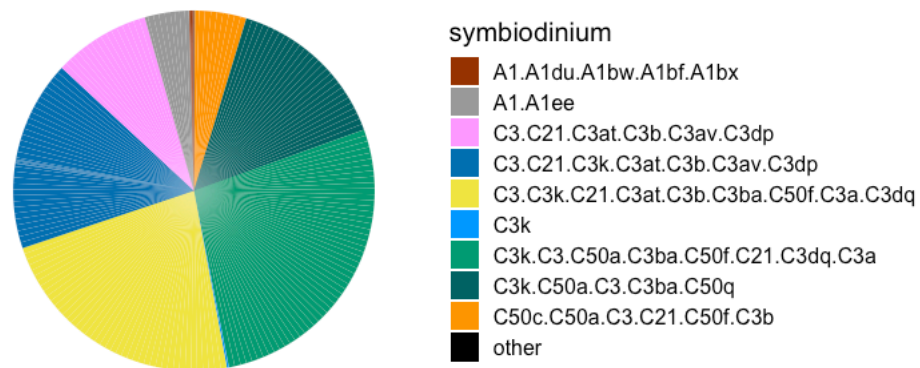
C.3 Adult fragments: Symbiodiniaceae

Table C.S 27 Statistical results of the permutational multivariate analysis of variance (PERMANOVA) of Symbiodiniaceae composition using Bray-Curtis distance.

	DF	Sums of squares	Mean squares	F value	R2	Pr(>F)
treatment t=1	2	0.496	0.248	1.100	0.007	0.34
treatment t=2	2	0.048	0.024	0.107	0.001	1.00
genotype	20	38.76	1.938	8.604	0.508	0.01

Residuals	164	36.939	0.225		0.484	
Total	188	76.243			1.000	

Figure C.S 7 Overall relative abundance of each group of Symbiodiniaceae type profiles and associated species in all adult fragments 4 weeks after transplantation (i.e., all treatment histories combined).



C.4 Adult fragments: Bacteria

Figure C.S 8 Rarefaction curves. 16S data analysis for bacterial communities

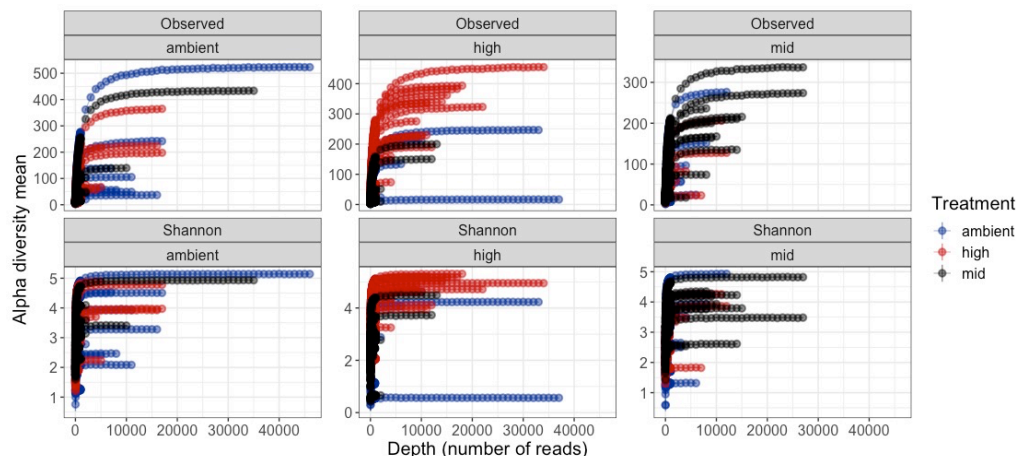


Table C.S 28 Coefficient estimates of the observed ASVs in adult coral fragments four weeks after transplantation, considering origin (t=4 weeks) and destination treatment (t=8 weeks).

	Estimate	Std. Error	z value	Pr(> z)
(Intercept) (A,A)	4.231	0.124	34.081	<0.001
treat_1M	-0.463	0.041	-11.249	<0.001
treat_1H	-0.413	0.040	-10.170	<0.001
treat_2M	-0.136	0.175	-0.775	0.438
treat_2H	0.048	0.175	0.276	0.783
treat_1M:treat_2M	1.153	0.053	21.479	<0.001
treat_1H:treat_2M	-0.027	0.061	-0.449	0.654
treat_1M:treat_2H	0.088	0.057	1.528	0.126
treat_1H:treat_2H	1.541	0.050	30.704	<0.001

contrast	ratio	SE	df	z.ratio	p.value
Ambient,Ambient / Mid,Ambient	1.590	0.066	Inf	11.249	0.000
Ambient,Ambient / High,Ambient	1.511	0.061	Inf	10.170	0.000
Ambient,Ambient / Ambient,Mid	1.146	0.202	Inf	0.775	0.998
Ambient,Ambient / Mid,Mid	0.575	0.101	Inf	-3.164	0.041
Ambient,Ambient / High,Mid	1.780	0.316	Inf	3.253	0.031
Ambient,Ambient / Ambient,High	0.953	0.167	Inf	-0.276	1.000
Ambient,Ambient / Mid,High	1.388	0.245	Inf	1.857	0.643
Ambient,Ambient / High,High	0.308	0.054	Inf	-6.755	0.000
Mid,Ambient / High,Ambient	0.950	0.043	Inf	-1.128	0.970
Mid,Ambient / Ambient,Mid	0.721	0.128	Inf	-1.852	0.647
Mid,Ambient / Mid,Mid	0.362	0.064	Inf	-5.783	0.000
Mid,Ambient / High,Mid	1.119	0.200	Inf	0.632	0.999
Mid,Ambient / Ambient,High	0.599	0.106	Inf	-2.901	0.088
Mid,Ambient / Mid,High	0.872	0.155	Inf	-0.769	0.998
Mid,Ambient / High,High	0.194	0.034	Inf	-9.358	0.000
High,Ambient / Ambient,Mid	0.758	0.134	Inf	-1.565	0.824
High,Ambient / Mid,Mid	0.381	0.067	Inf	-5.498	0.000
High,Ambient / High,Mid	1.178	0.210	Inf	0.918	0.992
High,Ambient / Ambient,High	0.630	0.111	Inf	-2.615	0.180
High,Ambient / Mid,High	0.918	0.163	Inf	-0.482	1.000
High,Ambient / High,High	0.204	0.036	Inf	-9.076	0.000
Ambient,Mid / Mid,Mid	0.502	0.017	Inf	-20.052	0.000
Ambient,Mid / High,Mid	1.553	0.071	Inf	9.663	0.000
Ambient,Mid / Ambient,High	0.831	0.146	Inf	-1.051	0.981
Ambient,Mid / Mid,High	1.211	0.214	Inf	1.083	0.977
Ambient,Mid / High,High	0.269	0.047	Inf	-7.525	0.000
Mid,Mid / High,Mid	3.095	0.127	Inf	27.512	0.000
Mid,Mid / Ambient,High	1.656	0.289	Inf	2.889	0.091
Mid,Mid / Mid,High	2.412	0.423	Inf	5.016	0.000

Mid, Mid / High, High	0.536	0.093	Inf	-3.599	0.010
High, Mid / Ambient, High	0.535	0.095	Inf	-3.528	0.012
High, Mid / Mid, High	0.779	0.139	Inf	-1.399	0.898
High, Mid / High, High	0.173	0.030	Inf	-9.967	0.000
Ambient, High / Mid, High	1.456	0.059	Inf	9.350	0.000
Ambient, High / High, High	0.324	0.010	Inf	-38.233	0.000
Mid, High / High, High	0.222	0.008	Inf	-43.953	0.000

Table C.S 29 Coefficient estimates of Chao1 index in adult coral fragments four weeks after transplantation, considering origin (t=4 weeks) and destination treatment (t=8 weeks).

	Value	Std.Error	DF	t-value	p-value
(Intercept) (A,A)	1.569	0.093	173	16.696	<0.001
treat_1M	-0.174	0.132	173	-1.310	0.197
treat_1H	-0.131	0.132	173	-1.993	0.321
treat_2M	0.031	0.132	6	0.239	0.818
treat_2H	-0.039	0.132	6	-0.293	0.779
treat_1M:treat_2M	0.498	0.187	173	2.652	0.008
treat_1H:treat_2M	-0.099	0.189	173	-0.524	0.600
treat_1M:treat_2H	0.230	0.187	173	1.225	0.222
treat_1H:treat_2H	0.839	0.187	173	4.467	<0.001

contrast	estimate	SE	df	t.ratio	p.value
Ambient,Ambient - Mid,Ambient	0.174	0.133	173.001	1.311	0.927
Ambient,Ambient - High,Ambient	0.132	0.133	173.001	0.994	0.986
Ambient,Ambient - Ambient, Mid	-0.032	0.133	46.996	-0.240	1.000
Ambient,Ambient - Mid, Mid	-0.356	0.133	46.996	-2.680	0.183
Ambient,Ambient - High, Mid	0.199	0.135	48.728	1.481	0.859
Ambient,Ambient - Ambient, High	0.039	0.133	46.996	0.293	1.000

Ambient,Ambient - Mid,High	-0.017	0.133	46.996	-0.129	1.000
Ambient,Ambient - High,High	-0.669	0.133	46.996	-5.032	0.000
Mid,Ambient - High,Ambient	-0.042	0.133	173.001	-0.317	1.000
Mid,Ambient - Ambient,Mid	-0.206	0.133	46.996	-1.551	0.825
Mid,Ambient - Mid,Mid	-0.530	0.133	46.996	-3.991	0.007
Mid,Ambient - High,Mid	0.025	0.135	48.728	0.187	1.000
Mid,Ambient - Ambient,High	-0.135	0.133	46.996	-1.017	0.982
Mid,Ambient - Mid,High	-0.191	0.133	46.996	-1.440	0.876
Mid,Ambient - High,High	-0.843	0.133	46.996	-6.342	0.000
High,Ambient - Ambient,Mid	-0.164	0.133	46.996	-1.234	0.945
High,Ambient - Mid,Mid	-0.488	0.133	46.996	-3.674	0.016
High,Ambient - High,Mid	0.067	0.135	48.728	0.500	1.000
High,Ambient - Ambient,High	-0.093	0.133	46.996	-0.700	0.999
High,Ambient - Mid,High	-0.149	0.133	46.996	-1.123	0.968
High,Ambient - High,High	-0.801	0.133	46.996	-6.025	0.000
Ambient,Mid - Mid,Mid	-0.324	0.133	173.001	-2.440	0.269
Ambient,Mid - High,Mid	0.231	0.135	173.281	1.718	0.735
Ambient,Mid - Ambient,High	0.071	0.133	46.996	0.533	1.000
Ambient,Mid - Mid,High	0.015	0.133	46.996	0.111	1.000
Ambient,Mid - High,High	-0.637	0.133	46.996	-4.792	0.001
Mid,Mid - High,Mid	0.556	0.135	173.281	4.128	0.002
Mid,Mid - Ambient,High	0.395	0.133	46.996	2.973	0.097
Mid,Mid - Mid,High	0.339	0.133	46.996	2.551	0.235
Mid,Mid - High,High	-0.313	0.133	46.996	-2.352	0.334
High,Mid - Ambient,High	-0.160	0.135	48.728	-1.192	0.955
High,Mid - Mid,High	-0.217	0.135	48.728	-1.609	0.795
High,Mid - High,High	-0.868	0.135	48.728	-6.450	0.000
Ambient,High - Mid,High	-0.056	0.133	173.001	-0.422	1.000
Ambient,High - High,High	-0.708	0.133	173.001	-5.325	0.000
Mid,High - High,High	-0.652	0.133	173.001	-4.903	0.000

Table C.S 30 Coefficient estimates of Shannon diversity index in adult coral fragments four weeks after transplantation, considering origin (t=4 weeks) and destination treatment (t=8 weeks).

	Value	Std.Error	DF	t-value	p-value
(Intercept) (A,A)	2.879	0.199	173	14.461	0.000
treat_1M	-0.365	0.264	173	-1.380	0.169
treat_1H	-0.222	0.264	173	-0.841	0.401
treat_2M	0.219	0.281	6	0.781	0.464
treat_2H	0.069	0.281	6	0.247	0.812
treat_1M:treat_2M	0.818	0.374	173	2.187	0.030
treat_1H:treat_2M	-0.347	0.376	173	-0.921	0.358
treat_1M:treat_2H	0.387	0.374	173	1.036	0.301
treat_1H:treat_2H	1.588	0.374	173	4.242	0.000

contrast	estimate	SE	df	t.ratio	p.value
Ambient,Ambient - Mid,Ambient	0.365	0.265	173.000	1.381	0.904
Ambient,Ambient - High,Ambient	0.223	0.265	173.000	0.842	0.995
Ambient,Ambient - Ambient,Mid	-0.220	0.282	32.933	-0.781	0.997
Ambient,Ambient - Mid,Mid	-0.673	0.282	32.933	-2.391	0.322
Ambient,Ambient - High,Mid	0.350	0.285	34.165	1.229	0.944
Ambient,Ambient - Ambient,High	-0.070	0.282	32.933	-0.248	1.000
Ambient,Ambient - Mid,High	-0.092	0.282	32.933	-0.328	1.000
Ambient,Ambient - High,High	-1.435	0.282	32.933	-5.097	0.000
Mid,Ambient - High,Ambient	-0.143	0.265	173.000	-0.539	1.000
Mid,Ambient - Ambient,Mid	-0.585	0.282	32.933	-2.079	0.504
Mid,Ambient - Mid,Mid	-1.039	0.282	32.933	-3.689	0.020
Mid,Ambient - High,Mid	-0.015	0.285	34.165	-0.054	1.000
Mid,Ambient - Ambient,High	-0.435	0.282	32.933	-1.546	0.826

Mid,Ambient - Mid,High	-0.458	0.282	32.933	-1.626	0.784
Mid,Ambient - High,High	-1.801	0.282	32.933	-6.395	0.000
High,Ambient - Ambient,Mid	-0.443	0.282	32.933	-1.572	0.812
High,Ambient - Mid,Mid	-0.896	0.282	32.933	-3.183	0.068
High,Ambient - High,Mid	0.127	0.285	34.165	0.446	1.000
High,Ambient - Ambient,High	-0.293	0.282	32.933	-1.039	0.979
High,Ambient - Mid,High	-0.315	0.282	32.933	-1.119	0.967
High,Ambient - High,High	-1.658	0.282	32.933	-5.888	0.000
Ambient,Mid - Mid,Mid	-0.453	0.265	173.000	-1.713	0.738
Ambient,Mid - High,Mid	0.570	0.268	173.205	2.126	0.459
Ambient,Mid - Ambient,High	0.150	0.282	32.933	0.533	1.000
Ambient,Mid - Mid,High	0.128	0.282	32.933	0.453	1.000
Ambient,Mid - High,High	-1.215	0.282	32.933	-4.316	0.004
Mid,Mid - High,Mid	1.023	0.268	173.205	3.817	0.006
Mid,Mid - Ambient,High	0.603	0.282	32.933	2.143	0.463
Mid,Mid - Mid,High	0.581	0.282	32.933	2.063	0.513
Mid,Mid - High,High	-0.762	0.282	32.933	-2.706	0.185
High,Mid - Ambient,High	-0.420	0.285	34.165	-1.474	0.859
High,Mid - Mid,High	-0.442	0.285	34.165	-1.553	0.822
High,Mid - High,High	-1.785	0.285	34.165	-6.269	0.000
Ambient,High - Mid,High	-0.022	0.265	173.000	-0.085	1.000
Ambient,High - High,High	-1.365	0.265	173.000	-5.158	0.000
Mid,High - High,High	-1.343	0.265	173.000	-5.074	0.000

Figure C.S 9 Alpha diversity of microbial communities in adult coral fragments four weeks after transplantation (t=8 weeks), considering origin (t=4 weeks) and destination treatment (t=8 weeks). Panel a: species richness (Observed ASV) Panel b: species diversity index (Chao 1) and panel c: Shannon index.

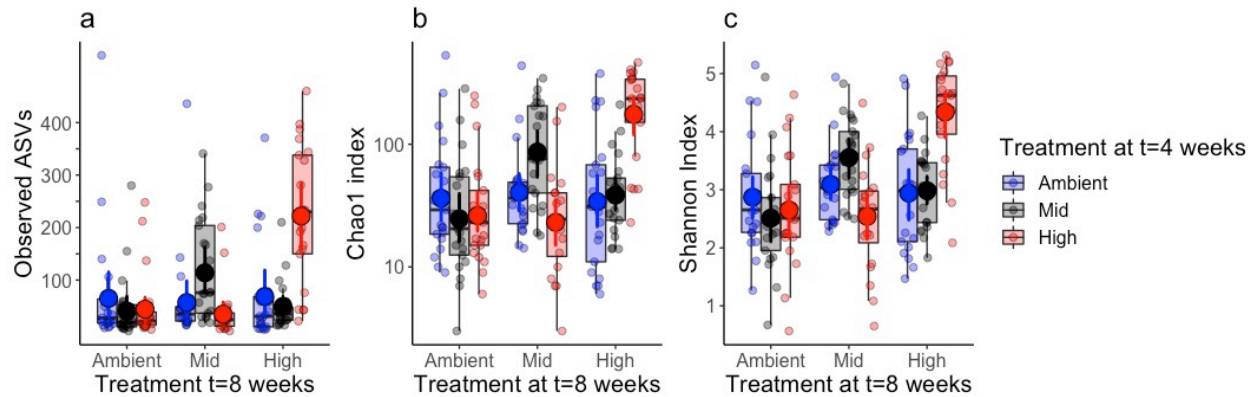


Figure C.S 10 Venn diagram corresponding to number of ASVs in all adult fragments 4 weeks after transplantation (t=8 weeks). Overlapping shades represent shared number of ASVs between treatment histories. Total number of ASVs at the destination treatment was 456 (AMBIENT), 453 (MID), and 465 (HIGH).

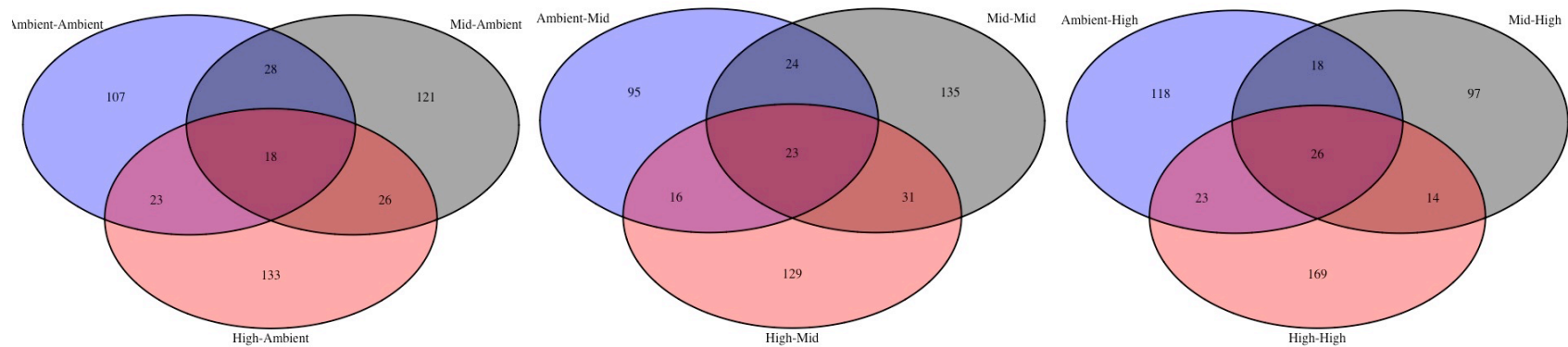


Table C.S 31 Presence and absence of bacterial taxa (ASV level) on a rarefied data set. For each treatment history, a number '1' represents presence of a particular ASVs classified according to treatment history, genotype and sample ID, whereas '0' represents absence; total appearances among treatment histories included.

(Available at: https://myjcu.edu-my.sharepoint.com/:f/g/personal/joseluis_montalvoproano_my_jcu_edu_au/EiShtWlQYNVCKvikyziQoooBK-FJxZ4ew28-GOOa_Nu1Sw?e=eS0s3q)

Table C.S 32 PERMANOVA test results (partial R^2 and p-values) for the effect of treatment on the relative composition of bacterial communities using Bray-Curtis similarity distance. Number of permutations=999

	Df	SumOfSqs	R^2	F	Pr(>F)	
treat_4weeks	2	1.104	0.01256	1.2802	0.018	***
treat_8weeks	2	1.555	0.01770	1.8039	0.001	***
tank	2	1.520	0.01730	1.7637	0.001	***
Genotype	18	12.760	0.14520	1.6447	0.001	***
treat_1:treat_2	4	2.404	0.02735	1.3942	0.001	***
Residual	159	68.535	0.77989			
Total	187	87.878	1.00000			

Number of permutations: 999

Table C.S 33 Permutation test for homogeneity of multivariate dispersions. Number of permutations=999

Df	Sum Sq	Mean Sq	F	N. perm	p-value
----	--------	---------	---	---------	---------

Groups	2	0.00819	0.0040951	4.1326	999	0.019
Residuals	185	0.18332	0.0009909			

Figure C.S 11 NMDS of bacterial communities in adult coral fragments four weeks after transplantation, considering origin (t=4 weeks) and destination treatment (t=8 weeks). Values in axis represent Bray-Curtis distances between samples.

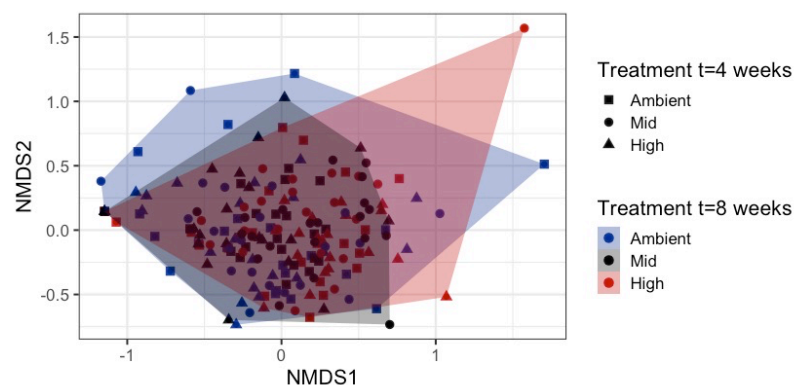


Table C.S 34 Indicator taxa for adult coral fragments four weeks after transplantation, considering origin (t=4) and destination treatment (t=8 weeks). Indval analysis done at the species level (ASV) and included alpha parameters of 0.05.

Treatment 1	Treatment 2	ASV	A (specificity)	B (fidelity)	stat	p_value	Kingdom	Phylum	Class	Order	Family	Genus	Species
Ambient	High	3c2be653f5cee06a9368e43dedbf6a13	0.6667	0.1905	0.356	0.0069	Bacteria	Epsilonbacteraeota	Campylobacteria	Campylobacteres	Arcobacteraceae	Arcobacter	NA

Ambient	High	efffffa2f37ff49f5c430e0b18af4c5	0.889	0.1429	0.356	0.02198	Bacteria	Firmicutes	Erysipelotrichia	Erysipelotrichales	Erysipelotrichaceae	Turicibacter	uncultured bacterium
Mid	Ambient	42efd8992f040edb8e6284153e9828ca	0.5774	0.1905	0.332	0.0016	Bacteria	Proteobacteria	Alphaproteobacteria	Rhodobacterales	Rhodobacteraceae	NA	NA
Mid	Mid	f2a8692e7d33fceb64a3f7050bf4e275	0.4667	0.2381	0.333	0.0012	Bacteria	Proteobacteria	Alphaproteobacteria	Rhodobacterales	Rhodobacteraceae	Roseobacter clade CHAB-I-5 lineage	Ambiguous_taxa
Mid	Mid	afbb6b175a089edbe6724015d1d86422	0.3028	0.5714	0.416	0.0002	Bacteria	Proteobacteria	Alphaproteobacteria	Rhodobacterales	Rhodobacteraceae	NA	NA
Mid	Mid	c698e34b0e4a752b6f0e1b37b1f03c63	0.8333	0.1429	0.345	0.0032	Bacteria	Proteobacteria	Alphaproteobacteria	Rhizobiales	Stappiaceae	Labrenzia	Ambiguous_taxa
Mid	High	f53625710a03f89025d95c493c3f2db2	0.500	0.2857	0.378	0.00599	Bacteria	Proteobacteria	Alphaproteobacteria	Sphingomonadales	Sphingomonadaceae	Erythrobacter	NA
Mid	High	8abb0ca2546c7f07c24300677e0b9100	0.5833	0.1429	0.289	0.004496	Bacteria	Proteobacteria	Alphaproteobacteria	Rhodobacterales	Rhodobacteraceae	NA	NA
High	Mid	7b7c9cbd3a402a3a7d3c9d48340b79ee	1.000	0.100	0.316	0.0015	Bacteria	Proteobacteria	Alphaproteobacteria	Rhodobacterales	Rhodobacteraceae	Roseobacter	uncultured alpha proteobacterium
High	Mid	cfe085ca82371939b4fc149f615c2012	0.8077	0.1000	0.284	0.0017	Bacteria	Proteobacteria	Gammaproteobacteria	Oceanospirillales	Endozoicomonadaceae	Endozoicomonas	Ambiguous_taxa
High	High	f01da61ef615a0968fa4116ad0f6a4ac	0.2535	0.6190	0.396	0.0015	Bacteria	Proteobacteria	Alphaproteobacteria	Rhodobacterales	Rhodobacteraceae	Ruegeria	Ambiguous_taxa

High	High	e2d07801858b8783b72867d25cc6affc	0.5714	0.2381	0.369	0.004	Bacteria	Proteobacteria	Alphaproteobacteria	Rhodobacterales	Rhodobacteraceae	Ruegeria	NA
High	High	a6aaaef3401ade4f24f385f8157916bd	0.7500	0.1429	0.327	0.044	Bacteria	Firmicutes	Erysipelotrichia	Erysipelotrichales	Erysipelotrichaceae	Turicibacter	uncultured bacterium
High	High	eeb8d4047341532d08f992e2b177bfe8	0.7500	0.1429	0.327	0.034	Bacteria	Proteobacteria	Alphaproteobacteria	Rhodobacterales	Rhodobacteraceae	Actibacterium	uncultured bacterium
High	High	e2250c863b1d3d72429b7ea7fc38fd48	0.7500	0.1429	0.327	0.048	Bacteria	Proteobacteria	Alphaproteobacteria	Rhodobacterales	Rhodobacteraceae	Roseobacter	NA
High	High	8292bdcea9217967192498aebdc36bac	0.7500	0.1429	0.327	0.029	Bacteria	Proteobacteria	Alphaproteobacteria	Rhizobiales	Hyphomicrobiales	Filomicrobium	uncultured bacterium
High	High	de505f410eefb69145848f97ed426ea9	0.5000	0.1905	0.309	0.029	Bacteria	Cyanobacteria	Oxyphotobacteria	Eurycoccales	Euryoccales Insertae Sedis	Synechococcus PCC-7336	Synechococcus sp. PCC 7336
High	High	771399a353b03df0e94367a225839475	0.3846	0.2381	0.303	0.030	Bacteria	Proteobacteria	Alphaproteobacteria	Rhodobacterales	Rhodobacteraceae	Tateyamaria	uncultured bacterium

Table C.S 35 Indicator taxa for adult coral fragments four weeks after transplantation, considering origin (t=4) and destination treatment (t=8 weeks). Indval analysis done at the family level and included alpha parameters of 0.05.

Treatment 1	Treatment 2	ASV	A (specificity)	B (fidelity)	stat	p_value	Kingdom	Phylum	Class	Order	Family	Genus	Species
Amb	Amb	736226d94c13a48ad6375e2123f08e11	0.5859	0.1905	0.334	0.05	Bacteria	Proteobacteria	Alphaproteobacteria	Rhodovibrionales	Kiloniellaceae	Pelagibius	Ambiguous_taxa

Amb	Mid	0f9384f2751706de751048f2848414ca	0.2465	0.4762	0.343	0.047	Bacteria	Planctomyces	Planctomycetacia	Pirellulales	Pirellulaceae	Blastopirellula	NA
Amb	High	3d10bf49b14e3f2c7a4a4e3b2e27e659e	0.3945	0.2381	0.306	0.037	Bacteria	Epsilonbacteraeota	Campylobacteria	Campylobacterales	Arcobacteraceae	Arcobacter	uncultured bacterium
Mid	High	fff0b2618b686e6bd4538b34f3f80572	1.000	0.1429	0.378	0.00699	Bacteria	Actinobacteria	Actinobacteria	Pseudonocardiales	Pseudonocardiaceae	Pseudonocardia	Ambiguous_taxa
Mid	High	6a4faf681b87814b636e13b42559797f	0.8571	0.1429	0.350	0.02298	Bacteria	Bacteroidetes	Bacteroidi	Chitinophagales	Saprospiraceae	Lewinella	uncultured bacterium
High	Mid	8c731445b7419a5eb700304897338f85	0.759	0.100	0.276	0.031	Bacteria	Proteobacteria	Alphaproteobacteria	uncultured	uncultured bacterium	NA	NA
High	High	5dc88811be88f7506bd5ca420ab0b7f6	0.2618	0.4286	0.335	0.026	Bacteria	Proteobacteria	Alphaproteobacteria	Rhizobiales	Hyphomicrobiales	Filomicrobium	NA

Table C.S 36 Individual models among bacterial families used to estimate difference in relative abundances from the top ten most abundant following a zero-inflated beta-regression.

(Available at: https://myjcu.edu-my.sharepoint.com/:f/g/personal/joseluis_montalvoproano_my_jcu_edu_au/EiShtWlQYNVckvikyziQoooBK-FJxZ4ew28-GOOa_Nu1Sw?e=eS0s3q)

Table C.S 37 Results from the posterior distribution of difference as the outcome for each model and bacterial family

term	estimate	std.error	conf.low	conf.high	Family
------	----------	-----------	----------	-----------	--------

b_Intercept	-2.5751482	0.50278312	-3.756359	-1.757007	Pirellulaceae
b_treat_1H	0.44560542	0.58017043	-0.5863336	1.71555721	Pirellulaceae
b_treat_1M	0.3404353	0.60749048	-0.7774285	1.69786914	Pirellulaceae
b_treat_2H	0.100298	0.59329856	-0.9591309	1.43694	Pirellulaceae
b_treat_2M	0.44981479	0.53422707	-0.4692337	1.6692494	Pirellulaceae
b_treat_1H:treat_2H	-0.2367644	0.68663617	-1.6598006	1.06466974	Pirellulaceae
b_treat_1M:treat_2H	-0.5441487	0.72627875	-2.0356211	0.8887743	Pirellulaceae
b_treat_1H:treat_2M	-0.214586	0.68913965	-1.6961676	1.05980207	Pirellulaceae
b_treat_1M:treat_2M	-0.5601823	0.67410617	-2.0251137	0.68857642	Pirellulaceae
phi	29.5336863	6.12380074	18.7502786	43.0788192	Pirellulaceae
zi	0.72112798	0.03295456	0.6554223	0.78289871	Pirellulaceae
b_Intercept	-0.4426503	0.25198536	-0.9567289	0.03095727	Rhodobacteraceae
b_treat_1H	0.28153759	0.35687388	-0.4084011	0.97775925	Rhodobacteraceae
b_treat_1M	0.09613766	0.34154676	-0.541739	0.77979925	Rhodobacteraceae
b_treat_2H	-0.2085495	0.33827094	-0.8533393	0.46271913	Rhodobacteraceae
b_treat_2M	0.03997425	0.32508592	-0.6072981	0.70301792	Rhodobacteraceae
b_treat_1H:treat_2H	0.13721196	0.47900603	-0.8103987	1.06346923	Rhodobacteraceae
b_treat_1M:treat_2H	0.17397505	0.45548907	-0.73635	1.04249199	Rhodobacteraceae
b_treat_1H:treat_2M	0.17360279	0.46310813	-0.7109955	1.07986283	Rhodobacteraceae
b_treat_1M:treat_2M	-0.2195015	0.45789733	-1.1329864	0.64491935	Rhodobacteraceae
phi	3.44950956	0.34800174	2.78482329	4.16503712	Rhodobacteraceae
zi	0.11142139	0.02157555	0.07124743	0.15672998	Rhodobacteraceae
b_Intercept	-2.8628468	0.54256717	-4.0074481	-2.002572	Methyloiligellaceae
b_treat_1H	0.03138978	0.68500182	-1.335989	1.46470897	Methyloiligellaceae
b_treat_1M	0.26264773	0.73913171	-1.167759	1.79360612	Methyloiligellaceae
b_treat_2H	0.46850043	0.65123963	-0.6815224	1.86012771	Methyloiligellaceae
b_treat_2M	0.57241578	0.58613924	-0.4235669	1.82441178	Methyloiligellaceae
b_treat_1H:treat_2H	-0.2173458	0.8360575	-1.9783874	1.46416411	Methyloiligellaceae
b_treat_1M:treat_2H	-0.2753877	0.87125064	-2.0896341	1.48694824	Methyloiligellaceae
b_treat_1H:treat_2M	0.50878751	0.78745626	-1.1654937	1.99171381	Methyloiligellaceae
b_treat_1M:treat_2M	-0.6426875	0.81581061	-2.2756938	0.96862527	Methyloiligellaceae
phi	31.6017218	8.4353522	17.8090767	51.0466825	Methyloiligellaceae

zi	0.81187865	0.02883828	0.75568543	0.86460647	Methyloligellaceae
b_Intercept	-0.8007979	0.53475889	-1.9112689	0.20063853	Phormidesmiaceae
b_treat_1H	-1.2968609	1.3812482	-4.2702935	1.14279754	Phormidesmiaceae
b_treat_1M	-1.4542419	0.98210181	-3.4779324	0.39291781	Phormidesmiaceae
b_treat_2H	-0.8235962	0.71231545	-2.1857608	0.65487369	Phormidesmiaceae
b_treat_2M	-0.9317781	1.31647032	-4.0634329	1.29745424	Phormidesmiaceae
b_treat_1H:treat_2H	1.78275217	1.5658057	-1.1280431	5.10890688	Phormidesmiaceae
b_treat_1M:treat_2H	0.8265867	1.34786417	-1.786144	3.35938277	Phormidesmiaceae
b_treat_1H:treat_2M	0.50813874	2.22129943	-3.9676909	5.14059164	Phormidesmiaceae
b_treat_1M:treat_2M	1.4759607	1.62214485	-1.4555131	5.125398	Phormidesmiaceae
phi	5.1607047	1.69876507	2.38472356	9.06884109	Phormidesmiaceae
zi	0.88286413	0.02280212	0.83635172	0.92231356	Phormidesmiaceae
b_Intercept	0.39035652	0.44353771	-0.486211	1.29215518	Kiloniellaceae
b_treat_1H	-2.8856114	1.40218561	-6.1170869	-0.5136915	Kiloniellaceae
b_treat_1M	-2.3423755	0.71888753	-3.7498598	-0.9342347	Kiloniellaceae
b_treat_2H	17.2331357	144.992515	-234.35146	281.90249	Kiloniellaceae
b_treat_2M	-2.4229408	1.36100858	-5.707558	-0.1282468	Kiloniellaceae
b_treat_1H:treat_2H	-16.445419	144.942071	-280.96249	236.309657	Kiloniellaceae
b_treat_1M:treat_2H	-16.92709	144.999156	-281.18133	235.648131	Kiloniellaceae
b_treat_1H:treat_2M	2.37270693	2.31876783	-2.50173	7.0697051	Kiloniellaceae
b_treat_1M:treat_2M	2.12178688	1.65567252	-0.8702999	5.63705334	Kiloniellaceae
phi	4.99183893	1.7350441	2.17982337	9.13380509	Kiloniellaceae
zi	0.88331763	0.02354412	0.83388123	0.92724856	Kiloniellaceae
b_Intercept	-1.8650647	0.19775878	-2.2628196	-1.4854757	Rhizobiaceae
b_treat_1H	-0.4828009	0.32472133	-1.1388899	0.12946181	Rhizobiaceae
b_treat_1M	0.26254799	0.26912606	-0.2622811	0.78720058	Rhizobiaceae
b_treat_2H	0.07495483	0.26310224	-0.448584	0.61137521	Rhizobiaceae
b_treat_2M	0.04977717	0.25970744	-0.4441473	0.562902	Rhizobiaceae
b_treat_1H:treat_2H	0.30586986	0.3983865	-0.472209	1.10486226	Rhizobiaceae
b_treat_1M:treat_2H	-0.7818209	0.39808161	-1.578457	0.02330748	Rhizobiaceae
b_treat_1H:treat_2M	0.15098644	0.45301464	-0.7581071	1.00054098	Rhizobiaceae
b_treat_1M:treat_2M	-0.6242157	0.36520952	-1.3745359	0.05702763	Rhizobiaceae

phi	17.9186649	2.5256469	13.1982462	23.1836745	Rhizobiaceae
zi	0.45218455	0.03640726	0.38039471	0.52248004	Rhizobiaceae
b_Intercept	-0.2419673	0.36179392	-0.9558818	0.46278986	Endozoicomonadaceae
b_treat_1H	0.62439864	0.50894107	-0.3849802	1.6511518	Endozoicomonadaceae
b_treat_1M	-0.0958666	0.48975472	-1.0393101	0.88214446	Endozoicomonadaceae
b_treat_2H	0.57939571	0.50397255	-0.4192784	1.55311862	Endozoicomonadaceae
b_treat_2M	0.23497624	0.47916725	-0.6919678	1.20090085	Endozoicomonadaceae
b_treat_1H:treat_2H	-2.0411931	0.89309529	-3.7973784	-0.2875093	Endozoicomonadaceae
b_treat_1M:treat_2H	-1.0302911	0.69069023	-2.3613551	0.36300824	Endozoicomonadaceae
b_treat_1H:treat_2M	-0.6556967	0.66998896	-1.9843608	0.62211325	Endozoicomonadaceae
b_treat_1M:treat_2M	-0.7206129	0.70568991	-2.1427878	0.60185418	Endozoicomonadaceae
phi	1.33859973	0.15748138	1.04212938	1.66546181	Endozoicomonadaceae
zi	0.46219733	0.03584079	0.39269228	0.5312463	Endozoicomonadaceae
b_Intercept	-2.1626135	0.52612196	-3.4418968	-1.3020425	Eurycoccales Incertae Sedis
b_treat_1H	0.53311836	0.64083529	-0.6518572	1.96946812	Eurycoccales Incertae Sedis
b_treat_1M	-0.3938431	0.61722569	-1.5083666	0.9719641	Eurycoccales Incertae Sedis
b_treat_2H	-0.1961649	0.6120295	-1.2852702	1.15616488	Eurycoccales Incertae Sedis
b_treat_2M	0.17166358	0.62370868	-0.9674855	1.58426292	Eurycoccales Incertae Sedis
b_treat_1H:treat_2H	-0.5854959	0.74939939	-2.1375884	0.786808	Eurycoccales Incertae Sedis
b_treat_1M:treat_2H	0.56783293	0.73731401	-0.9732918	1.92071159	Eurycoccales Incertae Sedis
b_treat_1H:treat_2M	-1.0882338	0.82725481	-2.8952313	0.44625431	Eurycoccales Incertae Sedis
b_treat_1M:treat_2M	0.15011321	0.78168136	-1.4410764	1.67084881	Eurycoccales Incertae Sedis
phi	18.7437926	3.92578898	11.8881466	26.8804187	Eurycoccales Incertae Sedis
zi	0.72111891	0.03162566	0.65584469	0.78089999	Eurycoccales Incertae Sedis
b_Intercept	-2.4077118	0.37704408	-3.236323	-1.759814	Sphingomonadaceae
b_treat_1H	0.30147099	0.45479937	-0.5508002	1.23800398	Sphingomonadaceae
b_treat_1M	0.43448334	0.44582275	-0.3949088	1.37092803	Sphingomonadaceae
b_treat_2H	0.32989003	0.44381428	-0.5183405	1.23179157	Sphingomonadaceae
b_treat_2M	-0.0142714	0.42325534	-0.7954575	0.87037529	Sphingomonadaceae
b_treat_1H:treat_2H	-0.6417586	0.54226264	-1.6962971	0.38350692	Sphingomonadaceae
b_treat_1M:treat_2H	-0.4668371	0.54728917	-1.5233467	0.64305593	Sphingomonadaceae
b_treat_1H:treat_2M	-0.205794	0.59706482	-1.4065275	0.91051169	Sphingomonadaceae

b_treat_1M:treat_2M	-0.2565856	0.55003214	-1.4050503	0.81088521	Sphingomonadaceae
phi	19.6033214	3.36621479	13.7076413	26.812627	Sphingomonadaceae
zi	0.61155432	0.03517344	0.54125636	0.6796009	Sphingomonadaceae
b_Intercept	-1.7244948	0.29814612	-2.346371	-1.1841971	Xenococcaceae
b_treat_1H	-0.1392482	0.40232198	-0.9262395	0.66152983	Xenococcaceae
b_treat_1M	0.01681333	0.45216716	-0.88833	0.88943106	Xenococcaceae
b_treat_2H	-0.5026109	0.49271413	-1.555006	0.43212499	Xenococcaceae
b_treat_2M	-0.7903385	0.50457742	-1.8503424	0.15540872	Xenococcaceae
b_treat_1H:treat_2H	0.17346893	0.6283099	-0.9804687	1.46043419	Xenococcaceae
b_treat_1M:treat_2H	0.18024848	0.7200675	-1.2185849	1.63660491	Xenococcaceae
b_treat_1H:treat_2M	1.45541796	0.64839269	0.17546917	2.72051101	Xenococcaceae
b_treat_1M:treat_2M	0.8670445	0.65655625	-0.406607	2.20114252	Xenococcaceae
phi	11.6409257	2.34973252	7.59438009	16.6124602	Xenococcaceae

Figure C.S 12 Relative abundance of the top 10 bacterial genera (y-axis) among individual genotypes of coral fragments (x-axis) at t=8 weeks, across each of the nine treatment histories (n= 1601 total genera).

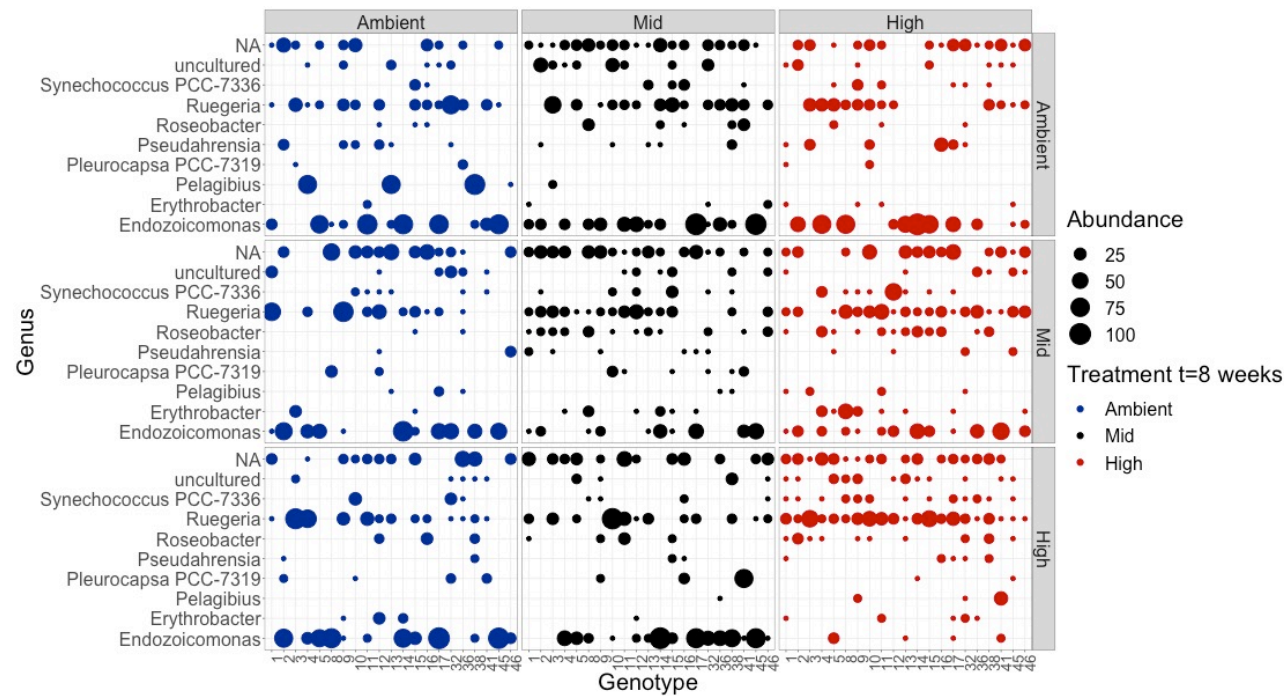


Table C.S 38 Individual models among bacterial genera used to estimate difference in relative abundances from the top ten most abundant following a zero-inflated beta-regression.

(Available at: https://myjcu.edu-my.sharepoint.com/:f/g/personal/joseluis_montalvoproano_my_jcu_edu_au/EiShtWlQYNVCKvikyziQoooBK-FJxZ4ew28-GOOa_Nu1Sw?e=eS0s3q)

Table C.S 39 Results from the posterior distribution of difference as the outcome for each model and bacterial genus (top 10 most abundant)

term	estimate	std.error	conf.low	conf.high	Genus
b_Intercept	-1.8816623	0.26366763	-2.4267035	-1.4071914	Pleurocapsa PCC-7319
b_treat_1H	0.36327397	0.32973435	-0.2749835	1.00912533	Pleurocapsa PCC-7319
b_treat_1M	0.45551169	0.31792557	-0.1550867	1.10873386	Pleurocapsa PCC-7319
b_treat_2H	0.05783406	0.33155717	-0.563609	0.70794059	Pleurocapsa PCC-7319
b_treat_2M	0.12137157	0.30548879	-0.4316882	0.75484579	Pleurocapsa PCC-7319
b_treat_1H:treat_2H	-0.2178971	0.41161018	-1.022481	0.52642619	Pleurocapsa PCC-7319
b_treat_1M:treat_2H	-0.2133631	0.41861279	-1.0485984	0.58659458	Pleurocapsa PCC-7319
b_treat_1H:treat_2M	-0.4025421	0.42041503	-1.225964	0.43886902	Pleurocapsa PCC-7319
b_treat_1M:treat_2M	-0.213329	0.38906173	-0.9795752	0.55301965	Pleurocapsa PCC-7319
phi	12.167352	1.49090591	9.44040205	15.166236	Pleurocapsa PCC-7319
b_Intercept	-1.8816623	0.26366763	-2.4267035	-1.4071914	(NA) Family Rhodobacteraceae
b_treat_1H	0.36327397	0.32973435	-0.2749835	1.00912533	(NA) Family Rhodobacteraceae
b_treat_1M	0.45551169	0.31792557	-0.1550867	1.10873386	(NA) Family Rhodobacteraceae
b_treat_2H	0.05783406	0.33155717	-0.563609	0.70794059	(NA) Family Rhodobacteraceae
b_treat_2M	0.12137157	0.30548879	-0.4316882	0.75484579	(NA) Family Rhodobacteraceae
b_treat_1H:treat_2H	-0.2178971	0.41161018	-1.022481	0.52642619	(NA) Family Rhodobacteraceae
b_treat_1M:treat_2H	-0.2133631	0.41861279	-1.0485984	0.58659458	(NA) Family Rhodobacteraceae
b_treat_1H:treat_2M	-0.4025421	0.42041503	-1.225964	0.43886902	(NA) Family Rhodobacteraceae
b_treat_1M:treat_2M	-0.213329	0.38906173	-0.9795752	0.55301965	(NA) Family Rhodobacteraceae
phi	12.167352	1.49090591	9.44040205	15.166236	(NA) Family Rhodobacteraceae
b_Intercept	-1.8816623	0.26366763	-2.4267035	-1.4071914	(NA) Family NA
b_treat_1H	0.36327397	0.32973435	-0.2749835	1.00912533	(NA) Family NA
b_treat_1M	0.45551169	0.31792557	-0.1550867	1.10873386	(NA) Family NA
b_treat_2H	0.05783406	0.33155717	-0.563609	0.70794059	(NA) Family NA
b_treat_2M	0.12137157	0.30548879	-0.4316882	0.75484579	(NA) Family NA
b_treat_1H:treat_2H	-0.2178971	0.41161018	-1.022481	0.52642619	(NA) Family NA
b_treat_1M:treat_2H	-0.2133631	0.41861279	-1.0485984	0.58659458	(NA) Family NA

b_treat_1H:treat_2M	-0.4025421	0.42041503	-1.225964	0.43886902	(NA) Family NA
b_treat_1M:treat_2M	-0.213329	0.38906173	-0.9795752	0.55301965	(NA) Family NA
phi	12.167352	1.49090591	9.44040205	15.166236	(NA) Family NA
b_Intercept	-1.8816623	0.26366763	-2.4267035	-1.4071914	Pseudahrensia
b_treat_1H	0.36327397	0.32973435	-0.2749835	1.00912533	Pseudahrensia
b_treat_1M	0.45551169	0.31792557	-0.1550867	1.10873386	Pseudahrensia
b_treat_2H	0.05783406	0.33155717	-0.563609	0.70794059	Pseudahrensia
b_treat_2M	0.12137157	0.30548879	-0.4316882	0.75484579	Pseudahrensia
b_treat_1H:treat_2H	-0.2178971	0.41161018	-1.022481	0.52642619	Pseudahrensia
b_treat_1M:treat_2H	-0.2133631	0.41861279	-1.0485984	0.58659458	Pseudahrensia
b_treat_1H:treat_2M	-0.4025421	0.42041503	-1.225964	0.43886902	Pseudahrensia
b_treat_1M:treat_2M	-0.213329	0.38906173	-0.9795752	0.55301965	Pseudahrensia
phi	12.167352	1.49090591	9.44040205	15.166236	Pseudahrensia
b_Intercept	-2.4625667	0.25900409	-3.0349061	-1.9872862	Pelagibius
b_treat_1H	-0.1674073	0.46846914	-1.1097405	0.67815955	Pelagibius
b_treat_1M	0.41537754	0.46931913	-0.5634485	1.34892915	Pelagibius
b_treat_2H	0.59103462	0.33414384	-0.0748209	1.24832334	Pelagibius
b_treat_2M	0.20828153	0.33122242	-0.4360628	0.87854573	Pelagibius
b_treat_1H:treat_2H	-0.4639851	0.58449167	-1.6081991	0.72921839	Pelagibius
b_treat_1M:treat_2H	-0.942848	0.60074236	-2.1057931	0.29455361	Pelagibius
b_treat_1H:treat_2M	-0.7445878	1.13749426	-3.466847	1.00889216	Pelagibius
b_treat_1M:treat_2M	-0.7495625	0.57146112	-1.9001015	0.37604647	Pelagibius
phi	30.5184007	7.26567087	18.0200234	46.3758078	Pelagibius
zi	0.77350349	0.03048561	0.71108751	0.83162326	Pelagibius
b_Intercept	-1.8816623	0.26366763	-2.4267035	-1.4071914	Ruegeria
b_treat_1H	0.36327397	0.32973435	-0.2749835	1.00912533	Ruegeria
b_treat_1M	0.45551169	0.31792557	-0.1550867	1.10873386	Ruegeria
b_treat_2H	0.05783406	0.33155717	-0.563609	0.70794059	Ruegeria
b_treat_2M	0.12137157	0.30548879	-0.4316882	0.75484579	Ruegeria
b_treat_1H:treat_2H	-0.2178971	0.41161018	-1.022481	0.52642619	Ruegeria
b_treat_1M:treat_2H	-0.2133631	0.41861279	-1.0485984	0.58659458	Ruegeria
b_treat_1H:treat_2M	-0.4025421	0.42041503	-1.225964	0.43886902	Ruegeria

b_treat_1M:treat_2M	-0.213329	0.38906173	-0.9795752	0.55301965	Ruegeria
phi	12.167352	1.49090591	9.44040205	15.166236	Ruegeria
b_Intercept	-1.8816623	0.26366763	-2.4267035	-1.4071914	uncultured
b_treat_1H	0.36327397	0.32973435	-0.2749835	1.00912533	uncultured
b_treat_1M	0.45551169	0.31792557	-0.1550867	1.10873386	uncultured
b_treat_2H	0.05783406	0.33155717	-0.563609	0.70794059	uncultured
b_treat_2M	0.12137157	0.30548879	-0.4316882	0.75484579	uncultured
b_treat_1H:treat_2H	-0.2178971	0.41161018	-1.022481	0.52642619	uncultured
b_treat_1M:treat_2H	-0.2133631	0.41861279	-1.0485984	0.58659458	uncultured
b_treat_1H:treat_2M	-0.4025421	0.42041503	-1.225964	0.43886902	uncultured
b_treat_1M:treat_2M	-0.213329	0.38906173	-0.9795752	0.55301965	uncultured
phi	12.167352	1.49090591	9.44040205	15.166236	uncultured
b_Intercept	-1.3687878	0.24770064	-1.8645016	-0.9106776	Endozoicomonas
b_treat_1H	0.26163948	0.39509996	-0.5247795	1.00052105	Endozoicomonas
b_treat_1M	0.47584834	0.39589313	-0.3027039	1.23462154	Endozoicomonas
b_treat_2H	-0.0460055	0.34860033	-0.7438109	0.6305776	Endozoicomonas
b_treat_2M	-0.254038	0.35274188	-0.9697661	0.39297213	Endozoicomonas
b_treat_1H:treat_2H	-0.0659211	0.51274836	-1.0332858	0.98293681	Endozoicomonas
b_treat_1M:treat_2H	-0.5132576	0.51202342	-1.5155443	0.50589605	Endozoicomonas
b_treat_1H:treat_2M	0.1217691	0.54184248	-0.9467471	1.22360243	Endozoicomonas
b_treat_1M:treat_2M	-0.6066018	0.53656014	-1.6511528	0.42673563	Endozoicomonas
phi	5.28865727	0.64576571	4.07186066	6.60068358	Endozoicomonas
zi	0.33766728	0.03367801	0.27537549	0.40564695	Endozoicomonas
b_Intercept	-2.4625667	0.25900409	-3.0349061	-1.9872862	Roseobacter
b_treat_1H	-0.1674073	0.46846914	-1.1097405	0.67815955	Roseobacter
b_treat_1M	0.41537754	0.46931913	-0.5634485	1.34892915	Roseobacter
b_treat_2H	0.59103462	0.33414384	-0.0748209	1.24832334	Roseobacter
b_treat_2M	0.20828153	0.33122242	-0.4360628	0.87854573	Roseobacter
b_treat_1H:treat_2H	-0.4639851	0.58449167	-1.6081991	0.72921839	Roseobacter
b_treat_1M:treat_2H	-0.942848	0.60074236	-2.1057931	0.29455361	Roseobacter
b_treat_1H:treat_2M	-0.7445878	1.13749426	-3.466847	1.00889216	Roseobacter
b_treat_1M:treat_2M	-0.7495625	0.57146112	-1.9001015	0.37604647	Roseobacter

phi	30.5184007	7.26567087	18.0200234	46.3758078	Roseobacter
zi	0.77350349	0.03048561	0.71108751	0.83162326	Roseobacter
b_Intercept	-2.4625667	0.25900409	-3.0349061	-1.9872862	Synechococcus PCC-7336
b_treat_1H	-0.1674073	0.46846914	-1.1097405	0.67815955	Synechococcus PCC-7336
b_treat_1M	0.41537754	0.46931913	-0.5634485	1.34892915	Synechococcus PCC-7336
b_treat_2H	0.59103462	0.33414384	-0.0748209	1.24832334	Synechococcus PCC-7336
b_treat_2M	0.20828153	0.33122242	-0.4360628	0.87854573	Synechococcus PCC-7336
b_treat_1H:treat_2H	-0.4639851	0.58449167	-1.6081991	0.72921839	Synechococcus PCC-7336
b_treat_1M:treat_2H	-0.942848	0.60074236	-2.1057931	0.29455361	Synechococcus PCC-7336
b_treat_1H:treat_2M	-0.7445878	1.13749426	-3.466847	1.00889216	Synechococcus PCC-7336
b_treat_1M:treat_2M	-0.7495625	0.57146112	-1.9001015	0.37604647	Synechococcus PCC-7336
phi	30.5184007	7.26567087	18.0200234	46.3758078	Synechococcus PCC-7336
zi	0.77350349	0.03048561	0.71108751	0.83162326	Synechococcus PCC-7336
b_Intercept	-1.8816623	0.26366763	-2.4267035	-1.4071914	Erythrobacter
b_treat_1H	0.36327397	0.32973435	-0.2749835	1.00912533	Erythrobacter
b_treat_1M	0.45551169	0.31792557	-0.1550867	1.10873386	Erythrobacter
b_treat_2H	0.05783406	0.33155717	-0.563609	0.70794059	Erythrobacter
b_treat_2M	0.12137157	0.30548879	-0.4316882	0.75484579	Erythrobacter
b_treat_1H:treat_2H	-0.2178971	0.41161018	-1.022481	0.52642619	Erythrobacter
b_treat_1M:treat_2H	-0.2133631	0.41861279	-1.0485984	0.58659458	Erythrobacter
b_treat_1H:treat_2M	-0.4025421	0.42041503	-1.225964	0.43886902	Erythrobacter
b_treat_1M:treat_2M	-0.213329	0.38906173	-0.9795752	0.55301965	Erythrobacter
phi	12.167352	1.49090591	9.44040205	15.166236	Erythrobacter

Table C.S 40 Estimates of differentially abundant bacteria (non-rarefied dataset) between origin and destination treatments. Only significantly different taxa displayed. Log2FoldChange (x) values compare abundances found in particular treatment combinations, where a positive value favours treatment history 1 and a negative value means significantly higher abundance in treatment history 2. Its value represents magnitude of difference (2^x).

history 1	history 2	ASV	base Mean	log2FoldChange	lfcSE	stat	pvalue	padj	Kingdom	Phylum	Class	Order	Family	Genus	Species
MC	CC	N/A													
HC	CC	8f0831ade3b3e4a5b7a972547804fff2	3.80167379	-22.40898	2.92235055	-7.6681356	1.75E-14	6.51E-12	Bacteria	Proteobacteria	Alphaproteobacteria	Rhodobacterales	Rhodobacteraceae	Ruegeria	NA
		e2d07801858b8783b72867d25cc6affc	11.2398342	-23.834724	2.65751133	-8.9688136	3.00E-19	2.24E-16	Bacteria	Proteobacteria	Alphaproteobacteria	Rhodobacterales	Rhodobacteraceae	Ruegeria	NA
HC	MC	N/A													
MM	CM	7ddd59056470e6021abe757ba23ec188	9.40551022	22.7463698	2.81600983	8.07751789	6.61E-16	6.59E-13	Bacteria	Proteobacteria	Alphaproteobacteria	Rhizobiales	Rhizobiaceae	NA	NA
		c698e34b0e4a752b6f0e1b37b1f03c63	28.3307172	9.96382528	2.12963893	4.67864536	2.89E-06	0.00073566	Bacteria	Proteobacteria	Alphaproteobacteria	Rhizobiales	Stappiaceae	Labrenzia	Ambiguous_taxa
		8abb0ca2546c7f07c24300677e0b9100	7.06970663	22.3464194	2.79494194	7.99530719	1.29E-15	6.59E-13	Bacteria	Proteobacteria	Alphaproteobacteria	Rhodobacterales	Rhodobacteraceae	NA	NA
		258f6ff0d19d4c22cfeb6861fc095355	9.35135621	22.736354	2.92049969	7.78509037	6.97E-15	2.37E-12	Bacteria	Proteobacteria	Alphaproteobacteria	Rhodospirillales	Rhodospirillaceae	Roseospira	uncultured bacterium

HH	CH	a6aaef3401ade4f24f385f8157916bd	7.68 547 625	6.288 45979	1.91 298 368	3.28 725 219	0.00 101 17	0.01 774 369	Bacteria	Firmicutes	Erysipelotrichia	Erysipelotrichales	Erysipelotrichaceae	Turicibacter	uncultured bacterium
		06ea2777273210625181a9375f748c71	6.44 199 414	6.032 4918	2.32 418 694	2.59 552 78	0.00 944 458	0.04 927 253	Bacteria	Cyanobacteria	Oxyphotobacteria	Eurycoccales	Eurycoccales Incertae Sedis	Synechococcus PCC-7336	Synechococcus sp. PCC 7336
		afbc701b739bc06bc30ede5b2eef9f0a	6.80 195 711	5.957 39402	1.93 036 237	3.08 615 321	0.00 202 764	0.02 421 754	Bacteria	Cyanobacteria	Oxyphotobacteria	Nostocales	Xenococcaeae	Pleurocapsa PCC-7319	NA
		ffd30ac895432741482e09dc9ca05171	9.11 200 384	6.531 87307	2.20 767 952	2.95 870 529	0.00 308 934	0.02 817 482	Bacteria	Cyanobacteria	Oxyphotobacteria	Nostocales	Nostocaceae	Rivularia PCC-7116	uncultured bacterium
		0097f3b74b88b7176c553d8cd4ed7beb	6.94 130 88	6.140 45123	2.17 097 757	2.82 842 684	0.00 467 774	0.03 677 671	Bacteria	Cyanobacteria	Oxyphotobacteria	Nostocales	Cyanobacteriaceae	Cyanobacterium CLg1	uncultured bacterium
		f2a8692e7d33fceb64a3f7050bf4e275	7.60 791 807	5.206 03707	1.72 208 892	3.02 309 423	0.00 250 204	0.02 593 027	Bacteria	Proteobacteria	Alphaproteobacteria	Rhodobacterales	Rhodobacteraceae	Roseobacter clade CHAB-I-5 lineage	Ambiguous_taxa
		75f5b4b1d3fb4c55b199b67a9debe61e	6.50 486 892	5.072 00572	1.95 347 392	2.59 640 309	0.00 942 055	0.04 927 253	Bacteria	Proteobacteria	Alphaproteobacteria	Rhizobiales	Rhizobiaceae	Pseudahrensia	uncultured bacterium
		a1ef686c65c83b720247e3da1bece48b	55.0 605 858	3.883 24929	1.49 740 132	2.59 332 567	0.00 950 527	0.04 927 253	Bacteria	Proteobacteria	Alphaproteobacteria	Rhizobiales	Rhizobiaceae	uncultured	Ambiguous_taxa
		bdc3917c51f88b15d5b0a9c81be2f3d4	14.2 128 236	7.173 10429	2.23 133 688	3.21 471 148	0.00 130 576	0.02 126 518	Bacteria	Proteobacteria	Alphaproteobacteria	Rhizobiales	Stappiaceae	Labrenzia	Ambiguous_taxa
		15db6cfde3ab615e3d99285035037e13	19.0 528 46	4.026 966	1.54 977 921	2.59 841 27	0.00 936 559	0.04 927 253	Bacteria	Proteobacteria	Alphaproteobacteria	Rhodobacterales	Rhodobacteraceae	Pseudoruegeria	uncultured bacterium

	cc17864c41a0b7e0e37ba57e7b080c47	6.61 248 063	6.069 71241	2.34 062 6	2.59 320 045	0.00 950 873	0.04 927 253	Ba cte ria	Prote obact eria	Alphapr oteobac teria	Rhodo bacter ales	Rhodobac teraceae	Pseudorueger ia	Pseudoruegeri a marinistellae
	29b44977b79597a88a8b2662d653e2e9	6.62 806 854	4.444 43151	1.57 789 968	2.81 667 559	0.00 485 235	0.03 678 156	Ba cte ria	Prote obact eria	Alphapr oteobac teria	Rhodo bacter ales	Rhodobac teraceae	uncultured	uncultured bacterium
	ad3f700c5632258c437f98b59f4dda55	18.5 434 026	4.163 58535	1.55 618 014	2.67 551 631	0.00 746 142	0.04 725 569	Ba cte ria	Prote obact eria	Alphapr oteobac teria	Rhodo bacter ales	Rhodobac teraceae	NA	NA
	842d96314b8659dead2becf79631b300	29.3 899 232	4.329 16598	1.46 238 501	2.96 034 625	0.00 307 293	0.02 817 482	Ba cte ria	Prote obact eria	Alphapr oteobac teria	Rhodo bacter ales	Rhodobac teraceae	NA	NA
	29d2e2719581e0bbd571b420482e6f6c	4.84 075 101	5.620 86676	2.00 246 824	2.80 696 924	0.00 500 1	0.03 678 156	Ba cte ria	Prote obact eria	Alphapr oteobac teria	Rhodo bacter ales	Rhodobac teraceae	NA	NA
	c5641fa0ea466dcbe87d60d8bae43cda	10.4 337 139	6.254 90069	1.72 941 034	3.61 678 229	0.00 029 829	0.00 870 362	Ba cte ria	Prote obact eria	Alphapr oteobac teria	Rhodo bacter ales	Rhodobac teraceae	Loktanella	NA
	416c81f69b4ea70bae0eb909f6ba78f8	9.49 635 341	6.591 6806	2.19 781 193	2.99 920 139	0.00 270 688	0.02 683 345	Ba cte ria	Prote obact eria	Alphapr oteobac teria	Rhodo bacter ales	Rhodobac teraceae	Silicimonas	uncultured bacterium
	1b4be9b77e6094a3ad87794878611458	14.3 966 671	4.443 76034	1.60 148 88	2.77 476 829	0.00 552 41	0.03 935 925	Ba cte ria	Prote obact eria	Alphapr oteobac teria	Rhodo bacter ales	Rhodobac teraceae	Silicimonas	uncultured bacterium
	41120b546c3b6240d4d7b891787369b4	128. 206 415	4.764 17702	1.28 484 321	3.70 798 318	0.00 020 892	0.00 823 518	Ba cte ria	Prote obact eria	Alphapr oteobac teria	Rhodo bacter ales	Rhodobac teraceae	NA	NA
	f01da61ef615a0968fa4116ad0f6a4ac	187. 589 036	2.931 19393	1.08 538 746	2.70 059 684	0.00 692 152	0.04 622 792	Ba cte ria	Prote obact eria	Alphapr oteobac teria	Rhodo bacter ales	Rhodobac teraceae	Ruegeria	Ambiguous_ta xa
	8c91f81c837dfb88c5328fdc01c0e1f8	8.54 180 169	6.439 99048	2.03 286 536	3.16 793 753	0.00 153 525	0.02 187 724	Ba cte ria	Prote obact eria	Alphapr oteobac teria	Rhodo bacter ales	Rhodobac teraceae	Ruegeria	Ambiguous_ta xa

	7db6bc9ca547 dccb30a8fb4e0 ba36a81	7.18 940 905	22.57 00382	2.92 081 383	7.72 731 145	1.10 E-14	2.50 E-12	Ba cte ria	Prote obact eria	Alphapr oteobac teria	Rhodo bacter ales	Rhodobac teraceae	Ruegeria	NA
	e2d07801858b 8783b72867d2 5cc6affc	89.9 901 067	7.091 98378	1.58 150 845	4.48 431 608	7.31 E-06	0.00 055 593	Ba cte ria	Prote obact eria	Alphapr oteobac teria	Rhodo bacter ales	Rhodobac teraceae	Ruegeria	NA
	07cbe0c6eb1e9 f6bdc20bbb5f6 30a1b5	18.3 276 177	5.020 25871	1.71 322 039	2.93 030 526	0.00 338 629	0.02 969 517	Ba cte ria	Prote obact eria	Alphapr oteobac teria	Rhodo bacter ales	Rhodobac teraceae	NA	NA
	ba292eac5b5b 02a5723d4629 787b4786	5.42 203 382	5.784 81786	2.14 866 338	2.69 228 67	0.00 709 639	0.04 622 792	Ba cte ria	Prote obact eria	Alphapr oteobac teria	Rhodo bacter ales	Rhodobac teraceae	Dinoroseobac ter	uncultured bacterium
	eeb8d4047341 532d08f992e2b 177bfe8	7.89 838 755	6.327 80941	1.77 721 423	3.56 052 146	0.00 037 012	0.00 937 635	Ba cte ria	Prote obact eria	Alphapr oteobac teria	Rhodo bacter ales	Rhodobac teraceae	Actibacterium	uncultured bacterium
	e2250c863b1d 3d72429b7ea7f c38fd48	7.85 139 325	6.317 93866	2.17 804 163	2.90 074 284	0.00 372 279	0.03 031 417	Ba cte ria	Prote obact eria	Alphapr oteobac teria	Rhodo bacter ales	Rhodobac teraceae	Roseobacter	NA
	c6e28c7522e60 3b8f62d858b0 2f12fa2	6.08 284 062	4.907 84895	1.35 925 728	3.61 068 432	0.00 030 539	0.00 870 362	Ba cte ria	Prote obact eria	Alphapr oteobac teria	Rhodo bacter ales	Rhodobac teraceae	Roseobacter	uncultured alpha proteobacteri um
	8a2ee2f7bd87c d5c5c5efe2cc9 1677ad	10.0 492 459	6.674 75869	1.90 832 618	3.49 770 325	0.00 046 928	0.01 069 965	Ba cte ria	Prote obact eria	Alphapr oteobac teria	Rhizobi ales	Rhizobiace ae	uncultured	NA
	91aa7f96235ff 49b6261337f19 1bdc81	18.8 280 161	4.057 20288	1.55 410 857	2.61 063 027	0.00 903 755	0.04 927 253	Ba cte ria	Prote obact eria	Alphapr oteobac teria	Rhizobi ales	Rhizobiace ae	uncultured	uncultured alpha proteobacteri um
	d84cc4258f4e5 56e74e94ad01 28e9ec7	8.87 198 255	5.434 11924	1.73 970 864	3.12 358 007	0.00 178 665	0.02 316 279	Ba cte ria	Prote obact eria	Alphapr oteobac teria	Rhizobi ales	Hyphomic robiaceae	Hyphomicrobi um	uncultured bacterium

	e015b60727107df3a701a9e132964ee7	8.48812348	6.43152859	1.89647997	3.39129792	0.00069562	0.01420184	Bacteria	Proteobacteria	Alphaproteobacteria	Rhizobiales	Methyloligellaceae	Methyloceani bacter	uncultured bacterium
	cb6b917a21080fee02e2a5aa2096b8d3	7.22465533	5.8922822	1.59307285	3.69868974	0.00021672	0.00823518	Bacteria	Proteobacteria	Alphaproteobacteria	Rhodobacteriales	Rhodobacteraceae	uncultured	uncultured alpha proteobacterium
	c5262485e098831e853876ebd93a5d61	8.25215577	4.51424406	1.70278645	2.65109231	0.00802319	0.04813915	Bacteria	Proteobacteria	Alphaproteobacteria	Rhodobacteriales	Rhodobacteraceae	uncultured	uncultured alpha proteobacterium
	3484d33fa1654e05e581062f42f699ac	7.73303368	5.61534081	1.82774736	3.07227407	0.00212435	0.02421754	Bacteria	Proteobacteria	Alphaproteobacteria	Parvibacterales	PS1 clade	uncultured bacterium	
	e2084ef86d740eab9541229ee9d710f3	8.09331098	6.3635645	1.67962729	3.78867653	0.00015145	0.00823518	Bacteria	Planctomycetes	Planctomycetacia	Pirellulales	Pirellulaceae	NA	NA
	2c1cf81ac2f4e4e6794b3eeffc4b531	4.37090131	5.47686274	1.72521003	3.17460636	0.0015004	0.02187724	Bacteria	Planctomycetes	Planctomycetacia	Pirellulales	Pirellulaceae	Blastopirellula	uncultured bacterium
	0f9384f2751706de751048f2848414ca	27.2167934	3.8681916	1.45312397	2.6619832	0.00776818	0.04786876	Bacteria	Planctomycetes	Planctomycetacia	Pirellulales	Pirellulaceae	Blastopirellula	NA
	0577e8efb35d17d66aa24b0297665603	11.1278078	4.93779582	1.62287607	3.0426204	0.00234528	0.02546304	Bacteria	Planctomycetes	Planctomycetacia	Pirellulales	Pirellulaceae	Blastopirellula	NA
	9620ec43dbab9c764d19413bfe05587	6.21558709	5.98066243	2.17087507	2.75495468	0.00587003	0.04055655	Bacteria	Planctomycetes	Planctomycetacia	Pirellulales	Pirellulaceae	Rhodopirellula	unidentified marine bacterioplankton
	095ceca3c61d9418671db120cd9789fa	5.80644908	5.88575179	1.74571108	3.37154976	0.00074747	0.01420184	Bacteria	Planctomycetes	Planctomycetacia	Pirellulales	Pirellulaceae	Rhodopirellula	Ambiguous_taxa

		b9c51c834dda 91a4faec58df2 9c5d645	5.53 910 114	5.815 89865	2.00 128 501	2.90 608 216	0.00 365 985	0.03 031 417	Ba cte ria	Prote obact eria	Deltapr oteobac teria	Bdellov ibriona les	Bdellovibri onaceae	OM27 clade	uncultured bacterium
		075e69e830e1 dfabb094eca7e f427857	29.8 142 694	8.243 81079	1.62 630 297	5.06 904 983	4.00 E-07	4.56 E-05	Ba cte ria	Prote obact eria	Alphapr oteobac teria	Sphing omona dales	Sphingom onadacea e	Parasphingop yxis	uncultured bacterium
		f44ed316686c0 00371fe14753d dde656	15.1 189 241	5.138 5268	1.64 868 754	3.11 673 781	0.00 182 864	0.02 316 279	Ba cte ria	Prote obact eria	Alphapr oteobac teria	Sphing omona dales	Sphingom onadacea e	Erythrobacter	NA
M H	CH	NA													
M H	HH	3140fc108962f bc0e8b3cc9a58 87a8a2	20.3 706 248	- 4.768 4186	1.60 457 059	- 2.97 177 24	0.00 296 086	0.03 924 146	Ba cte ria	Cyano bacte ria	Oxypho tobacte ria	Nostoc ales	Xenococca ceae	NA	NA
		fb14348fda73f 4a2a3bb01210 66d5afc	9.65 188 84	- 6.295 6821	2.07 047 147	3.04 069 98	0.00 236 029	0.03 924 146	Ba cte ria	Cyano bacte ria	Oxypho tobacte ria	Nostoc ales	Xenococca ceae	Pleurocapsa PCC-7319	NA
		822465ec1bb7 32365ea5fcc5c 0cfcf40	22.2 685 432	- 7.501 9195	2.00 406 786	- 3.74 334 6	0.00 018 159	0.00 832 667	Ba cte ria	Cyano bacte ria	Oxypho tobacte ria	Phormi desmia les	Phormides miaceae	Phormidium MBIC10003	cyanobacteriu m SC-1
		bdc3917c51f88 b15d5b0a9c81 be2f3d4	12.0 997 647	- 6.620 62	2.22 264 72	- 2.97 870 94	0.00 289 465	0.03 924 146	Ba cte ria	Prote obact eria	Alphapr oteobac teria	Rhizobi ales	Stappiace ae	Labrenzia	Ambiguous_ta xa
		f0cda7f00873c 61df80b7dc0f2 596fcf	7.21 402 316	- 5.876 4858	2.02 483 929	- 2.90 219 86	0.00 370 554	0.04 210 836	Ba cte ria	Prote obact eria	Alphapr oteobac teria	Rhizobi ales	Stappiace ae	Labrenzia	Ambiguous_ta xa

	d4ee0fcb2d6745f18745726de73faba5	7.76 770 682	- 5.984 7045	1.89 688 389	- 3.15 501 89	0.00 160 488	0.03 647 448	Ba cte ria	Prote obact eria	Alphapr oteobac teria	Rhodo bacter ales	Rhodobac teraceae	Ruegeria	Ambiguous_ta xa
	98d7e2d4d9eefd3350bf4307f0f4324	8.06 989 932	- 6.038 2802	2.03 339 825	- 2.96 955 12	0.00 298 235	0.03 924 146	Ba cte ria	Prote obact eria	Alphapr oteobac teria	Rhodo bacter ales	Rhodobac teraceae	Ruegeria	Ambiguous_ta xa
	d828b74e0fba3d6621ff180edca619e8	9.53 027 692	- 6.277 677	2.05 292 192	- 3.05 792 29	0.00 222 877	0.03 924 146	Ba cte ria	Prote obact eria	Alphapr oteobac teria	Rhodo bacter ales	Rhodobac teraceae	Silicimonas	uncultured bacterium
	ec81a17f16cb389e0bcd06c49438a027	17.7 549 593	- 5.603 7766	1.30 081 117	- 4.30 790 94	0.00 1.65 E-05	0.00 206 006	Ba cte ria	Prote obact eria	Alphapr oteobac teria	Rhodo bacter ales	Rhodobac teraceae	Ruegeria	NA
	c40fc572929282c726cedc1c52ac8081	27.1 107 318	- 7.785 9595	1.97 878 637	- 3.93 471 46	0.00 8.33 E-05	0.00 694 13	Ba cte ria	Prote obact eria	Alphapr oteobac teria	Rhodo bacter ales	Rhodobac teraceae	NA	NA
	8c91f81c837dfb88c5328fdc01c0e1f8	7.31 861 349	- 5.897 5384	2.02 576 871	- 2.91 125 95	0.00 359 975	0.04 210 836	Ba cte ria	Prote obact eria	Alphapr oteobac teria	Rhodo bacter ales	Rhodobac teraceae	Ruegeria	Ambiguous_ta xa
	e2d07801858b8783b72867d25cc6affc	78.2 477 626	- 9.321 5973	1.48 202 013	- 6.28 979 13	3.18 7.95 E-10	7.95 E-08	Ba cte ria	Prote obact eria	Alphapr oteobac teria	Rhodo bacter ales	Rhodobac teraceae	Ruegeria	NA
	07cbe0c6eb1e9f6bdc20bbb5f630a1b5	15.3 402 042	- 6.965 2276	1.85 606 46	- 3.75 268 6	0.00 017 495	0.00 832 667	Ba cte ria	Prote obact eria	Alphapr oteobac teria	Rhodo bacter ales	Rhodobac teraceae	NA	NA

	915bf7ca1f5f8a18e36dbde6615996de	40.1019505	-4.5894263	1.23397594	3.7192186	0.00019984	0.00832667	Bacteria	Proteobacteria	Alphaproteobacteria	Rhodobacterales	Rhodobacteraceae	NA	NA
	7b7c9cbd3a402a3a7d3c9d48340b79ee	6.60012092	-5.7500377	1.90175955	3.0235356	0.0024984	0.03924146	Bacteria	Proteobacteria	Alphaproteobacteria	Rhodobacterales	Rhodobacteraceae	Roseobacter	uncultured alpha proteobacterium
	771399a353b03df0e94367a225839475	7.36550028	-5.9082472	1.79185946	3.2972716	0.00097629	0.02440726	Bacteria	Proteobacteria	Alphaproteobacteria	Rhodobacterales	Rhodobacteraceae	Tateyamaria	uncultured bacterium
	a81e40f018e6522e6b21a3d91d843675	4.58236843	-5.2258902	1.74796578	2.9896982	0.00279253	0.03924146	Bacteria	Proteobacteria	Alphaproteobacteria	Rhodobacterales	Rhodobacteraceae	Tateyamaria	uncultured bacterium
	91aa7f96235ff49b6261337f191bdc81	15.9115188	-4.8253502	1.65610674	2.913671	0.00357206	0.04210836	Bacteria	Proteobacteria	Alphaproteobacteria	Rhizobiales	Rhizobiaceae	uncultured	uncultured alpha proteobacterium
	d84cc4258f4e556e74e94ad0128e9ec7	7.47006334	-5.9294295	1.77745424	3.3359112	0.0008502	0.02440726	Bacteria	Proteobacteria	Alphaproteobacteria	Rhizobiales	Hyphomicrobiaceae	Hyphomicrobium	uncultured bacterium
	c5262485e098831e853876ebd93a5d61	6.92957688	-4.6924704	1.66327801	2.8212183	0.00478416	0.04983503	Bacteria	Proteobacteria	Alphaproteobacteria	Rhodobacterales	Rhodobacteraceae	uncultured	uncultured alpha proteobacterium
	e2084ef86d740eab9541229ee9d710f3	6.86805962	-5.3410439	1.60983769	3.317753	0.00090745	0.02440726	Bacteria	Planctomycetes	Planctomycetacia	Pirellulales	Pirellulaceae	NA	NA

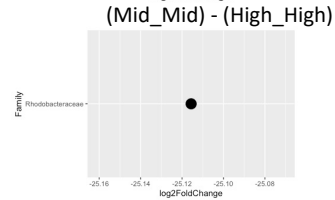
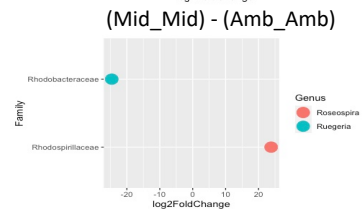
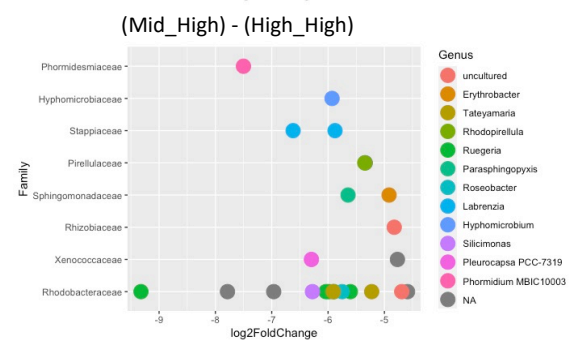
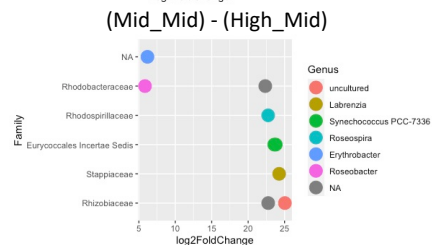
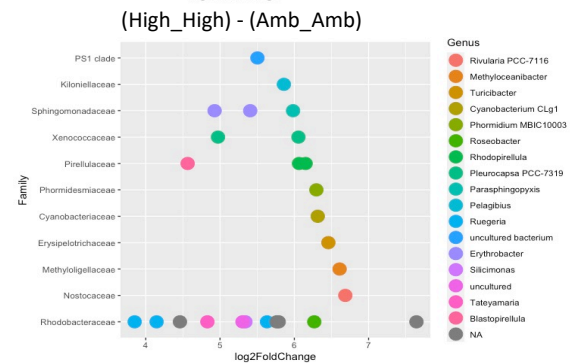
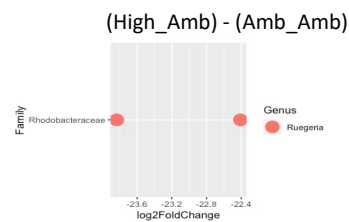
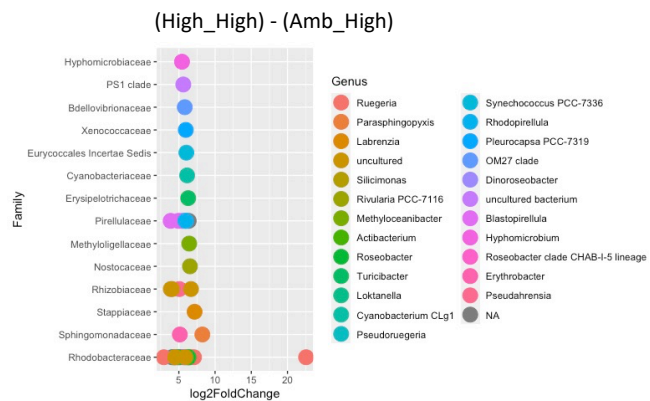
		095ceca3c61d9 418671db120c d9789fa	4.98 617 739	- 5.348 2146	1.74 029 729	3.07 316 15	0.00 211 804	0.03 924 146	Ba cte ria	Planct omyc etes	Plancto myceta cia	Pirellul ales	Pirellulace ae	Rhodopirellul a	Ambiguous_ta xa
		075e69e830e1 dfabb094eca7e f427857	26.1 409 863	- 5.645 3671	1.68 064 724	3.35 904 34	0.00 078 213	0.02 440 726	Ba cte ria	Prote obact eria	Alphapr oteobac teria	Sphing omona dales	Sphingom onadacea e	Parasphingop yxis	uncultured bacterium
		f44ed316686c0 00371fe14753d dde656	12.9 032 673	- 4.916 8512	1.73 288 908	2.83 737 21	0.00 454 866	0.04 944 192	Ba cte ria	Prote obact eria	Alphapr oteobac teria	Sphing omona dales	Sphingom onadacea e	Erythrobacter	NA
H H	CC	a6aaaef3401ad e4f24f385f815 7916bd	8.47 423 393	6.458 42548	1.92 363 844	3.35 740 092	0.00 078 679	0.02 562 685	Ba cte ria	Firmic utes	Erysipel otrichia	Erysipe lotrich ales	Erysipelotr ichaceae	Turicibacter	uncultured bacterium
		afbc701b739bc 06bc30ede5b2 eef9f0a	7.16 857 129	6.055 59046	1.93 536 443	3.12 891 483	0.00 175 453	0.03 636 665	Ba cte ria	Cyano bacte ria	Oxypho tobacte ria	Nostoc ales	Xenococca ceae	Pleurocapsa PCC-7319	NA
		822465ec1bb7 32365ea5fcc5c 0cfcf40	29.0 071 57	6.297 072	1.93 502 055	3.25 426 621	0.00 113 686	0.03 240 042	Ba cte ria	Cyano bacte ria	Oxypho tobacte ria	Phormi desmia les	Phormides miaceae	Phormidium MBIC10003	cyanobacteriu m SC-1
		ffd30ac895432 741482e09dc9c a05171	9.94 852 631	6.686 41518	2.21 942 827	3.01 267 46	0.00 258 956	0.04 217 29	Ba cte ria	Cyano bacte ria	Oxypho tobacte ria	Nostoc ales	Nostocace ae	Rivularia PCC- 7116	uncultured bacterium
		0097f3b74b88 b7176c553d8c d4ed7beb	7.68 721 059	6.315 54385	2.18 436 637	2.89 124 752	0.00 383 716	0.04 374 36	Ba cte ria	Cyano bacte ria	Oxypho tobacte ria	Nostoc ales	Cyanobact eriaceae	Cyanobacteri um CLg1	uncultured bacterium
		98d7e2d4d9eef df3350bf4307f 0f4324	10.6 120 012	5.632 47073	1.91 845 005	2.93 594 859	0.00 332 529	0.04 374 36	Ba cte ria	Prote obact eria	Alphapr oteobac teria	Rhodo bacter ales	Rhodobac teraceae	Ruegeria	Ambiguous_ta xa
		29d2e2719581 e0bbd571b420 482e6f6c	5.33 499 875	5.789 66323	2.01 394 435	2.87 478 809	0.00 404 299	0.04 389 529	Ba cte ria	Prote obact eria	Alphapr oteobac teria	Rhodo bacter ales	Rhodobac teraceae	NA	NA

	1b4be9b77e60 94a3ad877948 78611458	15.5 657 851	5.341 57428	1.75 892 482	3.03 684 058	0.00 239 072	0.04 192 953	Ba cte ria	Prote obact eria	Alphapr oteobac teria	Rhodo bacter ales	Rhodobac teraceae	Silicimonas	uncultured bacterium
	8fea15bbdcf6 8306ef3d37dd 0c7e63e	2.62 898 802	3.850 9075	1.34 835 572	2.85 600 265	0.00 429 012	0.04 446 12	Ba cte ria	Prote obact eria	Alphapr oteobac teria	Rhodo bacter ales	Rhodobac teraceae	Ruegeria	NA
	ec81a17f16cb3 89e0bcd06c49 438a027	23.6 465 551	4.146 23993	1.43 346 199	2.89 246 589	0.00 382 231	0.04 374 36	Ba cte ria	Prote obact eria	Alphapr oteobac teria	Rhodo bacter ales	Rhodobac teraceae	Ruegeria	NA
	41120b546c3b 6240d4d7b891 787369b4	139. 322 853	5.763 10347	1.56 550 647	3.68 130 287	0.00 023 205	0.02 110 268	Ba cte ria	Prote obact eria	Alphapr oteobac teria	Rhodo bacter ales	Rhodobac teraceae	NA	NA
	07cbe0c6eb1e9 f6bdc20bbb5f6 30a1b5	19.2 950 287	7.644 12316	1.86 889 528	4.09 018 271	4.31 E-05	0.00 982 756	Ba cte ria	Prote obact eria	Alphapr oteobac teria	Rhodo bacter ales	Rhodobac teraceae	NA	NA
	915bf7ca1f5f8a 18e36dbde661 5996de	51.7 364 337	4.460 3712	1.23 664 208	3.60 684 089	0.00 030 995	0.02 110 268	Ba cte ria	Prote obact eria	Alphapr oteobac teria	Rhodo bacter ales	Rhodobac teraceae	NA	NA
	4d6c7413002bf b6f892578760b b9f7d3	7.43 818 883	6.268 54473	2.03 844 879	3.07 515 438	0.00 210 394	0.03 997 479	Ba cte ria	Prote obact eria	Alphapr oteobac teria	Rhodo bacter ales	Rhodobac teraceae	Roseobacter	uncultured bacterium
	771399a353b0 3df0e94367a22 5839475	9.70 877 274	4.830 20507	1.74 186 315	2.77 301 066	0.00 555 403	0.04 973 552	Ba cte ria	Prote obact eria	Alphapr oteobac teria	Rhodo bacter ales	Rhodobac teraceae	Tateyamaria	uncultured bacterium
	e015b6072710 7df3a701a9e13 2964ee7	9.41 094 131	6.609 51253	1.90 799 362	3.46 411 668	0.00 053 198	0.02 110 268	Ba cte ria	Prote obact eria	Alphapr oteobac teria	Rhizobi ales	Methylolig ellaceae	Methyloceani bacter	uncultured bacterium
	f9c44c9fce9289 ff88e5b2f6734 8d798	10.1 810 946	5.859 63264	2.02 641 431	2.89 162 616	0.00 383 254	0.04 374 36	Ba cte ria	Prote obact eria	Alphapr oteobac teria	Rhodo vibrion ales	Kiloniellac eae	Pelagibius	uncultured alpha proteobacteri um

		c5262485e098831e853876ebd93a5d61	8.88630841	5.30247406	1.69160599	3.13457985	0.001721	0.03636665	Bacteria	Proteobacteria	Alphaproteobacteria	Rhodobacterales	Rhodobacteraceae	uncultured	uncultured alpha proteobacterium
		3484d33fa1654e05e581062f42f699ac	8.73989333	5.50361904	1.89977635	2.8969826	0.00376771	0.0437436	Bacteria	Proteobacteria	Alphaproteobacteria	Parvibacterales	PS1 clade	uncultured bacterium	
		eced8c897c76f2e2c70effdc3b2bda5b	3.37921299	4.9727442	1.75437454	2.83448266	0.00458999	0.04550082	Bacteria	Cyanobacteria	Oxyphotobacteria	Nostocales	Xenococcaceae	Pleurocapsa PCC-7319	Pleurocapsa sp. PCC 7319
		0f9384f2751706de751048f2848414ca	29.3702138	4.5641463	1.43052446	3.19054056	0.00142007	0.03597508	Bacteria	Planctomycetes	Planctomycetacia	Pirellulales	Pirellulaceae	Blastopirellula	NA
		9620ec43dbab9c764d19413bfe05587	6.86555568	6.15201585	2.18386678	2.81702891	0.00484702	0.04604665	Bacteria	Planctomycetes	Planctomycetacia	Pirellulales	Pirellulaceae	Rhodopirellula	unidentified marine bacterioplankton
		095ceca3c61d9418671db120cd9789fa	6.43166002	6.06321764	1.75616107	3.45254074	0.00055533	0.02110268	Bacteria	Planctomycetes	Planctomycetacia	Pirellulales	Pirellulaceae	Rhodopirellula	Ambiguous_taxa
		075e69e830e1dfabb094eca7ef427857	33.4133701	5.98310146	1.71219226	3.49440983	0.00047511	0.02110268	Bacteria	Proteobacteria	Alphaproteobacteria	Sphingomonadales	Sphingomonadaceae	Parasphingomyxis	uncultured bacterium
		d4449bc64fe461d40efda856ccecceaf8	6.91772847	5.40615775	1.848647	2.92438619	0.00345136	0.0437436	Bacteria	Proteobacteria	Alphaproteobacteria	Sphingomonadales	Sphingomonadaceae	Erythrobacter	NA
		f44ed316686c000371fe14753ddde656	16.5806126	4.9269717	1.78114171	2.76618736	0.00567159	0.04973552	Bacteria	Proteobacteria	Alphaproteobacteria	Sphingomonadales	Sphingomonadaceae	Erythrobacter	NA
M	CC	e2d07801858b8783b72867d25cc6affc	13.8583632	-24.582704	2.62364266	9.3696847	7.27E-21	7.61E-18	Bacteria	Proteobacteria	Alphaproteobacteria	Rhodobacterales	Rhodobacteraceae	Ruegeria	NA

		258f6ff0d19d4c22cf6b6861fc095355	11.6 209 677	23.82 76684	2.92 046 498	8.15 886 12	3.38 E-16	1.77 E-13	Ba cte ria	Prote obact eria	Alphapr oteobac teria	Rhodos pirillale s	Rhodospiri llaceae	Roseospira	uncultured bacterium
M M	HH	9b1561230b5cf602e7357494364f1b01	20.5 196 31	- 25.11 5616	2.42 583 868	10.3 533 74	4.04 E-25	5.75 E-22	Ba cte ria	Prote obact eria	Alphapr oteobac teria	Rhodo bacter ales	Rhodobac teraceae	NA	NA

Figure C.S 13 Estimates of differentially abundant bacteria (non-rarefied dataset) between origin and destination treatments. Only significantly different taxa displayed. Log2FoldChange (x) values compare abundances found in particular treatment combinations, where a positive value favours treatment history 1 and a negative value means significantly higher abundance in treatment history 2. Its value represents magnitude of difference (2^x).



EDMUNDS, P. J. 2017. Intraspecific variation in growth rate is a poor predictor of fitness for reef corals. *Ecology*, 98, 2191-2200.

WEISS, S., XU, Z. Z., PEDDADA, S., AMIR, A., BITTINGER, K., GONZALEZ, A., LOZUPONE, C., ZANEVELD, J. R., VAZQUEZ-BAEZA, Y., BIRMINGHAM, A., HYDE, E. R. & KNIGHT, R. 2017. Normalization and microbial differential abundance strategies depend upon data characteristics. *Microbiome*, 5, 27.